THE UNIVERSITY OF HULL

Pollution Reduction with Processed Waste Materials

A thesis being submitted for the degree of

Doctor of Philosophy

in the University of Hull

By

Sunday Enenche ELAIGWU (B.Sc, M.Sc)

October 2013

Acknowledgements

I am highly grateful to my major supervisor Professor Gillian M. Greenway for her consistent support, scientific guidance and making time for me from her tight schedule throughout the period of this research, and for giving me a great deal of freedom to carry out the research at my own pace.

I am also very grateful to my second supervisor, Dr. John Adam for his time, and the ideas he brought into the composting aspect of this research, most especially with the enzyme and statistical analysis.

I am highly indebted to Bob Knight, my friend and colleague for giving me space in his laboratory throughout the period of my research, and also for his invaluable and continual assistance with the microwave and ICP-OES instrumentation. I am also grateful to him for always finding out time to go through my work with me. I always felt at home with him.

I would also like to thank Dr. Georgios Kyriakou for all his assistance. Dr. Yan Zhou for help with different computer skills I needed during my write up. Dr. Vincent Rocher for helping with the characterization of materials. Dr. Mark Lorch and Rahul Saurabh are appreciated for all their help with NMR, Ian Dobson for FT-IR, and Tony Sinclair for SEM. I would like to thank Dean and Sean Moore for all their assistance and fun in the teaching laboratory, I am going to miss all that. I would like to express my great appreciation to everyone in the Analytical Chemistry group, my fellow postgraduate students and friends at the University of Hull for all their support. I also highly appreciate all the support I got from the Catholic community in Hull, and my other friends outside and within the UK.

I would like to express my great appreciation to the Nigerian government for providing the financial support for this research through the Petroleum Technology Development Fund (PTDF) overseas scholarship scheme.

Finally, I would like to say a big thank you to all members my family: my wife Anita, my parents and siblings for all your love, encouragement, understanding, prayers and moral support throughout my academic pursuits. I thank you all for believing in me and to my son Chris; I thank you for coming into my life at this point. I lack words to express the joy you have brought to my life.

Publications and Presentations

The work contained in this thesis has led to the following publications and presentations:

Publications:

1. S.E. Elaigwu, G.M. Greenway**.** Biomass derived mesoporous carbon monoliths via an evaporation-induced self-assembly. *Materials Letters* 2014; 115: 117-120.
2. S.E. Elaigwu, V. Rocher, G. Kyriakou, G.M. Greenway. Removal of Pb^{2+} and Cd^{2+} from aqueous solution using chars from pyrolysis and microwave-assisted hydrothermal carbonization of *Prosopis africana* shell. **Accepted**: *Journal of Industrial and Engineering Chemistry* (2013)

Presentations:

1. Sunday E. Elaigwu, Gillian M. Greenway**.** Synthesis of Carbonaceous Material Utilizing Pyrolysis and Microwave Assisted Hydrothermal Carbonization of Waste Material. *Oral presentation.* University of Hull, Research Colloquia, 9th July, 2012.
2. Sunday E. Elaigwu, Vincent Rocher, Gillian M. Greenway. Synthesis of Novel Materials Utilizing Microwave Assisted Hydrothermal Carbonization of Waste Material. *Poster presentation.* University of Hull, Research Colloquia, 11th July, 2011.
3. Sunday E. Elaigwu, Gillian M. Greenway. Biochar from *Prosopis africana* shell and palm kernel seeds for heavy metal remediation. *Poster presentation.* Analytical Research Forum 2010**.** Loughborough University, United Kingdom, 26 - 28 July 2010.

Abstract

This research aimed at providing an understanding into the waste management options available for developing countries and also to provide insight into the possible application of the processed materials during the waste management processes, thereby helping in converting the waste materials which would have been a nuisance into useful products. Pyrolysis and composting were utilized as the waste management techniques for processing the waste materials for use in pollution reduction.

Carbon materials (biochar and hydrochar) were prepared in the pyrolysis aspect of this research through dry and wet (hydrothermal carbonization) pyrolysis respectively. Under the wet pyrolysis, comparisons were made between the conventional and the microwave-assisted hydrothermal process for carbonisation of waste materials. Three waste materials were investigated *Prosopis africana* shell (from Nigeria), rapeseed waste (from the UK) and coconut husks (a well-studied material in carbon science). The result shows that the microwave-assisted hydrothermal carbonization process reduced the processing time from 4 hours to 20 minutes for the same level of carbonisation. The biochar and the hydrochar from the pyrolysis and microwave-assisted hydrothermal carbonization of one of the waste materials (*Prosopis africana* shell) were applied in the adsorption of Pb^{2+} and Cd^{2+} from aqueous solution. In terms of adsorbing the heavy metal ions from aqueous solution, the materials proved to have high adsorption capacities than some previously studied adsorbents. Maximum adsorption capacities for the hydrochar and biochar were 45.3 and 31.3 mg/g for Pb^{2+} and 38.3 and 29.9 mg/g for Cd^{2+} respectively. Interestingly, the hydrochar from microwave-assisted hydrothermal carbonization, which is a green chemistry approach, was capable of adsorbing the metal ions more than the biochar from aqueous solution. The adsorption process was dominated by chemisorptions as it followed the pseudo-second-order kinetics and the adsorption data fitted the Langmuir isotherm model. The thermodynamics study of the adsorption processes showed that it was spontaneous and endothermic.

Microwave-assisted hydrothermal process and evaporation-induced self-assembly (EISA) were also used to synthesize carbon monoliths, using a waste plant material as the carbon precursor. The microwave-assisted hydrothermal process was not successful in the synthesis of the carbon monolith; however novel carbon monolith was produced

using the EISA approach. The carbon monolith in comparison to the biochar and hydrochar from the same material is not powdered, has higher surface area and porosity which could enhance its adsorption capacities for heavy metal ions.

In the composting aspect of the research, the *Prosopis africana* shell showed that it can be composted. The effect of an organic pollutant, in this case anthracene during a starch amended co-composting process was evaluated through total dry matter and extracellular enzyme activities of both starch specific (α-glucosidase) and non-specific (β-glucosidase) substrate. The result showed that the effect of anthracene amendment alone was not highly significant on the process. However, the interaction between the anthracene and starch have consistent effects on the process, which is novel and should be studied further to know the magnitude of sure interaction.

This research showed that the waste material (*Prosopis africana* shell) from Nigeria can be processed into useful products using pyrolysis and composting. Further work will be required in Nigeria outside the laboratory to see the real applicability of these processed materials.

Table of Contents

Chapter 4: Preparation and Characterization of Carbonaceous Materials from Pyrolysis and Hydrothermal Carbonization

List of Abbreviations

Abbreviations	**Meaning**
R-PAS	Raw *Prosopis africana* shell
B-PAS	*Prosopis africana* shell biochar
M-PAS	Microwave-assisted *Prosopis africana* shell hydrochar
C-PAS	Conventional oven *Prosopis africana* shell hydrochar
M-RSH	Microwave-assisted rapeseed husk hydrochar
C-RSH	Conventional oven rapeseed husk hydrochar
M-CS	Microwave-assisted coconut shell hydrochar
C-CS	Conventional coconut shell hydrochar
HTC-G	Microwave-assisted glucose hydrochar
$CM_{100\text{-}20}$	Carbon monolith synthesized at 100 °C for 20 minutes
$CM_{100\text{-}15}$	Carbon monolith synthesized at 100 °C for 15 minutes
$CM_{100\text{-}10}$	Carbon monolith synthesized at 100 °C for 10 minutes
$CM_{100\text{-}5}$	Carbon monolith synthesized at 100 °C for 5 minutes
ss	Sums of square
df	Degree of freedom
ms	Mean square
p	Probability
F	F-statistics test
MSE	Root mean square error
adj R-squared	Adjusted R-square for degree of freedom
t	t-statistics

Chapter 1

General Introduction

1. 1 Aims of the Project

This work investigates the waste management options for a developing country (Nigeria). It is specifically aimed at studying how waste materials generated as a result of population growth, agricultural practices, and from the huge natural resources present in the country can be transformed into a form that will be of benefit in solving other problems in the country, rather than being a nuisance by converting the waste materials into useful products. These products can find application in solving environmental problems, such as, remediating petrochemical pollution that usually result from the exploration, refining and distribution of petroleum products from the large oil reserve in the country. In addition, this project will provide an understanding into the changes that took place in the waste materials during the processes of conversion and how these materials have being converted to a useful form. In order to achieve these aims the following objectives were set:

- To use dry and wet pyrolysis as a waste management technique for converting the waste material into a biochar and hydrochar respectively, and to evaluate their performance in the removal of heavy metal ions from wastewater.
- To use composting as a low cost waste management technique and monitor the effect of organic pollutant on the composting process.
- To evaluate the possibility of converting the waste material into carbon monolith.

The findings from this project will be useful in tackling waste management and recycling problems in developing countries like Nigeria. This project as a whole will help the Nigerian Government in meeting their Millennium Development Goals of protecting the environment. It will provide possible alternatives to the available methods for managing different varieties of organic waste materials mostly from agricultural activities, which is the major occupation in the country, and lead to the development of an effective and sustainable waste management strategy that will help in the reduction of the volume of agricultural waste going to landfills and being incinerated.

1.2 The Need to Recycle Waste

Waste recycling refers to the collection, separation, clean-up and processing of waste material into a material or product that is marketable [1]. Sustainable development is something that is now of increasing importance to the world-wide community. World leaders signed a global environment and development action plan called Agenda 21 at the Earth Summit in Rio, 1992 [2], and since then a series of actions aimed at waste reduction and increasing recycling have been taken by individual governments.

However, waste management has been and is still a major problem developing countries are facing, arising from population increase, and agricultural and industrial activities. There is the need to manage the environment properly to meet environmental standards and regulations as this is vital for sustainable development and remains the central objective of the United Nation Millennium Declaration of September, 2000 [3]. The European community (EC) for example has passed its Landfill Directive since April 1999, which asked European countries to reduce biodegradable waste sent to landfill by 75% of their 1995 levels by 2006, 50% by 2009 and 35% by 2016 [4]. In this regard, Nigeria still has a long way to go when compared to the European community. Waste piles are still often seen by roadsides, rivers and other open spaces in Nigerian cities causing environmental and health problems.

Traditional waste management techniques, such as, incineration and landfill produce a low-value alternative due to their environmental impact which includes generation of greenhouse gases, such as, carbon dioxide and methane. Leachate from landfills is difficult to treat and may contaminate the water resources, this is in addition to the large space required to meet the increasing land use for landfills. There is a need to look for an alternative, such as, pyrolysis and composting. This led to the Nigerian government funding this project to look into these alternatives.

1.3 Waste Management and Treatment Technologies

The concept of waste management has led to the development of alternative waste treatment and disposal options which have minimal environmental impact, with the aim of recycling and energy recovery with low pollution. These techniques include

pyrolysis, gasification, composting and anaerobic digestion [1]. These techniques can serve two important purposes: utilize large amount of waste produced in concentrated areas and convert it into useful value-added material at a low cost. In recent times studies have been conducted to analyse the feasibility of applying these techniques to some less traditional waste, such as municipal sewage sludge and animal manure.

1.3.1 Pyrolysis

Pyrolysis is the thermal breakdown of biomass or organic waste in the absence of oxygen to produce carbonaceous char (biochar), oil (bio-oil) and combustible gases (syngas) [1]. The biochar is a high-energy-density solid (approximately 18 $MJkg^{-1}$), the bio-oil is high-energy-density liquid (approximately 17 $MJkg^{-1}$), while the syngas is a relatively low-energy-density gas (approximately 6 $MJkg^{-1}$) [5,6]. The amount of each of the products formed is dependent on the conditions of the process particularly the heating rate and the temperature. Waste materials are usually made up of complex chemical compounds. For example municipal solid waste contains paper and cardboard which are made up of large, complex polymeric, organic molecular chains namely hemicelluloses, lignin and cellulose. In the same way waste originating from the forest and other biomass are mainly composed of hemicelluloses, lignin and cellulose. Oil and gas formation during pyrolysis results from these shorter molecules present in the waste [1]. Generally, pyrolysis involves the heating of organic materials to temperatures less than 400 °C in the absence of oxygen. Organic materials thermally decompose releasing a vapour phase and a residual solid phase (biochar) at these temperatures. During the process of cooling of the pyrolysis vapour, the polar and high-molecular-weight compounds condense into liquid (bio-oil). The low-molecular-weight volatile compounds remain in the gas phase (syngas) [7]. The physics and chemistry occurring during the pyrolysis of waste biomass are very complex and depend on both the nature of material and the reactor conditions [8,9]. The exact mechanisms of thermal degradation of waste are not clear [1].

1.3.1.1 Pyrolysis Technology

The use of pyrolysis in waste management is a very recent development, though the use of pyrolysis for the production of biochar known as charcoal has been known for thousands of years. The use of traditional earthen, brick, and steel kilns typically emit volatiles to the environment during the production of biochar [1,7]. These have

poor environmental reputations as they are associated with air pollution and deforestation [10]. The designs of modern pyrolysers are such that they capture volatiles for the production of bio-oil and syngas [11]. The bio-oil produced during pyrolysis in particular has been investigated with the aim of either using the oil directly in fuel applications or after upgrading to produce refined fuels. The bio-oil derived during the pyrolysis of different varieties of waste has been shown to have complex composition. It contains a wide variety of chemicals which may be used as chemical feedstock. The bio-oil is characterised by a high energy density, which is a higher energy content per unit weight, than the raw weight. The biochar can be used directly as solid fuel or alternatively, it can be upgraded to activated carbon. The gases generated during the pyrolysis process have a medium to a high calorific value and may contain energy sufficient enough to meet the energy requirement of the pyrolysis plant [12].

The thermochemical process conditions for transforming waste biomass into renewable energy products can be altered to produce the desired biochar, bio-oil and syngas, with the heating rate and the pyrolysis temperature influencing the product distribution most. One advantage that pyrolysis has is that the gases or oil products derived from the waste during the process can be used to provide fuel for the process itself. The thermochemical technologies can be classified into four general categories namely slow pyrolysis, flash pyrolysis, gasification, and fast pyrolysis [7]. Slow pyrolysis involves heating the biomass to a temperature > 400 ºC in the absence of oxygen in a batch or continuous system. The heating rate is moderate usually in the range of about 20 °C/min to 100 °C and a maximum temperature of 600 ºC [1,7]. The approximate product yields from slow pyrolysis are 35% biochar, 30% bio-oil, and 35% syngas by mass [13]. Flash pyrolysis is carried out to maximise biochar production. It involves heating of the waste biomass under moderate to high pressure in a retort. Typical yield from flash pyrolysis are 60% biochar and 40% volatiles that is the bio-oil and syngas [7]. The design of gasification is to maximise the production of syngas. A typical gasifier is designed in such a way that it permits a small and carefully controlled amount of oxygen to enter the reaction chamber. The oxygen allowed into the reaction chamber causes partial combustion of the waste biomass which produces the heat needed to keep the reaction going. A high temperature is required for the reaction (800-1200 ºC). At this high temperature a gasifier produces very small amount

of biochar or bio-oil. The amount usually produced is 5-15% of biochar and traces of bio-oil referred to as ‘tar’ can be produced by a commercial gasifier [7]. Fast pyrolysis is carried out to maximise the production of bio-oil. The fast pyrolyzers are continuous flow systems. Product yield during fast pyrolysis are typically 50-70% bio-oil, 10-30% biochar, and 15-20% syngas by mass. Before putting the waste biomass into the fast pyrolyzer it must be dried and ground to a particle size of less than 2 mm [7]. The biomass is heated in the absence of oxygen within the pyrolyzer typically to a temperature of greater than 400 °C in less than one second using one of various technologies such as mixing biomass with pre-heated sand in a fluidized bed reactor. As a result of the rapid heating, there is a thermal decomposition of the biomass to vapour, aerosol and light gases. The volatiles must be rapidly separated from the solids and cooled to maximise the bio-oil yield. A series of condensers are typically used to accomplish these later processes [7].

1.3.1.2 Uses of Pyrolysis Products

Biochar

Biochar produced from pyrolysis is a combustible solid which can be burned to produce heat energy in most systems that are currently burning pulverised coal. It has been used for centuries as the method of producing charcoal for use as fuel and the common charcoal product yields are within the range of 30-40%. Waste material pyrolysis also gives a char product; the amount produced depends on the process conditions [1,7]. Biochar has a low sulphur content [7]; hence technology for removing SOx from emission is not required in the industrial combustion of biochar. The feedstock type is substantially responsible for the ash content of biochar. Some biomass sources contain relatively high silicon and after pyrolysis the silicon is concentrated in the biochar. Examples of such sources with high silicon content include rice husks and *Miscanthus giganteus* [7]. Scaling of the combustion chamber occurs during the combustion of high Si biochar and this decreases the usable life of those chambers. In metallurgy low-ash biochar is used as feedstock in the production of activated carbon, which has many uses, such as, an adsorbent in removal of heavy metals and organic contaminants from waste-water streams as well as to remove odour from air streams [7]. The use of biochar as a soil conditioner is an emerging application which is gaining more ground.

Biochars have been reported to show the following benefits in some soil types and certain crop species [11, 14-16]

- Increase soil pH
- Increase soil carbon levels
- Increase water holding capacity of the soil
- Increase biomass (crop) production
- Increase CEC, especially over the long-term
- Decrease emissions from soil of the greenhouse gases CO_2, N_2O and CH_4
- Improve soil conditions for microorganism population (eg bacteria)
- Reduces fertiliser requirement in soil

However, it is important to note that the benefits listed above are dependent on the feedstock materials used in the preparation of the biochar, the process conditions and applications and have led to a huge and diverse range of responses that are often contradictory. Some biochars have been seen to have adverse effects on crop productivity, while some have been shown not to have any influence on some of the factors noted above. There is need for more research to verify these effects and to differentiate beneficial from detrimental biochar. The greatest positive effects of biochar applications from studies have been in highly degraded, acidic or nutrient-depleted soils.

Syngas

The gases produced during pyrolysis (syngas) of solid waste and biomass waste are primarily a mixture of carbon monoxide and hydrogen. It also contains carbon dioxide, methane, water and lower concentrations of other low-molecular-weight volatile organic compounds (VOCs) [1,6]. The high carbon monoxide and carbon dioxide concentrations are due to the oxygenated structures present in the original materials, such as, lignin, cellulose and hemicelluloses. The gas also contains a significant proportion of uncondensed pyrolysis oil in addition to these. Syngas has a relatively low heating value (approximately 6 $MJKg^{-1}$) when compared to that of

natural gas (approximately 54 $MJKg^{-1}$). Syngas, however is burned to produce heat energy for various applications which include electricity generation and drying [7]. A potential use of syngas formed through the pyrolysis of biomass for a small and medium-scale pyrolyzer will be to produce the heat and electricity needed to sustain the pyrolyzer itself.

Bio-oil

Bio-oil produced during the pyrolysis of biomass could be used in conventional electricity generating systems, such as, gas turbines and diesel engines. However, the properties of the bio-oil fuel may not match the specification of a petroleum derived fuel and may need upgrading of the fuel or require the modification of the power plant. The heating value and the chemistry of bio-oil vary substantially depending on the nature of the feedstock and the conditions under which the pyrolysis of the feedstock was carried out. In some instances the oil product is described as a liquid. It may represent, a true oil, an oil/aqueous phase, separated oil and aqueous phase or for some waste feedstocks, a waxy material [1]. Production of oil product from waste has the advantages that the oil can be transported away from the pyrolysis process plant, thereby de-coupling the processing of the waste from the product utilization. The oil may be applied directly as a fuel, used as a chemical feedstock, upgraded using catalyst to a premium grade fuel or added to petroleum refinery stocks [1]. Bio-oil from biomass has high oxygen content, of the order of 35% by weight; due to the content of lignin, cellulose and hemicelluloses in the biomass which are large polymeric structures consisting mainly of carbon, hydrogen and oxygen. In the same way municipal solid waste derived bio-oils have high oxygen content due to the cellulosic components present in the waste, such as, paper, cardboard and wood. Bio-oils derived from flash pyrolysis of biomass and municipal solid wastes tend to have a low viscosity and consist of a single water/oil phase. The caloric value of the oil is reduced due to the high water content. Higher viscosity liquid products are produced by slow pyrolysis and tend to have two phases due to the more extensive degree of secondary reactions which occur. Bio-oils produced from the pyrolysis of tyres and plastics are composed mainly of carbon and hydrogen [1].

1.3.2 Hydrothermal Carbonization

If pyrolysis is carried out in water under pressure, it is often called hydrothermal carbonization. Such wet processes have been widely studied and are known by various names. Hydrothermal carbonization is used here because it appears to be the most accepted name for the process [17]. Other names by which the process is known include wet torrefaction, hydrothermal pre-treatment, hot compressed water, hydrous pyrolysis and coalification. Hydrothermal carbonization is a process that has been known for a long time now; but fell into relative obscurity after its initial discovery, and research activity to understand natural coal formation in the early 20^{th} century [18]. Recently, reviews of this process were published [19,20] and since then several other authors have also reviewed this topic [18,21-24].

The use of conventional or dry pyrolysis has some drawbacks, such as, using only dry feedstocks, generation of harmful gases such as CO, CH_4, C_2-hydrocarbons and PAHs (polycyclic aromatic hydrocarbons), and production of oils. The gases need to be recovered and converted into another useable form such as bioenergy, as their release into the environment is harmful and should be avoided. This requires the use of sophisticated and expensive equipment; thereby increasing the energy requirement and the cost of the process. The process of pyrolysis also requires very harsh conditions and high temperature [25-29]. Therefore it has become necessary to look for alternative methods of preparing the material, of which hydrothermal carbonization offers such an alternative.

The hydrothermal carbonization process involves the heating of biomass or other materials under pressure in water at a temperature of about 180–200 °C to form char and water-soluble organic substances [30,31]. During the hydrothermal carbonization of biomass, decomposition of the carbohydrate structure takes place via hydrolysis, an exothermic process, forming free sugar and other by-products [31,32]. It represents an environmentally friendly and a simple technique in which biomass or sugars are first converted into precondensed polymers and subsequently following further dehydration/polymerization/condensation process into carbon rich, coal-like derivatives [33]. A mechanism of transformation of carbohydrates into carbonaceous material has been investigated using characterization techniques such as, ^{13}C solid state NMR and GC-MS and it was found that the process of hydrothermal carbonization

takes place via 5-hydroxymethyl-fur-fural-1-aldehyde (HMF) as a monomer, while C-C- linkages towards the final carbonaceous material occur via this intermediate involving cycloaddition, polymerization and aldol condensation reactions, with the latter being presumably reversible under the applied conditions (Figure 1.1) [26,30,34].

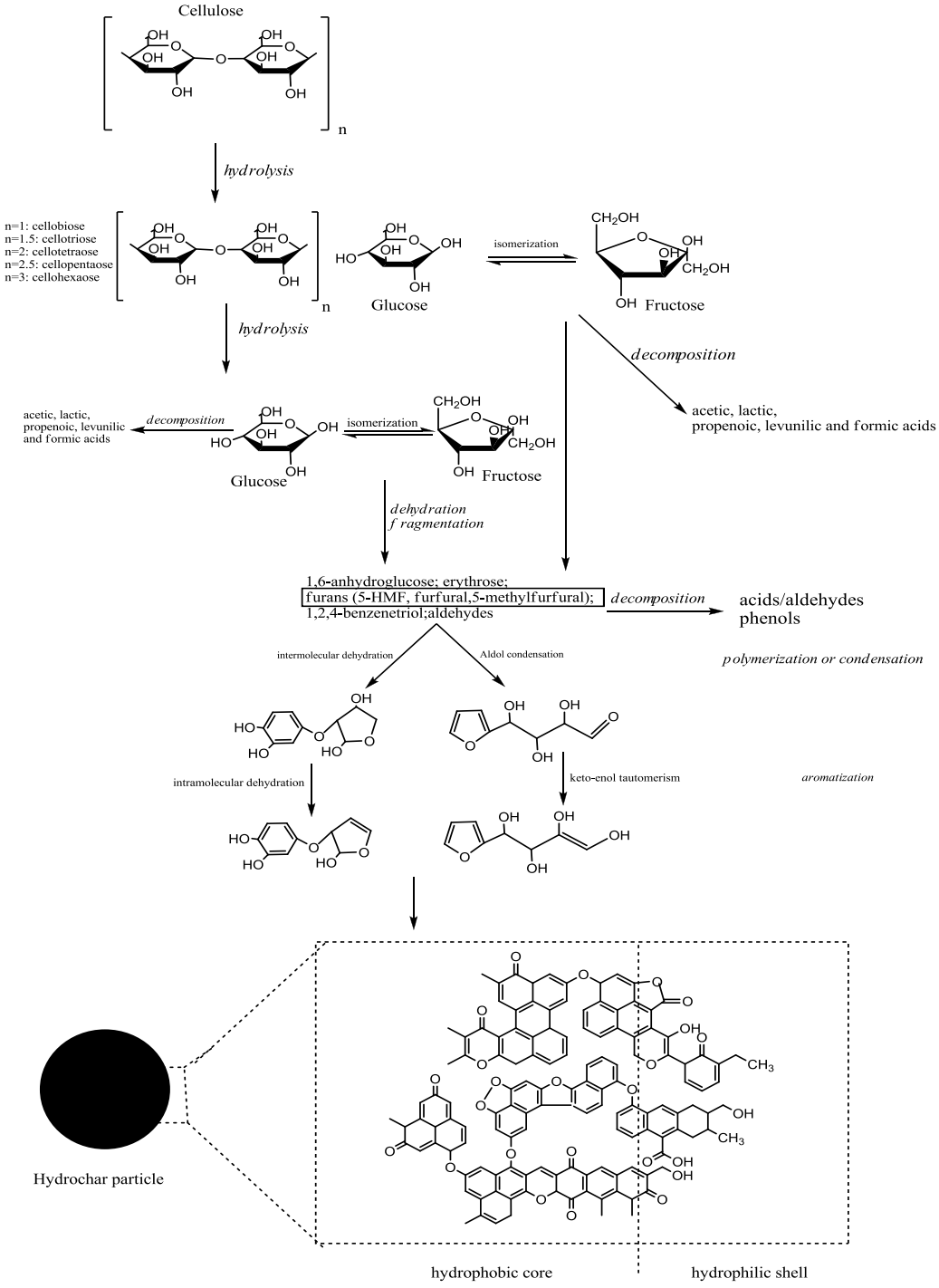

Figure 1.1: Mechanism of formation of hydrochar particles from cellulose by hydrothermal carbonization as proposed by Sevilla and Fuertes [30]. Permission for reproduction of figure has been obtained from Elsevier [License Number: 3254781425848].

The advantage of hydrothermal carbonization is that it involves mild reaction conditions of temperature and pressure, and the material does not need to be dry, thus eliminating the significant energy input required to remove water by evaporation. The hydrothermal carbonization of biomass, unlike the pyrolysis, does not produce a lot of harmful gases and the gases produced in the process are contained within the system. The hydrothermal carbonization process can convert wet feedstock into carbonaceous material at relative high yield without going through the energy-intensive drying before or during the process. It is possible for the process to accommodate a variety of non-traditional feedstocks which represent large, continuously generated, renewable residual streams that need to be managed, treated and/or processed to ensure protection to the environment. Examples are wet animal manure, sewage sludge, municipal solid waste (MSW), human waste, as well as aquaculture and algae residue [35].

1.3.3 Energy Balance of Pyrolysis and Hydrothermal Carbonization

The energy balance is an important factor in determining the feasibility of a biomass conversion process. This is usually the case when the char is used as a fuel. It is also necessary for energy requirements determination to judge the economic feasibility of using the processes for other purposes, such as, value-added products or in soil amendment [35]. Some initial results have been published for biochar obtained via pyrolysis [36,37]. However, a detailed energy use balance analysis for the hydrothermal carbonization cannot be given yet as the research on the technical development is still at the early stage. What can be discussed now is a comparison of the energy balance of pyrolysis and hydrothermal carbonization on the basis of reaction enthalpy, and followed by a qualitative comparison of the energy differences in production processes [35].

1.3.3.1 Reaction Enthalpy

Pyrolysis and hydrothermal carbonization reactions can be exothermic. The reaction parameters (temperature and time) and the nature of feedstock used determine the amount of heat released. The approximate stoichiometric equations (Equation 1.1 and 1.2) give a rough estimate of the heat of reaction for each process. The equations were deduced from experimental results in which cellulose ($C_6H_{10}O_5$) was used as a model material. Equation 1.1 is for pyrolysis adopted from Klason *et al.* [38] and Equation 1.2 is for hydrothermal carbonization adopted from Bergius and Specht [39].

	Pyrolysis (Equation 1)	**Hydrothermal carbonization (Equation 2)**
Temperature range (°C)	300-500	180-250
Higher heating value of feed (MJ/kg)	-17.6	-17.6
Heat of reaction (MJ/kg cellulose)	-0.8	-1.6
Higher heating value of solid product (MJ/kg cellulose)	-11.3	-16.0
Higher heating value of liquid by-product (MJ/kg cellulose)	-5.1	0
Higher heating value of gaseous by-product (MJ/kg cellulose)	-0.4	0

Table 1.1: Comparison of the calorific nature of slow pyrolysis and hydrothermal carbonization of cellulose [35]

Table 1.1 summarizes the higher heating values as obtained from Equation 1.1 and 1.2

$$C_6H_{10}O_5 \rightarrow C_{3.75}H_{2.25}O_{0.5} + 0.5CO_2 + 0.25CO + 2.88H_2O + C_{1.5}H_2O_{0.3} \quad \text{(Equation 1.1)}$$

$$C_6H_{10}O_5 \rightarrow C_{5.25}H_4O_{0.5} + 0.75CO_2 + 3H_2O \quad \text{(Equation 1.2)}$$

Since the chemistry of neither the pyrolysis nor hydrothermal carbonization is fully understood, these approximations should be treated with care [35]. It is important to note that liquid organic reaction by-products that represent an important fraction were not considered by Equation 1.2. Also, biomass, because of its high degree of chemical complexity and heterogeneity, cannot be regarded as a well-defined reactant. These theoretical estimations were supported by results of experimental calorimetric measurements with cellulose. Mok *et al.* [40] reported values between 0.4-0.7 $MJ/kg_{cellulose}$ for the slow pyrolysis of cellulose, while unpublished data reported by Libra *et al.* [35] for a similar measurement for hydrothermal carbonization produced approximately 1 $MJ/kg_{cellulose}$ values. Therefore, the calorific values of pyrolysis and hydrothermal carbonization reactions are comparable to each other.

It is important to note that the reaction mechanisms involved in the processes are complex and are highly dependent on the conditions of the reactions. For instance, despite the overall reaction being exothermic, the initial phases of both pyrolysis and

hydrothermal carbonization are endothermic. As a result of this, mild pyrolysis and hydrothermal carbonization is endothermic, because of the endothermic nature of cellulose hydrolysis [35].

1.3.3.2 Process Comparison

Some guidance in the choice between pyrolysis and hydrothermal carbonization can be obtained through the theoretical energetic considerations. From the point of view of thermodynamics, at certain water content the use of pyrolysis becomes uneconomical. There exists a threshold at which hydrothermal carbonization becomes more energetically efficient than the pyrolysis process. Theoretical comparison of wood combustion with and without hydrothermal carbonization as a pre-treatment process has been used for the illustration. Erlach *et al.* [41] reported that pre-treatment with hydrothermal carbonization is more efficient for feedstocks having a water content of more than 50%, while a comparison of the amount of heat required for the evaporation of water to the heat of cellulose pyrolysis reaction (Equation 1.1) showed that when the water content is above 30%, the energy required to evaporate the water is more than that supplied by the heat released during pyrolysis [35]. In some process designs, the feedstock is preheated by the product gas [38]. A process in which such a design is used is capable of converting cellulose with up to 70% water content without an external energy supply, but pyrolyzing cellulose with a higher water content will result in part of the char being burnt which reduces the yield. For example at approximately 90% water content all the char would need to be burnt [35]. This value will be lower for biomass because less energy is released during carbonization.

In the case of hydrothermal carbonization, the feedstock does not need to be dried therefore heat for water evaporation is avoided. However, the water has to be heated, but the amount of external heat required is accepted to be substantially lower than that of drying in pyrolysis. Also, other aspects that require energy, such as, transportation of energy of water-rich feedstocks and post-processing of the hydrochar e.g. dewatering need to be considered as well. An advantage of the hydrothermal process in terms of energy can be expected if the product can be utilized without predrying, or when their dewaterability of the hydrochar compared with that of the drying of feedstock in pyrolysis is improved [35].

1.3.4 Composting

Composting is the science of degradation of organic waste into a useful product by the action of micro-organisms. It is an aerobic process, rather than anaerobic. The process of composting occurs in nature at various levels, on a small scale at the household level and on the large scale via composting schemes where organic waste from different collection points are composted at large central facilities. It is a relatively fast degradation process reaching a stabilized product within 4-6 weeks. Several modifications have been made to this natural process with a careful monitoring of the process to attain the goal of having high quality end products. Composting is associated with reclamation and recycling a way of saving and reusing natural resources, where the degraded product is a stabilized product which is added to soil to improve soil structure, especially for clay soils, or where it can act as a fertilizer improving the nutrient content, or as a mulch to retain moisture in the soil [42]. The process of composting helps to remove a large fraction of organic biodegradable waste from a waste stream and in this way helps compliance with environmental standards. Food, garden waste, paper and board, wood and some textiles constitute the biodegradable part of municipal solid waste and therefore have the capacity to be composted [1]. There are other major sources of organic waste suitable for composting apart from organic waste from domestic sources and park and garden waste deposited at civic amenity sites and these include agricultural waste, sewage sludge, food waste and forestry waste [43]. In terms of management of biodegradable waste, a large scale centralised composting facility is viewed as an alternative to incineration and waste landfill.

As stated earlier, the process of composting is aerobic; therefore it relies on a plentiful supply of oxygen. There is a need for a regular aeration to maintain the aerobic conditions. Three stages usually characterize the composting process. The first stage which is usually characterized by an increase in temperature, and a high rate of microbial activity. During this stage, simple carbohydrates and proteins are readily biologically degraded by mesophilic micro-organisms, followed by thermotolerant and thermophilic micro-organisms as the temperature rises above 45 °C [44]. The second stage is the stabilisation stage and it involves the biodegradation of the waste by thermophilic micro-organisms, the process is exothermic, therefore the temperature in the compost pile can reach up to 70 °C [45]. This is the active phase of composting.

Thermal destruction of weed seeds and pathogenic micro-organisms occur at the high temperature stage. The third stage is the maturation stage and this stage is characterized by lower temperatures and the presence of humic substances. The maturation stage takes several weeks to reach completion and it involves further biodegradation of intermediate compounds. After maturity, sieving and grading to remove un-composted materials and contaminants, such as, glass, plastics and metals are carried out.

1.3.4.1 Biological Processes Taking Place in Composting

During the composting process metabolism and mineralization of simple carbon compounds, such as soluble sugars and organic acids takes place by heterotrophic and heterogeneous micro-organisms. The exothermic process taking place and the high metabolic activity produces an increased temperature in the compost heap which cannot be dissipated because of the low thermal conductivity and consequently the temperature rises. The rise in temperature kills pathogenic micro-organisms and allows only thermophilic micro-organism to be active. Fungi and actinomycetes degrade cellulose, lignin, starch and pectin. The activity of the fungi and actinomycetes micro-organisms increases with decrease in temperature and also moisture and pH. Intense decomposition of cellulose occurs throughout the process, but particularly during the final stages, mostly through degradation by a eumycete micro-organism. The basidiomycete group of fungi are responsible for the degradation of lignin [1]. During the process nitrogen content also decreases through the formation of ammonia and volatilization. An overall decrease in C:N ratio results from the loss of carbon dioxide and water from the carbon- and hydrogen-containing constituents of the waste, representing a relative increase in nitrogen overall to carbon. In addition, nitrogen fixation from micro-organisms slightly increases the nitrogen content later [1].

1.3.4.2 Factors Influencing Composting

For the composting process to progress smoothly and to obtain good quality compost as the end product, the following factors are necessary. Natural decomposition progresses faster and yields a quality product under controlled conditions. The rate of composting, just like the rate of animal or plant growth, can be affected by many factors. In addition, organic substances to be used for composting should be free of any kind of contaminant or toxic compounds, such as, surfactants, detergents, phenolics,

and pharmaceuticals, which either directly or through their metabolism is capable of posing health risks. The following factors were identified by Williams [1]:

Oxygen Content: For the aerobic condition to be maintained, a minimum oxygen content of 18% is recommended in the compost.

Temperature: A temperature in the range of 30-35 °C is necessary to give maximum micro-organism activity.

Moisture Content: High moisture content should be avoided, since this produces anaerobic conditions by occupying intraparticle spaces. Biodegradation is significantly reduced at moisture content below 40%.

pH: Fungi develop better in acidic conditions. Bacteria prefer a pH that is near neutral. A pH in the range of 5.5-8 is necessary for optimal composting to be achieved.

C:N Ratio: Slow decomposition results from higher values of C:N ratio while lower ratios result in nitrogen loss. The optimal ratio in the starting waste material should be about 25.

Size Range of Waste Material: The surface area of the waste material increases with the shredding of the starting material and results in enhanced rates of composting.

1.3.4.3 Composting Technology

As mentioned previously, the composting process is an aerobic biodegradation process and therefore aeration of the waste is required. Several methods are available for the aeration to be achieved. The cost increases as the process increases in sophistication and control. The aeration processes include ‘windrow’ system, aerated static piles, in-vessel systems and vermicomposting.

The ‘Windrow’ System: In this system the biodegradable waste is being piled into an elongated conical heap or windrow, which is about 50 m in length, 3-4 m in width and 2 m high. Mechanical turning is used to turn the waste periodically. The process begins with the turning rate of one turn per day at the initial stage of the composting to one turn per five days towards the end of the process. The purpose of the turning is to release trapped heat, moisture and stale air and introduce fresh air. The windrows are usually placed on a gravel bed to help in the collection of any leachate formed during

the process. They are usually arranged in rows to allow mechanical vehicles to move up and down each row turning the waste, hence fully aerating the pile periodically [1].

This method has several advantages over other methods which include simple management, low cost, and in some cases the windrows can be constructed near the fields where the composted material may be applied later. It is also possible to use standard farming equipment to shred and turn the material. However, windrow composting when compared with other composting technologies is laborious and are subject to exposure from the weather.

Aerated Static Pile or Forced Aeration Systems: In this system a fan is used to blow or suck air through the pile of the composting waste. The compost pile remains undisturbed and is located on an aeration block. Here, finished compost acts as a filter for even distribution of air via a perforated pipe covered with a porous based material. The filter and perforated pipe allows the compost pile for composting to be constructed over it. Height of 2-3 m, 2-6 m width and 30 m length are typical dimensions of a forced aeration system. The passage of the air through the pile is carried out either continuously or periodically. The odours from the compost are contained in the system if the air is drawn through the pile, this also allows for treatment and control if required. Heat is transferred from the inner pile to outer region, when air is blown up through the compost pile [1]. Once the pile is formed, no turning or agitation will be required as long as the air supply is sufficient and distributed uniformly, the active composting may be complete in approximately 3-5 weeks.

This method is a more concentrated method of composting as it allows for higher and broader piles requiring less land area than the windrows. This makes it easier for the system to be covered with a roof or enclosed within a building. Forced aeration can shorten the composting period, since it allows for closer process control. Variations in temperature are reduced in the larger pile size as a result of the homogenous aeration. It also improves conditions for destroying pathogens. Lack of turning and insulation layer conserves nitrogen, limiting release of odours. In the suction aerated systems the odours can be collected and treated. The main disadvantages associated with this process are the potential for short circuiting by channelling of the airflow and clogging of the aeration pipes resulting in an uneven compost product.

In-vessel Systems: In this system closer control of temperature, moisture, aeration and waste mixing rates are allowed [46]. These include containers, such as, enclosed halls, silos or towers, tunnels, rotating drums or reactor tank systems [44]. In silos or tower systems biodegradable waste is fed to the top of the silo and composting takes place as the waste moves down the tower. It is a vertical unit operating on a continuous basis. After several days duration the compost is collected at the bottom of the tower, this is followed by a maturation stage. Large floor area where composting takes place inside a purpose-built composting building is required in composting in enclosed hall. Some form of mechanical agitation may be involved in tunnel composting systems which are large systems which may be either batch or continuous. In rotating drum systems the waste is being placed in a long rotating drum having typically dimension of 3-4 m in diameter and 50 m long. It is also combined with forced aeration [44]. While the waste is continuously stirred and tumbled, the air continuously passes through the rotating drum. Several days in the drum is the typical residence times and the composting process would require a subsequent maturation stage to reach completion. A more sophisticated composting system is the composting tank reactor. Here, a series of augers which are perforated are used to stir the waste, which allows air to be blown into the composting waste pile [1].

The advantages of this method are minimal weather problems, reduced labour requirements, better control of odour, faster composting, closer process control, reduction in land area requirements and consistent quality composted organic material. In-vessel composting however, does not guarantee the realization of these advantages. Many problems may arise which require expensive solutions. The disadvantage of the in-vessel technology is the high capital cost. The maintenance and operation of these systems requires a lot of expense and a higher level of knowledge and skill when compared to the other technologies.

Vermicomposting: This involves using selected species of earthworm, such as, brandling worms (*Eisenia foetida*) and redworms or red wigglers (*Lumbricus rubellus*) to carry out composting of biodegradable waste. The temperature of the process is normally kept below 35 °C and the process takes place in long troughs. The earthworms are relied on to mix, aerate and fragment the waste, combined with the biodegradable process of the micro-organisms in vermicomposting process [1].

The advantage of this method is that it does not require the use of heavy and expensive equipment as used in the other technologies. The earthworm in this technology carries out the roles of turning and maintaining the material in an aerobic condition reducing the need for expensive equipment. The product from vermicomposting is homogenous, has the desirable qualities and may have reduced levels of contaminants. The major drawback in this technology is the temperature requirement which must be maintained below 35 °C for the survival of the earthworm. This temperature is low when compared with other thermophilic technologies where the thermophilic bacteria can raise the temperature of the material to above 70 °C. The temperature of the vermicomposting is lower than the acceptable level to kill pathogens. Hence, the product fails the EPA rules for pathogen reduction [47].

1.3.4.4 Drawbacks of the Composting Process

The composting process is a biodegradable process and as a result leads not only to formation of compost, but also to the formation of other products in which product treatment and control may be required. If the moisture content is high it may result in the formation of leachate, which may have composition and properties similar to the leachate formed during the early stages of landfill. The leachate is usually collected via channels and depending on the level formed is either treated on site or discharged to the sewer. Volatile organic compounds (VOCs) are usually the constituents of gaseous emission from the composting process. The emissions are potentially toxic and characterized by malodour [1]. Micro-organisms, such as, bacteria, fungi spores and actinomycetes also constitute part of airborne emissions resulting from the composting process [44,48].

1.4 Conclusion

Management of waste materials is very critical considering the impact waste materials have on the quality of life and the environment. Globally, billons of tonnes of waste materials are generated annually from human and non human activities, there is an urgent need for these waste materials to be removed from the environment and converted into a form that will be beneficial to humans and the environment rather than being a nuisance. Traditional waste management techniques, such as, incineration and landfill which have been used in the past have environmental impacts, such as, generation of greenhouse gases, carbon dioxide and methane, and also pollution of

water bodies arising from run-offs from landfills. Alternative waste treatment and disposal techniques such as pyrolysis and composting have minimal environmental impact, and have been on the increase in recent times. The products from these processes have been utilized in pollution reduction and have also served as source of energy. Considering the advantages the pyrolysis and composting techniques have over the traditional method of waste management, the potentials of these techniques should be explored further and new waste materials should be investigated.

1.5 References

[1] Williams, PT. Waste Treatment and Disposal. 2nd Edition, John Wiley & Sons, Chichester, England, 2005.

[2] European Commission, Agenda 21, The First Five years, 1997.

[3] http://www.un.org/millennium/declaration/ares552e.htm. Accessed June 19, 2013.

[4] Landfill of Waste: Council Directive 1999/31/EC.

[5] Bridgwater, AV, Meier, D, Radlein, D. An Overview of Fast Pyrolysis of Biomass. Organic Geochem 1999; 30: 1479-1493.

[6] Ioannidou, O, Zabaniotou, A, Antonakou, EV, Papazisi, KM, Lappas, AA, Athanassiou, C. Investigating the Potential for Energy, Fuel, Materials and Chemicals Production from Corn Residues (Cob and Stalks) by Non-Catalytic and Catalytic Pyrolysis In Two Reactor Configurations. Renew Sustain Energy Rev 2009; 13: 750-762.

[7] Laird, DA, Brown, RC, Amonette, JE, Lehmann, J. Review of Pyrolysis Platform for Coproducing Bio-oil and Biochar. Biofuels Bioprod Bioref 2009; 3: 547-562.

[8] Di Blasi, C. Modeling Chemical and Physical Process of Wood and Biomass Pyrolysis. Prog Energ Combust Sci 2008; 34: 47-90.

[9] Babu, BV. Biomass Pyrolysis: A State of Art Review. Biofuels Bioprod Bioref 2008; 2: 393-414.

[10] Namaalwa, J, Sankhayan, PL, Hofstad, OA. Dynamic Bio-Economic Model for Analyzing Deforestation and Degradation: An Application to Woodland in Uganda. Forest Policy Econ 2007; 9: 479-495.

[11] Brown, R. Biochar Production Technology: In Biochar for Environmental Management, ed by Lehmann, J, Joseph, S. Earthscan, London, England, 2009.

[12] Bridgwater, AV, Grassi, G. Biomass Pyrolysis Liquid, Upgrading and Utilization. Elsevier Applied Science, London, England, 1991.

[13] Goyal, HB, Seal, D, Saxena, RC. Bio-fuels from Thermochemical Conversion of Renewable Resources: A Review. Renew Sustain Energy Rev 2008; 12: 504-517.

[14] Xu, G, Lv, Y, Sun, J, Shao, H, Wei, L. Recent Advances in Biochar Applications in Agricultural Soils: Benefits and Environmental Implications. Clean-Soil Air Water 2012; 40: 1093-1098.

[15] Rondon, MA, Molina, D, Hurtado, M, Ramirez, J, Lehmann, J, Major, J, *et al*. Enhancing the Productivity of Crops and Grasses while Reducing Greenhouse Gas Emissions through Bio-Char Amendments to Unfertile Tropical soils. Proceeding of the 18th World Congress of Soil Science; Pennsylvania, USA, 2006.

[16] Lehmann, J. A Handful of Carbon. Nature 2007; 447: 143-144.

[17] Hoekman, SK, Broch, A, Robbins, C. Hydrothermal Carbonization (HTC) of Lignocellulosic Biomass. Energy Fuels 2011; 25: 1802-1810.

[18] Funke, A, Ziegler F. Hydrothermal Carbonization of Biomass: A Summary of Discussion of Chemical Mechanisms for Process Engineering. Biofuel Bioprod Bioref 2010; 4: 160-177

[19] van Krevelen, DW. Coal: Typology, Physics, Chemistry and Constitution. 3rd Edition, Elsevier, Amsterdam, Netherlands, 1993.

[20] Bobleter, O. Hydrothermal Degradation of Polymers Derived from Plants. Prog Polym Sci 1994; 19: 797-841.

[21] Funke, A, Ziegler F. Hydrothermal Carbonization of Biomass: A Literature Survey Focusing on its Technical Application and Prospects. Proceedings of the 17th European Biomass Conference; Hamburg, Germany, 2009.

[22] Peterson, AA, Vogel, F, Lachance, RP, Froeling, M, Antal, MJ. Thermochemical Biofuel Production in Hydrothermal Media: A Review of Sub- and Supercritical Water Technologies. Energy Environ Sci 2008; 1: 32-65.

[23] Yu, Y, Lou, X, Wu, H. Some Recent Advances in Hydrolysis of Biomass in Hot-Compressed Water and Its Comparisons with Other Hydrolysis Methods. Energy Fuels 2008; 22: 46-60.

[24] Titirici, M, Antonietti, M. Chemistry and Material Options of Sustainable Carbon Materials Made Under Hydrothermal Carbonization. Chem Soc Rev 2010; 39: 103-116.

[25] Titirici, MM, Demir-Cakan, R, Baccile, N, Antonietti, M. Carboxylate-Rich Carbonaceous Materials via One-Step Hydrothermal Carbonization of Glucose in the Presence of Acrylic Acid. Chem Mater 2009; 21: 484-490.

[26] Sevilla, M, Fuertes, AB. Chemical and Structural Properties of Carbonaceous Products Obtained by Hydrothermal Carbonization of Saccharides. Chem-Eur J 2009; 15: 4195-4203.

[27] Beaumontt, O, Schwob, Y. Influence of Physical and Chemical Parameters on Wood Pyrolysis. Ind Eng Chem Process Des Dev 1984; 23: 637-641.

[28] Di Blasi, C, Signorelli, G, Di Russo, C, Rea, G. Product Distribution from Pyrolysis of Wood and Agricultural Residues. Ind Eng Chem Res 1999; 38: 2216-2224.

[29] Sevilla, M, Macia-Agullo, JA, Fuertes AB. Hydrothermal Carbon of Biomass as a Route for the Sequestration of CO_2: Chemical and Structural Properties of the Carbonized Products. Biomass Bioenerg 2011; 35: 3152-3159.

[30] Sevilla, M, Fuertes, AB. The Production of Carbon Materials by Hydrothermal Carbonization of Cellulose. Carbon 2009; 47: 2281-2289.

[31] Heilmann, SM, Davis, HT, Jader, LR, Lefebvre, PA, Sadowsky, MJ, Schendel, FJ, *et al*. Hydrothermal Carbonization of Microalgae. Biomass Bioenerg 2010; 34: 875-882.

[32] Guiotoku, M, Rambo, CR, Hansel, FA, Magalhaes, WLE, Hotza, D. Microwave-assisted Hydrothermal Carbonization of Lignocellulosic Materials. Mater Lett 2009; 63: 2707-2709.

[33] Titirici, MM, Antonietti, M, Baccile, N. Hydrothermal Carbon from Biomass: A Comparison of the Local Structure from Poly- to Monosaccharides and Pentoses/Hexoses. Green Chem 2008; 10: 1204-1212.

[34] Antonietti, M, Titirici MM. Coal from Carbohydrates: The "Chimie Douce" of Carbon. CR Chim 2010; 13: 167-173.

[35] Libra, JA, Ro, KS, Kammann, C, Funke, A, Berge, ND, Neubauer, Y, *et al*. Hydrothermal Carbonization of Biomass Residuals: A Comparative Review of the Chemistry, Processes and Applications of Wet and Dry Pyrolysis. Biofuels 2011; 2: 89-124.

[36] Gaunt, JL, Lehmann, J. Energy Balance and Emissions Associated with Biochar Sequestration and Pyrolysis Bioenergy Production. Environ Sci Technol 2008; 42: 4152-4158.

[37] Roberts, KG, Gloy, BA, Joseph, S, Scott, NR, Lehmann, J. Life Cycle Assessment of Biochar Systems: Estimating the Energetic, Economic and Climate Change Potential. Environ Sci Technol 2010; 44: 827-833.

[38] Klason, P, von Heidenstam, G, Norlin E. Untersuchungen zur Holzverkohlung. Angew Chem Int Ed 1909; 25: 1205-1214.

[39] Bergius, F, Specht, H. Die Anwendung hoher Drucke bei chemischen Vorgangen und eine Nachbildung des Entstehungsprozesses der Steinkohle. Wilhelm Knapp Halle ad Saale 1913; 41-58.

[40] Mok, WSL, Antal, MJ, Szabo, P, Varhegyi, G, Zelei, B. Formation of Charcoal from Biomass in a Sealed Reactor. Ind Eng Chem Res 1992; 31: 1162-1166.

[41] Erlach, B, Tsatsaronis, G. Upgrading of Biomass by Hydrothermal Carbonization: Analysis of an Industrial-Scale Plant Design. Presented at: The 23rd International Conference on Efficiency, Cost, Optimization, Simulation and Environmental Impact of Energy System; Lausanne, Switzerland, 2010.

[42] Mclanaghan, SRB. Delivering the Landfill Directive: The Role of New and Emerging Technologies. Associate in Industrial Ecology, Penrith, England, 2002.

[43] Border, D. Taking a Green Product to Market. Waste Age 1995; 24: 12-15.

[44] Swan, JRM, Crook, B, Gilbert, EJ. Microbial Emissions from Composting Sites. In Issues in Environmental Science: Environmental and Health Impact of Solid Waste Management Activities, ed by Hester, RE, Harrison, RM. RSC Press, Cambridge, England, 2002.

[45] Warmer Bulletin 29. Compost, Warmer Fact Sheet. The World Resource Foundation, Tonbridge, Kent, England, 1991.

[46] Diaz, LF, Savage, GM, Eggerth, LL, Golueke, CG. Composting and Recycling of Municipal Solid Waste. Lewis Publishers, Boca Raton, USA, 1993.

[47] Ndegwa, PM, Thompson, SA. Integrating Composting and Vermicomposting in the Treatment and Bioconversion of Biosolids. Bioresource Technol 2001; 76: 107-112.

[48] Newport, HA, Bardos, RP, Hensler, K, Gosss, E, Willet, S, King, L. Municipal Waste Composting, Report No. CWM/074/93. DoE, HMSO, London, England, 1993.

Chapter 2

Pollutants in the Environment

2.1 Introduction

A pollutant is defined by the United State Environmental Protection Agency (USEPA) as any substance introduced into the environment that has the capacity to adversely affect the usefulness of a resource [1]. It can also be defined as any chemical that can cause harm to the environment [2]. Introduction of pollutants into the environment can be through point source (single source, usually through industrial activities) or through non-point source (non-specific source, usually through agricultural activities). In general, pollutant introduction is significantly through the form of waste, sewage, by-product of a manufacturing process, accidental discharge, agriculture, or by other human activities [3]. These pollutants can easily enter the human body via food, water, air or absorption through skin contact in agriculture, industrial or residential settings [4]. Damage to the central nervous system, lungs, kidneys, liver, blood compositions and other organs, as well as, lower energy levels may result from such pollutants at high exposure levels, and in extreme cases, may result in, insanity, paralysis, coma and even death may follow within weeks of the onset of symptoms [5,6]. The following summaries the damage caused to the environment by pollutants [3].

- Human health damage arising from specific chemical substances present in air, water and food.
- Damage to the natural environment which subsequently affect soil, water, vegetation, crops and animals.
- Damage caused by smoke, dust, chemical fumes, noise, refuse dumps that affect the beauty of the environment.
- Long-term damage which may not be noticed immediately, for example low-level absorption of carcinogenic substances into the body.

There has been increasing global concern, over the last three decades about the public health impacts of environmental pollution, particularly, the global burden of disease. It has been estimated by The World Health Organization (WHO) that a quarter of the diseases facing mankind today arise from prolonged exposure to environmental

pollutants. However, most of these environment-related diseases are not detected easily and may have been acquired during childhood and manifested later in adulthood [7].

2.2 Types of Pollutants in the Environment

Pollution of the environment could be by heavy metals, organic pollutants or both. Heavy metal pollution occurs through natural and anthropogenic sources. Mineral weathering, erosion and volcanic activity are the most significant natural sources, while anthropogenic sources include industrial and agriculture activities, such as, mining and mineral processing, battery manufacturing, electroplating, smelting, application of fertilizers and pesticides, and also through waste dumping [8-13]. Organic pollutants on the other hand are released into the environment through sources, such as, burning of fossil fuels, incineration of waste, petrochemical production and automobile exhaust processes. Various industrial activities and technological development have also led to the discharge of these pollutants, such as, insecticides, fungicides, herbicides, butadiene, and dyes posing a significant threat to environment and public health [14,15]. Safe and effective disposal of waste from various industries processes is always a challenge for industries and environmentalists, as any unsuitable disposal may affect the environment adversely because of their accumulation in the food chain, toxicity and persistent nature [14].

2.2.1 Heavy Metals

Some metals are referred to as heavy metals because of their toxicity and high densities. For example, Cd = 8.64 g cm^{-3}, and Pb = 11.3 g cm^{-3}, in comparison with other common metals such as Mg with density of 1.7 g cm^{-3}. Elemental toxicity depends on the element's chemistry and concentration as well as the mode of contact and biochemistry of the host organism. Ironically, some metals which are toxic at high concentrations may be essential to life at low concentration. Heavy metals are of concern in the environment because of their toxicity to humans and other animals, and their non-biodegradable nature. Heavy metals occur naturally, but their concentrations in natural waters can be increased by anthropogenic activities [16]. Heavy metals such as lead and cadmium and their compounds are characterised by very low volatility and

it is assumed that these metals are transported in the atmosphere only in the composition of aerosol particles [17].

Cadmium

Cadmium is a toxic and non-essential element which is released into the environment through natural (geogenic) and anthropogenic (industrial and agricultural) activities [18-21]. Cadmium is similar to zinc chemically, and both metals frequently undergo geochemical processes together. Both metals have +2 oxidation states in water. Acute cadmium poisoning in humans has resulted in kidney damage, high blood pressure, damage to testicular tissue and destruction of red blood cells [22]. Its chemical similarity to zinc is responsible for most of the physiological action of cadmium. In some enzymes cadmium may replace zinc, thereby altering the stereostructure of the enzyme and impairing its catalytic activity, causing disease symptoms [22]. The cadmium concentration in drinking water should be very low. The permissible concentration of cadmium in drinking water is 0.003 mg/L according to the World Health Organisation (WHO) guidelines [23]. The natural and anthropogenic activities through which cadmium enters the environment include weathering of parent rock, volcanic eruption, mining, metal plating, waste disposal, sewage sludge disposal, composts, or fertilizers application and have led to its accumulation and leaching to water bodies under certain soil and environmental conditions. This eventually results in an increase in its concentration in food crops [24-26]. The concern about cadmium is its accumulation in the environment and entry into the food chain.

Lead

Lead exists naturally in the Earth's crust, and is usually found in soils, plants, and water at trace levels with lead bearing limestone and galena (PbS) contributing lead to natural water in some locations in addition to other pollutant sources [22,27]. The occurrence of metallic lead in nature is rare; however, occurrence of lead ores is widespread, which has made it the most widely scattered toxic metal in the world due to man's actions [27]. Lead pollution arises from a number of sources; industrial, waste incineration, coal burning and mining processes and also formerly from leaded gasoline. Lead occurs in water in the +2 oxidation state and is a toxic heavy metal which can enter the human body via inhalation and ingestion from different sources,

such as, contaminated air, water, soil, and food [27]. In adults, acute lead poisoning has caused dysfunction in the kidneys, liver, peripheral and central nervous systems, reproductive system, blood pressure and also resulted in sickness or death, while mild lead poisoning causes anaemia [22,28]. The susceptibility to lead is more in children than in adults, with the exposure causing effects which are irreversible on the cognitive performance during childhood [29]. Recently, the focus on lead poisoning has been on the larger population of asymptomatic children with lesser exposures than adults exposed to high doses in industrial settings [28]. Environmental pollution due to lead became a cause of major concern in the 1970s, and led to the ban on the use of lead additives in gasoline in the western world. Body burdens of this toxic metal have been on the decrease in recent decades as evidenced from hair samples and blood [30], largely the result of the reduction in lead used in plumbing, paint and other products that come in contact with food or drink [22]. Lead is not a major problem in drinking water except in isolated cases and the lead concentration in drinking water should also be very low, with the permissible concentration of 0.01 mg/L according to the World Health Organisation (WHO) guidelines [22,23].

2.2.2 Organic Pollutants

Organic pollutants in the environment are compounds which are made up of a carbon skeleton and are usually associated with atoms of oxygen, hydrogen, nitrogen, sulphur and phosphorous. These atoms could be an integral part of the molecule, or alternatively could be present in the functional groups. The functional groups present in the molecule are responsible for certain properties of the molecule. For example, the presence of carboxyl (-COOH) and hydroxyl (-OH) functional groups in a molecule increase its polarity, making it more water soluble [16]. The –COOH is also capable of making the molecule acidic as a result of dissociation of H^+. The various structural forms in which an organic molecule exists, for example saturated and unsaturated chains and rings has resulted in a diverse range of organic contaminants [16]. Organic pollutants in the environment can originate from natural and anthropogenic sources.

Organic pollutants present in the soil environment can interact or move into the mineral fractions and organic matter, as well as the atmosphere and water. In the long run, however, the organic pollutants will either dissipate or persist. Compounds which

persist are those with low volatility, low solubility or those that have molecular structures that resist degradation (e.g. polycyclic aromatic hydrocarbons). On the other hand, highly volatile, highly soluble or easily degraded compounds (e.g. aldehydes, alcohols and ketones) will be destroyed or lost to the environment [16]. The vapour pressure of a compound controls its volatility, while the polarity governs its solubility and this depends upon molecular structure, molecular weight and functional groups. Degradation is a subject of both biological and abiological processes, although with large quantity of microorganisms in soil the potential for biodegradation is high. Abiological degradation process takes place through oxidation, reduction, hydrolysis and photo-oxidation [16].

In the soil, organic pollutants interact mainly with either the mineral or organic component of soils through two possible routes, namely, (a) adsorption, which is a surface phenomenon, and (b) entrapment within the soil mineral or components [16]. The properties of the molecule, that is, its aqueous solubility, vapour pressure; concentration and hydrophobicity as well as the properties of the soil determine the nature and the extent of the interaction. Soil factors include the type and amount of soil organic matter, clay content and mineralogy, pore size and pore structure and the microorganism present. The end result of the two processes of adsorption and entrapment is the decrease in both the biological and chemical availability of soil-associated contaminants with time. As a result, the proportion of the compound in the available fraction decreases with time, while the proportion of compound in the non available fraction increases with time. The process which is called ‘ageing’ could cause a decrease in the rate and extent of degradation an organic pollutant suffers in the soil environment [16]. Organic pollutants attached to soil particles exist in four fractions which can be differentiated by the ease with which they can be released or desorbed from the particles. These include (a) a rapidly desorbed fraction (b) a slowly desorbed fraction (c) a very slowly desorbed fraction (d) non-extractable (bound) residues. The non-extractable residue refers to the fraction of an organic compound (or its metabolites) that persists in the matrix following an extraction process that has not changed either the compound or matrix substantially. Bound residues usually represent an extreme end-member of ageing. The size of each of these fractions is dependent on the length of contact time between the soil and the pollutants. [16].

Polycyclic Aromatic Hydrocarbon (PAHs)

Polycyclic aromatic hydrocarbons (PAHs) are chemicals that are composed of two or more fused aromatic rings which can occur naturally (from volcanic activity and forest fires) in the environment and can also originate from anthropogenic activities, such as, incomplete combustion of coal, oil spillage, gasoline, and garbage [31]. Many PAHs are highly carcinogenic, even at relatively low concentrations, mutagenic and are toxic to aquatic life. PAHs are of concern in the environment because they are toxic, bioaccumulate and persistent in the environment for a long time, with persistence increasing with increase in the molecular weight [32]. They vary in behaviour, some vapourise easily in air, while others do not break down easily in water. Solubility in water decreases with increase in molecular weight [33]. PAHs are used in the production of dyes, plastics and pesticides. Although, PAHs are major air pollutant, soil acts as the ultimate depository for them. They enter the human body through different routes, such as, breathing of contaminated air, skin contact with contaminated soil or products like coal tar and heavy oil. Once in the body, PAHs can spread and target fat tissues and organs like kidney and liver [32].

2.3 General Concerns about Pollutants in the Environment

Concern about environmental pollution has been on the increase globally over the years, due to the exponential growth in human population and the changes in productivity and consumption habits, increase in affluent lifestyles and use of resources, increase in number of industries and continuing development in technologies. These have led to rapid generation of municipal and industrial solid wastes, which in turn has resulted in the pollution of the air, water and soil [34]. In Nigeria, there has been a dramatic increase in lead, cadmium and PAHs emissions into the environment in recent times, mostly from anthropogenic activities, such as, industrial activities, oil spillage, vehicular exhaust, and bush burning. Although the government is still working to have a proper document on the level of the pollution, they are already putting adequate measures in place in order to minimize the risk of the adverse health effects of such exposure, which this project set out to address.

2.3.1 Air Pollution

The major cause of air pollution is through anthropogenic activities, although a number of natural activities may release different pollutants in the environment. Hazardous chemicals can also get into the environment through accidental discharge; however, a number of air pollutants are released into the environment from industrial processes and other human activities and may have an adverse effect on human health and the environment [35].

Gases, volatile organic compounds (VOCs) and particulates can cause air pollution. They can be in the form of persistent organic compounds, such as, polycyclic aromatic hydrocarbon; and heavy metals, such as lead and cadmium [35]. The nature of these compounds is an important consideration for compounds that escape into the atmosphere. Hydrophobic compounds are compounds that have no affinity for water and they include a number of VOCs and semivolatile organic compounds, while hydrophilic compounds readily dissolve in water and are removed by precipitation (rain) [36]. Methanol is an example of a hydrophilic compound, while dichloromethane is an example of a hydrophobic compound [36]. These pollutants can be emitted to the atmosphere by a range of sources, namely anthropogenic emissions from human activities, such as, burning fossil fuel and biogenic emissions through the breakdown of organic materials by microorganisms. It can also be emitted from natural sources, such as, volcanic eruptions, forest fire and desert dust.

There are a number of atmospheric pollutants which are in the form of particulate matter or aerosol, mostly referred to as particulates. They are emitted from various industrial processes into the atmosphere via sources, such as, power plants emitting fly ash, combustion of coal, wood, biomass, oil, gasoline/petrol and diesel [36]. They could also be formed by the reaction of gases which occur when particles characteristic of photochemical smog are formed from sunlight, VOCs, and nitrogen oxides in the atmosphere. Particles which are heavy tend to settle rapidly and deposit on buildings, surface of plant leaves and on soil, while the lighter ones remain in the atmosphere longer and travel further away from their sources. Hydrophilic particles are readily removed during rainfall and may enter into water sources thereby polluting the hydrosphere [36].

2.3.2 Water Pollution

Increase in industrialization, agricultural and human activities have resulted in increase in the pollutants, such as, heavy metals, dyes, pesticides, pharmaceuticals, detergents and other persistent organic pollutants (POPs) entering water bodies in recent times [37]. Many of these pollutants remain unknown, due to new chemical compounds that are continuously developed and brought to the market as a result of this rapid industrialization and sooner or later will find their way into the aquatic systems [37]. These are in addition to pathogenic microorganisms that enter water bodies via untreated sewage, septic tanks, and runoff from farms, waste dumps and landfills. This has led to unprecedented health hazards that were not previously in existence coming to light and has resulted in the need for further legislation [38].

Water bodies become polluted either by the direct discharge of the pollutant into the water bodies or from water coming from diffuse sources, such as, soil runoff or the atmosphere. Surface water as well as ground water can become polluted. Pollutants can get into the ground water from contaminated surface water that flows from the surface downward. Leachate from waste that has been improperly disposed of on the surface or in landfills can move through the soil into ground water or surface water, this is another pollutant source of great concern. Hydrophilic chemicals in particular have the tendency to remain dissolved in water and move with the flow of surface water or ground water, while hydrophobic species, such as, PAHs in water have a greater tendency to be held in sediments or mineral surfaces as the water moves from surface to ground water [36].

2.3.3 Soil Pollution

Soil is a very precious resource which needs protection and conservation because we live on it, but its utility by humans has resulted in its contamination [39]. Pollution of the soil arises from industrial, agricultural, waste disposal and deposition of particulates from the atmosphere which could result in an excess of any element or compound, through direct or secondary exposure [40]. The concern about soil pollution is on the increase in many countries worldwide, this is due to the detrimental effects on humans, other life-forms, and the subsequent migration of the pollutants to water bodies which could have a short-term or long-term effect on the environment [41]. Amongst the ubiquitous soil pollutants are the persistent organic pollutants and heavy metals. Significantly elevated levels of these pollutants co-exist in soils in previously

heavily industrialised areas [42]. Soil characteristics and individual geochemical associations of each of these pollutants control whether their elevated concentrations are transferable to soluble, bioavailable and mobile fractions. In the soil, the transport of the pollutants is largely through the movement of groundwater and leachate through rock formations composing aquifers [36]. The pollutants in the groundwater are continuously exposed to the mineral surface and may be adsorbed by it in cases where the aquifer mineral is composed of finely divided matter, such as, sand. Usually, the aquifer is made up solid rock fractured into fragments through which the ground water may flow quickly and over a long distance. When this is the case the pollutants do not have a good opportunity to be taken up by the mineral surface. This leads to a rapid appearance of pollutants from an infiltrating water source in well water supplies of drinking water. At lot of cases have resulted in which pollution at the surface due to heavy metal or organic solvent have moved through the groundwater source to appear in a well used as water source [36]. Researchers have been challenged as a result of these, to urgently develop new, effective, less expensive and innovative techniques to help in the cleaning up of polluted sites [43].

2.4 Environmental Remediation Techniques

With the concern and level of pollutants in the environment, there is a need for remediation in order to alleviate worries and restore the way of life in contaminated communities. Remediation is a process of reclamation or restoration of the polluted environment to its natural condition as possible and it aims to convert the pollutants to a harmless product or to remove them completely from the environment through chemical processes, such as, chemical oxidation, solvent extraction, photocatalytic degradation, and electrokinetic/electrodialytic remediation; biological processes, such as, bioremediation and phytoremediation; and physical processes, such as, thermal processes and adsorption. Remediation processes however, rarely takes place without side effects, which can be expensive, disruptive socially, or cause damage to the environment [44]. The feasibility and perceived success of environmental remediation processes is dependent not only on the reduction or complete removal of the pollutant and the direct economic costs of remediation, but can be constrained by other factors,

which include, social and environmental consequences, and broader economic and political implications of the processes [44].

Soil pollution with organic and inorganic pollutants occurs globally; therefore remediation is necessary to reduce the risk of transfer of these pollutants to proximal waters or receptor organisms by using approaches that are more environmentally friendly than unsustainable waste disposal options [40,45]. The modern agenda seeks to apply processes that are cost effective to meet remediation needs of polluted soils and bind or remove pollutants, while providing conditions that are favourable to plant growth and stimulate ecological restoration [46-48]. Bioavailability and mobility of pollutants are now being recognised by regulators on environmental risk and have led to adoption of a risk-based approach when assessing soil quality [49,50]. Such regulators are more concerned with the pollutants effect, rather than just the total soil concentration and encourage remediation strategies that address such pollution consequences rather than merely reducing total soil concentrations [40].

2.4.1 Chemical Techniques for Environmental Remediation

Solvent Extraction

Solvent extraction strategy involves removing the pollutants from soil using a single solvent or mixtures of solvents and involves the extraction of a compound by desorption from the binding site in the matrix, followed by elution from the solid into the extraction fluid in soils [51]. A typical example is soil washing in which the pollutants are separated from the soil matrix by solubilizing them in a washing solution, such as water, methanol, acetone, dichloromethane and propanol [52]. It is usually applied as an *ex-situ* process. This process has been used successfully in the removal of heavy metals, hydrocarbons and semi-volatile organic compounds from polluted soils, but it is less effective in the treatment of soils polluted with volatile organic compounds and pesticides [52]. Pollutants, such as, heavy metals with low aqueous solubilities, usually require the presence of an acid or chelating agent for effective removal [53], this is because there are four ways in which solvents can be used to mobilize metals in soils: (a) changes in the acidity, (b) changes in solution ionic strength, (c) changes in the redox potential and (d) formation of complexes. The

efficiency of metal removal however depends mainly on the characteristics of the soil and metal (e.g. crystallinity, solubility), chemistry of the extractant and the processing conditions [52,54]. Other approaches in solvent extraction include using non-toxic and biodegradable extraction agents, such as, cyclodextrins and vegetable oil as well as using supercritical and subcritical fluids [55]. The advantage of this approach is that it can treat organics and heavy metal. However, it cannot reduce the toxicity of the heavy metals and leads to the introduction of chemicals into the environment [56].

Chemical Oxidation

Oxidation reactions can be utilised to remediate polluted soils, sediments and water. It is a versatile remediation technique, which provides a rapid and extensive removal of both high and low recalcitrant compounds [57]. Chemical oxidants are used to oxidize organic pollutants into water and carbon dioxide or some other products, such as, alcohols, ketones, aldehydes and carboxylic acids which are easily biodegradable [58]. This aggressive process removes pollutants that are either adsorbed to the soil organic matter or present as non-aqueous phase liquids. Different kinds of oxidants have been used [59,60], which include the more commonly used Fenton's reagent (hydrogen peroxide and ferrous iron) and ozone [55,57]. The advantage of this approach is that it is suitable for the remediation of organics; however it generates hazardous oxidizing chemicals [61].

Photocatalytic Degradation

Photocatalytic degradation has recently been applied in the remediation of polluted soils. This process uses photocatalysts, such as, TiO_2, ZnO and ZrO_2 semiconductor particles to promote redox reactions capable of destroying or mineralising organic pollutants in the presence of ultraviolet-irradiation and/or sunlight to carbon dioxide and water. The technology has been widely used for wastewater treatment [55,62,63]. The advantage of the approach is that it is inexpensive as it uses sunlight and ultraviolet radiation. However, widespread use of the photocatalyst could lead to its accumulation in the environment, which could also have potential health impacts on people exposed to it [64].

Electrokinetic/Electrodialytic Remediation

Electrokinetic remediation can be used in the *in-situ* treatment of low permeable soils polluted with heavy metals, organic pollutants and radionuclides [55]. The technique is based on the principle of applying a low level direct current electric potential through electrodes, placed in the polluted soil. Ionic pollutants are transported by electromigration to the oppositely charged electrodes. Electroosmotic flow in addition, provides a driving force for the movement of soluble pollutants [55]. The technology has been known and applied for over a decade; however, it is only recently that it has been applied to remove hydrophobic and strongly adsorbed pollutants, such as, PAHs, especially from low permeability soils and in this case solubilising agents (surfactants, chelants and cyclodextrins) are utilized to enhance the removal efficiency of PAHs [55].

In the electrodialytic technique, water soluble ions in water and soils are allowed to pass under the influence of electric current (DC) through ion selective semi-permeable membranes [65,66]. The ion membranes are made of ion exchange material which are selective in nature and may be cation or anion exchangers permitting the out flow of cations and anions respectively. The process could be operated either in a batch or continuous mode having two electrodes on which a voltage is applied. In order to obtain the desired demineralization degree, the membranes are either arranged in parallel or in series [67]. The effectiveness of the process in water depends on pH, temperature, applied current, nature of pollutants, selectivities of the membranes, and flow rate of wastewater, scaling and fouling of wastewater, and number and configuration of stages [68]. This approach is effective under acidic conditions; however acidification may not be environmentally friendly and may be time consuming [56].

2.4.2 Biological Techniques for Environmental Remediation

Bioremediation

Bioremediation technology is believed to be a cost-effective and environmentally friendly strategy developed to encourage the microbial (e.g. bacteria, fungi) metabolism of pollutants, by changing the water, air and nutrient condition of

the polluted environment. It can be an aerobic or anaerobic process and is usually achieved through biostimulation (addition of a bulking agent) or bioaugmentation (addition of microorganisms capable of degrading the pollutants) of the contaminated environment [55,69]. There are different ways through which bioremediation of contaminated soils, water, and sediments are carried out. It could be through *in-situ* treatment, such as, landfarming or via *ex-situ* methods, such as, bio-piling and composting [69]. It is also possible to treat the waste in bioreactors, but the technology is expensive when compared with the *in-situ* treatment. In choosing a bioremediation technology for soil, it is important that the technology is comparable in cost and success to treatment processes of polluted land, such as, landfilling, incineration and soil washing [69]. The choice of a bioremediation technique depends on the site conditions. It is therefore necessary to have a thorough understanding of site conditions and this will allow for a proper optimisation of the bioremediation technique and subsequently lead to a better result [69]. The advantage of this approach is that it is cheap and effective in the removal of organics; however it is not very effective with heavy metals and can form toxic metabolites with the organics [56].

Phytoremediation

Phytoremediation is an *in-situ* remediation technique that is relatively new. It uses plants to remove, sequester and detoxify environmental pollutants in the soil, sediments and water and is very effective for the removal of heavy metals [55]. Over the last two decades, different plant species have been widely studied in order to understand their different endogenous genetic, physiological and biochemical capabilities to mineralise a wide range of complex organic pollutants into non-toxic constituents, such as, carbon dioxide, ammonia, nitrate, and chlorine [70]. Plants are known to enhance remediation through biophysical and biochemical processes, such as, adsorption of nutrients bound with pollutants, promoting a more acidic environment to enhance pollutant uptake by plant, secretion of enzymes which act as surfactants to increase the pollutants bioavailability, ability to store and sequester pollutants to 0.1–1% of the plant dry weight and chemical transformation of toxic elements into relatively harmless forms via their metabolic course [71,72]. In addition, the synergistic interactions that exist between plants and microbial communities in the rhizosphere have been shown to be effective in the remediation of recalcitrant organic compounds [73]. This approach is very effective for a wide range of pollutants, cost effective and

can completely breakdown organic pollutants to H_2O and CO_2 instead of transferring toxicity. However, the approach is dependent on climate and can be used seasonally; pollutants can enter into the food chain through the animals that feed on the plant and special disposal of the used plant is required. It is usually restricted to soil less than one meter from the surface [74].

2.4.3 Physical Techniques for Environmental Remediation

Thermal Processes

The thermal approach is a physical separation process that uses heat to either volatilise or destroy the organics in polluted soils. It usually involves the incineration of the soil, sediments and sludge at high temperatures of about 870-1200 °C which effectively destroys organic pollutants, such as, PAHs and PCBs [55]. If the process is aimed at changing the organics into a treatable form rather than destroying it, it is called thermal desorption and should be differentiated from soil incineration [74]. Microwave energy can also be utilize for the remediation of the soil, since most soil constituents are microwave transparent, allowing the applied energy to be concentrated on the pollutants and the water in the soil pores [75]. Depending on the pollutant types and soil properties, the microwave energy may immobilize or remove pollutants through various mechanisms, such as, thermal desorption and destruction [75]. The thermal approach is effective in treating halogenated and non-halogenated volatiles and semi-volatiles, fuel hydrocarbons and pesticides. It however failed to demonstrate an ability to remove heavy metals from polluted soils [56].

Adsorption

In the adsorption process there is an increase in the amount of a particular component on the surface of another component and therefore it is a surface phenomenon. The process efficiency depends on certain parameters, such as, pH, temperature, pollutants concentration, contact time, and the nature of adsorbents and the pollutants [68]. Different types of adsorbents, such as, natural and synthetic zeolite, alumina, fly ash, carbon aerogel, clinoptilolites, phosphate rock, and biopolymer [76-82] have been used in adsorption process for the removal of heavy metals and organic pollutants from wastewater. Recently the process has been applied in the remediation

of polluted soil using biochars [40,42]. This approach is cost effective as the adsorbent can be prepared from readily available waste materials. It is also effective in removing heavy metals and organics. The disadvantage of this approach has to do with the regeneration of the adsorbent, the adsorbent life, and the management of the exhausted adsorbent [68].

2.4.4 Integrated Remediation Techniques

As stated, the different remediation techniques discussed above have their advantages and disadvantages. In order to address the limitations of these remediation techniques and achieve better removal efficiencies for the pollutants has led to different combinations of physical, chemical and biological techniques. Some examples are shown in Table 2.1.

Combination	Environment	Details	Ref
Physical-chemical	Synthetic wastewater contaminated with 2-chlorophenol	Adsorption + photocatalysis	[83]
Physical-biological	Soil contaminated with trace metals	Adsorption + bioremediation	[42]
Biological-chemical	Aged industrial soil and spiked soil	Bioremediation + chemical oxidation with ozone	[84]

Table 2.1: Examples of integrated remediation techniques

2.5 Conclusion

In this chapter, an overview of environmental pollution, causes, effect, concern and remediation has been provided. Anthropogenic activities, such as, industrial and agricultural activities are the major cause of environmental pollution and have resulted in the release of different pollutants into the environment globally with detrimental effect on humans and the environment. There is therefore an urgent need for the remediation of the environment. Different environmental remediation techniques are in existence, namely chemical, biological and physical processes. These processes differ

from each other in terms of principles, scope, speed and cost. The feasibility of using any of these techniques is dependent on the type of the pollutant, the extent of the pollution, nature of the matrix and cost, as each of these techniques has its merits and demerits. It is important to note that no single remediation technique has the solution for the effective removal of all kind of pollutants present in the environment. An integrated technique which is a hyphenated procedure that combines the advantages of these techniques appears to be the way forward in the remediation of polluted environment, but could be costly. Therefore, in this thesis the focus was on the biological and physical processes because that are inexpensive, and do not require the use of extra energy or chemicals that can further pollute the environment.

2.6 References

[1] Hill, MK. Understanding Environmental Pollution. Cambridge University Press, Cambridge, England, 1997.

[2] Crathorne, B, Dobbs, AJ, Rees, Y. Chemical Pollution of the Aquatic Environment by Priority Pollutants and its Control. In Pollution: Causes, Effects, and Control, ed by Harrison, RM. RSC Press, Cambridge, England, 1996.

[3] Dix, HM. Environmental Pollution: Atmosphere, Land, Water, and Noise. John Wiley & Sons, Chichester, England, 1981.

[4] Idris, AM, Ibrahim, A, Abulkibash, AM, Saleh, TA, Ibrahim, K. Rapid Inexpensive Assay Method for Verapamil by Spectrophotometric Sequential Injection Analysis. Drug Test Anal 2011; 3: 380-386.

[5] Franklin, LB. Wastewater Engineering: Treatment, Disposal and Reuse. McGraw Hill, New York, USA, 1991.

[6] Kjellstrom, T, Shiroishi, K, Erwin, PE. Urinary. Beta. /Sub 2/-Microglobulin Excretion among People Exposed to Cadmium in the General Environment. Environ Res 1977; 13: 318-344.

[7] United Nations Environment Programme (UNEP). Environmental Pollution and Impacts on Public Health: Implications of the Dandora Municipal Dumping Site in Nairobi, Kenya. Report Summary (undated).

[8] Ali, H, Khan, E, Sajad, MA. Phytoremediation of Heavy Metals-Concepts and Applications. Chemosphere 2013; 91: 869-881.

[9] Modaihsh, A, Al-Swailem, M, Mahjoub, M. Heavy Metal Contents of Commercial Inorganic Fertilizer Used in the Kingdom of Saudi Arabia. Agri Mar Sci 2004; 9: 21-25.

[10] Chehregani, A, Malayeri, BE. Removal of Heavy Metals by Native Accumulator Plants. Int J Agri Biol 2007; 9: 462-465.

[11] Fulekar, M, Singh, A, Bhaduri, AM. Genetic Engineering Strategies for Enhancing Phytoremediation of Heavy Metals. Afr J Biotechnol 2009; 8: 529-535.

[12] Sabiha, J, Mehmood, T, Tufai, M, Irfan, N. Heavy Metal Pollution from Phosphate Rock used for the Production of Fertilizer in Pakistan. Microchem J 2009; 91: 94-99.

[13] Wuana, RA, Okieimen, FE. Heavy Metals in Contaminated Soils: A Review of Sources, Chemistry, Risks and Best Available Strategies for Remediation. Ecology 2011; 1-20.

[14] Gupta, VK, Saleh TA. Sorption of Pollutants by Porous Carbon, Carbon Nanotubes and Fullerene - An Overview. Environ Sci Pollut Res 2013; 20: 2828-2843.

[15] Garg, UK, Kaur, MP, Garg, VK, Sud, D. Removal of Hexavalent Cr from Aqueous Solutions by Agricultural Waste Biomass. J Hazard Mater 2007; 140: 60-68.

[16] Andrew, JE, Brimblecomble, P, Jickells, TD, Liss, PS, Reid, B. An Introduction to Environmental Chemistry. Wiley-Blackwell, Oxford, England, 2004.

[17] Ospar Commission. Atmospheric Deposition of Selected Heavy Metals and Persistent Organic Pollutants to the OSPAR Maritime Area (1990-2005), 2008.

[18] Handy, RD. Intermittent Exposure to Aquatic Pollutants: Assessment, Toxicity and Sublethal Responses in Fish and Invertebrates. Comp Biochem Physiol 1994; 107: 171-184.

[19] Pascoe, D, Mattery, DL. Studies on the Toxicity of Cadmium to the Three-spined Stickleback, *Gasterostens aculeatus* L. J Fish Biol 1977; 11: 207-215.

[20] Satarug, S, Baker, JR, Urbenjapol, S, Haswell-Elkins, M, Reilly, PEB, Williams, DJ, *et al*. A Global Perspective on Cadmium Pollution and Toxicity in Non-Occupationally Exposed Population. Toxicol Lett 2003; 137: 65-83.

[21] Rashed, MN. Cadmium and Lead Levels in Fish (*Tilapia nilotica*) Tissues as Biological Indicator for Lake Water Pollution. Environ Monit Assess 2001; 68: 75-89.

[22] Madronová, L, Kozler, J, Čežíková, J, Novák, J, Janoš, P. Humic Acids from Coal of the North-Bohemia Coal Field: III. Metal-Binding Properties of Humic Acids-Measurements in a Column Arrangement. React Funct Polym 2001; 47: 119-123.

[23] Pedro, F, Nyer, EK. The Water Encyclopedia: Hydrologic Data and Internet Resources; CRC Press, Boca Raton, FL, USA, 2006.

[24] Alloway, BJ. Heavy Metals in Soils. Blackie, Glasgow, Scotland, 1990.

[25] Naidu, R, Kookana, RS, Sumner, ME, Harter, RD, Tiller, KG. Cadmium Sorption and Transport in Variable Charge Soils: A Review. J Environ Qual 1997; 26: 602-617.

[26] McLaughlin, MJ, Singh, BR. Cadmium in Soils and Plants. In Developments in Plant and Soil Sciences, ed by McLaughlin, MJ, Singh BR. Academic Publishers, Dordrecht, Netherlands, 1999.

[27] Cheng, H, Hu, Y. Lead (Pb) Isotopic Fingerprinting and its Applications in Lead Pollution Studies in China: A Review. Environ Pollut 2010; 158: 1134-1146.

[28] Needleman, H. Lead Poisoning. Annu Rev Med 2004; 55: 209-222.

[29] Hilary, AG. The Biological Chemistry of Lead. Curr Opin Chem Biol 2001; 5: 223-227.

[30] Schuhmacher, M, Belles, M, Rico, A, Domingo, JL, Corbellab, J. Impact of Reduction of Lead in Gasoline on the Blood and Hair Lead Levels in the Population of Tarragona Province, Spain, 1990-1995. Sci Total Environ 1996; 184: 203-209.

[31] Lorenzi, D, Cave, M, Dean, JR. An Investigation into the Occurrence and Distribution of Polycyclic Aromatic Hydrocarbons in Two Soil Size Fractions at a Former Industrial Site in NE England, UK using *in situ* PFE-GC-MS. Environ Geochem Health 2010; 32: 553-565.

[32] Haritash, AK, Kaushik, CP. Biodegradation Aspects of Polycyclic Aromatic Hydrocarbons (PAHs): A Review. J Hazard Mater 2009; 169: 1-15.

[33] Patnaik, P. A Comprehensive Guide to the Properties of Hazardous Chemical Substances. John Wiley & Sons, Hoboken, NJ, USA, 1999.

[34] Foo, KY, Hameed, BH. An Overview of Landfill Leachate Treatment via Activated Carbon Adsorption Process. J Hazard Mater 2009; 171: 54-60.

[35] Kampa, M, Castanas, E. Human Health Effects of Air Pollution. Environ Pollut 2008; 151: 362-367.

[36] Manahan, SE. Environmental Chemistry. 9th Edition, CRC Press, London, England, 2010.

[37] Reddy, DHK, Lee, SM. Water Pollution and Treatment Technologies. J Environ Anal Toxicol 2012; 2: e103.

[38] Schwarzenbach, RP, Escher, BI, Fenner, K, Hofstetter, TB, Johnson, CA, von Gunten, U, *et al*. The Challenge of Micropollutants in Aquatic Systems. Science 2006; 313: 1072-1077.

[39] Dean, JR. Bioavailability, Bioaccessibility and Mobility of Environmental Contaminants. John Wiley & Sons, Chichester, England, 2007.

[40] Beesley, L, Moreno-Jiménez, E, Gomez-Eyles, JL, Harris, E, Robinson, B, Sizmur, T. A Review of Biochars' Potential Role in the Remediation, Revegetation and Restoration of Contaminated Soils. Environ Pollut 2011; 159: 3269-3282.

[41] Gan, VS, Ng, HK. Current Status and Prospects of Fenton Oxidation for the Decontamination of Persistent Organic Pollutants (POPs) in Soils. Chem Eng J 2012; 213: 295-317.

[42] Beesley, L, Moreno-Jiménez, E, Gomez-Eyles, JL. Effects of Biochar and Greenwaste Compost Amendments on Mobility, Bioavailability and Toxicity of Inorganic and Organic Contaminants in a Multi-Element Polluted Soil. Environ Pollut 2010; 158: 2282-2287.

[43] Reddy, DR, Kosgi, S, Zhou, J. A Review of *in-situ* Air Sparging for the Remediation of VOC-Contaminated Saturated Soil and Groundwater. Hazard Waste Hazard 1995; 2: 97-118.

[44] Oughton, DH. Social and Ethical Issues in Environmental Remediation Projects. J Environ Radioactiv 2013; 119: 21-25.

[45] Mench, M, Lepp, N, Bert, V, Schwitzguébel, JP, Gawronski, SW, Schöder, P, *et al*. Successes and Limitations of Phytotechnologies at Field Scale: Outcomes, Assessment and Outlook from COST action 859. J Soils Sediments 2010; 10: 1039-1070.

[46] Adriano, DC, Wenzel, WW, Vangronsveld, J, Bolan, NS. Role of Assisted Natural Remediation in Environmental Cleanup. Geoderma 2004; 122: 121-142.

[47] Bernal, MP, Clemente, R, Walker, DJ. The Role of Organic Amendment in the Bioremediation of Heavy Metal-Polluted Soils. In Environmental Research at the Leading Edge, ed by Gore, RW. Nova, New York, USA, 2006.

[48] Vangronsveld, J, Herzig, R, Weyens, N, Boulet, J, Adriaensen, K, Ruttens, A, *et al*. Phytoremediation of Contaminated Soils and Groundwater: Lessons from the Field. Environ Sci Pollut R 2009; 16: 765-794.

[49] Swartjes, FA. Risk-Based Assessment of Soil and Groundwater Quality in the Netherlands: Standards and Remediation Urgency. Risk Anal 1999; 19: 1235-1249.

[50] Fernández, MD, Cagigal, E, Vega, MM, Urzelai, A, Babín, M, Pro, J, *et al*. Ecological Risk Assessment of Contaminated Soils through Direct Toxicity Assessment. Ecotox Environ Safe 2005; 62: 174-184.

[51] Kubátová, A, Jansen, B, Vaudoisot, JF, Hawthorne, SB. Thermodynamic and Kinetic Models for the Extraction of Essential Oil from Savory and Polycyclic Aromatic Hydrocarbons from Soil with Hot (subcritical) Water and Supercritical CO_2. J Chromatogr A 2002; 975: 175–188.

[52] Peters, WR. Chelant Extraction of Heavy Metals from Contaminated Soil. J Hazard Mater 1999; 66: 151-210.

[53] Moutsatsou, A, Gregou, M, Matsas, D, Protonotarios, V. Washing as a Remediation Technology Applicable in Soils Heavily Polluted by Mining-Metallurgical Activities. Chemosphere 2006; 63: 1632-1640.

[54] Mann, JM. Full-Scale and Pilot-Scale Soil Washing. J Hazard Mater 1999; 66: 119-136.

[55] Gan, S, Laua, EV, Ng, HK. Remediation of Soils Contaminated with Polycyclic Aromatic Hydrocarbons (PAHs). J Hazard Mater 2009; 172: 532-549.

[56] Virkutytea, J, Sillanp, M, Latostenmaa, P. Electrokinetic Soil Remediation-Critical Overview. Sci Total Environ 2002; 289: 97-121.

[57] Sutton, NB, Grotenhuis, JTC, Langenhoff, AAM, Rijnaarts, HHM. Efforts to Improve Coupled *in situ* Chemical Oxidation with Bioremediation: A Review of Optimization Strategies. J Soils Sediments 2010; 11: 129-140.

[58] Bigda, RJ. Consider Fenton Chemistry for Wastewater Treatment. Chem Eng Prog 1995; 91: 62-66.

[59] Seol, Y, Zhang, H, Schwartz, FW. A Review of *in situ* Chemical Oxidation and Heterogeneity. Environ Eng Geosci 2003; 9: 37-49.

[60] Watts, RJ, Teel, AL. Chemistry of Modified Fenton's Reagent (Catalyzed H_2O_2 Propagations-CHP) for *in situ* Soil and Groundwater Remediation. J Environ Eng 2005; 131: 612-622.

[61] Karpenko, O, Lubenets, V, Karpenko, E, Novikov, V. Chemical Oxidants for Remediation of Contaminated Soil and Water: A Review. Chemist Chem Technol 2009; 3: 41-45.

[62] Zhang, L, Li, P, Gong, Z, Li, X. Photocatalytic Degradation of Polycyclic Aromatic Hydrocarbons on Soil Surfaces using TiO_2 under UV Light. J Hazard Mater 2008; 158: 478-484.

[63] Rababah, A, Matsuzawa, S. Treatment System for Solid Matrix Contaminated with Fluoranthene. II-Recirculating Photodegradation Technique. Chemosphere 2002; 46: 49-57.

[64] Ibhadon, AO, Fitzpatrick, P. Heterogeneous Photocatalysis: Recent Advances and Applications. Catalysts 2013; 3: 189-218.

[65] von Gottberg, AJM, Siwak, LR. Re-engineering of the Electrodialysis Reversal Process Int Desalin Water Reuse Q 1998; 7: 33-37.

[66] Tongwen, X. Electrodialysis Processes with Bipolar Membrane (EPBM) in Environmental Protection-A Review. Resour Conserv Recycl 2002; 37: 1-22.

[67] Jakobsen, MR, Fritt-Rasmussen, J, Nielsen, S, Ottosen, LM. Electrodialytic Removal of Cadmium from Wastewater Sludge. J Hazard Mater 2004; 106: 127-132.

[68] Gupta, VK, Ali, I, Saleh, TA, Nayaka, A, Agarwal S. Chemical Treatment Technologies for Wastewater Recycling-An Overview. RSC Adv 2012; 2: 6380-6388.

[69] Bamforth, SM, Singleton, I. Bioremediation of Polycyclic Aromatic Hydrocarbons: Current Knowledge and Future Directions. J Chem Technol Biotechnol 2005; 80: 723-736.

[70] Vidali, M. Bioremediation. An Overview. Pure Appl Chem 2001; 73: 1163-1172.

[71] Meagher, RB. Phytoremediation of Toxic Elemental and Organic Pollutants. Curr Opin Plant Biol 2000; 3: 153-162.

[72] Parrish, ZD, Banks, MK, Schwab, AP. Assessment of Contaminant Liability during Phytoremediation of Polycyclic Aromatic Hydrocarbon Impacted Soil. Environ Pollut 2005; 137: 187-197.

[73] Chaudry, Q, Blom-Zandstra, M, Gupta, S, Joner, EJ. Utilising the Synergy between Plants and Rhizosphere Microorganisms to Enhance Breakdown of Organic Pollutants in the Environment. Environ Sci Pollut Res 2005; 12: 34-48.

[74] Khan, FI, Husain, T, Hejazi, R. An Overview and Analysis of Site Remediation Technologies. J Environ Manage 2004; 71: 95-122.

[75] Wu, TN. Environmental Perspectives of Microwave Applications as Remedial Alternatives: Review. Pract Period Hazard Toxic Radioact Waste Manage 2008; 12: 102-115.

[76] Motsi, T, Rowson, NA, Simmons, MJH. Adsorption of Heavy Metals from Acid Mine Drainage by Natural Zeolite. Int J Miner Process 2009; 92: 42-48.

[77] Genc-Fuhrman, H, Mikkelsen, PS, Ledin, A. Simultaneous Removal of As, Cd, Cr, Cu, Ni and Zn from Stormwater: Experimental Comparison of 11 Different Sorbents. Water Res 2007; 41: 591-602.

[78] Cetin, S, Pehlivan, E. The Use of Fly Ash as a Low Cost, Environmentally Friendly Alternative to Activated Carbon for the Removal of Heavy Metals from Aqueous Solutions. Colloid Surfaces A 2007; 298: 83-87.

[79] Kadirvelu, K, Goel, J, Rajagopal, CJ. Sorption of Lead, Mercury and Cadmium Ion in Multi-Component System using Carbon Aerogel as Adsorbent. J Hazard Mater 2008; 153: 502-507.

[80] Çoruh, S. The Removal of Zinc Ions by Natural and Conditioned Clinoptilolites. Desalination 2008; 225: 41-57.

[81] Mavropoulos, E, da Rocha, NCC, Moreira, JC, Bertolinod, LC, Rossi, AM. Pb^{2+}, $Cu^{2+}$and Cd^{2+} Ions Uptake by Brazilian Phosphate Rocks. J Braz Chem Soc 2005; 16: 62-68.

[82] Debbandt, AL, Ferreira, ML, Gschaider, ME. Theoretical and Experimental Study of M^{2+} Adsorption on Biopolymer. III. Comparative Kinetic Pattern of Pb, Hg and Cd. Carbonhydr Polym 2004; 56: 321-332.

[83] Ilisz, I, Dombia, A, Mogyorósi, K, Farkas, A, Dékány, I. Removal of 2-Chlorophenol from Water by Adsorption Combined with TiO_2 Photocatalysis. Appl Catal B-Environ 2002; 39: 247-256.

[84] Derudi, M, Venturini, G, Lombardi, G, Nano, G, Rota, R. Biodegradation Combined with Ozone for the Remediation of Contaminated Soils. Eur J Soil Biol 2007; 43: 297-303.

Chapter 3

Techniques for Characterizing Carbonaceous Materials

3.1 Introduction

The increasing search for carbonaceous materials for different applications requires a clear picture of the properties of the final carbonaceous materials [1]. Several techniques have been used for the interpretation of the structural and chemical properties of different carbon materials obtained from the pyrolysis and hydrothermal carbonization of materials, such techniques include, but not limited to the, BET (Brunauer–Emmett–Teller) surface area and porosity analysis, scanning electron microscopy (SEM), Fourier transform infrared analysis (FT-IR), ^{13}C solid state magic angle spinning nuclear magnetic resonance (NMR), and elemental analysis (CHN). In order to know the structural and chemical composition of the different carbon materials prepared in this thesis, the different characterisation and analytical techniques used are briefly discussed.

3.2 The Surface Area and Porosity Analysis

The surface area and porosity are very important in the determination of the quality, utility and behaviour of many materials, such as, catalysts, adsorbents, pigments, and pharmaceuticals in different applications. It is therefore essential that these characteristics be determined correctly.

The BET (Brunauer–Emmett–Teller) surface area and porosity analyzer has been applied in the determination of the surface area and porosity of different biochars, hydrochars and carbon monoliths using nitrogen sorption measurements. The surface area and porosity of biochars depend on the nature of precursor material and pyrolysis condition [2,3]. Slow pyrolysis (< 400 °C) results in biochars with low surface area and porosity [4,5], which is due to the condensation of the volatile organic compounds produced during the pyrolysis process on the char which block the pores and their adsorption potential [6,7]. The hydrochars from the hydrothermal carbonization also have the characteristic of having small number of micropores and therefore a small surface area when compared to activated carbons from the BET surface area analysis of the materials and this is because the process of hydrothermal carbonization involves carbonization as well as solubilisation of the organics and the formation of tarry

substances which block the pores [8-11]. Low surface areas in the range of 1.9-8.3 m^2/g have been reported for biochar and hydrochars obtained under different conditions [4,9,10]. Nitrogen sorption isotherm from the BET analysis performed to quantify the porosity and surface area of the carbon monoliths have shown a typical Type-IV isotherm with hysteresis loop, which is usually a characteristic exhibited by mesoporous materials and it is associated with the filling of mesopores due to capillary condensation. The carbon monoliths also showed a high surface area and a narrow pore size distribution [12-15] when compared with other carbon materials, such as, biochar and hydrochar.

3.3 Scanning Electron Microscope (SEM) Analysis

The scanning electron microscope (SEM) has been used in providing information about the structural morphologies of different materials. The physical structure of biochar, hydrochar and carbon monoliths are often described using the scanning electron microscopy (SEM). Biochar produced from cellulosic plant materials usually have macropore, with pores of approximately 1 μm diameter, which are usually a product of the architecture of the feedstock [16], this is potentially important to its adsorption and waterholding capacity in soil [17-19]. In the case of hydrochars, the morphology is often different from that of the precursor material. Irregular surfaces and numerous microspheres with different shapes and sizes in the range of 1-10 μm have been seen on the surface of hydrochar prepared by different authors [9,10,20-22], while SEM images of carbon monoliths illustrate the morphology of the dispersed microspheres with a smooth surface and a broad size distribution ranging from hundreds of nanometers to a few micrometers [23-25].

3.4 Fourier Transform Infrared (FT-IR) Analysis

Infrared spectrometric analysis is regarded as a powerful technique for investigating the chemical functionality of carbonaceous materials. A range of different methods, such as, diffuse reflectance infrared Fourier transform (DRIFT) spectroscopy, where the carbon materials are mixed with KBr to form a wafer, and the attenuated total reflectance Fourier transform infrared (ATR-FTIR) spectroscopy have been applied in the infrared analysis to characterise carbon materials [26]. The FT-IR spectrum of biochar and hydrochar can be complex, with different compositions identified due to the different kinds of chemical bonds in the material [26].

Carbonization temperature has effects on the FT-IR spectrum of the biochar, with the charring temperature altering the functional group on the biochar, by showing a weaker adsorption intensity for oxygen, hydrogen, and aliphatic carbon, but stronger adsorption intensity for aromatic carbon as the charring temperature increases [27,28]. FT-IR spectra reveal the type of functional groups present on the hydrochars, which point to their very polar surface structure, such as, phenolic residues, carbonyl and hydroxyl functional groups, as well as aliphatic double bonds [22,29-31]. FT-IR of polymer monoliths obtained using phenolic precursor and triblock copolymer show functional groups of the phenolic resin and the triblock copolymer, however, carbonization leads to the disappearance of most of these functional groups leaving only those of the phenolic resin due to the decomposition of the triblock copolymer [13,32,33].

3.5 Nuclear Magnetic Resonance (NMR) Analysis

^{13}C solid-state nuclear magnetic resonance (NMR) spectroscopy has been used to characterize carbonaceous materials. The most frequently used is the ^{13}C cross-polarization magic-angle spinning (CP/MAS) technique, which has the advantage of excellent spectral resolution and sensitivity enhancement by narrowing the signals, and has helped to significantly advance the understanding of the chemical structures of carbonaceous materials [34]. The fastest approach to obtain preliminary information about chemical composition at one single contact time has in general been with cross-polarization [35]. Recently, a range of advanced solid-state ^{13}C NMR techniques, have been developed and applied to characterize various kinds of natural organic matter samples and these applications have revealed detailed insights into the chemical structures of natural organic matter [36-38].

A detailed ^{13}C solid-state NMR analysis of biochar and hydrochars has provided deeper information into the chemical structures and possible mechanisms behind the production of these carbon materials and has been used to further confirm the results from the FT-IR. The results obtained from different studies showed that biochars from slow pyrolysis are chemically different from hydrochars. Biochars have aromatics as their most dominant components, while the hydrochars are dominated by aliphatic components [34,35], and this is in agreement with the FT-IR results. Aromatization of a material is less during hydrothermal carbonization than during the

pyrolysis of the same material and there is variation in the chemical structures of hydrochars produced under different processing conditions [34].

3.6 Elemental Analysis (CHN) Analysis

Elemental (CHN) analysis has been used to measure the level of organic matter degradation during the carbonization process. CHN analysis has provided a reliable measure of both the extent of carbonization and the level of oxidative alteration of chars in the soil, and are relatively straightforward to determine [16]. Elemental (CHN) analysis, is usually carried out using analytical instruments which operate based on the complete combustion of the material in pure oxygen atmosphere [39]. Biochars and hydrochars differ in their chemical composition which is usually attributed to the incomplete and uncontrolled physical and chemical transformations that take place which is a function of the temperature of pyrolysis, nature of feedstock, cooling and other post-production conditions [40,41]. Char yields (dry weight percentage of the starting material) typically decrease with increase in the temperatures of carbonization, with the preference shifting towards other products (gaseous and liquid) at such higher temperature [42]. The decrease is related to the deoxygenating reactions, such as, dehydration and decarboxylation, as the oxygen contents become lower at such high temperature [43]. However, the amount of fixed carbon in the chars increases with increase in temperature [44].

3.7 Conclusion

Characterization of carbonaceous materials is very important, although carbon materials prepared under different conditions may have similar physical appearance; their chemical properties are usually different due to the different thermochemical reactions and carbonization processes. For example, the biochar prepared from pyrolysis usually displays predominantly aromatics, while hydrochar prepared from hydrothermal carbonization shows mainly aliphatics. It is therefore crucial to carry out characterization of the chars in order to understand the different reaction mechanisms involved in the pyrolysis and hydrothermal carbonization processes. In addition a clear knowledge of char properties is important for the beneficial use of char products, which is dependent on the physical and chemical characteristics of the chars.

3.8 References

[1] Falco, C, Caballero, FP, Babonneau, F, Gervais, C, Laurent, G, Titirici, MM. Hydrothermal Carbon from Biomass: Structural Differences between Hydrothermal and Pyrolyzed Carbons via ^{13}C Solid State NMR. Langmuir 2011; 27: 14460-14471.

[2] Lehmann, J, Rillig, MC, Thies, J, Masiello, CA, Hockaday, WC, Crowley, D. Biochar Effects on Soil Biota - A Review. Soil Biol Biochem 2011; 43: 1812-1836.

[3] Atkinson, CJ, Fitzgerald, JD, Hipps, NA. Potential Mechanisms for Achieving Agricultural Benefits from Biochar Application to Temperate Soils: A Review. Plant Soil 2010; 337: 1-18.

[4] Angın, D. Effect of Pyrolysis Temperature and Heating Rate on Biochar Obtained from Pyrolysis of Safflower Seed Press Cake. Bioresource Technol 2013; 128: 593-597.

[5] Ronsse, F, van Hecke, S, Dickinson, D, Prins, W. Production and Characterization of Slow Pyrolysis Biochar: Influence of Feedstock Type and Pyrolysis Conditions. GCB Bioenergy 2013; 5: 104-115.

[6] Kwon, S, Pignatello, JJ. Effects of Natural Organic Substances on the Surface and Adsorptive Properties of Environmental Black Carbon (Char): Pseudo Pore Blockage by Model Lipid Components and its Implications for N_2-Probed Surface Properties of Natural Sorbents. Environ Sci Technol 2005; 39: 7932-7939.

[7] Pignatello, JJ, Kwon, S, Lu, Y. Effects of Natural Organic Substances on the Surface and Adsorptive Properties of Environmental Black Carbon (Char): Attenuation of Surface Activity by Humic and Fulvic acids. Environ Sci Technol 2006; 40: 7757-7763.

[8] Titirici, MM, Antonietti, M. Chemistry and Materials Options of Sustainable Carbon Materials Made by Hydrothermal Carbonization. Chem Soc Rev 2010; 39: 103-116.

[9] Sevilla, M, Macia-Agullo, JA, Fuertes, AB. Hydrothermal Carbon of Biomass as a Route for the Sequestration of CO_2: Chemical and Structural Properties of the Carbonized Products. Biomass Bioenerg 2011; 35: 3152-3159.

[10] Sevilla, M, Fuertes, AB. Chemical and Structural Properties of Carbonaceous Products Obtained by Hydrothermal Carbonization of Saccharides. Chem-Eur J 2009; 15: 4195-4203.

[11] Mochidzuki, K, Sato, N, Sakoda, A. Production and Characterization of Carbonaceous Adsorbents from Biomass Wastes by Aqueous Phase Carbonization. Adsorption 2005; 11: 669-673.

[12] Hao, G, Li, W, Li, W, Wang, S, Wang, G, Qi, L, *et al*. Lysine-assisted Rapid Synthesis of Crack-free Hierarchical Carbon Monoliths with a Hexagonal Array of Mesopores. Carbon 2011; 49: 3762-3772.

[13] Liu, L, Wang, FY, Shao, G, Yuan, Z. A Low Temperature Autoclaving Route to Synthesize Carbon Materials with an Ordered Mesostructure. Carbon 2010; 48: 2089-2099.

[14] Tanaka, S, Nakatani, N, Doi, A, Miyake, Y. Preparation of Ordered Mesoporous Carbon Membranes by a Soft-templating Method. Carbon 2011; 49: 3184-3189.

[15] Huang, Y, Cai, H, Feng, D, Gu, D, Deng, Y, Tu, B, *et al*. One-step Hydrothermal Synthesis of Ordered Mesostructured Carbonaceous Monoliths with Hierarchical Porosities. Chem Comm 2008; 2641-2643.

[16] Sohi, SP, Krull, E, Lopez-Capel, E, Bol, R. A Review of Biochar and Its Use and Function in Soil. Adv Agron 2010; 105: 47-82.

[17] Day, D, Evans, RJ, Lee, JW, Reicosky, D. Economical CO_2, SO_x, and NO_x capture from Fossil-Fuel Utilization with Combined Renewable Hydrogen Production and Large-scale Carbon Sequestration. Energy 2005; 30: 2558-2579.

[18] Ogawa, M, Okimori, Y, Takahashi, F. Carbon Sequestration by Carbonization of Biomass and Forestation: Three Case Studies. Mitigat Adaptat Strateg Global Change 2006; 11: 429-444.

[19] Yu, XY, Ying, GG, Kookana, RS. Sorption and Desorption Behaviors of Diuron in Soils Amended with Charcoal. J Agric Food Chem 2006; 54: 8545-8550.

[20] Guiotoku, M, Maia, CMBF, Rambo, CR, Hotza, D. Synthesis of Carbon-Based Materials by Microwave Hydrothermal Processing. In Microwave Heating, ed by Chandra, U. InTech, New York, USA, 2011.

[21] Xiao, LP, Shia, ZJ, Xua, F, Sun, RC. Hydrothermal Carbonization of Lignocellulosic Biomass. Bioresource Technol 2012; 118: 619-623.

[22] Sevilla, M, Fuertes, AB. The Production of Carbon Materials by Hydrothermal Carbonization of Cellulose. Carbon 2009; 47: 2281-2289.

[23] Liu, D, Lei, JH, Guoa, LP, Deng, KJ. Simple Hydrothermal Synthesis of Ordered Mesoporous Carbons from Resorcinol and Hexamine. Carbon 2011; 49: 2113-2119.

[24] Wang, Z, Li, F, Ergang, NS, Stein, A. Effects of Hierarchical Architecture on Electronic and Mechanical Properties of Nanocast Monolithic Porous Carbons and Carbon-Carbon Nanocomposites. Chem Mater 2006; 18: 5543-5553.

[25] Sevilla, M, Fuertes, AB. Fabrication of Porous Carbon Monoliths with a Graphitic Framework. Carbon 2013; 56: 155-166.

[26] Chia, CH, Gong, B. Joseph, SD, Marjob, CE, Munroea, P, Rich, AM. Imaging of Mineral-Enriched Biochar by FTIR, Raman and SEM–EDX. Vib Spectrosc 2012; 62: 248-257.

[27] Lehmann, J, Liang, B, Solomon, D, Lerotic, M, Luiza, F, Kinyangi, J, *et al*. Near-Edge X-ray Absorption Fine Structure (NEXAFS) Spectroscopy for Mapping Nano-Scale Distribution of Organic Carbon Forms in Soil: Application to Black Carbon Particles. Glob Biogeochem Cycles 2005; 19: 1013-1025.

[28] Fuertes AB, Arbestain MC, Sevilla M, Maciá-Agulló JA, Fiol S, López R, *et al*. Chemical and Structural Properties of Carbonaceous Products Obtained by Pyrolysis and Hydrothermal Carbonisation of Cornstover. Soil Res 2010; 48: 618-626.

[29] Titirici, MM, Thomas, A, Yu, SH, Jens-O. Muller, JO, Antonietti, M. A Direct Synthesis of Mesoporous Carbons with Bicontinuous Pore Morphology from Crude Plant Material by Hydrothermal Carbonization. Chem Mater 2007; 19: 4205-4212.

[30] Jamari, SS, Howse, JR. The Effect of the Hydrothermal Carbonization Process on Palm Oil Empty Fruit Bunch. Biomass Bioenerg 2012; 47: 82-90.

[31] Parshetti, GK, Hoekman, SK, Balasubramanian, R. Chemical, Structural and Combustion Characteristics of Carbonaceous Products Obtained by Hydrothermal Carbonization of Palm Empty Fruit Bunches. Bioresource Technol 2013; 135: 683-689.

[32] Ryu, J, Suh, YW, Suh, DJ, Ahn, DJ. Hydrothermal Preparation of Carbon Microspheres from Mono-saccharides and Phenolic Compounds. Carbon 2010, 48: 1990-1998.

[33] Zhang, FQ, Meng, Y, Gu, D, Yan, Y, Yu, CZ, Tu, B, et al. A Facile Aqueous Route to Synthesize Highly Ordered Mesoporous Polymer and Carbon Framework with Ia^3d Bicontinous Cubic Structure. J Am Chem Soc 2005; 127: 13508-13509.

[34] Cao, X, Ro, KS, Chappell, M, Li, Y, Mao, J. Chemical Structures of Swine-Manure Chars Produced under Different Carbonization Conditions Investigated by Advanced Solid-State ^{13}C Nuclear Magnetic Resonance (NMR) Spectroscopy. Energy Fuels 2011; 25: 388-397.

[35] Baccile, N, Laurent, G, Babonneau, F, Fayon, F, Titirici, MM, Antonietti, M. Structural Characterization of Hydrothermal Carbon Spheres by Advanced Solid-State MAS ^{13}C NMR Investigations. J Phys Chem C 2009; 113: 9644-9654.

[36] Mao, J, Ajakaiye, A, Lan, Y, Olk, DC, Ceballos, M, Zhang, T, *et al*. Chemical Structures of Manure from Conventional and Phytase Transgenic Pigs Investigated by Advanced Solid-State NMR Spectroscopy. J Agric Food Chem 2008; 56: 2131-2138.

[37] Mao, J, Holtman, KM, Scott, JT, Kadla, JF, Schmidt-Rohr, K. Differences between Lignin in Unprocessed Wood, Milled Wood, Mutant Wood, and Extracted Lignin Detected by ^{13}C Solid-State NMR. J Agric Food Chem 2006; 54: 9677-9686.

[38] Mao, JD, Schimmelmann, A, Mastalerz, M, Hatcher, PG, Li, Y. Structural Features of a Bituminous Coal and Their Changes during Low-Temperature Oxidation and Loss of Volatiles Investigated by Advanced Solid-State NMR Spectroscopy. Energy Fuels 2010; 24: 2536-2544.

[39] Manyà, JJ. Pyrolysis for Biochar Purposes: A Review to Establish Current Knowledge Gaps and Research Needs. Environ Sci Technol 2012; 46: 7939-7954.

[40] Boehm, HP. Some Aspects of the Surface Chemistry of Carbon Blacks and Other Carbons. Carbon 1994; 32: 759-769.

[41] Antal, MJ, Grønli, M. The Art, Science, and Technology of Charcoal Production. Ind Eng Chem Res 2003; 42: 1619-1640.

[42] Bridgwater, AV, Meier, D, Radlein, D. An Overview of Fast Pyrolysis of Biomass. Org Geochem 1999; 30: 1479-1493.

[43] Kang, S, Li, X, Fan, J, Chang, J. Characterization of Hydrochars Produced by Hydrothermal Carbonization of Lignin, Cellulose, D-Xylose, and Wood Meal. Ind Eng Chem Res 2012; 51: 9023-9031.

[44] Spokas, KA. Review of the Stability of Biochar in Soils: Predictability of O:C Molar Ratios. Carbon Manag 2010; 1: 289-303.

Chapter 4

Preparation and Characterization of Carbonaceous Materials from Pyrolysis and Hydrothermal Carbonization

4.1 Introduction

Various methods, such as, pyrolysis and hydrothermal carbonization have been used for the preparation of carbonaceous materials, with the aim of preparing materials that are useful for different applications in the environment, catalysis, and separation science. Preparation of carbonaceous material from biomass also offers the option to sequester carbon from plant materials, binding CO_2 efficiently in a useful way by taking carbon out of the short term carbon cycle [1].

However, the production of biochar from the pyrolysis of biomass has some drawbacks. One example is that during the pyrolysis of the biomass gases, such as, CO, CH_4, C_2-hydrocarbons and PAHs (polycyclic aromatic hydrocarbons) as well as oils are produced [2-4]. These gases need to be recovered and converted into another useable form such as bioenergy, as their release into the environment is harmful and should be avoided. This requires the use of sophisticated and expensive equipment increasing the cost of the process [5]. Also pyrolysis of biomass usually requires very harsh conditions and high temperature [6]. Therefore; it becomes necessary to search for alternative methods of preparing the material of which hydrothermal carbonization offers such an alternative.

Hydrothermal carbonization experiments were first reported by Bergius and Specht in 1913 [7]. The process involves the heating of biomass or other materials in a closed vessel under pressure in water at a temperature of about 180-200 °C to form char and water-soluble organic substances [8,9]. Thus, in hydrothermal carbonization the stored energy in the biomass is used more efficiently. Water acts in the process as both the reagent and reactive environment, aiding the different reactions that take place. During the hydrothermal carbonization of biomass, decomposition of the carbohydrate structure takes place via hydrolysis, an exothermic process, forming free sugar and other by-products [8,10]. It represents an environmentally friendly and a simple technique in which biomass or sugars are first converted into precondensed polymers

and subsequently following further dehydration/polymerization/condensation process into carbon rich derivatives [11].

Hydrothermal carbonization has been applied in the synthesis of different types of carbonaceous material by different authors in recent times, with some specializing in the hydrothermal carbonization of biomass [1,5,10-14]. Some of these were with the aim of sequestration of CO_2. Others studied synthesis of carbonaceous materials from several types of saccharides using a hydrothermal carbonization process [4,6,15], as well as from swine manure [16], cellulose [9,10] and microalgae [8]. However, the conventional hydrothermal process requires special systems that support pressure and temperature, and usually an autoclave with pressure safety device is used. Also, the time for the reaction ranges from hours to days. These make the process expensive and time consuming.

Microwave technology has been shown to be more energy efficient than conventional methods of heating in many applications. It has the advantage of providing selective, fast and homogenous heating and this reduces processing time and costs significantly [17]. When a material is been processed in the microwave oven, the material interacts with the electromagnetic radiation and since the heat is being produced by the material itself in its bulk, makes the heating faster and selective. When properly monitored, these characteristics result in a homogenous material, with a significant reduction in energy losses and with a faster production in contrast to the conventional ovens [18].

Considering the advantages of microwave heating mentioned above, it can be applied in the hydrothermal process in place of a conventional oven. Although, microwave heating has been applied in the synthesis of materials over the last decade by different authors; its use in the hydrothermal carbonization of material started only recently [10]. Therefore, more research is necessary in order to fully understand the process of using microwave heating because of the aforementioned advantages and other widespread applications of microwave irradiation.

Three waste materials were investigated in this study, namely *Prosopis africana* shell (from Nigeria), rapeseed husk (from the UK) and coconut shell (a model material that has been widely studied in carbon science). Glucose (monosaccharide) is used in this study as a model material (pure chemical material) that has been previously studied

using the conventional hydrothermal process, to compare the effectiveness of the microwave-assisted hydrothermal carbonization process with the previous reports for glucose and other saccharides using the conventional hydrothermal carbonization method of oven heating [4,6,11,19]. To the best of my knowledge, this is the first time comparison is been made between the hydrochars prepared using the microwave-assisted and conventional hydrothermal carbonization of the same material.

Prosopis africana (*Mimosaceae*) is found in the guinea savanna region of Nigeria. It is a multi-purpose tree of great economic value among the rural communities. The fruit of the tree is used as a feed for animals, while the seeds are fermented to make a highly proteinaceous condiment called *'ukpehe'*. The tree is not cultivated. Products from the hard wood, such as some kitchen utensils, wooden farm implements, and planks for construction, are traded extensively. The tree is a good source of fire wood and charcoal, while the secondary roots are useful in medicine [20]. As a result of these uses, a lot of waste materials are generated and the shell is one of such waste materials.

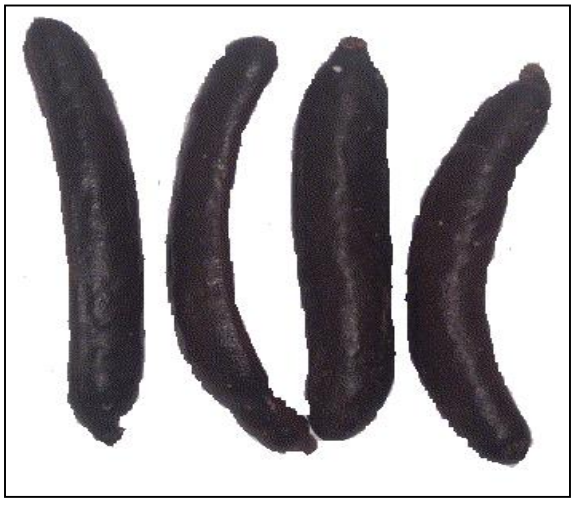

Figure 4.1: *Prosopis africana* shell [21]. One of the waste products obtained from the different uses of the *Prosopis africana*.

Rapeseed (*Brassica napus*) belongs to the family of the *Brassicaceae*. It is a crop found in Northern England and mainly cultivated because of its nutritious oil-rich seed. The oil has been a source of lubricant for steam engines since the 19th century. The rapeseed husk is a residue from crushing of the rapeseeds to remove rape oil. The waste has been used in the preparation of cattle feed known as cattle cake over the years.

Figure 4.2: Rapeseed [22]. The husk is a residue from crushing of the rapeseeds to remove rape oil.

The coconut (*Cocos nucifera*) is member of the family *Arecaceae*. It has a lot of uses as seen in the domestic, commercial and industrial use of the different parts. The shell is one of the waste products from these different uses and it is available in large quantities throughout the tropical and subtropical countries of the world. It has been used extensively in the preparation of activated carbon in the past. It is used in this study as a readily available and well studied waste plant material in carbon science to act as a baseline material for the comparison of the microwave-assisted and conventional hydrothermal carbonization process of a hard waste biomass.

Figure 4.3: Coconut shell [23]. A waste material obtained from the different uses of coconut.

Therefore the aim of this chapter is:

- To compare biochar and hydrochar from the the pyrolysis and green chemistry process of hydrothermal carbonization of *Prosopis africana* shell respectively.
- To compare the green chemistry processes of the microwave-assisted and conventional hydrothermal carbonization of *Prosopis africana* shell, rapeseed husk, and coconut shell.

4.2 Materials and Methods

Prosopis africana shell was collected locally in Benue State, North Central, Nigeria. The rapeseed husk was donated by Ian Dobson of the Institute for Chemistry in Industry, University of Hull, while the coconut shells were from coconuts bought from Tesco supermarket (Hull, UK). The materials were washed, dried, crushed and then sieved using 2 mm sieve and stored for use in the preparation of the biochar and hydrochar. The anhydrous D-Glucose was purchased from Fisher Scientific, UK.

4.2.1 Preparation of Pyrolytic Char (Biochar)

20 g of dried 2 mm sized *Prosopis africana* shell was pyrolysed in a muffle furnace (Carbolite CWF 1200, Carbolite, Sheffield, UK) at 350 °C for 10 minutes to produce a solid char. The char was removed from the furnace, allowed to cool down and stored in a dessicator. It is referred to as the biochar (B-PAS) and was used directly without further treatment in subsequent experiments.

4.2.2 Preparation of the Hydrothermal Char (Hydrochar)

4.2.2.1 Microwave-Assisted Hydrothermal Carbonization

The waste materials were hydrothermally carbonized using microwave heating in a 2.45 GHz microwave oven (MARS, CEM, Milton Keynes, UK equipped with XP1500 digestion vessels). The pressure was monitored in the reference vessel during the reaction using a pressure sensor and the temperature was monitored using an infrared fibre optic sensor installed in a ceramic sleeve in the same vessel.

For the *Prosopis africana* shell, rapeseed husk and coconut shell; 2 g each of the ground raw materials (2 mm sized) were weighed into a microwave reaction vessels made of Teflon and 30 mL of de-ionised water was added to each of the vessels to cover the solid. The vessels were sealed and placed in the microwave oven. The samples were heated between 150-200 °C in the microwave oven which was set to ramp to a given temperature in 5 minutes and then held at the temperature for 5-45 minutes (pressure at 200 °C was around 1.80 MPa). The reaction system was allowed to cool down to room temperature and the carbonized materials were filtered off using filter paper (Whatman filter paper number 3, ashless 11 cm). The solid chars obtained were washed several times with de-ionised water until neutral pH was obtained and dried in a conventional oven at 80 °C for 16 hours. The hydrochars prepared from the

microwave-assisted hydrothermal carbonization of *Prosopis africana* shell, rapeseed husk, and coconut shell are referred to as M-PAS, M-RSH and M-CS respectively.

For the glucose, 5 g of the glucose was dissolved in 5 mL of de-ionised water in a microwave reaction vessel made of Teflon to form a supersaturated solution and it was hydrothermally carbonized in the microwave oven using the procedure stated above. The hydrochar is referred to as HTC-G.

4.2.2.2 Conventional Oven Hydrothermal Carbonization

2 g of *Prosopis africana* shell, rapeseed husk and coconut shell were weighed each into different 50 mL non-stirred Teflon-lined stainless steel Parr autoclaves; 30 mL each of deionised water was added to each of the autoclaves. The autoclaves were sealed and placed in a programmable conventional oven and were heated at 150-200 °C for 2-4 hours. The oven was allowed to cool down to room temperature before removing the autoclaves. The chars produced were filtered, washed with deionised water until a neutral pH was obtained and dried in the oven at 80 °C for 16 hours. The hydrochars prepared from the conventional hydrothermal carbonization of *Prosopis africana* shell, rapeseed husk, and coconut shell are referred to as C-PAS, C-RSH and C-CS respectively.

In each case, the dry mass of the carbonized materials was measured and the percentage yield (dry mass percentage of the raw material) were calculated.

$$\%\ Yield = \frac{Mass\ of\ carbonized\ material}{Mass\ of\ raw\ material} \times 100 \qquad \text{(Equation 4.1)}$$

4.2.3 Ash Content Determination

2 g each of the carbonized materials were placed into weighed ceramic crucibles. The carbonized material and crucibles were dried for 16 hours at 80 °C and reweighed to obtain the dry carbon weight. The samples were heated in a furnace at 760 °C for 6 hrs. The crucibles were removed from the furnace, cooled in a dessicator and the remaining solids (ash) were weighed. Percentage ash was calculated by

$$\%\ Ash = \frac{Remaining\ solid\ weight}{Original\ carbon\ weight} \times 100 \qquad \text{(Equation 4.2)}$$

4.2.4 pH Measurement

1 % (wt/wt) suspension carbon materials in deionized water were prepared. The pH of the suspensions was measured with a pH meter (FisherBrand Hydrus 500, Fisher Scientific, Loughborough, UK). The pH meter was calibrated with pH 4 and pH 7 buffer solutions. The calibration was confirmed by analysis of a pH 7 buffer after every five analyses and a recalibration done if the value varied by more than ± 0.1 pH units.

All experiments were carried out in triplicate for all the materials.

4.3 Characterization Methods

The characterizations of the materials were carried out using the following instruments. The elemental (CHN) analysis was carried out using Fisons instruments EA 1108 CHN analyser (Fison Instrument, Crawley, UK); the samples were ground into fine powder and weighed into tin capsules. They were then placed on the autosampler for analysis. The surface area and pore size distribution were measured on a Micromeritics Tristar BET-N_2 surface area analyser (Micromeritics, Hexton, UK). Before carrying out the analysis the samples were degassed at 120 °C for 3 hrs. FT-IR spectra were recorded using Thermo Scientific Nicolet 380 FT-IR (Themo Scientific, Hemel Hempstead, UK), equipped with attenuated total reflectance (ATR) where the samples were in direct contact with the ATR diamond crystal. Each sample was investigated in the wavenumber range of 4000–525 cm^{-1} using 16 scans at a spectral resolution wavenumber of 4 cm^{-1}. The morphology and particle size was visualised using a ZEISS EVO 60 SEM (Carl Zeiss, Cambridge, UK); the samples were coated with gold and platinum alloy and impregnated on a sticky disc before analysis. ^{13}C solid-state magic angle spinning NMR experiment was carried out using a Bruker Avance II 500 MHz (11.74T) spectrometer (Bruker, Coventry, UK); the samples were packed without further treatment into a 4 mm zirconia rotor sample holder spinning at MAS rate ν_{MAS} = 8 KHz. Carbon sensitivity was enhanced using Proton-to-carbon CP MAS: recycle delay for all CP experiments was 3 s and TPPM decoupling was applied during signal acquisition. Cross polarization transfer was carried out under adiabatic tangential ramps to enhance the signal with respect to other known methods. CP time t_{CP} = 500 ms. The number of transients was 200 for all the carbon samples.

4.4 Results and Discussion

The biochar was prepared at 350 °C for 10 minutes due of the nature of the material. At a temperature > 350 °C, the *Prosopis africana* shell burned into ash. Similar observation was made when the time was > 10 minutes at 350 °C. In the hydrothermal processes, the Teflon vessels have a melting point of 250 °C and at temperatures close to that, the vessel will be too soft and can burst if the reaction generates too much heat and pressure. Reactions at 200 °C and below produce only low and weak pressure with the CO_2, methane and other gases produced during the decomposition process playing a minor role [1]. It has also been reported that in the temperature range of 200–250 °C, the carbon content remains relatively constant [24].

Temperature and Time	**C (%)**	**H (%)**	**N (%)**	**O[a] (%)**	**pH**	**Ash**
Raw *Prosopis africana* shell	46.58±0.01	6.44±0.04	1.57±0.09	45.41±0.10	5.34±0.02	
Biochar	70.84±0.06	4.67±0.09	1.57±0.01	22.92±0.16	6.48±0.05	25.23±1.02
Microwave (Hydrochar)						
200°C for 45 mins	57.23±0.90	5.68±0.04	1.49±0.02	35.54±0.88	4.57±0.02	9.25±0.10
200°C for 30 mins	56.06±1.05	6.47±0.08	1.58±0.01	35.89±0.98	4.54±0.00	9.17±0.80
200°C for 20 mins	58.08±1.12	6.18±0.80	1.61±0.01	34.13±0.31	4.05±0.03	9.32±0.50
200°C for 15 mins	55.81±0.06	6.61±0.09	1.60±0.01	35.98±0.14	4.21±0.01	9.05±0.45
200°C for 10 mins	55.69±0.00	6.92±0.03	1.57±0.02	35.82±0.05	4.37±0.01	9.10±0.10
200°C for 5 mins	55.46±0.08	6.71±0.05	1.48±0.00	36.35±0.06	4.51±0.00	8.72±0.85
170°C for 20 mins	54.41±0.15	6.22±0.01	1.50±0.00	37.87±0.14	4.59±0.01	8.80±0.30
150°C for 20 mins	52.47±0.09	6.36±0.02	1.57±0.01	39.60±0.08	4.77±0.01	8.51±0.70
Conventional						
200 °C for 4 hours	56.56±1.10	6.77±0.06	1.46±0.05	35.21±1.21	4.34±0.01	9.25±0.45
200 °C for 3 hours	53.85±1.02	6.53±0.01	1.40±0.05	38.22±0.96	4.41±0.02	9.01±0.32
200 °C for 2 hours	53.25±0.90	6.02±0.02	1.65±0.03	39.08±0.95	4.57±0.01	8.87±0.75
170 °C for 4 hours	52.53±1.00	6.60±0.12	1.40±0.07	39.47±0.95	4.77±0.01	8.45±0.30
170 °C for 3 hours	52.51±0.75	6.25±0.15	1.63±0.01	39.61±0.59	4.85±0.00	8.40±0.90
170 °C for 2 hours	51.70±1.05	6.37±0.23	1.57±0.04	40.36±1.32	4.97±0.01	8.23±0.55
150 °C for 4 hours	51.87±0.80	6.50±0.05	1.51±0.09	40.12±0.76	5.16±0.01	8.20±0.95
150 °C for 3 hours	49.29±1.22	6.55±0.01	1.41±0.07	42.75±1.14	5.37±0.00	8.13±0.63
150 °C for 2 hours	48.73±1.01	6.37±0.09	1.36±0.04	43.54±1.06	5.43±0.02	8.01±0.22

[a] The oxygen content was determined by difference [100% - (C%+H%+N%)] [10]

Table 4.1: CHN analysis, pH and ash contents of the chars from *Prosopis africana* shell (n=3)

Temperature and Time	C (%)	H (%)	N (%)	O[a] (%)	pH	Ash
Raw Rapeseed Husk	42.56±0.08	6.62±0.02	6.41±0.01	44.41±0.11	6.18±0.02	
Microwave						
200°C for 45 mins	55.70±1.29	6.85±0.30	6.63±0.20	30.82±0.79	5.72±0.01	10.86±0.53
200°C for 30 mins	54.03±0.90	6.61±0.01	5.84±0.49	33.52±1.38	5.12±0.00	10.90±0.33
200°C for 20 mins	54.62±1.02	6.45±0.13	6.74±0.22	34.19±1.37	5.26±0.01	10.80±0.75
200°C for 15 mins	50.86±0.80	6.40±0.25	6.53±0.14	37.21±0.41	5.38±0.01	10.21±0.42
200°C for 10 mins	48.01±1.00	6.37±0.38	6.45±0.09	39.17±1.47	5.45±0.00	10.05±0.73
200°C for 5 mins	46.35±0.52	6.32±0.21	6.39±0.02	40.94±0.29	5.60±0.02	9.65±0.82
170°C for 20 mins	46.21±1.12	6.35±0.32	6.61±0.11	40.83±1.55	5.78±0.00	9.83±0.55
150°C for 20 mins	44.13±0.75	6.38±0.22	6.40±0.01	43.09±0.54	5.92±0.01	9.13±1.05
Conventional						
200 °C for 4 hours	54.04±1.00	6.28±0.12	6.12±0.25	33.56±0.87	5.65±0.00	10.43±0.25
200 °C for 3 hours	54.33±0.74	6.65±.0.08	6.78±0.08	32.24±0.58	5.45±0.00	10.40±0.80
200 °C for 2 hours	55.45±0.53	6.43±0.10	5.93±0.17	32.19±0.46	5.48±0.00	10.35±0.10
170 °C for 4 hours	51.25±0.90	6.71±0.04	5.94±0.20	36.10±0.74	5.45±0.01	9.45±0.13
150 °C for 4 hours	46.72±0.95	6.58±0.22	6.17±0.05	40.53±1.12	5.95±0.01	9.00±0.33

Table 4.2: CHN analysis, pH and ash contents of hydrochars from rapeseed husk (n=3)

Raw Coconut Shell	**46.77±0.03**	**5.44±0.01**	**0.00±0.00**	**47.79±0.04**	**6.87±0.01**	
Microwave						
200°C for 45 mins	52.09±0.75	5.59±0.10	0.00±0.00	42.32±0.65	4.06±0.01	18.25±0.50
200°C for 30 mins	54.78±0.80	5.78±0.08	0.13±0.04	39.31±0.92	4.35±0.02	18.30±0.75
200°C for 20 mins	53.84±0.25	5.31±0.10	0.00±0.00	40.85±0.35	4.36±0.01	18.12±0.23
200°C for 15 mins	53.24±0.45	5.25±0.03	0.01±0.00	41.50±0.48	4.35±0.00	18.05±0.93
200°C for 10 mins	52.01±0.80	5.74±0.12	0.00±0.00	42.25±0.92	4.60±0.01	17.76±0.10
200°C for 5 mins	51.55±0.69	5.87±0.30	0.00±0.00	42.58±0.99	4.88±0.00	15.24±1.02
170°C for 20 mins	52.36±0.97	5.69±0.23	0.00±0.00	41.95±1.2	4.90±0.02	15.15±0.92
150°C for 20 mins	49.92±0.85	5.53±0.13	0.03±0.01	44.92±0.99	5.26±0.01	14.33±1.10
Conventional						
200 °C for 4 hours	52.61±1.05	5.83±0.05	0.00±0.00	41.56±1.10	5.22±0.05	18.00±0.75
200 °C for 3 hours	52.12±0.70	5.81±0.28	0.00±0.00	42.07±0.42	5.53±0.02	17.83±0.23
200 °C for 2 hours	51.43±0.65	5.73±0.20	0.01±0.00	42.83±0.85	5.60±0.01	17.55±0.45
170 °C for 4 hours	51.93±0.86	5.80±0.35	0.00±0.00	42.27±1.21	5.72±0.00	14.90±0.60
150 °C for 4 hours	49.21±0.70	5.48±0.01	0.00±0.00	45.31±0.69	5.96±0.00	14.40±0.35

Table 4.3: CHN analysis, pH and ash contents of hydrochars from coconut shell (n=3)

Temperature and Time	C (%)	H (%)	N (%)	O[a] (%)	pH	Ash
Raw Glucose	39.84±0.06	6.84±0.09	0.00	53.32±0.15	7.63±0.01	
200 °C for 45 mins	62.32±1.80	4.31±0.70	0.00	33.37±1.10	3.56±0.01	1.31±0.05
200 °C for 30 mins	58.64±0.60	4.90±0.55	0.00	36.46±1.15	3.59±0.01	1.13±0.10
200°C for 20 mins	60.66±2.15	4.64±1.58	0.00	34.70±0.57	3.61±0.01	1.10±0.15
200°C for 15 mins	52.81±0.12	4.61±0.10	0.00	42.58±0.02	3.72±0.00	0.73±0.21
200°C for 10 mins	NC	NC	NC	NC		
200°C for 5 mins	NC	NC	NC	NC		
170°C for 20 mins	NC	NC	NC	NC		
150°C for 20 mins	NC	NC	NC	NC		

NC (No carbonization)

Table 4.4: CHN analysis, pH and ash contents of the hydrochars from glucose (n=3)

4.4.1 Chemical Characteristics

The chemical characteristics of the materials were studied using elemental (CHN) analysis, attenuated total reflectance Fourier transform infrared (ATR-FTIR) and ^{13}C solid-state magic angle spinning nuclear magnetic resonance (NMR).

4.4.1.1 Elemental (CHN) Analysis, % Yield, pH and Ash Content

The carbon, hydrogen and nitrogen (CHN) compositions, pH, and ash content of the raw materials, biochar from *Prosopis africana* Shell, and hydrochars prepared using both the microwave-assisted and conventional hydrothermal carbonization of *Prosopis africana* shell, rapeseed husk, coconut shell and glucose are shown in Tables 4.1-4.4. The carbon contents of the chars were higher than that of raw materials, while the hydrogen and oxygen content were higher in the raw materials. The gradual increase in the carbon content in the chars with increase in temperature is due to the loss of hydrogen and oxygen due to deoxygenating, dehydration and decarboxylation reactions that occur during the hydrothermal carbonization process [5,24-26]. The increase in the carbon content was more in the biochar than the hydrochar from the *Prosopis africana* shell. A similar trend has been reportedly demonstrated with corn stover feedstock [27]. This shows that, pyrolysis at 350 °C decomposes the material more than hydrothermal carbonization at 200 °C and suggests more aromatization in the biochar as a result of the higher decrease in the amount of oxygen and hydrogen

content [10]. Similarly, the higher carbon content in the microwave-assisted process shows that it is faster in decomposing the raw materials to obtain carbon-enriched materials than the conventional method of oven heating [10].

The lower ash content in the hydrochar when compared with the biochar is due to the fact that most inorganic compounds contained in the *Prosopis africana* shell dissolved in the water during the hydrothermal process, and are therefore not retained in the hydrochar resulting in the increased acidic nature of the aqueous product released when compared with the raw material [27,28]. In all cases the acidity and ash content of the hydrochar increases as the carbon content increases, implying that the acidity and ash content could be dependent on the decomposition of the biomass. The acidity decreased in the biochar from the *Prosopis africana* shell due to the volatiles that were lost during the pyrolysis process. The result obtained in this study is consistent with previous reports as acidic pHs have been reported for hydrochar, and biochar produced from pyrolysis at temperatures of <400 °C [27,29].

Figure 4.4 and Figure 4.5 show the effects of temperature and time on the percentage yield by weight of the hydrochars. The % yield decreased gradually as the temperature and time of the carbonization increases in both the microwave-assisted and conventional hydrothermal carbonization for the *Prosopis africana* shell and rapeseed husk. This decrease in % yield is due to the loss of oxygen during the increasing liquefaction and gasification reactions, which are parallel reactions to the hydrothermal process of the biomass at a higher temperature and time [24,30,31]. A similar trend had been reported by Liu *et al*. [32] for coconut fibre and dead eucalyptus leaves using the conventional method of oven heating.

The coconut shell presents an opposite behaviour, the % yield increased as the temperature and time of the carbonization increases in both the microwave-assisted and conventional hydrothermal carbonization. The reason for this could be attributed to the nature of the material. The amount of volatile compounds could be higher in the *Prosopis africana* shell and rapeseed husk which reduces the solid yield in the carbonization step [33].

At temperature below 170 °C, there was no carbonization in the microwave-assisted hydrothermal process of the glucose; rather the supersaturated solution becomes homogenous. This is in agreement with previous reports that hydrothermal

carbonization of glucose in an autoclave produces a char yield at temperatures > 170 °C, due to the high solubility of glucose in water making it difficult for solid residues to be recovered by filtrations at low temperatures [4,24]. The maximum yield for the hydrothermal carbonization of glucose has been reported to be achieved at 200 °C, after which a gradual decrease in yield begins; the reason being that the increase in temperature favours gasification reactions [30] and this results in part of the hydrothermal carbon being lost in the form of volatile compounds [26]. Falco *et al*. [24] using conventional hydrothermal carbonization process reported a maximum yield of about 40% at 200 °C for glucose which is consistent with the yield obtained in this study under microwave heating.

In all the waste materials studied, the % yield at 200 °C for 20 minutes and 4 hours for the microwave-assisted and conventional hydrothermal carbonization processes respectively were close to each other. Hence, further discussions were carried out using the hydrochars prepared under these conditions.

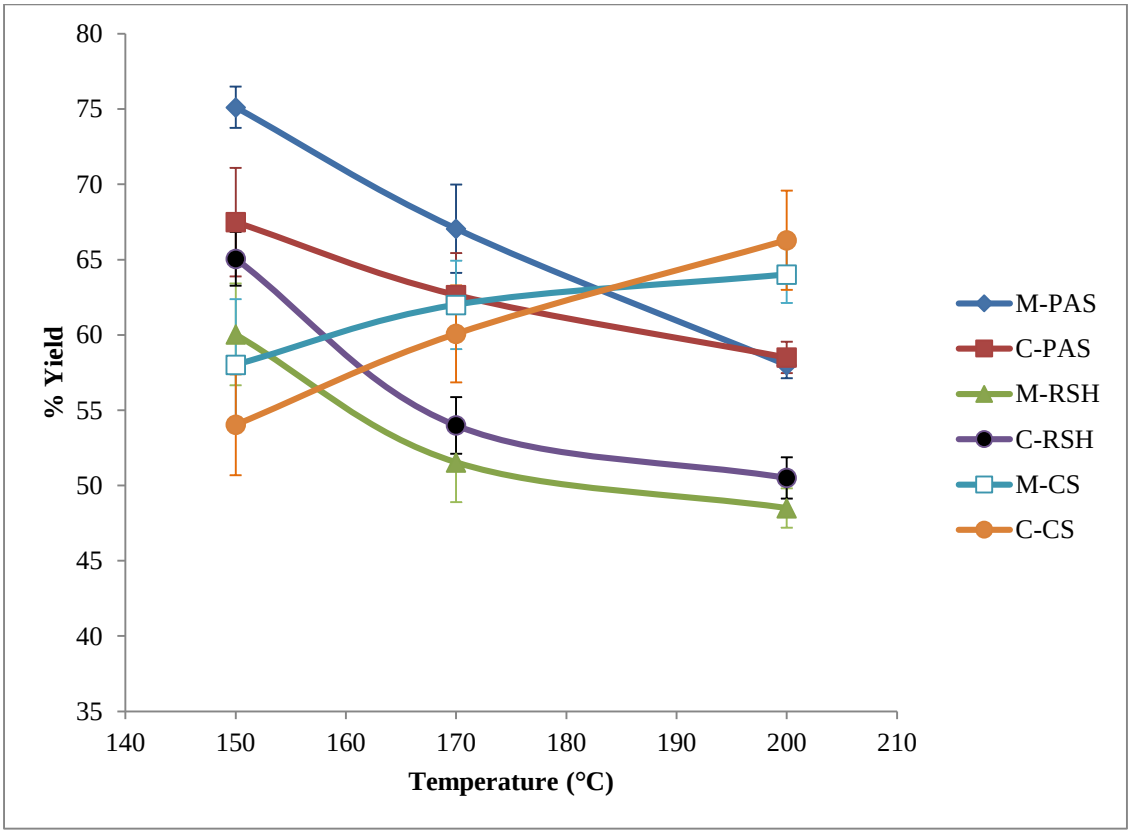

Figure 4.4: Effect of temperature on microwave-assisted and conventional process (n=3)

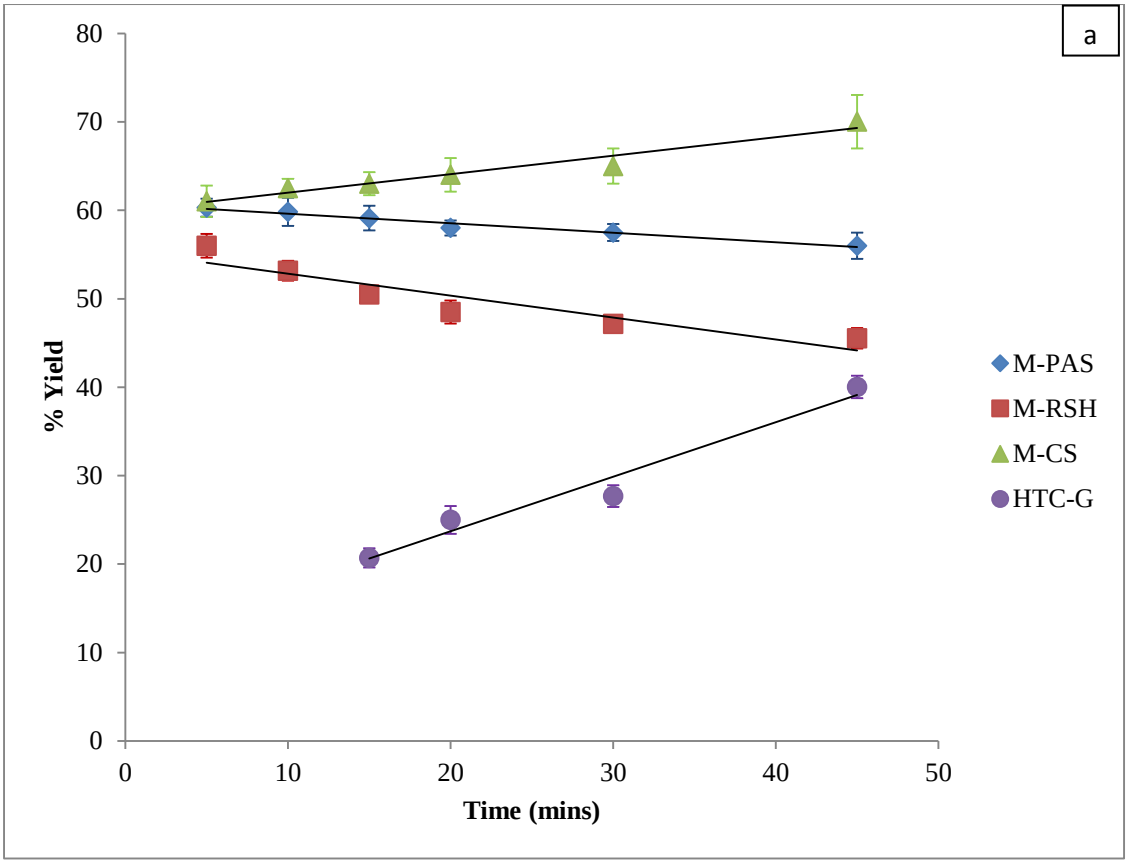

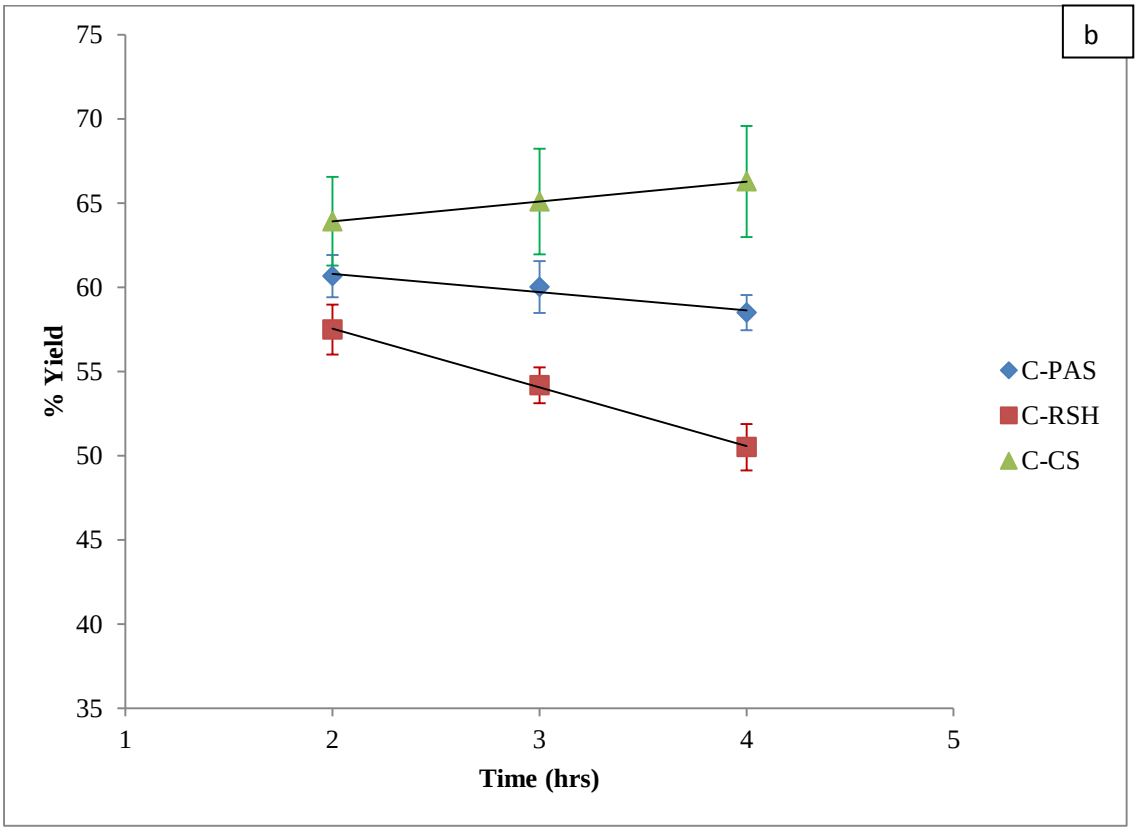

Figure 4.5: Effect of (a) time on the microwave-assisted hydrothermal process, (b) time on the conventional hydrothermal process (n=3)

4.4.1.2 ATR-FTIR Analysis

Section	Wavelength range (cm^{-1})	Functional group	Description
1	3700-3000	O-H stretching	Broad peak due to the presence of water, alcohols from cellulose or phenols from lignin.
2	3000-2800	C-H stretching	Small double peaks showing the stretching vibrations of aliphatic C-H bond.
3	1800-1650	C=O stretching	The vibration due to the esters, carboxylic acids or aldehydes present in the cellulose and lignin.
4	1650-1500	C=C stretching	Due to the vibration from the aromatic rings present in lignin.
5	1450-1200	C-H bending	Small peaks due to absorption from CH bond of aliphatic carbon, methylene, and methyl groups.
6	1200-950	C-O stretching	Due to vibration from esters, phenols, aliphatic alcohols.
7	< 950	C-H bending	Due to the deformation of the CH bond in aromatic compounds.

Table 4.5: Assignment of functional groups to FTIR-ATR peaks of the biochar and hydrochars

ATR-FTIR gave further insight into the chemical composition of the materials. In Figure 4.6 (a-d), the differences in the thermal decomposition process during pyrolysis of the *Prosopis africana* shell, and hydrothermal carbonization of the waste materials were illustrated by a comparison of their surface spectroscopy. The determination of the main functional groups for a given wavelength is based on previous reports [4,6,9,11,34]. Table 4.5 shows each of the major wavelength range that have been detected in the different materials and the associated functional groups. Similar results have been found in coal and other carbonized products [27,35]. The strong presence of single bond components, such as, C-O, C-H and O-H is expected since the raw materials used, apart from glucose, are lignocellulosic biomass which contains cellulose, hemicelluloses and lignin [36]. The presence of the lignin on the *Prosopis africana* shell (Figure 4.6 a), rapeseed husk (Figure 4.6 b) and coconut shell (Figure 4.6 c) is indicated by the peaks in the region of 1800-1500 cm^{-1} (C=O and C=C bonds) [34]. These peaks remained after the carbonization process, showing the presence of lignin fragments and intermediate structures in the resulting chars, indicating that under the studied conditions lignin did not totally decompose [32]. The higher intensity observed in the hydrochars from the coconut shell (Figure 4.6 c) is an indication that it has higher lignin content. The lower intensity of the spectrum of the chars shows that the functional groups on the raw materials decomposed via deoxygenating and dehydration reactions during the high temperature pyrolysis and

hydrothermal carbonization [32]. Due to the greater degree of decomposition during the pyrolysis process, the spectrum of the biochar (Figure 4.6 (a)) has low intensity for C-H and oxygen containing groups, and as a result showed higher level of aromaticity by the peaks below 950 cm^{-1} [34,35]. This observation is consistent with the results of elemental analysis.

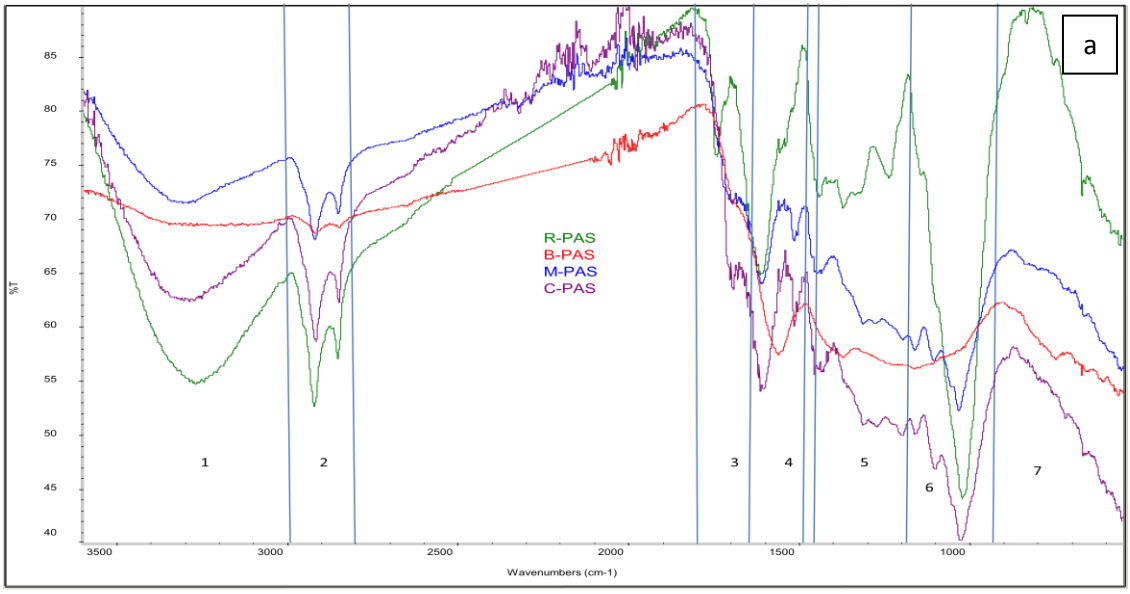

Figure 4.6 (a): ATR-FTIR spectra of raw and carbonized *Prosopis africana* shell showing the different sections and changes in the spectra due to different carbonization treatment (assignment of functional group is in Table 4.5)

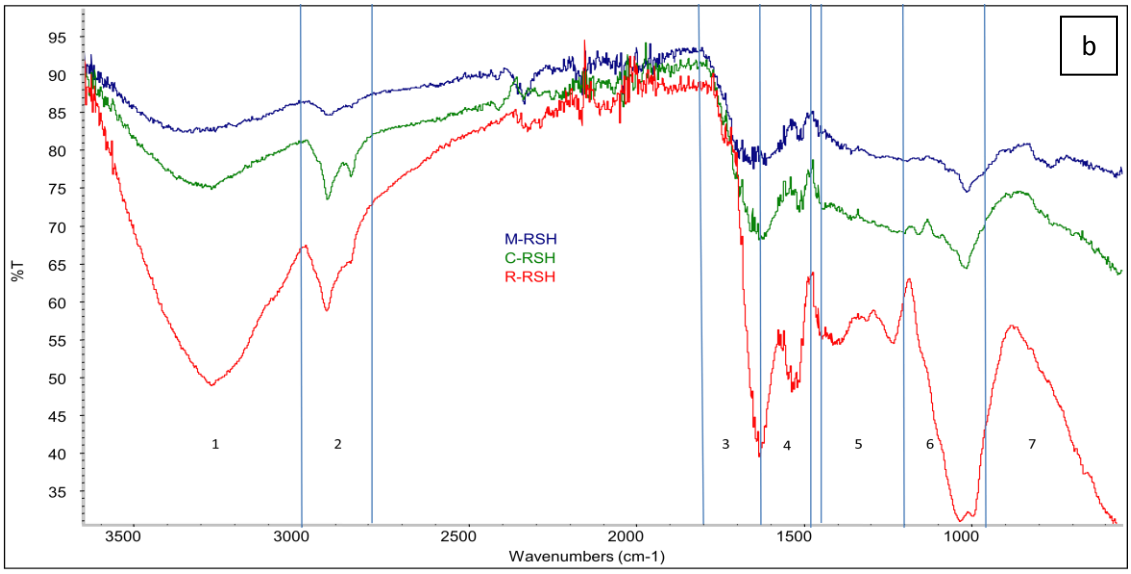

Figure 4.6 (b): ATR-FTIR spectra of raw and carbonized rapeseed husk showing the different sections and changes in the spectra due to different carbonization treatment (assignment of functional groups is in Table 4.5)

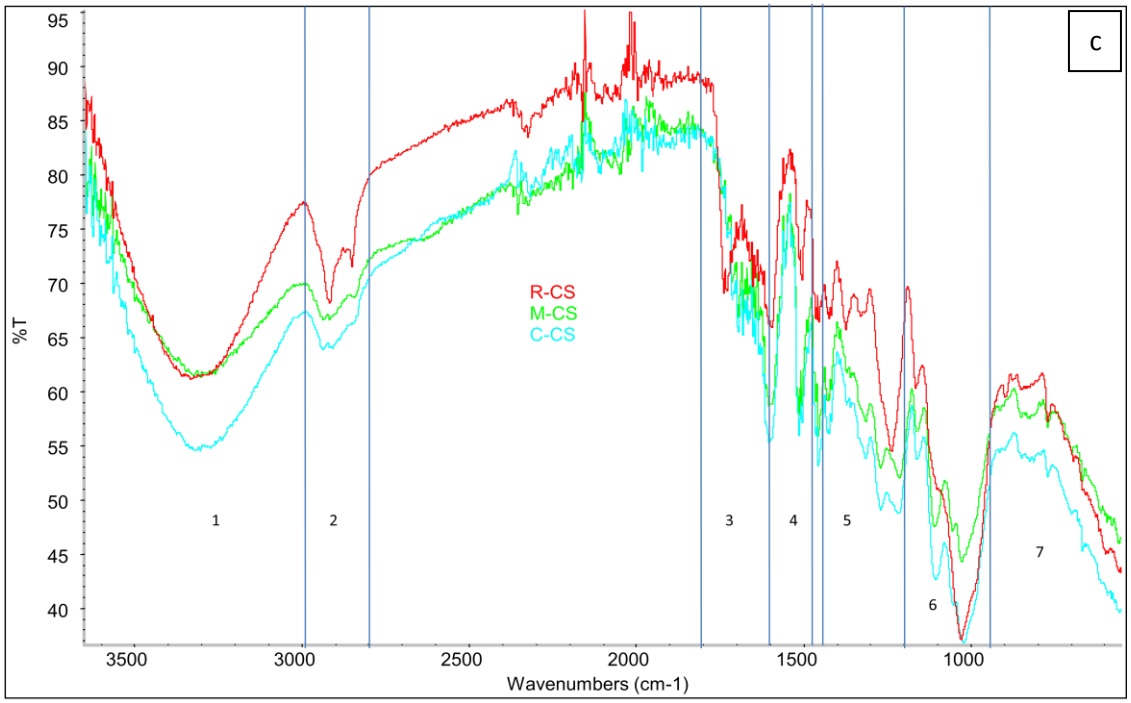

Figure 4.6 (c): ATR-FTIR spectra of raw and carbonized coconut shell showing the different sections and changes in the spectra due to different carbonization treatment (assignment of functional group is in Table 4.5)

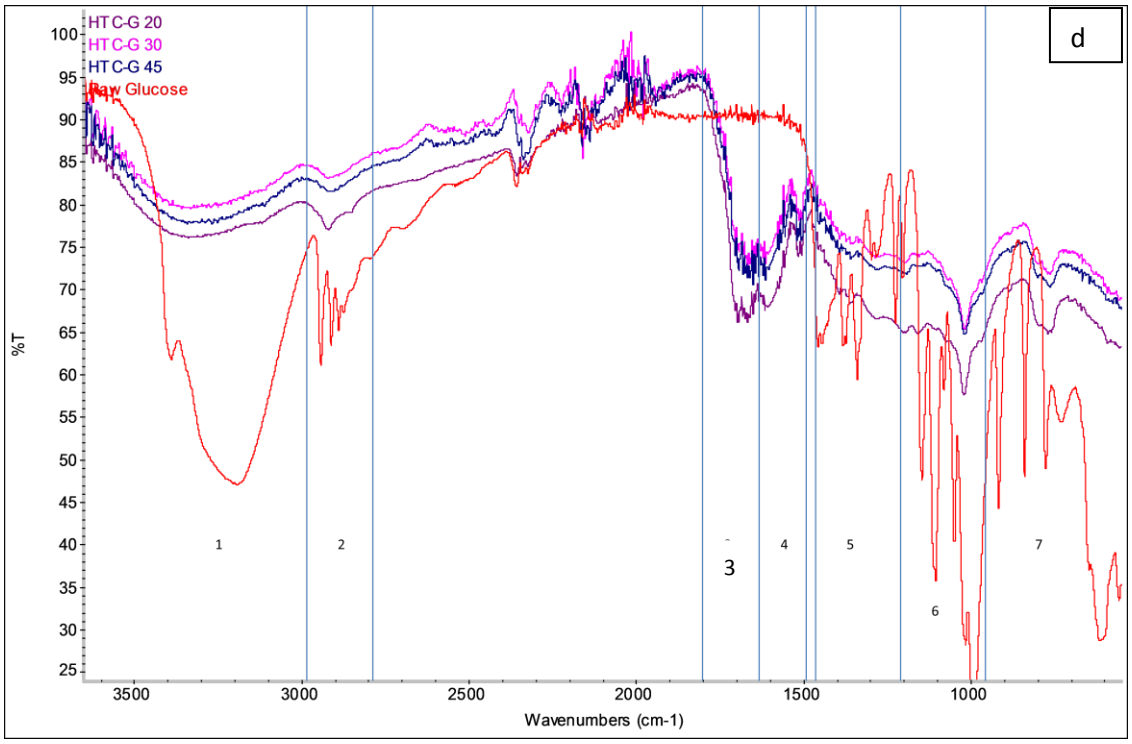

Figure 4.6 (d): ATR-FTIR spectra of raw and carbonized glucose showing the different sections and changes in the spectra due to different carbonization treatment (assignment of functional group is in Table 4.5). 20, 30, 45 are the time in the microwave.

4.4.1.3 ^{13}C Solid State NMR Analysis

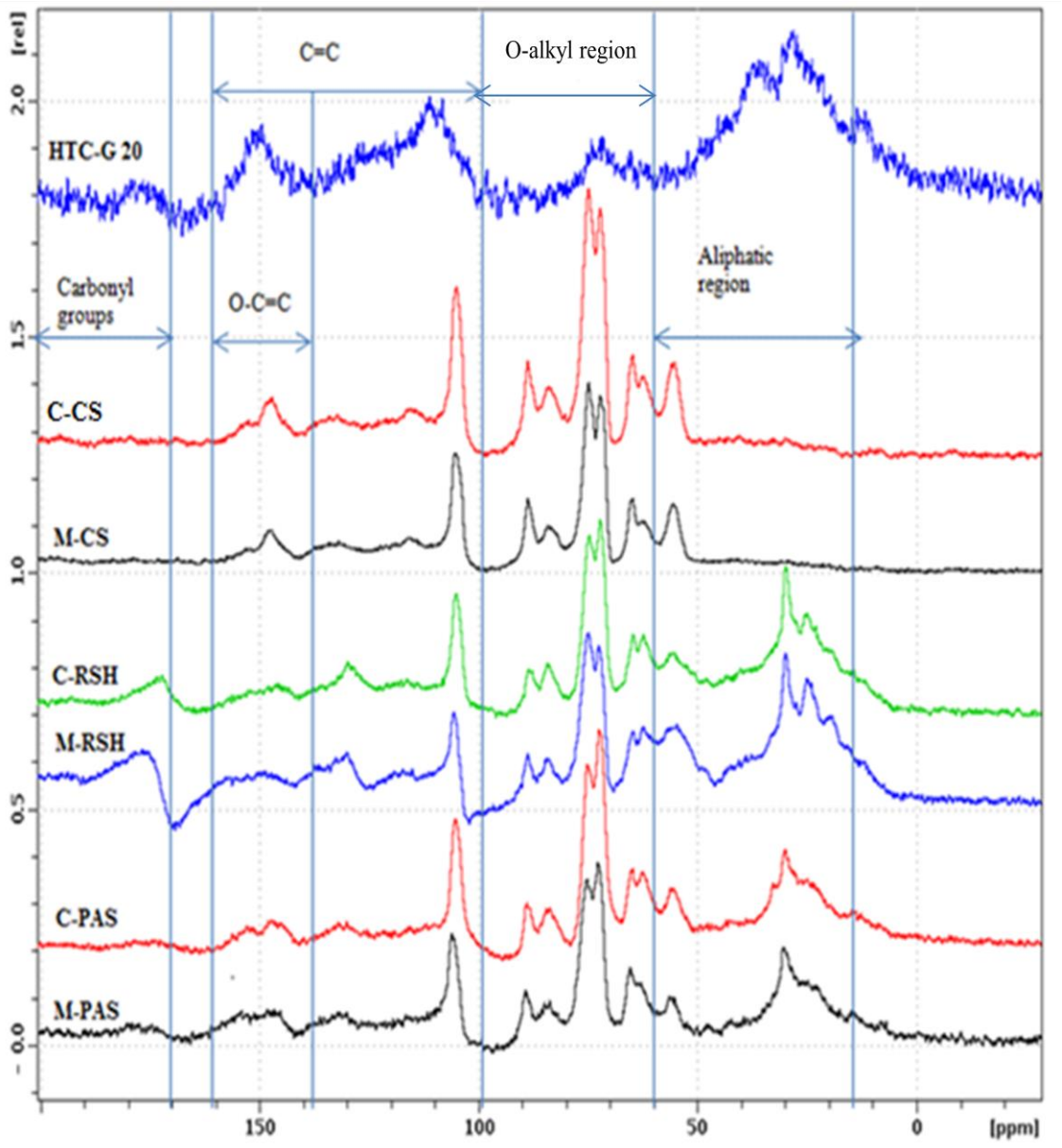

Figure 4.7: ^{13}C solid state cross-polarization magic-angle spinning NMR spectra showing the different functional groups present in the hydrothermal carbons obtained from microwave-assisted and conventional hydrothermal carbonization of glucose (HTC-G 20), coconut shell (C-CS, M-CS), rapeseed husk (C-RSH, M-RSH), and *Prosopis africana* shell (C-PAS, M-PAS)

The ^{13}C solid state NMR analysis of the hydrochars provides further information on the chemical structures and is used to further confirm the results from the FT-IR. ^{13}C solid state cross-polarization magic-angle spinning nuclear magnetic resonance spectroscopy (NMR) studies of the materials are shown in Figure 4.7. A close comparison between the NMR spectra of the hydrochars shows

very similar features. It was also observed that weaker signals were obtained for the microwave-assisted hydrothermal carbonization process, when compared to the hydrochar from the conventional hydrothermal process. The peaks between 14-60 ppm shows the presence of aliphatic carbons [6,37], while those in the region between 100-160 ppm usually referred to as the aromatic region are all due to C=C double bond from lignin, but between 140-160 ppm are specifically due to the oxygen bound O-C=C (O-aryl) [37]. The peaks in the region between 170-200 ppm present in the rapeseed and glucose hydrochars are due to the presence of carboxylic acid, aldehydes or ketones moieties [38]. Due to the cellulose and hemicellulose content of the materials, the spectra show carbohydrate resonances (specifically CH_2OH groups around 62 ppm, CHOH groups around 72 ppm and and anomeric O-C-O carbons around 90 ppm) in the O-alkyl region between 60 and 100 ppm [39,40]. The result is in good agreement with that of the FT-IR and a further confirmation of the nature of functional groups present in the materials. The NMR spectra in this study are similar to those of previous reports for hydrothermal carbonization of coconut fiber [32], poultry litter and swine solid [38]

4.4.2 Structural Characteristics

4.4.2.1 SEM Analysis

The scanning electron microscope (SEM) provided information about the structural morphologies of the different materials. The scanning electron microscopy (SEM) images of the raw and carbonised materials are shown in Figures 4.8-4.11. The SEM of the raw *Prosopis africana* shell (Figure 4.8 a), rapeseed husk (Figure 4.9 a) and coconut shell (Figure 4.10 a) show cellular structures which are typical of lignocellulosic materials, while that of the rapeseed husk showed in addition an oily surface morphology. The SEM image of the biochar from the *Prosopis africana* shell (Figure 4.8 b) shows a smooth surface that is non-porous. The smooth surface results from the melting and fusion process of lignin and other small molecules in the raw material, such as, pectin and inorganic compounds [41,42]. Although, residual cellular structure of the raw material can be seen on the biochar, this could be because the raw material was not destroyed completely due to short time and low temperature of the pyrolysis process [43]. The hydrochars from the *Prosopis africana* shell (Figures 4.8 c and d) and rapeseed husk (Figures 4.9 b and c) showed substantial changes in the

morphology from the raw material. However, in the coconut shell hydrochars (Figures 4.10 b and c) some features of the raw materials are still preserved. These results imply that the materials have undergone hydrolysis and partial carbonization as expected for hydrochars [5]. The aggregates of sphere-like microparticles (1-10 μm in diameter) seen on the hydrochars have their origin from the decomposition of cellulose during the hydrothermal carbonization, while the features that are preserved are due to the lignin present in the raw materials which has a greater chemical stability and thus can only undergo partial degradation [5,12]. More sphere-like particles were found on the SEM images of the hydrochars from the microwave-assisted process than in the conventional hydrothermal process, showing that decomposition of cellulose tend to be more under the microwave heating than the conventional oven heating in this study. The results also showed that the nature of the material affects the decomposition, and this is obvious from the SEM images of the raw coconut shell (Figures 4.10 a) and the hydrochar from the conventional hydrothermal carbonization of coconut shell (Figures 4.10 c) where the change in the morphology is minimal. Romero-Anaya *et al*. [44] reported that natural bio-fibres are classified into hard and soft biomass, and that the structural disintegration pathway for hard biomass tissue with a crystalline scaffold differs from that of the soft biomass. The melting point of the crystalline cellulose in the hard biomass is well above it's decomposition temperature, making the macro and microstructure of the biological tissue to be preserved as shown in the SEM image of the hydrochars from the coconut shell, while soft biomass has no crystalline cellulose scaffolds, forms liquid intermediates that polymerize or cyclise later to form fraction of spherical particles [1].

In the case of the glucose (Figure 4.11) the morphological features of the carbonized material (Figures 4.11 b) as visualised by using SEM are completely different from that of the raw glucose (Figures 4.11 a). Sphere-like microparticles of different sizes (1-10 μm) are seen on the SEM image of the microwave-assisted hydrothermal carbonized glucose, which is in contrast to the block of material observed in the raw glucose. A mechanism in which these microspheres are generated has been proposed and the mechanism is based on hydrolysis followed by dehydration and polymerization of saccharides and the spherical nuclei are formed in order to minimise the energy interface [9,10,19]. The SEM result obtained for the microwave-assisted

hydrothermal carbonization of glucose is consistent with those in the literature [4,6] using the conventional method of hydrothermal carbonization.

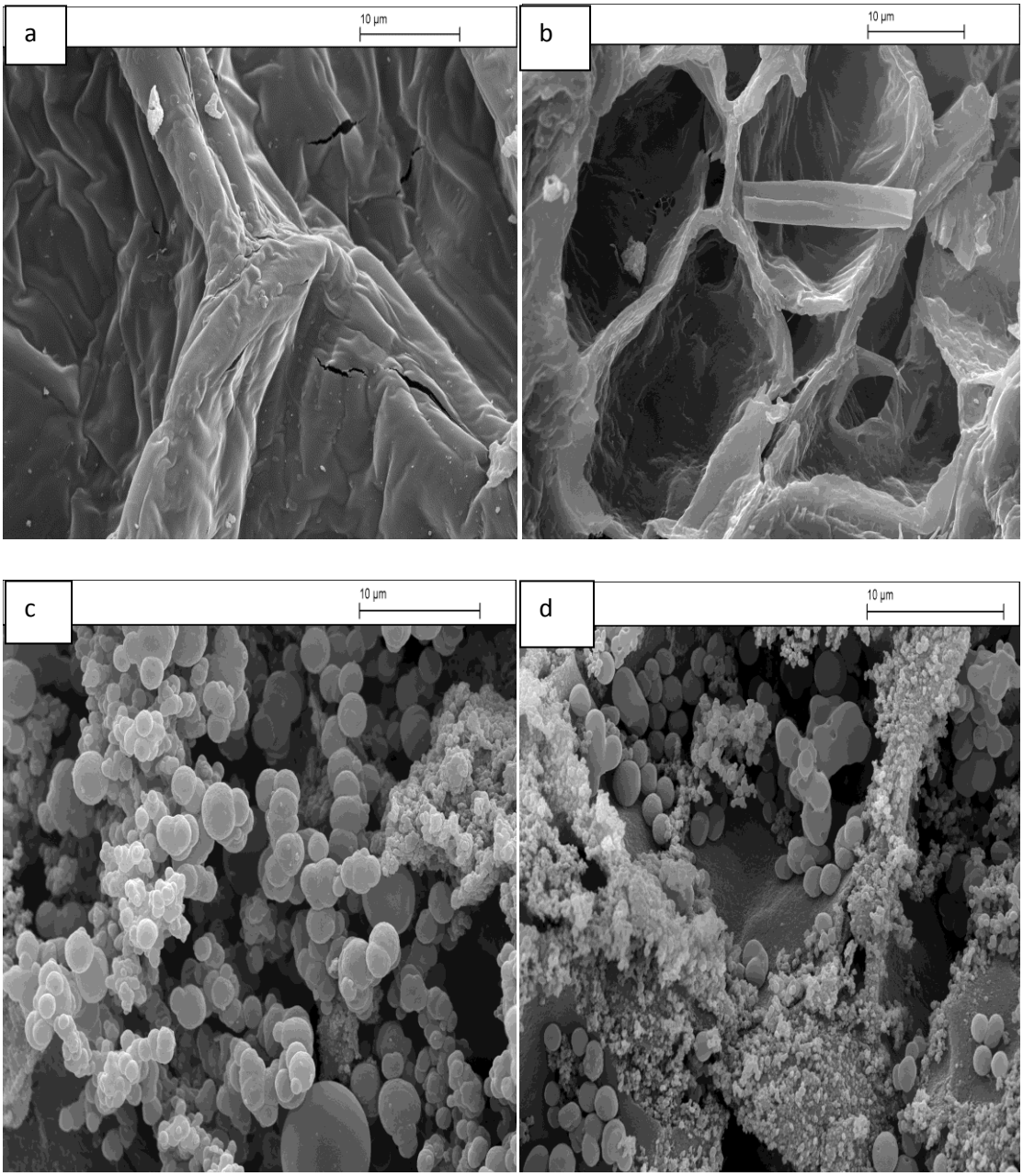

Figure 4.8: SEM images of (a) raw *Prosopis africana* shell showing cellular structure, (b) *Prosopis africana* shell biochar showing residual cellular structure due to high decomposition of the raw material during the pyrolysis process, (c) *Prosopis africana* shell microwave-assisted hydrochar showing decomposition of cellulose in the raw material indicated by sphere-like microparticles, (d) *Prosopis africana* shell conventional oven hydrochar showing less decomposition of cellulose indicated by fewer sphere-like microparticle

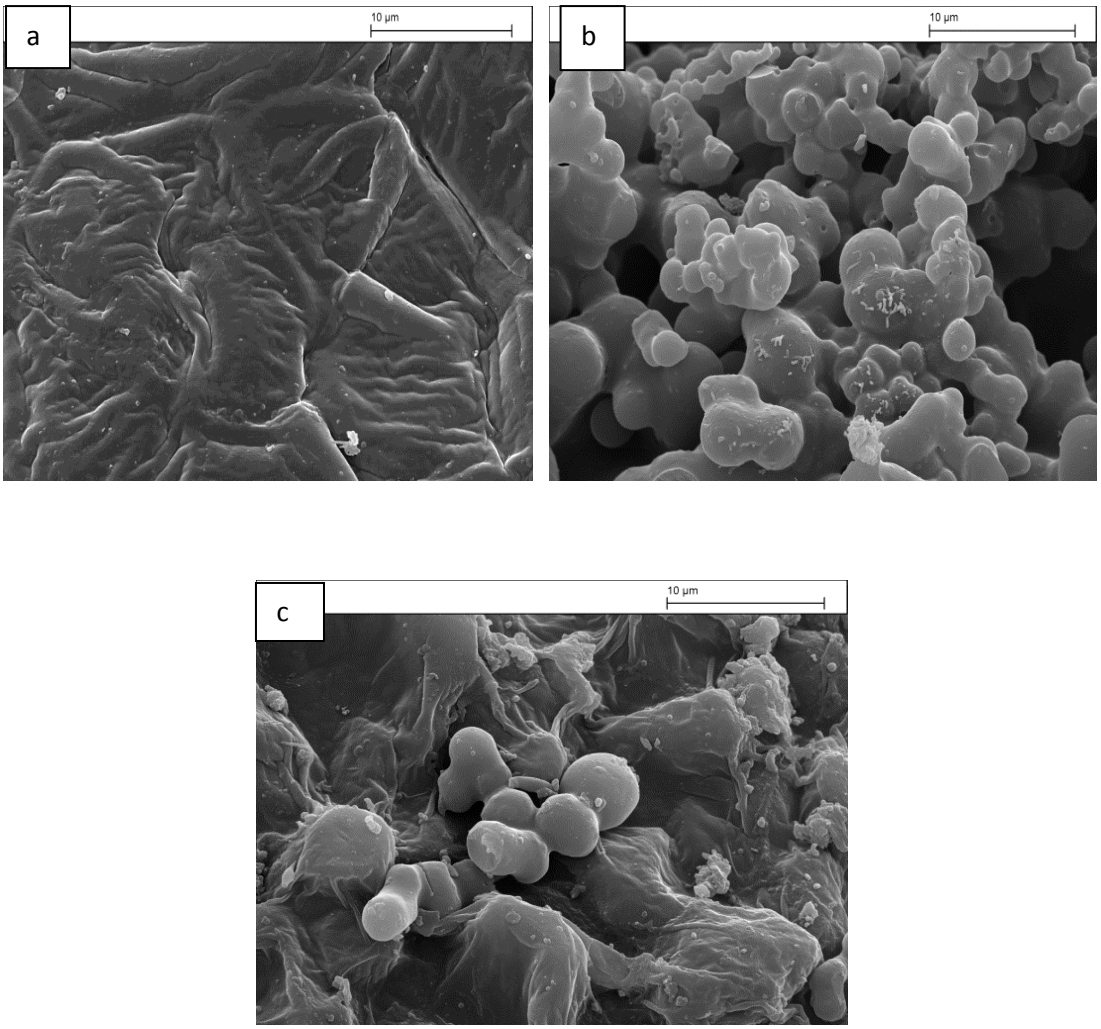

Figure 4.9: SEM images of (a) raw rapeseed showing cellular structure, (b) rapeseed microwave-assisted hydrochar showing decomposition of cellulose in the raw material indicated by sphere-like microparticles, (c) rapeseed conventional oven hydrochar showing less decomposition of cellulose indicated by fewer sphere-like microparticle

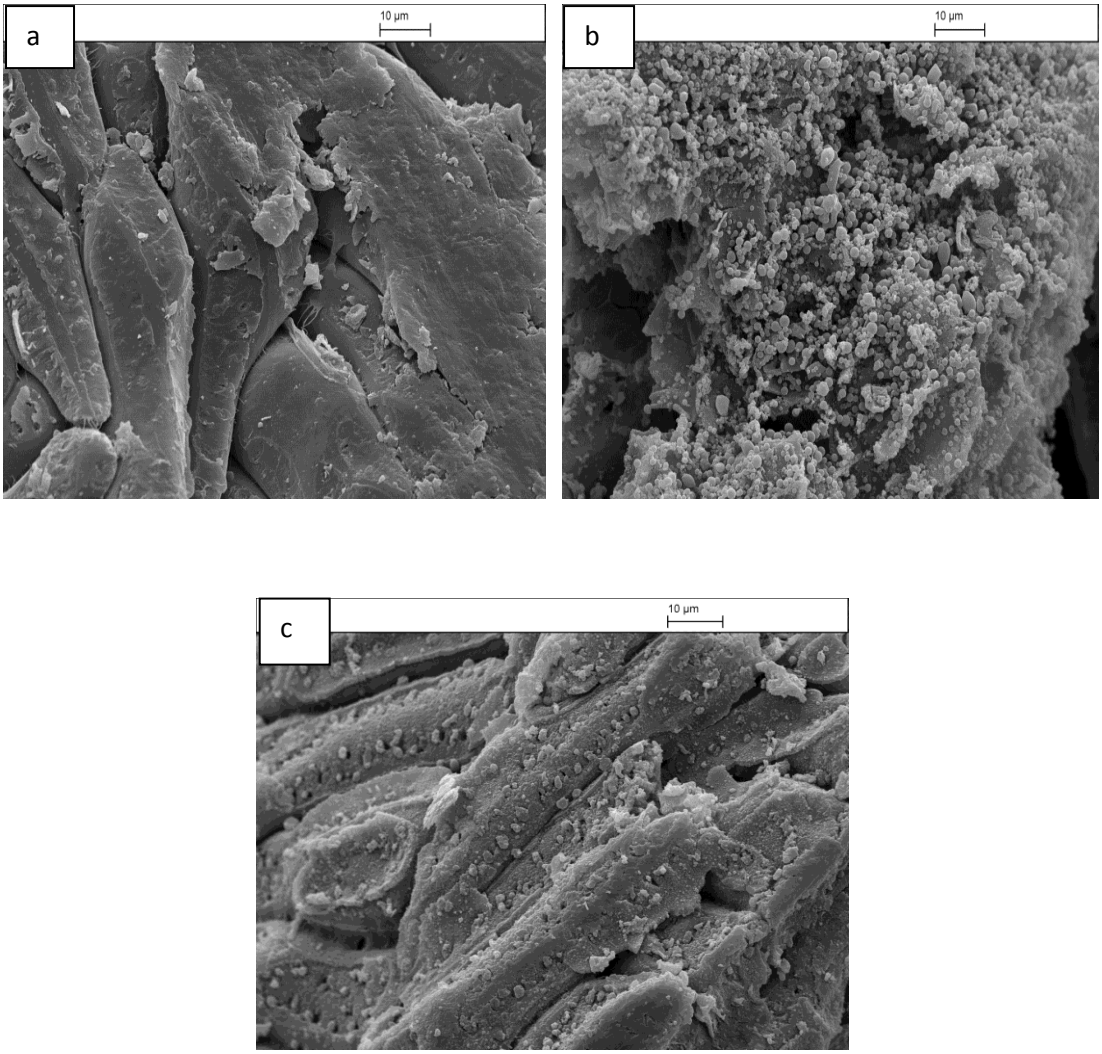

Figure 4.10: SEM images of (a) raw coconut shell showing cellular structure, (b) coconut shell microwave-assisted hydrochar showing decomposition of the raw material indicated by sphere-like microparticles, (c) coconut shell conventional oven hydrochar showing less decomposition of cellulose indicated by fewer sphere-like microparticle

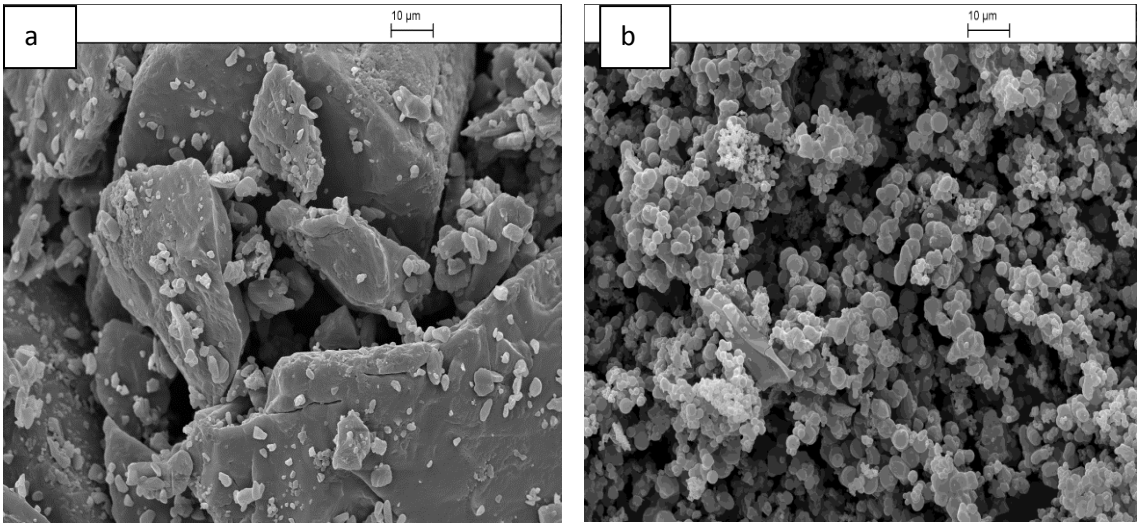

Figure 4.11: SEM images of (a) raw glucose, (b) microwave-assisted glucose hydrochar showing microspheres generated via hydrolysis, dehydration and polymerization

4.4.2.2 BET Surface Area Analysis

The nitrogen sorption measurements provided further insight into the changes in the waste materials and pore generation on carbonization. The nitrogen adsorption-desorption isotherm for the carbon materials prepared from the pyrolysis of *Prosopis africana* shell, microwave-assisted and conventional hydrothermal carbonization of *Prosopis africana* shell, rapeseed husk, coconut shell and glucose are shown in Figure 4.12 (a-h). All the prepared materials in this study showed characteristics that are representative of Type II isotherms based on the IUPAC system of classification, which is a typical type of isotherm obtained with non-porous materials [45]. It was not surprising therefore, that the prepared materials have relatively small BET surface areas due to the absence of porosity (Table 4.6), and in such situation the values of the specific surface area calculated only correspond to the external surface [27]. Slow pyrolysis (< 400 °C) results in biochars with low surface area and porosity, which is due to the condensation of the volatile organic compounds produced during the pyrolysis process on the char which block the pores and their adsorption potential [46-49], while the hydrothermal carbonization process involves carbonization as well as solubilisation of the organics and the formation of tarry substances, the hydrochar produced becomes contaminated with these substances thereby plugging the pores and this tends to make the apparent BET surface area of the sample to be very small [50].

The surface areas obtained in this study is consistent with previous studies which have reported low surface areas of 4.4 m^2/g and 8.3 m^2/g, less than 3 m^2/g, and 5.3 m^2/g for hydrochars from eucalyptus sawdust and barley straw, saccharides, and Japanese cedar (*Cryptomeria*) respectively [4,5,50], and 2.7-3.4 m^2/g for biochar from safflower seed cake [46]. Therefore, improvements of the porosity and the surface area of hydrochars are usually necessary to enable them fit into specific applications, such as, hydrogen storage or electrical energy storage (supercapacitors) [51], which has been achieved by carrying out further post synthesis processes, such as, combination of thermal and chemical activation that have resulted in a high surface area of >2000 m^2/g [52].

Material	**Method**	**Surface Area (m^2/g)**
Prosopis africana shell	Pyrolysis	3.1±1.0
Prosopis africana shell	Microwave-Assisted	6.1±2.2
Prosopis africana shell	Conventional method	5.9±1.8
Rapeseed husk	Microwave-Assisted	6.6±3.2
Rapeseed husk	Conventional method	3.2±1.2
Coconut Shell	Microwave-Assisted	5.7±2.4
Coconut Shell	Conventional method	3.3±1.1
Glucose	Microwave-Assisted	3.3±0.7

Table 4.6: Surface areas of the prepared carbon materials

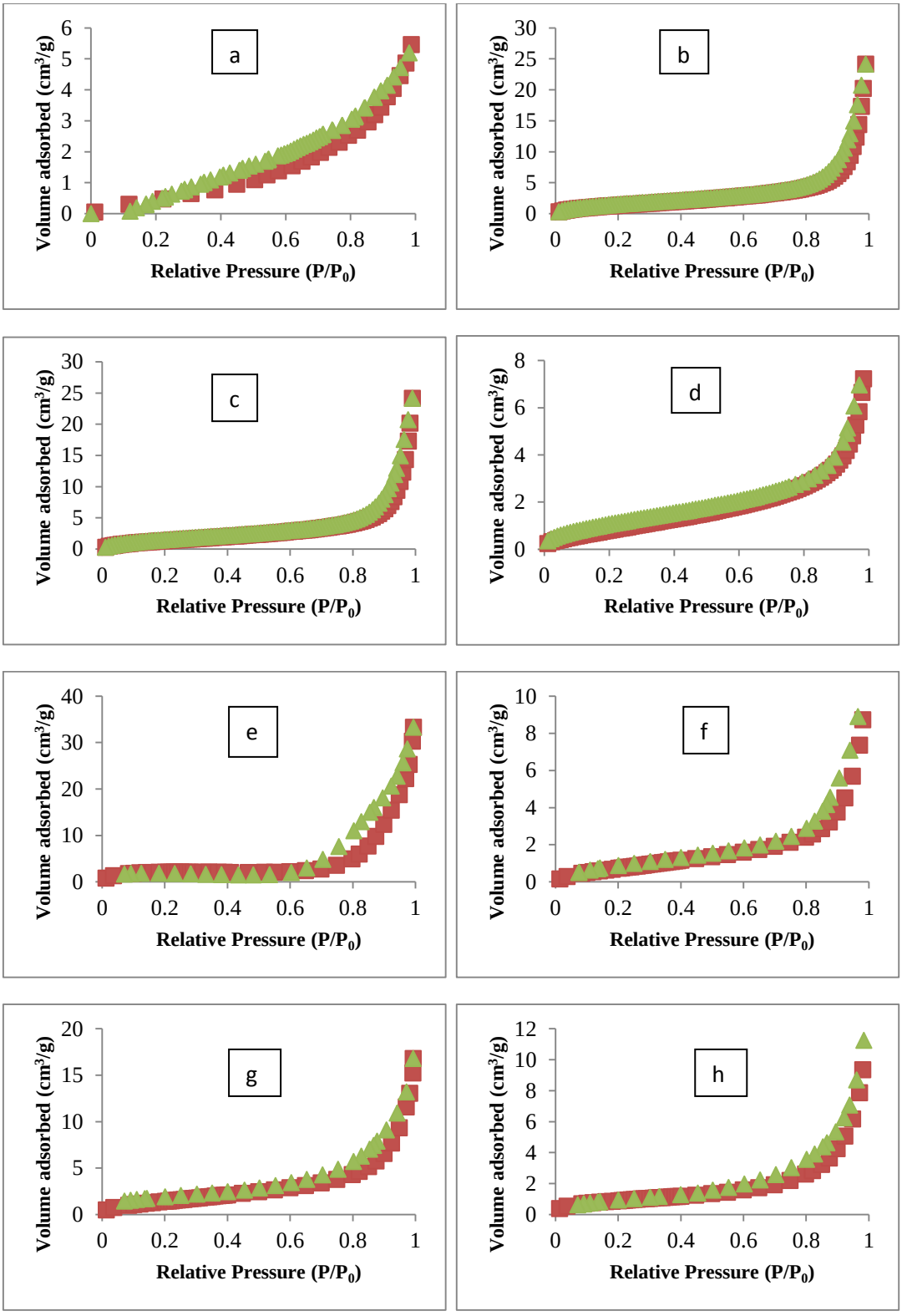

Figure 4.12: N_2 sorption isotherms of (a) *Prosopis africana* shell biochar, (b) *Prosopis africana* shell microwave-assisted hydrochar, (c) *Prosopis africana* shell conventional oven hydrochar, (d) microwave-assisted glucose hydrochar (e) rapeseed microwave-assisted hydrochar, (f) rapeseed conventional oven hydrochar, (g) coconut shell microwave-assisted hydrochar, (h) coconut shell conventional oven hydrochar, showing a Type II isotherm which is typical isotherm for non-porous materials.

4.5 Conclusion

Carbonaceous materials have been successfully prepared from waste plant materials and glucose using pyrolysis, microwave-assisted and the conventional method of hydrothermal carbonization. The prepared materials were characterized structurally and chemically using different analytical and spectroscopic techniques. Interestingly, the results obtained using the microwave-assisted hydrothermal process are consistent with that of the conventional method of oven heating. Therefore, the microwave-assisted hydrothermal approach offers a newer method to synthesize hydrothermal materials through hydrolysis and subsequent carbonization of the raw materials and also provides a way of converting a waste materials into a useful form. It has advantage over the conventional method of hydrothermal carbonization using oven heating as it requires a shorter time (20 minutes) to achieve the result that was obtained in 4 hours using the conventional method of oven heating. This method could be important in the development of new materials and have a positive impact in green chemistry.

4.6 References

[1] Antonietti, M, Titirici, MM, Thomas, A, Yu, SH, Muller, JO. A Direct Synthesis of Mesoporous Carbons with Bicontinuous Pore Morphology from Crude Plant Material by Hydrothermal Carbonization. Chem Mater 2007; 19: 4205-4212.

[2] Beaumontt, O, Schwob, Y. Influence of Physical and Chemical Parameters on Wood Pyrolysis. Ind Eng Chem Process Des Dev 1984, 23: 637-641.

[3] Di Blasi, C, Signorelli, G, Di Russo, C, Rea, G. Product Distribution from Pyrolysis of Wood and Agricultural Residues. Ind Eng Chem Res 1999; 38: 2216-2224.

[4] Sevilla, M, Fuertes, AB. Chemical and Structural Properties of Carbonaceous Products Obtained by Hydrothermal Carbonization of Saccharides. Chem-Eur J 2009; 15: 4195-4203.

[5] Sevilla, M, Macia-Agullo, JA, Fuertes, AB. Hydrothermal Carbon of Biomass as a Route for the Sequestration of CO_2: Chemical and Structural Properties of the Carbonized Products. Biomass Bioenerg, 2011, 35: 3152-3159.

[6] Titirici, MM, Demir-Cakan, R, Baccile, N, Antonietti, M. Carboxylate-Rich Carbonaceous Materials via One-Step Hydrothermal Carbonization of Glucose in the Presence of Acrylic Acid. Chem Mater 2009; 21: 484-490.

[7] Bergius, F, Specht, H. Die Anwendung hoher Drucke bei chemischen Vorgangen und eine Nachbildung des Entstehungsprozesses der Steinkohle. Wilhelm Knapp Halle ad Saale 1913; 41-58.

[8] Heilmann, SM, Davis, HT, Jader, LR, Lefebvre, PA, Sadowsky, MJ, Schendel, FJ, *et al*. Hydrothermal Carbonization of Microalgae. Biomass Bioenerg 2010; 34: 875-882.

[9] Sevilla, M, Fuertes, AB. The Production of Carbon Materials by Hydrothermal Carbonization of Cellulose. Carbon 2009; 47: 2281-2289.

[10] Guiotoku, M, Rambo, CR, Hansel, FA, Magalhaes, WLE, Hotza, D. Microwave-assisted Hydrothermal Carbonization of Lignocellulosic Materials. Mater Lett 2009; 63: 2707-2709.

[11] Titirici, MM, Antonietti, M, Baccile, N. Hydrothermal Carbon from Biomass: A Comparison of the Local Structure from Poly- to Monosaccharides and Pentoses/Hexoses. Green Chem 2008; 10: 1204-1212.

[12] Antonietti, M, Titirici, MM. Coal from Carbohydrates: The "Chimie Douce" of Carbon. CR Chim 2010; 13: 167-173.

[13] Yu, SH, Hu, B, Wang, K, Wu, LH, Antonietti, M, Titirici, MM. Engineering Carbon Materials from the Hydrothermal Carbonization Process of Biomass. Adv Mater 2010; 22: 813-828.

[14] Hoekman, SK, Broch, A, Robbins, C. Hydrothermal Carbonization (HTC) of Lignocellulosic Biomass. Energ Fuel 2011; 25: 1802-1810.

[15] Baccile, N, Laurent, G, Coelho, C, Babonneau, F, Zhao, L, Titirici, MM. Structural Insights on Nitrogen-Containing Hydrothermal Carbon Using Solid-State Magic Angle Spinning ^{13}C and ^{15}N Nuclear Magnetic Resonance. J Phys Chem C 2011; 115: 8976-8982.

[16] Mao, JD, Cao, XY, Ro, KS, Chappell, M, Li, YA. Chemical Structures of Swine-Manure Chars Produced under Different Carbonization Conditions Investigated by Advanced Solid-State ^{13}C Nuclear Magnetic Resonance (NMR) Spectroscopy. Energ Fuel 2011; 25: 388-397.

[17] Nüchter, M, Ondruschka, B, Bonrath, W, Gum, A. Microwave Assisted Synthesis-A Critical Technology Overview. Green Chem 2004; 6: 128-141.

[18] Clarke, E, Sutton, WH. Microwave Processing of Material. Annu Rev Mater Sci 1996; 26: 299-331.

[19] Yao, C, Shin, Y, Wang, LQ, Windisch, CF, Samuels, WD, Arey, BW, *et al*. Hydrothermal Dehydration of Aqueous Fructose Solutions in a Closed System. J Phys Chem C 2007; 111: 15141-15145.

[20] Agboola, DA. *Prosopis africana* (Mimosaceae): Stems, Roots and Seeds in the Economy of the Savannah Areas of Nigeria. Econ Bot 2004; 58 (Suppl): S34–S42.

[21] Akaaimo, DI, Raji, AO. Some Physical and Engineering Properties of *Prosopis africana* Seed. Biosyst Eng 2006; 95: 197-205.

[22] http://www.naturalfoodfinder.co.uk/rapeseedcanolablog. Accessed June 20, 2013.

[23] http://originexports.com/products/coconut-products/coconut-shell. Accessed June 20, 2013.

[24] Falco, C, Baccile, N, Titirici, MM. Morphological and Structural Differences between Glucose, Cellulose and Lignocellulosic Biomass Derived Hydrothermal Carbons. Green Chem 2011; 13: 3273-3281.

[25] Kang, S, Li, X, Fan, J, Chang, J. Characterization of Hydrochars Produced by Hydrothermal Carbonization of Lignin, Cellulose, D-Xylose, and Wood Meal. Ind Eng Chem Res 2012; 51: 9023-9031.

[26] Berge, ND, Ro, KS, Mao, J, Flora, JRV, Chappell, MA, Bae, S. Hydrothermal Carbonization of Municipal Waste Streams. Environ Sci Technol 2011; 45: 5696-5703.

[27] Fuertes, AB, Arbestain, MC, Sevilla, M, Maciá-Agulló, JA, Fiol, S, López, R, *et al*. Chemical and Structural Properties of Carbonaceous Products Obtained by Pyrolysis and Hydrothermal Carbonisation of Corn Stover. Aust J Soil Res 2010; 48: 618-626.

[28] Liu, Z, Zhang, FS, Wu, J. Characterization and Application of Chars Produced from Pinewood Pyrolysis and Hydrothermal Treatment. Fuel 2010; 89: 510-514.

[29] Calvelo-Pereira, R, Pardo-Lorenzo, R, Aitkenhead, W, Macias, F, Hedley, M, Macia-Agullo, JA, *et al*. Influence of Pyrolysis Temperature on Heterotrophic Basal Soil in Biochar/Soil Mixtures. New Zealand Biochar Research Centre Workshop; Palmerston North, New Zealand, 2010.

[30] Kruse, A, Gawlik, A. Biomass Conversion in Water at 330-410 °C and 30-50 MPa. Identification of Key Compounds for Indicating Different Chemical Reaction Pathways. Ind Eng Chem Res 2003; 42: 267-279.

[31] Möller, M, Nilges, P, Harnisch, F, Schröder, U. Subcritical Water as Reaction Environment: Fundamentals of Hydrothermal Biomass Transformation. ChemSusChem, 2011; 4: 566-579.

[32] Liu, Z, Quek, A, Hoekman, SK, Balasubramania, R. Production of Solid Biochar Fuel from Waste Biomass by Hydrothermal Carbonization. Fuel 2013; 103: 943-949.

[33] Macías-García, A, Cuerda-Correa, EM, Olivares-Marín, M, Díaz-Paralejo, A, Díaz-Díez, MÁ. Development and Characterization of Carbon-Honeycomb Monoliths from Kenaf Natural Fibers: A Preliminary Study. Ind Crop Prod 2012; 35: 105-110.

[34] Jamari, SS, Howse, JR. The Effect of the Hydrothermal Carbonization Process on Palm Oil Empty Fruit Bunch. Biomass Bioenerg 2012; 47: 82-90.

[35] Ibarra, JV, Muñoz, E, Moliner, R. FTIR Study of the Evolution of Coal Structure during the Coalification Process. Org Geochem 1996; 24: 725-735.

[36] Vassilev, SV, Baxter, D, Andersen, LK, Vassileva, CG, Morgan, TJ. An Overview of the Organic and Inorganic Phase Composition of Biomass. Fuel 2012; 94: 1-33.

[37] Baccile, N, Laurent, G, Babonneau, F, Fayon, F, Titirici, MM, Antonietti, M. Structural Characterization of Hydrothermal Carbon Spheres by Advanced Solid-State MAS ^{13}C NMR Investigations. J Phys Chem C 2009; 113: 9644-9654.

[38] Sun, K, Ro, K, Guo, M, Novak, J, Mashayekhi, H, Xing, B. Sorption of Bisphenol A, 17α-Ethinyl Estradiol and Phenanthrene on Thermally and Hydrothermally Produced Biochars. Bioresource Technol 2011; 102: 5757-5763.

[39] Cao, X, Ro, KS, Chappell, M, Li, Y, Mao, J. Chemical Structures of Swine-Manure Chars Produced under Different Carbonization Conditions Investigated by Advanced Solid-State ^{13}C Nuclear Magnetic Resonance (NMR) Spectroscopy. Energ Fuels 2011; 25: 388-397.

[40] Mao, J, Holtman, KM, Scott, JT, Kadla, JF, Schmidt-Rohr, K. Differences between Lignin in Unprocessed Wood, Milled Wood, Mutant Wood, and Extracted Lignin Detected by ^{13}C Solid-State NMR. J Agric Food Chem 2006; 54: 9677-9686.

[41] Sharma, RK, Wooten, JB, Baliga, VL, Lin, X, Chan, WG, Hajaligol MR. Characterization of Chars from Pyrolysis of Lignin. Fuel 2004; 83: 1469-1482.

[42] Cetin, E, Moghtaderi, B, Gupta, R, Wall, TF. Influence of Pyrolysis Conditions on the Structure and Gasification Reactivity of Biomass Chars. Fuel 2004; 83: 2139-2150.

[43] Mohan, D, Rajput, S, Singh, VK, Steele, PH, Pittman Jr, CU. Modeling and Evaluation of Chromium Remediation from Waste Water using Low Cost Bio-Char, a Green Adsorbent. J Hazard Mater 2011; 188: 319-333.

[44] Romero-Anaya, AJ, Lillo-Ródenas, MA, de Lecea, CS, Linares-Solano, A. Hydrothermal and Conventional H_3PO_4 Activation of Two Natural Bio-Fibers. Carbon 2012; 50: 3158-3169.

[45] Sing, KSW, Everett, DH, Haul, RAW, Moscou, L, Pierotti, RA, Rouquerol, J, *et al*. Reporting Physisorption Data for Gas/Solid Systems. Pure Appl Chem 1985; 57: 603-619.

[46] Angın, D. Effect of Pyrolysis Temperature and Heating Rate on Biochar Obtained from Pyrolysis of Safflower Seed Press Cake. Bioresource Technol 2013; 128: 593-597.

[47] Ronsse, F, van Hecke, S, Dickinson, D, Prins, W. Production and Characterization of Slow Pyrolysis Biochar: Influence of Feedstock Type and Pyrolysis Conditions. GCB Bioenergy 2013; 5: 104-115.

[48] Kwon, S, Pignatello, JJ. Effects of Natural Organic Substances on the Surface and Adsorptive Properties of Environmental Black Carbon (Char): Pseudo Pore Blockage by Model Lipid Components and its Implications for N_2-Probed Surface Properties of Natural Sorbents. Environ Sci Technol 2005; 39: 7932-7939.

[49] Pignatello, JJ, Kwon, S, Lu, Y. Effects of Natural Organic Substances on the Surface and Adsorptive Properties of Environmental Black Carbon (Char): Attenuation of Surface Activity by Humic and Fulvic acids. Environ Sci Technol 2006; 40: 7757-7763.

[50] Mochidzuki, K, Sato, N, Sakoda, A. Production and Characterization of Carbonaceous Adsorbents from Biomass Wastes by Aqueous Phase Carbonization. Adsorption 2005; 11: 669-673.

[51] Parshetti, GK, Hoekman, SK, Balasubramanian, R. Chemical, Structural and Combustion Characteristics of Carbonaceous Products Obtained by Hydrothermal Carbonization of Palm Empty Fruit Bunches. Bioresource Technol 2013; 135: 683-689.

[52] Sevilla, M, Fuertes, AB, Mokaya, R. High Density Hydrogen Storage in Superactivated Carbons from Hydrothermally Carbonized Renewable Organic Materials. Energy Environ Sci 2011; 4: 1400-1410.

Chapter 5

Application of the Biochar and Hydrochar from *Prosopis africana* shell for the Adsorption of Lead and Cadmium Ions from Aqueous Solution

5.1 Introduction

The rapid growth in industries, such as, fertilizer, tannery, petroleum, pesticides, paper, etc and also due to the increase in other human activities, such as, agriculture, mining and metal plating have led to the direct and indirect discharge of untreated wastewater into the environment, most especially in the developing countries of the world. Heavy metals are elements with high densities and are toxic to humans and other animals. Heavy metals, unlike the organic contaminants, tend to accumulate and persist in the living organism or environment because they are not biodegradable [1], their existence in the environment can only be managed by removal. Water pollution caused by heavy metals is already a known fact and has been a serious environmental problem worldwide with cumulative, chronic and harmful effects on the environment and human health. Elements such as lead, cadmium, chromium and nickel are classified as heavy metals and are associated with water pollution with lead and cadmium being amongst the most toxic to human beings found in higher concentrations in aqueous industrial wastewater [2]. Lead is used in various industrial activities, such as, electrical goods, batteries, chemical catalysis, metal surface finishing and in the manufacturing of alloys, while cadmium is used in the plastic industries, and other activities, such as, metal plating, batteries and pigment manufacturing [3]. During the various activities lead and cadmium are discharged in the effluent into the environment, mostly water bodies. Damage to the liver and kidney, infertility and abnormalities in pregnancy, mental retardation, and reduction in haemoglobin formation are some of the effects of lead poisoning, while exposure to cadmium can cause kidney dysfunction with high levels of exposure resulting in death [1]. In some cases, the effluents are discharged untreated into the water bodies, which is usually the case in most developing countries due to poor environmental regulations and government policies. Heavy metal concentration in drinking water should be very low in the microgram per litre (μg/L) range. For example, the permissible concentration of lead and cadmium are respectively 0.01 and 0.003 mg/L according to the World Health Organisation (WHO) guidelines [4].

There are various methods for heavy metals removal from wastewater. These methods include precipitation, ion exchange, electrodialysis, coagulation/flocculation, reverse osmosis, electrochemical operation, ultra filtration, biological treatment and complexation/sequestration. The use of these methods for the removal of heavy metals at low concentration has shown to be economically unviable [5]. Adsorption has been used as an excellent technique in the treatment of wastewater because of its simplicity. Different kinds of adsorbents have been investigated by different authors for the removal of heavy metals, these include, but not limited to natural and synthetic zeolite [6], alumina [7], fly ash [8], carbon aerogel [9], clinoptilolites [10], phosphate rock [11], biopolymer [12] etc and more recently different nanomaterials such as magnetic nanoparticles [13], carbon nanotubes [14], nano zeolite composite [15], nano metal oxide [16] and nanostructure alumina [5]. However, the use of some of these adsorbents has economical and technical limitations, which has to do with the method of preparation and the cost of the adsorbent. The preparation of adsorbents, such as, activated carbon usually involves the use of high temperature, takes a very long time and consumes a lot of chemicals. Therefore, it has become necessary to explore and develop cheaper adsorbents using effective/alternative techniques to meet the growing demand [17]. This can be achieved by utilising waste materials as a source of cheap and readily available raw material for the production of adsorbents for the removal of toxic metals and organic species from wastewater.

The use of biochars and hydrochars from biomass as a low-cost adsorbent for the adsorption of heavy metals and organics from aqueous solution is an emerging and promising wastewater treatment technology which has been reported by some authors for their ability to adsorb various heavy metals and organics, such as copper, zinc, arsenic, nickel, cadmium, lead and atrazine [2,17-22]. It is anticipated that as pyrolysis and hydrothermal carbonization of biomass into liquid and gas fuels grows in importance, very large amount of char from these processes will become available for use. The use of biochar and hydrochar prepared from pyrolysis and green chemistry process of microwave-assisted hydrothermal carbonization of *Prosopis africana* shell to adsorb heavy metals from aqueous solution to the best of my knowledge has not been previously reported. It will therefore be important if these chars can studied and compared for their ability to remove heavy metals from aqueous solution, as a way of managing and reusing this waste material.

In this chapter, the aims are to apply the chars prepared in Chapter 4 from pyrolysis (biochar) and green chemistry approach of microwave-assisted hydrothermal carbonization (hydrochar) of *Prosopis africana* shell as adsorbents for the adsorption of heavy metals from aqueous solution (using lead and cadmium as representative heavy metal), and also to evaluate which of these materials is more effective in the adsorption of the heavy metals by varying different parameters.

5.2 Materials and Methods

5.2.1 Preparation of the Biochar and Hydrochar

The materials and the methods used for the preparation and characterization of the biochar and hydrochar from *Prosopis africana* shell have been previously described in Chapter 4.

5.2.2 Adsorption Studies

All chemicals used were of analytical grade and were used without further purification. Pb^{2+} and Cd^{2+} solutions were obtained from Lead (II) nitrate and Cadmium (II) nitrate which were purchased from Fisher Scientific, United Kingdom. Synthetic stock solutions (1000 mg/L) of lead and cadmium ions were prepared in de-ionised water from their respective salts and were diluted to the required concentration before use. The effects of different parameters, such as, pH, adsorbent dosage, time, and concentration on the adsorption process of a single component system were studied using batch adsorption experiment. A brief description of the process is given below.

The adsorbent material (0.01-0.08 g) was placed in a 250 mL conical flask and 50 mL of 10-100 mg/L aqueous solution of Pb^{2+} or Cd^{2+} was added. The batch adsorption experiment was carried out on a shaker at room temperature (22±1 °C) for 10-60 minutes for equilibrium to be attained. The pH was adjusted between 4 and 10 using 2% nitric acid and 5M NH_4OH. After equilibration the suspension was filtered using a filter paper (Whatman filter paper number 3, ashless 11 cm) and the filtrates were immediately analysed using an inductively coupled plasma optical emission spectrophotometer (ICP-OES, Optima 5300 DV, Perkin Elmer, Seer Green,

Beaconsfield, UK), which has both axial and radial viewing mode and is equipped with an autosampler. It uses WinLab 32 software and has the capacity to detect a wide range of elements, with sensitivities in the range of ppb. The exact sensitivity depends on the specific element and emission wavelength used. Before use, it was calibrated using commercial standards of known concentrations (Romil, Cambridge UK, PrimAg). By subtracting the equilibrium solution concentration from the initial metal ion concentration, the amounts of metal ions adsorbed on the biochar and hydrochar in mg/g at equilibrium q_{eq} were calculated using the mass balance equation.

$$q_{eq} = \left(\frac{C_0 - C_{eq}}{m}\right) v \qquad \text{(Equation 5.1)}$$

where v is the volume of the solution in litres (L), m is the amount of adsorbent in grams (g); C_0 and C_{eq} are the initial and equilibrium concentrations of the metal ions (mg/L) respectively.

The adsorption study was carried out in triplicate and the average of the repeated runs is presented for reliability. Adsorption of metal ions by the raw *Prosopis africana* shell and on the walls of the glass flasks were checked by blank experiments that were run in parallel to establish reliability and reproducibility, and it was found to be negligible. All glassware were pre-soaked in a 5% HNO_3 solution, rinsed with deionized water and oven-dried before use.

5.2.2.1 Adsorption Kinetics

The kinetics study was carried out at room temperature (22±1 °C) using 0.05 g of adsorbent and 50 mL of 10 mg/L solution of the adsorbates at pH 6 and 8 for Pb^{2+} and Cd^{2+} respectively, while the contact time was varied between 10-60 minutes. The adsorption kinetics were tested using the linear plots of the following well-known models: the pseudo-first-order, pseudo-second-order and intraparticle diffusion model to establish the adsorption kinetic parameters of the adsorption process.

The pseudo-first-order rate equation suggested by Lagergren [23] and cited by Olgun and Atar [24] is given by

$$\frac{1}{q_t} = \left(\frac{k_1}{q_{eq}}\right)\left(\frac{1}{t}\right) + \frac{1}{q_{eq}} \qquad \text{(Equation 5.2)}$$

where q_{eq} and q_t are the amount of metal ion adsorbed per unit mass of the adsorbent (mg/g) at equilibrium and time t (mins) respectively, k_1 (min^{-1}) is the first-order rate constant. By plotting $1/q_t$ against $1/t$, the values of k_1 and q_{eq} can be calculated from slope and intercept of the graph.

The pseudo-second-order rate equation expressed by Ho and McKay [25] is given by

$$\frac{t}{q_t} = \frac{1}{k_2 q_{eq}^2} + \frac{1}{q_{eq}} t \qquad \text{(Equation 5.3)}$$

where q_{eq} and q_t are the amount of metal ion adsorbed per unit mass of the adsorbent (mg/g) at equilibrium and time t (mins) respectively, k_2 (g mg^{-1} min^{-1}) is the pseudo-second-order rate constant. By plotting t/q_t against t, the second-order sorption rate constant k_2, and q_{eq} can be calculated from the slope and intercept of the graph.

The intraparticle diffusion model is expressed by the equation described by Weber and Morris [26]

$$q_t = k_p t^{1/2} + C \qquad \text{(Equation 5.4)}$$

Where q_t (mg/g) is the amount of metal ion adsorbed at time t (mins), k_p (mg g^{-1} $min^{-1/2}$) is the intraparticle diffusion rate constant, C (mg/g) is the intercept when q_t is plotted against $t^{1/2}$.

5.2.2.2 Equilibrium Adsorption Isotherms

Freundlich and Langmuir isotherms were used to model the experimental equilibrium data for the adsorption of Pb^{2+} or Cd^{2+} on the biochar and hydrochar. This study was carried out at room temperature (22±1 °C) for 30 minutes with 0.05 g of adsorbent and 50 mL of different concentration of adsorbate solutions (10-100 mg/L) at pH 6 and 8 for Pb^{2+} and Cd^{2+} respectively. The linear forms of the Langmiur and Freundlich models can be represented as follows

$$\frac{C_{eq}}{q_{eq}} = \frac{1}{K_L . q_{max}} + \frac{C_{eq}}{q_{max}} \quad \text{(Langmuir model)} \qquad \text{(Equation 5.5)}$$

$$\log q_{eq} = \log K_F + \frac{1}{n} \log C_{eq} \quad \text{(Freundlich Model)} \qquad \text{(Equation 5.6)}$$

where q_{max} is the maximum adsorption capacity (mg/g), q_{eq} is the amount of metal adsorbed per unit mass of the adsorbent (mg/g), C_{eq} is the equilibrium solution concentration (mg/L), n is the intensity of the adsorption constant, K_F (mg/g) is the adsorption capacity for Freundlich model, K_L (L/mg) is the Langmuir constant relating to the adsorption strength or intensity.

5.2.2.3 Thermodynamics Studies

The effect of temperature on the adsorption process was carried out for 30 minutes using 50 mL of 10 mg/L of the adsorbate solutions and 0.05 g of adsorbent at different temperatures (22, 30 and 35 °C) and pH 6 and 8 for Pb^{2+} and Cd^{2+} respectively. The thermodynamic parameters of the adsorption processes were calculated using the following equations:

Chen *et al.* [19] reported that the equilibrium constant (K_{eq}) of the adsorption processes can be evaluated using the following equation:

$$K_{eq} = \frac{q_{eq}}{C_{eq}} \qquad \text{(Equation 5.7)}$$

The free energy change (ΔG°) of the adsorption process is given by the following equation:

$$\Delta G^{\circ} = -RT\ln K_{eq} \qquad \text{(Equation 5.8)}$$

The van't Hoff equation gives the relationship between equilibrium constant (K_{eq}) and temperature (T)

$$\Delta G^{\circ} = \Delta H^{\circ} - T\Delta S^{\circ} \qquad \text{(Equation 5.9)}$$

$$\ln K_{eq} = \frac{\Delta S^{\circ}}{R} - \frac{\Delta H^{\circ}}{RT} \qquad \text{(Equation 5.10)}$$

where q_{eq} (mg/g) is the amount of metal ions adsorbed on the adsorbent from solution at equilibrium, C_{eq} (mg/L) is the equilibrium concentration of metal ions in the solution, R (J/mol.K) is the gas constant 8.314, T (K) is the absolute temperature, K_{eq} (L/g) is the equilibrium constant of the adsorption, ΔG°, ΔH° and ΔS° are the changes in the Gibbs free energy, enthalpy and entropy of the adsorption process respectively. By

plotting lnK_{eq} against $1/T$, ΔH° and ΔS° values can be calculated from the slopes and intercepts of the graphs. The values of ΔG° can be obtained from the corresponding ΔH° and ΔS° values.

5.3 Results and Discussion

5.3.1 Effect of pH

pH is one of the most important parameters that influences the adsorption of metal ions from aqueous solution [27]. The effect of pH on the adsorption of Pb^{2+} or Cd^{2+} from aqueous solution by the biochar and hydrochar is shown in Figure 5.1. The experiment was performed at room temperature (22±1 °C) using 10 mg/L adsorbate concentrations, and 1 g/L of adsorbent dosage. The adsorption of Pb^{2+} and Cd^{2+} on both chars increased with pH until maximum adsorption of 8.5 and 7.5 mg/g on the hydrochar and biochar respectively were reached at pH 6 for Pb^{2+} (Figure 5.1 a), and 7.8 and 6.5 mg/g on hydrochar and biochar respectively at pH 8 for Cd^{2+} (Figure 5.1 b). After this, there was a gradual decrease in adsorption for both metals ions. A situation where this kind of adsorption trend is observed shows that the mechanisms involved in the adsorption process is ion exchange, followed by precipitation [28]. The observed trend in this study is consistent with previous studies for the adsorption of Pb^{2+} and Cd^{2+} using chars obtained from pyrolysis and hydrothermal liquefaction [20,22,28]. Depending on the pH and the initial metal ion concentration Pb^{2+} or Cd^{2+} may exist in different forms in aqueous solution. At a low pH (2-6), they are likely to be found as free ions (Pb^{2+} >98% and Cd^{2+} >99.9%), in equilibrium with solvated species [29], while at a pH above 8 they tend to be precipitated in the formation of complexes because of the presence of the OH^- ion [20]. Two mechanisms exist through which adsorption onto carbon materials is considered to take place; one of the routes is coordination with the functional groups on the surface of the carbon material and it is affected by the pH value of the solution, while the second is physical adsorption relating to the surface area and porosity of the carbon [30]. The coordination route played an important role here; since the biochar and hydrochar have small surface area and are non-porous. At a lower pH value there is competition between the metal ions and the H^+ in solution, the H^+ linked with hydrophilic functional groups making it difficult for the metal ions to be adsorbed due to the neutralization of the adsorption

sites. As the pH value increases H^+ concentration decreases, deprotonation of the hydrophilic functional group makes it possible for coordination with the metal ions, hence higher adsorption [22]. In such a situation, Equation 5.11 is in competition with Equation 5.12.

$$*^{(-)} + H^+ \leftrightarrow *H \qquad K_1 \qquad \text{(Equation 5.11)}$$

$$*^{(-)} + M^+ \leftrightarrow *M \qquad K_2 \qquad \text{(Equation 5.12)}$$

Where * is the generic adsorption site and K is the equilibrium constant.

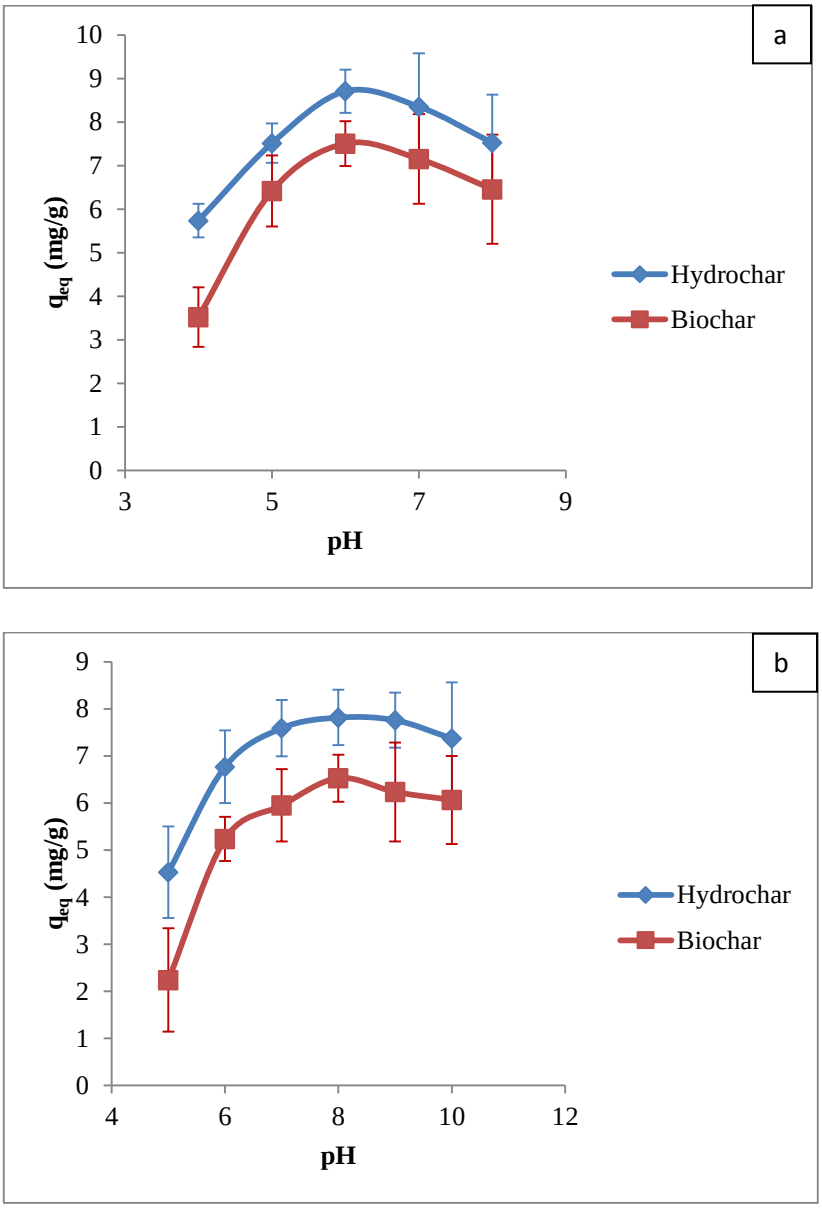

Figure 5.1: Effect of pH on the adsorption of (a) lead (b) cadmium ions onto biochar and hydrochar. The adsorption of the metal ions increased as pH values increases. The highest adsorption was obtained at pH 6 and 8 for the Pb^{2+} and Cd^{2+} respectively (n=3).

5.3.2 Effect of Adsorbent Dosage

The effect of adsorbent dose on the adsorption of Pb^{2+} or Cd^{2+} from aqueous solution is shown in Figure 5.2. This study is crucial because it shows the capacity of adsorbent for a given concentration of metal ion [31]. The effect was studied over the range of 0.2-1.6 g/L adsorbent dosage, 10 mg/L adsorbate concentrations at pH of 6 and 8 for Pb^{2+} and Cd^{2+} at room temperature (22±1 °C) respectively. It was observed that as the dose of the adsorbents increased from 0.2-1.0 g/L, the amount of metal ions adsorbed from aqueous solution increased about two fold (4.6-8.7 mg/g and 3.1-7.8 mg/g, and 4.2-7.6 mg/g and 3.1-6.5 mg/g for Pb^{2+} and Cd^{2+} on the hydrochar and biochar respectively) before equilibrium was attained. This is expected because as the adsorbent dosage is increased, while the metal ion concentration is kept constant more surface and adsorption sites become available for the metal ions to be adsorbed [32]. However, there was no significant change in the adsorption of the metal ions after the dosage of 1 g/L, which was found to be the equilibrium adsorbent concentration in this study and this could be due to the overlapping of the active sites at such high dosage [3], suggesting that there is a threshold dosage at which maximum adsorption occurs after which no significant increase will be observed [33]. Atar *et al*. [34], and Naiya *et al*. [35] have reported a similar trend.

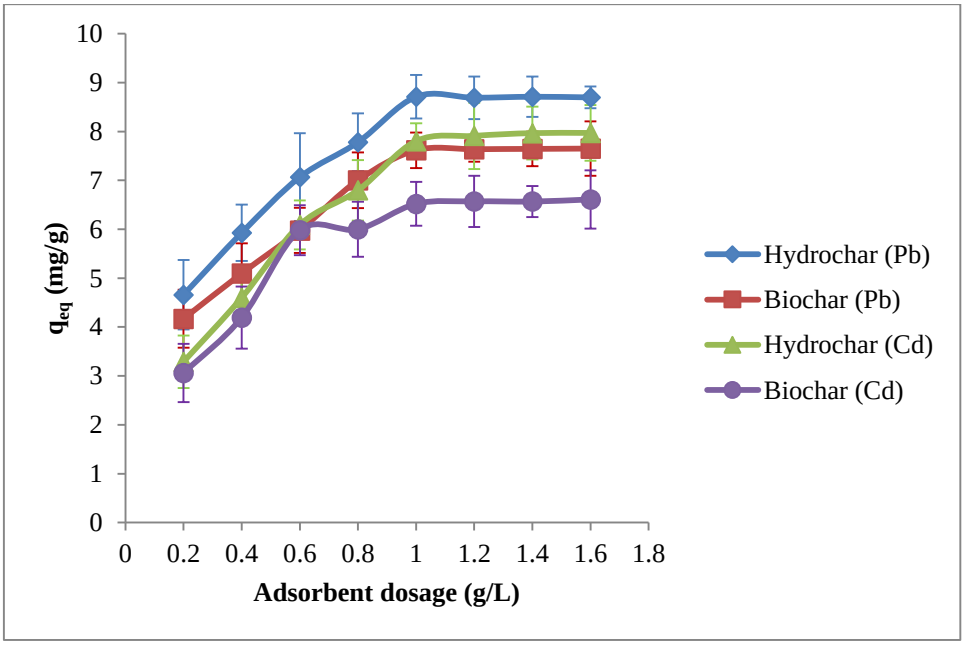

Figure 5.2: Effect of adsorbent dose on adsorption of Pb^{2+} or Cd^{2+} onto biochar and hydrochar. Adsorption increases as the adsorbent dose is increased with the adsorption at 1 g/L almost twice that at 0.2 g/L before equilibrium was reached (n=3).

5.3.3 Effect of Time

The effect of time on the adsorption of Pb^{2+} or Cd^{2+} from aqueous solution by the biochar and hydrochar is shown in Figure 5.3. The experiment was performed at room temperature (22±1 °C) using 10 mg/L adsorbate concentrations, 1 g/L adsorbent dose at pH 6 and 8 for the Pb^{2+} and Cd^{2+} respectively, while the contact time was varied between 10-60 minutes in order to establish to appropriate time for equilibrium to be reached. The adsorption of Pb^{2+} and Cd^{2+} increased rapidly within the first 10 minutes, followed by a gradual increase up to 30 minutes and remained almost constant thereafter for both the biochar and hydrochar. Most of the metal ion removal occurred within 30 minutes accounting for about 8.5 and 7.8 mg/g on the hydrochar, and 7.4 and 6.4 mg/g on the biochar at equilibrium for Pb^{2+} and Cd^{2+} respectively. Similar trends in heavy metal adsorption have been previously reported [24,31]. The increase in adsorption at the initial stage is due to large number of vacant adsorption sites, which become saturated with time and as a result adsorption is less efficient after 30 minutes [24]. Therefore, 30 minutes was taken as the equilibrium time for adsorption in this study.

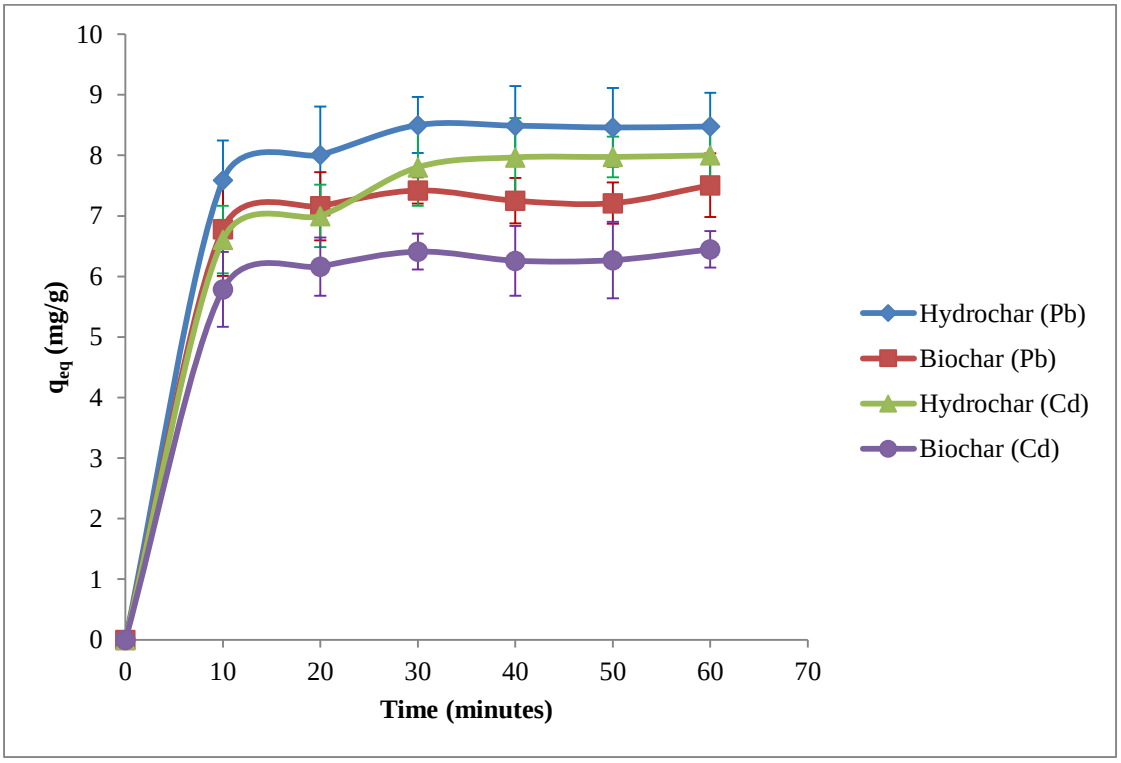

Figure 5.3: Effect of time on adsorption of Pb^{2+} or Cd^{2+} onto biochar and hydrochar. The adsorption of the metal ions was rapid within the first 10 minutes and gradually increased up to 30 minutes before equilibrium was obtained (n=3).

5.3.4 Effect of Initial Metal Ion Concentration

The effect of initial metal ion concentration is shown in Figure 5.4. The experiment was performed at room temperature (22±1 °C) for 30 minutes using 10-100 mg/L adsorbate concentrations, 1 g/L adsorbent dose at pH 6 and 8 for the Pb^{2+} and Cd^{2+} respectively. There was a gradual increase in the total amount of metal ions adsorbed as the metal ion concentration increases, but the percentage adsorbed decreased from 85-46% and 74-27% for Pb^{2+}, and 78-24% and 64-20% for Cd^{2+} on hydrochar and biochar respectively with increase in metal ion concentration from 10-100 mg/L. At low metal ion concentration, the hydrochar and biochar are exposed to a small number of metal ions and as a result the adsorption is not dependent on the initial concentration of metal ion [24]. However, as the metal ion concentration increased without increase in the amount of the adsorbent the extent of adsorption drops due to saturation or decrease in the available adsorption sites on the adsorbents [24]. Similar trend have been reported previously on boron waste [36] and sawdust [37].

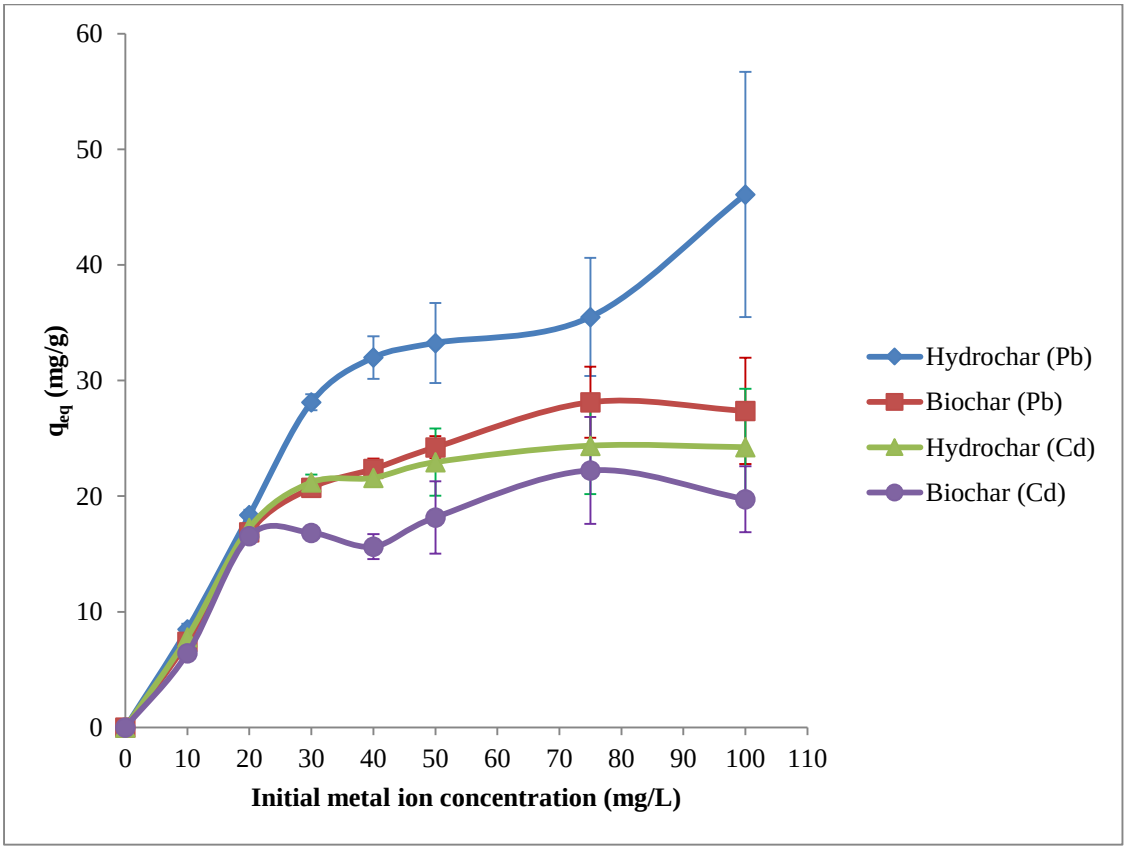

Figure 5.4: Effect of concentration on adsorption of Pb^{2+} or Cd^{2+} onto biochar and hydrochar showing gradual increase in the total metal ions adsorbed as the initial metal ion concentration increases (n=3).

5.3.5 Adsorption Kinetics

The metal adsorption rate is an important factor and a criterion for determining the reactor design and optimization of the process for a successful practical application [28]. Three steps are involved in the adsorption on an adsorbent from aqueous phase [38]: (a) external transfer (the transport of the adsorbate from the bulk phase to the exterior surface of the adsorbent either through molecular or convective diffusion), (b) the internal transfer (the transport into the adsorbent through either pore diffusion and/or surface diffusion), and (c) the adsorption on the active sites on the surface of the adsorbent (through chemisorption or physisorption). The rate of the adsorption process is determined by the slowest of these steps (rate determining), which governs the overall rate of the removal of the adsorbate from solution [28]. The pseudo-first-order, pseudo-second-order, and intraparticle diffusion models were therefore used to obtain the kinetic parameters of the adsorption process. These are the most commonly used models to describe the adsorption kinetics of metal ions, and organics, such as, dyes and herbicides from aqueous solution on different adsorbents [28].

The results for the pseudo-first-order and pseudo-second-order kinetics respectively are presented in Figures 5.5 and 5.6, and Table 5.1. The low values of the correlation coefficient (R^2) between the theoretical (q_{eq}) and the experimental ($q_{eq(exp)}$) values obtained for the pseudo-first-order model compared to that for the pseudo-second-order kinetics is an indication that the adsorption of both metal ions on the biochar and hydrochar did not follow the pseudo-first-order reaction. The R^2 values were found to be close to unity for both metals when the kinetic data were modelled with the pseudo-second-order equation. This is an indication that the experimental data fit well into the second-order model, suggesting that it can be used for the entire process of adsorption [19]. The kinetic process that is fitted by the pseudo second-order kinetic model has chemisorption as the rate-determining step and involves the chemical bonding between divalent metal ions and polar functional groups, such as, phenolics, acids, ketones, and aldehydes on the adsorbent which are responsible for the sharing or exchange of electrons between the adsorbent and the adsorbate [19,28,39,40]. The theoretical values q_{eq} for the pseudo-second-order kinetic model and the experimental values $q_{eq(exp)}$ were very close to each other. This uniformity is a further confirmation that the adsorption processes followed second-order kinetics. The kinetics results obtained in this study is consistent with previous studies for the adsorption of metal

ions by chars prepared from pyrolysis and hydrothermal liquefaction of biomass [19,22].

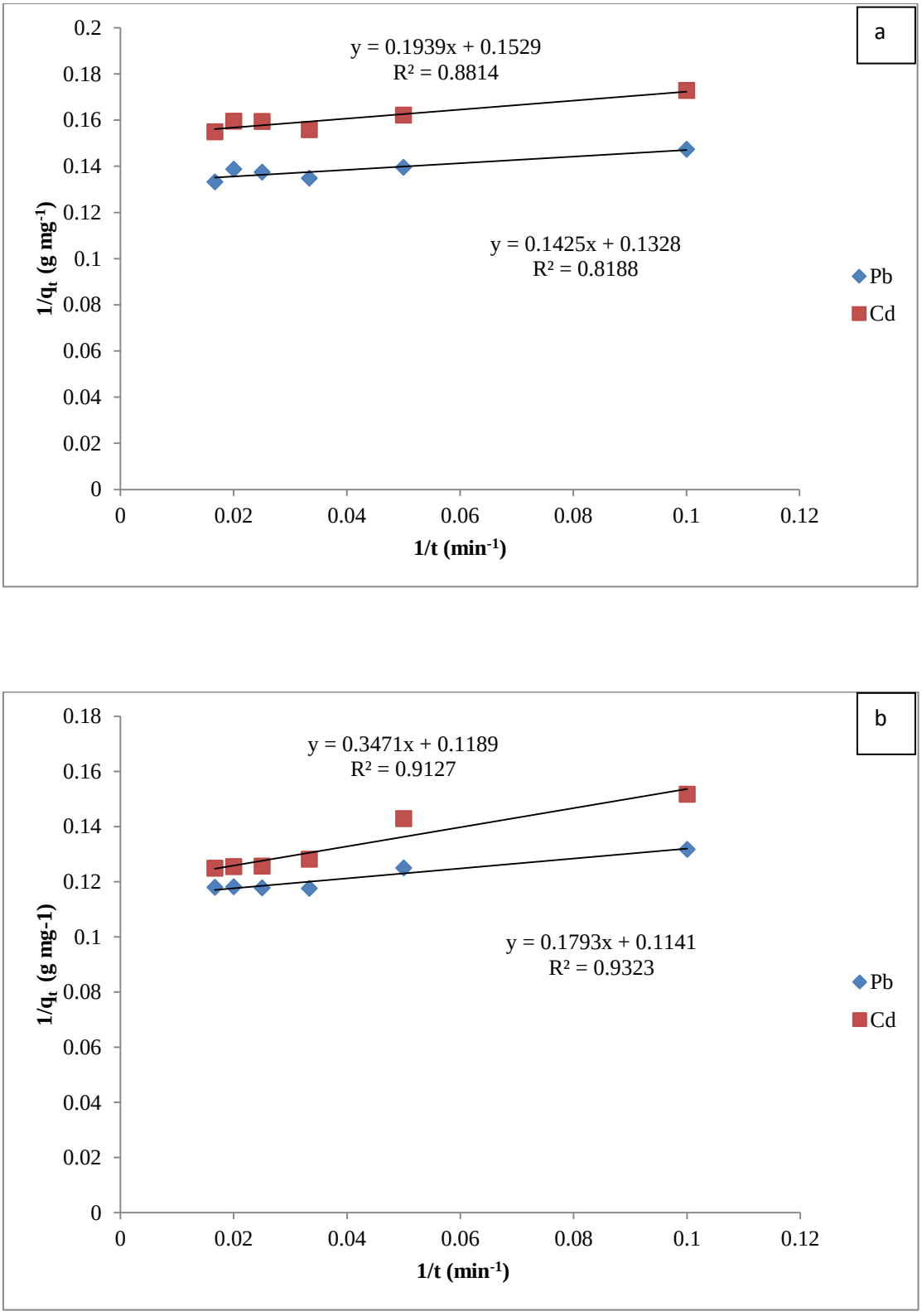

Figure 5.5: Pseudo-first-order kinetic plot for the adsorption of Pb^{2+} and Cd^{2+} onto (a) biochar (b) hydrochar, calculated from Equation 5.2

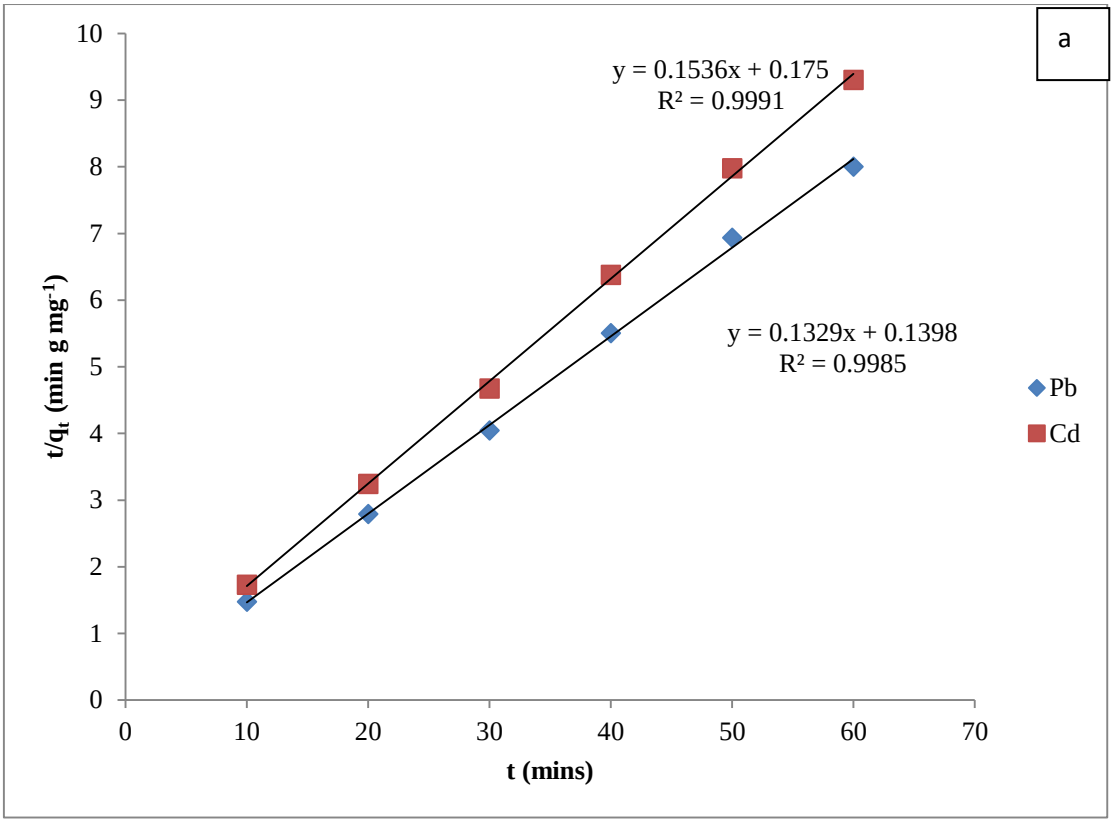

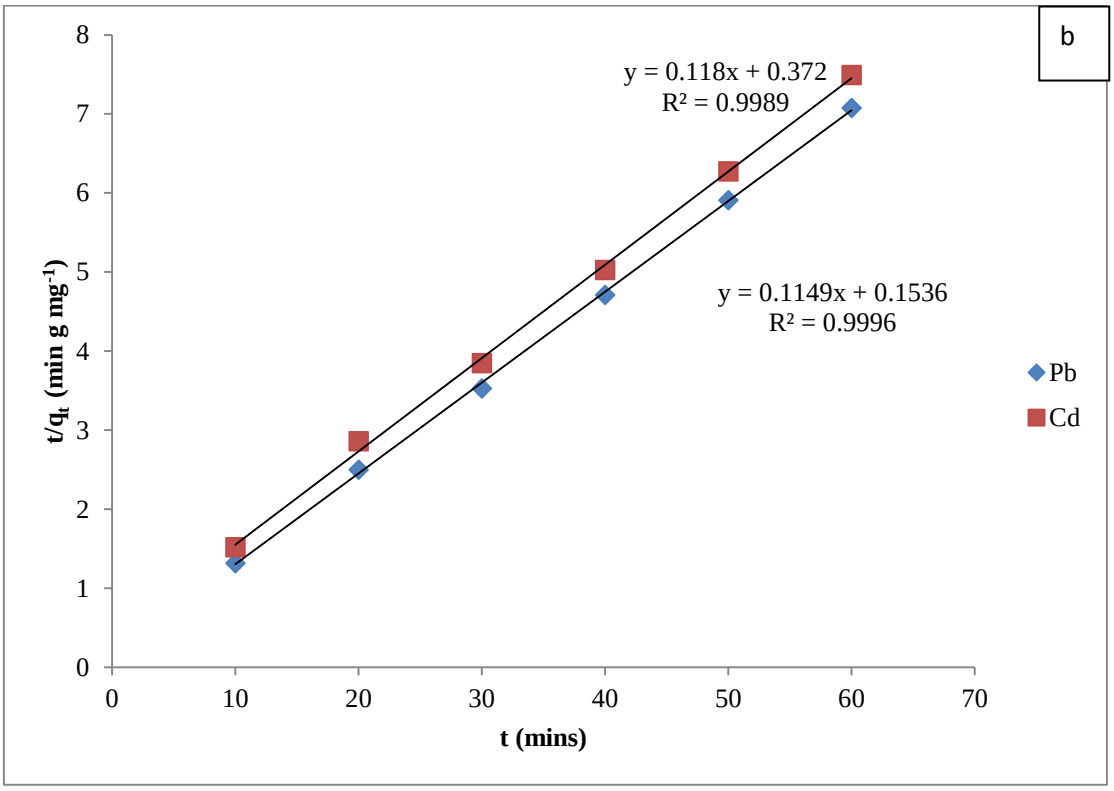

Figure 5.6: Pseudo-second-order kinetic plot for the adsorption of Pb^{2+} and Cd^{2+} onto (a) biochar (b) hydrochar, calculated from Equation 5.3

			Pseudo-first-order kinetics			Pseudo-second-order kinetics		
Adsorbent	**Metals**	$q_{eq(exp)}$ **(mg/g)**	k_1 **(min^{-1})**	q_{eq} **(mg/g)**	R^2	k_2 **(g mg^{-1} min^{-1})**	q_{eq} **(mg/g)**	R^2
Biochar	Pb^{2+}	7.4	1.07	7.5	0.8188	12.63×10^{-2}	7.5	0.9985
	Cd^{2+}	6.4	1.27	6.5	0.8814	13.48×10^{-2}	6.5	0.9991
Hydrochar	Pb^{2+}	8.5	1.57	8.8	0.9323	85.95×10^{-3}	8.7	0.9996
	Cd^{2+}	7.8	2.92	8.4	0.9127	37.43×10^{-3}	8.5	0.9989

Table 5.1: Kinetic parameters for the adsorption of Pb^{2+} and Cd^{2+} onto biochar and hydrochar, calculated from Equations 5.2 and 5.3 using values from Figures 5.5 and 5.6, showing the correlation coefficients and the theoretical and experimental values for the amount of metal ions adsorbed at equilibrium.

The details of the diffusion mechanism cannot be identified by the pseudo-first-order and pseudo-second-order models; therefore an intraparticle diffusion model was used to analyze the kinetic results to show whether or not the movement of the metal ions from the aqueous solution into the pores of the chars is the only rate determining step. If it is, a straight line graph passing through the origin should be obtained [41]. Figure 5.7 shows the intraparticle diffusion plot (q_t against $t^{1/2}$) for the adsorption of the Pb^{2+} and Cd^{2+} on the biochar and hydrochar. The graphs obtained showed gradual increase and a plateau, with no zero intercept indicating that metal ion diffusion into pores is not the dominating factor that controlled the mechanism of the process [24,28]. This is not surprising because the biochar and hydrochar are non-porous. Table 5.2 gives the values for the intraparticle diffusion parameters calculated from the graph.

Adsorbent	**Metals**	k_p **(mg g^{-1} $min^{-1/2}$)**	C **(mg/g)**	R^2
Biochar	Pb^{2+}	11.90×10^{-2}	6.5	0.6536
	Cd^{2+}	11.76×10^{-2}	5.6	0.6904
Hydrochar	Pb^{2+}	19.59×10^{-2}	7.1	0.7768
	Cd^{2+}	33.39×10^{-2}	5.7	0.8751

Table 5.2: Intraparticle diffusion parameters for the adsorption of Pb^{2+} and Cd^{2+} onto biochar and hydrochar, calculated from Equation 5.4 using values from Figure 5.7. The *C* values are not zero indicating that intraparticle diffusion is not the rate determining step of the adsorption processes.

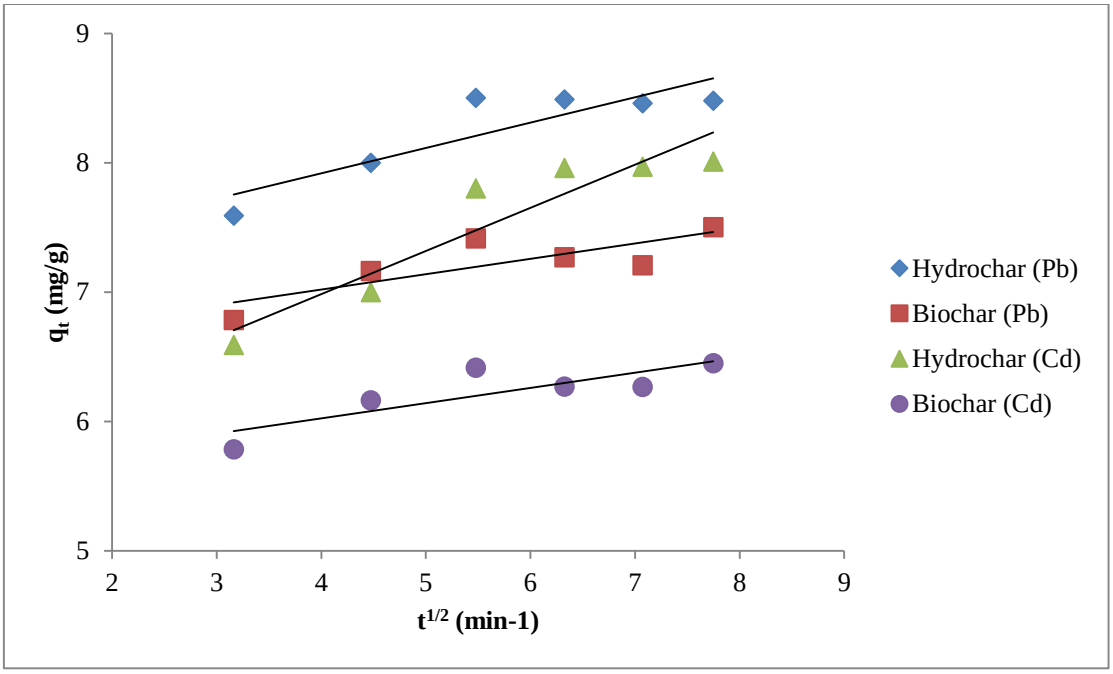

Figure 5.7: Intraparticle diffusion model for the adsorption of Pb^{2+} and Cd^{2+} onto biochar and hydrochar, calculated from Equation 5.4 showing lines of best fit.

5.3.6 Equilibrium Adsorption Isotherms

The distribution of metal ions between the solid adsorbent and liquid phase is the measure of the equilibrium position in the adsorption process and can be expressed using any of the popular isotherm models [42]. In the design of an adsorption system, this is a basic requirement, as the data obtained give information about the capacity of the adsorbent for the adsorbate under the system conditions [5]. Therefore, well-known isotherm models; the Langmuir and Freundlich isotherms were employed to describe the adsorption characteristic of Pb^{2+} and Cd^{2+} onto the biochar and hydrochar. The Langmuir isotherm is employed to describe the equilibrium of a homogenous adsorption surface implying that all the adsorption sites have equal adsorbate affinity and that adsorption taking place at one site does not affect the adsorption at the adjacent site. It assumes a monolayer capacity, while the Freundlich isotherm model assumes the heterogeneity of adsorption surfaces and describes the equilibrium of such surface. It does not assume monolayer capacity [20]. A summary of the theoretical parameters for these isotherms and the corresponding correlation coefficient R^2 for each of the adsorbates onto the adsorbents is shown in Table 5.3. Figures 5.8 and 5.9 show the linear plots of the Langmuir and Freundlich models for the adsorption of Pb^{2+} and Cd^{2+} onto the biochar and hydrochar respectively.

Char	Adsorbate	Langmuir model			Freundlich model		
		q_{max} (mg/g)	K_L	R^2	n	K_F	R^2
Hydrochar	Pb^{2+}	45.3	0.23	0.9713	4.05	15.96	0.9579
Biochar	Pb^{2+}	31.3	0.70	0.9988	4.26	12.80	0.8291
Hydrochar	Cd^{2+}	38.3	0.16	0.9625	3.71	11.67	0.9554
Biochar	Cd^{2+}	29.9	0.07	0.9151	3.94	7.71	0.8817

Table 5.3: Langmuir and Freundlich isotherm parameters for the adsorption of Pb^{2+} and Cd^{2+} onto the biochar and hydrochar, calculated from Equation 5.5 and 5.6 using values from Figures 5.8 and 5.9.

The correlation coefficients (R^2) for the adsorption of Pb^{2+} and Cd^{2+} onto the hydrochar and biochar were higher for the Langmuir model than the Freundlich model, implying that the adsorption data fitted the Langmuir model better than the Freundlich model, with maximum adsorption capacities of 45.3 and 31.3 mg/g for Pb^{2+} and 38.3 and 29.9 mg/g for Cd^{2+} on the hydrochar and biochar respectively. This is expected as an adsorption process that follows the pseudo second-order kinetics also fits the Langmuir isotherm model and the adsorption process is controlled by chemisorption [40]. The poor fitting of the adsorption data into the Freundlich model could be attributed to the fact that the supply of adsorption sites on the adsorbent surface was not unlimited [17,22]. The biochar and hydrochar used in this study have good adsorption for Pb^{2+} and Cd^{2+}, this is because, *n* values between 2-10 have been reported to indicate good adsorption [24]. The *n* values for both metal ions in Table 5.3 fall within this range. Pb^{2+} has a higher adsorption capacity than Cd^{2+}, which is usually attributed to the metal ion properties, such as, electronegativity and ionic radius [29]. The Pb^{2+} have a better electrostatic interaction with the hydrophilic functional group of the chars due to its high electronegativity [2], while the hydrated ionic radius of cadmium (0.275 nm) is higher than that of lead (0.261 nm), which could have caused a quick saturation of adsorption sites, due to steric hindrance [3]. The hydrochar has a higher adsorption capacity for both Pb^{2+} and Cd^{2+} than the biochar due to the presence of more functional groups on the surface [25,43,44].

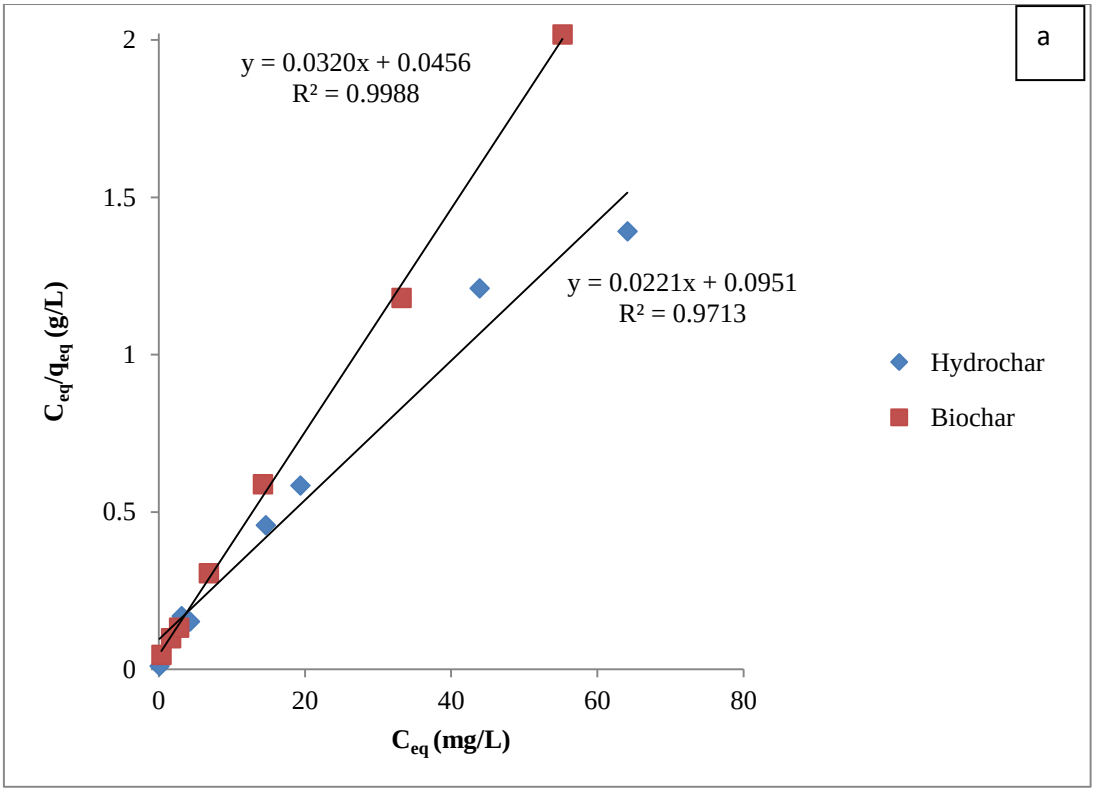

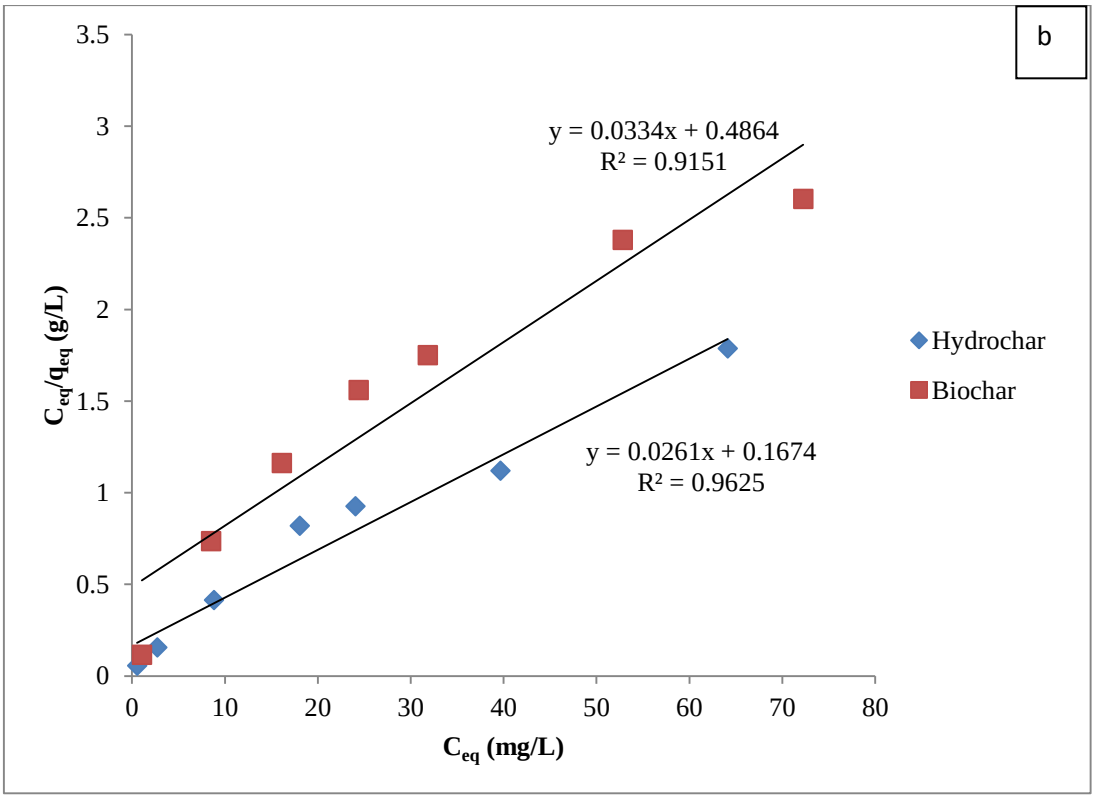

Figure 5.8: Linear Langmuir isotherm plot for (a) Pb^{2+}, (b) Cd^{2+} adsorption onto the biochar and hydrochar, calculated from Equation 5.5 showing lines of best fit.

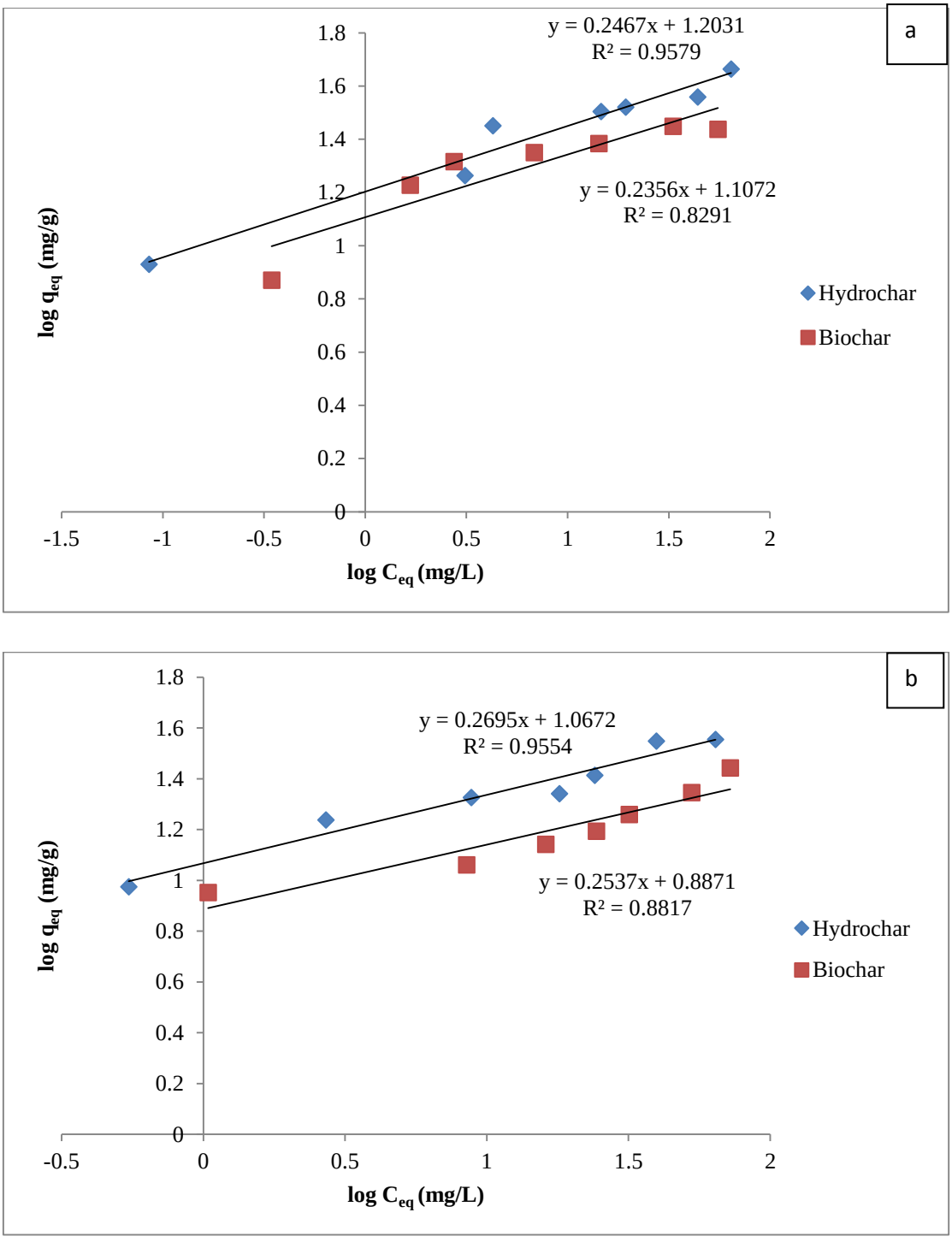

Figure 5.9: Linear Freundlich isotherm plot for (a) Pb^{2+}, (b) Cd^{2+} adsorption onto the biochar and hydrochar, calculated from Equation 5.6 showing lines of best fit.

The adsorption capacities in this study is higher than, or comparable with other previous studies using carbonaceous or other adsorbent materials (Table 5.4), which shows that chars prepared under mild condition of microwave-assisted hydrothermal carbonization and slow pyrolysis of *Prosopis africana* shell are suitable for the removal of Pb^{2+} and Cd^{2+} from aqueous solutions.

Adsorbent	Adsorption Capacities (mg/g)		References
	Pb^{2+}	Cd^{2+}	
Hydrochar from *Prosopis africana* shell	45.3	38.3	This study
Biochar from *Prosopis africana* shell	31.3	29.9	This study
Biochars from pinewood	3.9		[22]
Biochars from rice husk	1.8		[22]
Pigeon peas hulls	20.8	-	[31]
Activated carbon from tamarind wood	43.9	-	[45]
Activated carbon from *Ceiba pentandra* hull	-	19.6	[46]
Loess soil	-	8.2	[47]
Multiwalled carbon nanotube	-	10.9	[14]
Coffee residue	-	37.0	[48]
Carbon aerogel	34.7	15.5	[9]
Chitosan-Pectin pellets	11.2	1.2	[12]
Charcoal	1.2	2.9	[49]

Table 5.4: Adsorption capacities of different adsorbents for Pb^{2+} and Cd^{2+}, showing that the hydrochar and biochar used in this study have higher or comparable adsorption capacities.

5.3.7 Thermodynamic Studies

The thermodynamic parameters, Gibbs free energy (ΔG°), enthalpy (ΔH°) and entropy (ΔS°) are useful in defining whether an adsorption process is endothermic or exothermic, and if properly studied can give in-depth information about the inherent energy and structural changes after adsorption [31]. In environmental engineering practice, determination of both energy and entropy factors is very important and must be carried out in order to know the processes that are spontaneous [50].

The effect of temperature on the adsorption process carried out at 22, 30, and 35 °C for 30 minutes using 50 mL of 10 mg/L of the adsorbate solutions and 0.05 g of adsorbent at pH 6 and 8 for Pb^{2+} and Cd^{2+} respectively are shown in Figure 5.10. The adsorption of both Pb^{2+} and Cd^{2+} onto the hydrochar and biochar increased slightly with increase in temperature, indicating an endothermic process. The adsorption capacity of Pb^{2+} increased from 8.5-9.0 mg/g on the hydrochar and 7.4-8.1 mg/g on the biochar, while that of Cd^{2+} increased from 7.8-8.3 mg/g on the hydrochar and 6.4-7.0 mg/g on the biochar at 22 °C and 35 °C respectively. The results obtained in this study are consistent with Mohan *et al*. [20] in which adsorption increased with increase in temperature for oak wood and oak bark chars in the temperature range of 5-40 °C.

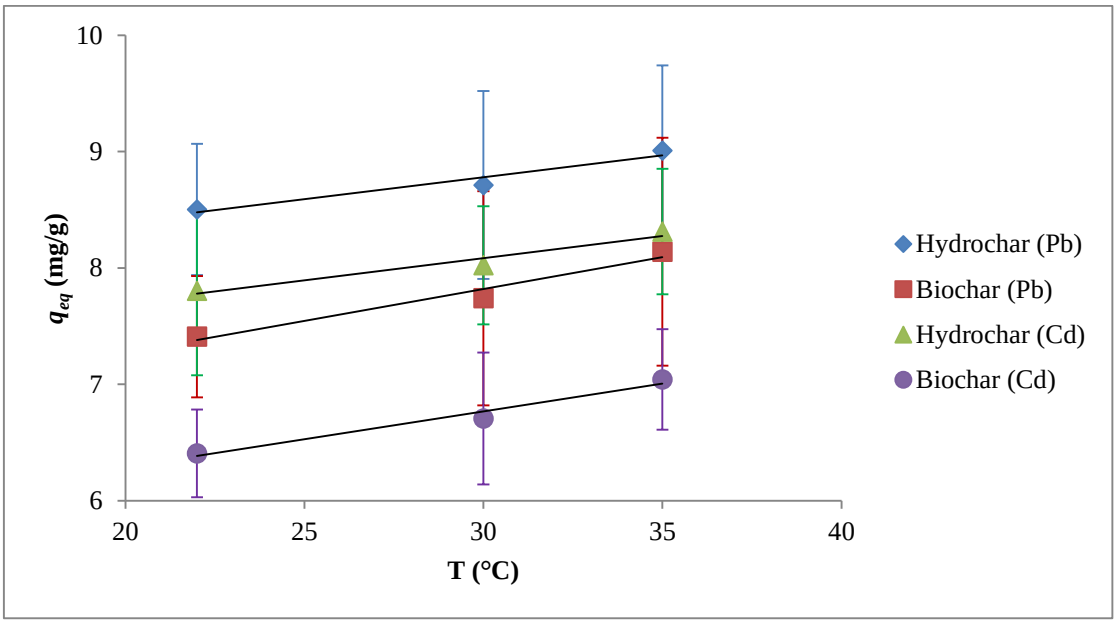

Figure 5.10: Effect of temperature on adsorption of Pb^{2+} and Cd^{2+} onto biochar and hydrochar. The adsorption of the metal ions increased slightly as temperature increases showing that the adsorption processes are endothermic (n=3).

The values of the thermodynamic parameters (ΔG°, ΔH° and ΔS°) of the adsorption of Pb^{2+} and Cd^{2+} onto the hydrochar and biochar were obtained from the van't Hoff plots (lnK_{eq} against $1/T$) in Figure 5.11 and are presented in Table 5.5. The negative values of ΔG° indicates that the adsorption of Pb^{2+} and Cd^{2+} onto the biochar and hydrochar were spontaneous [22,28]. The decreasing (increasingly negative) values of the Gibbs free energy with increasing temperature is an indication that higher temperatures favour the adsorption processes of both metal ions onto the hydrochar and biochar [19,31]. The positive values of ΔH° further confirm the endothermic nature of

the adsorption of Pb^{2+} and Cd^{2+} onto the hydrochar and biochar which the effect of temperature on the adsorption process earlier indicated. ΔS° values on the other hand are also positive indicating an increase in randomness at the interface of the solid/liquid during the adsorption process of Pb^{2+} and Cd^{2+} onto the biochar and hydrochar, which shows the good affinity of the adsorbents for the adsorbed species [28,31]. The trend observed in this study for the thermodynamic parameters is consistent with previous reports in metal ion adsorption [28,31].

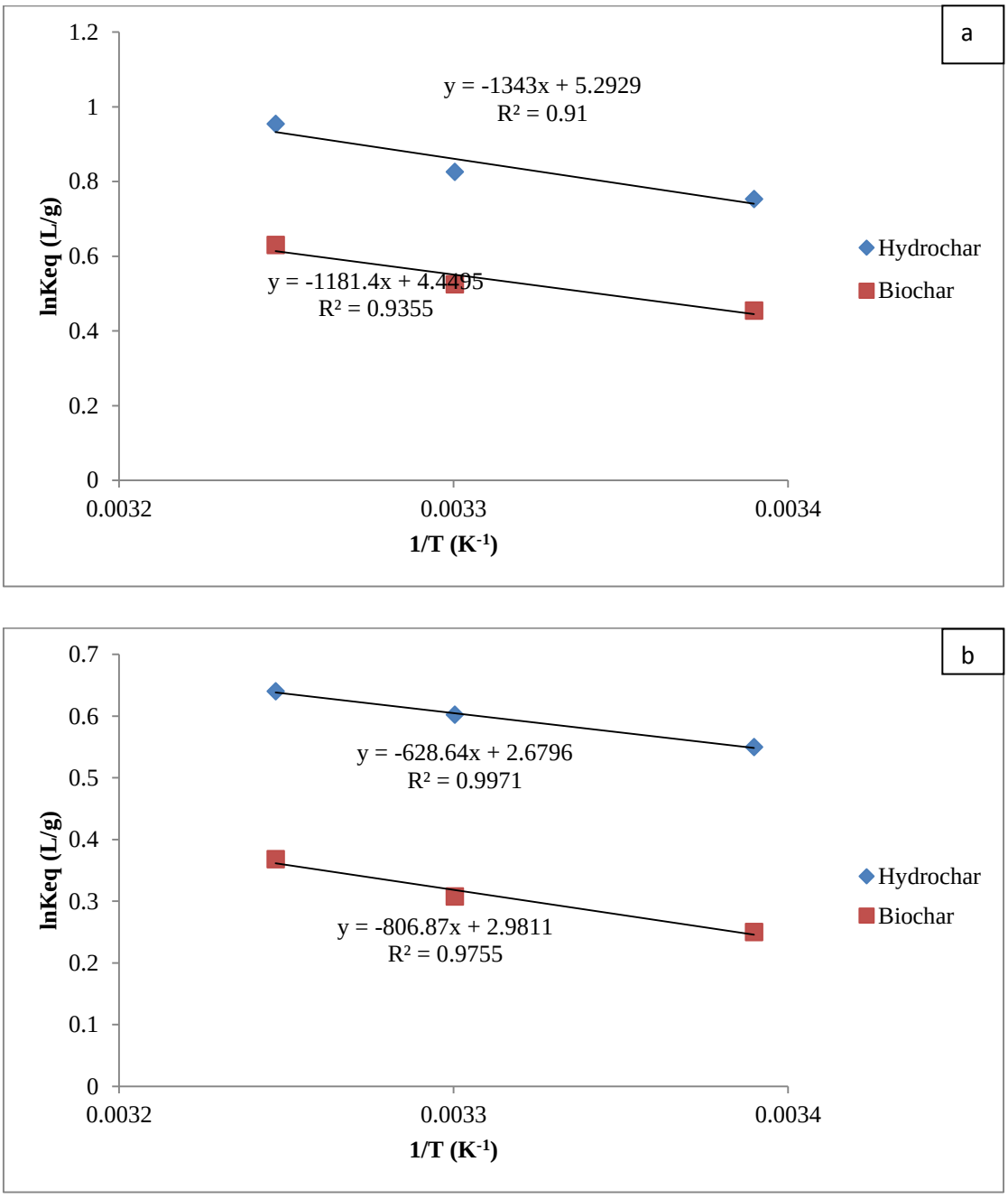

Figure 5.11: van't Hoff plot for (a) Pb^{2+}, (b) Cd^{2+} adsorption onto biochar and hydrochar, calculated from Equation 5.10.

Adsorbent	Heavy Metal	Temperature (K)	Thermodynamic Parameters		
			ΔG° (kJ/mol)	**ΔH° (kJ/mol)**	**ΔS° (J/molK)**
Biochar	Pb^{2+}	295	-1.10	9.82	36.99
		303	-1.39		
		308	-1.57		
	Cd^{2+}	295	-0.60	6.71	24.79
		303	-0.80		
		308	-0.93		
Hydrochar	Pb^{2+}	295	-1.81	11.17	44.01
		303	-2.17		
		308	-2.39		
	Cd^{2+}	295	-1.34	5.23	22.28
		303	-1.52		
		308	-1.63		

Table 5.5: Thermodynamic parameters for Pb^{2+} and Cd^{2+} adsorption onto the biochar and hydrochar, calculated from Equation 5.10 using values from Figure 5.11. The negative values of ΔG° show that the adsorption processes are spontaneous, while the positive values of ΔH° indicate endothermic process. The positive values of ΔS° shows increase in randomness at the interface of the solid/liquid during the adsorption process.

5.4 Conclusion

In this study, biochar and hydrochar prepared from pyrolysis and microwave-assisted hydrothermal carbonization of a waste material (*Prosopis africana* shell)

respectively have been used to adsorb metal ions from aqueous solution using a batch adsorption process. The result shows that the adsorption of the metal ions is dependent on the pH of the solution, with the adsorption decreasing in more acidic solutions and was rapid for the first 30 minutes after which equilibrium was attained. The uptake of the metal ions depends appreciably on the amount of the adsorbent. Interestingly, the hydrochar from the microwave-assisted hydrothermal carbonization, which is a green chemistry approach, was capable of adsorbing the metal ions more effectively from aqueous solution than the biochar, because of the presence of more functional groups on the surface. The kinetics of the adsorption of the heavy metals followed the pseudo-second-order rate expression and the adsorption data could be better described using the Langmuir model than the Freundlich model with the maximum adsorption capacities of 45.3 and 31.3 mg/g for Pb^{2+} and 38.3 and 29.9 mg/g for Cd^{2+} on the hydrochar and biochar respectively from single component solution, which is higher when compared with some adsorbent materials previously reported. The thermodynamics study shows that the adsorption process for both metal ions was spontaneous and endothermic. The results indicate the possibility of using low cost carbonaceous materials produced from plant residue or agricultural waste under mild conditions like these as effective adsorbents for water treatment and purification, and could be an attractive alternative, especially in developing countries of the world.

5.5 References

[1] Fu, F, Wang, Q. Removal of Heavy Metal Ions from Wastewaters: A Review. J Environ Manage 2011; 92: 407-418.

[2] Titirici, MM, Demir-Cakan, R, Baccile, N, Antonietti, M. Carboxylate-Rich Carbonaceous Materials via One-Step Hydrothermal Carbonization of Glucose in the Presence of Acrylic Acid. Chem Mater 2009; 21: 484-490.

[3] Benhima, H, Chiban, M, Sinan, F, Seta, P, Persin, M. Removal of Lead and Cadmium Ions from Aqueous Solution by Adsorption onto Micro-Particle of Dry Plant. Colloids Surface B 2008; 61: 10-16.

[4] Pedro, F, Nyer, EK. The Water Encyclopedia: Hydrologic Data and Internet Resources; CRC Press, Boca Raton, FL, USA, 2006.

[5] Rahmani, A, Mousavi, HZ, Fazli, M. Effect of Nanostructure Alumina on Adsorption of Heavy Metals. Desalination 2010; 253: 94-100.

[6] Motsi, T, Rowson, NA, Simmons, MJH. Adsorption of Heavy Metals from Acid Mine Drainage by Natural Zeolite. Int J Miner Process 2009; 92: 42-48.

[7] Genc-Fuhrman, H, Mikkelsen, PS, Ledin, A. Simultaneous Removal of As, Cd, Cr, Cu, Ni and Zn from Stormwater: Experimental Comparison of 11 Different Sorbents. Water Res 2007; 41: 591-602.

[8] Cetin, S, Pehlivan, E. The Use of Fly Ash as a Low Cost, Environmentally Friendly Alternative to Activated Carbon for the Removal of Heavy Metals from Aqueous Solutions. Colloids Surfaces A 2007; 298: 83-87.

[9] Kadirvelu, K, Goel, J, Rajagopal, CJ. Sorption of Lead, Mercury and Cadmium Ion in Multi-Component System using Carbon Aerogel as Adsorbent. J Hazard Mater 2008; 153: 502-507.

[10] Çoruh, S. The Removal of Zinc Ions by Natural and Conditioned Clinoptilolites. Desalination 2008; 225: 41–57.

[11] Mavropoulos, E, da Rocha, NCC, Moreira, JC, Bertolinod, LC, Rossi, AM. Pb^{2+}, $Cu^{2+}$and Cd^{2+} Ions Uptake by Brazilian Phosphate Rocks. J Braz Chem Soc 2005; 16: 62-68.

[12] Debbandt, AL, Ferreira, ML, Gschaider, ME. Theoretical and Experimental Study of M^{2+} Adsorption on Biopolymer. III. Comparative Kinetic Pattern of Pb, Hg and Cd. Carbonhyd Polym 2004; 56: 321-332.

[13] Ngomsik, A, Bee, A, Draye, M, Cote, G, Cabuil, V. Magnetic Nano- and Microparticles for Metal Removal and Environmental Applications: A Review. CR Chimie 2005; 8: 963–970.

[14] Li, YH, Ding, ZK, Luan, ZK, Di, ZC, Zhu, YF, Xu, CL, *et al*. Competitive Adsorption of Pb^{2+}, Cu^{2+} and Cd^{2+} Ions from Aqueous Solution by Multiwalled Carbon Nanotube. Carbon 2003; 41: 2787-2792.

[15] Lu, J, Xu, F, Cai, W. Adsorption of MTBE on Nano Zeolite composites of Selective Supports. Micropor Mesopor Mat 2008; 108: 50-55.

[16] Zhang, L, Huang, T, Zhang, M, Guo, X, Yuan, Z. Studies on the Capability and Behavior of Adsorption of Thallium on Nano-Al_2O_3. J Hazard Mater 2008; 157: 352-357.

[17] Liu, Z, Zhang, FS, Wu, J. Characterization and Application of Chars Produced from Pinewood Pyrolysis and Hydrothermal Treatment. Fuel 2010; 89: 510-514.

[18] Inyang, M, Gao, B, Yao, Y, Xue, Y, Zimmerman, AR, Pullammanappallil, P, *et al*. Removal of Heavy Metals from Aqueous Solution by Biochars Derived from Anaerobically Digested Biomass. Bioresource Technol 2012; 110: 50-56.

[19] Chen, X, Chen, G, Chen, L, Chen, Y, Lehmann, J, McBride, MB, *et al*. Adsorption of Copper and Zinc by Biochars Produced from Pyrolysis of Hardwood and Corn Straw in Aqueous Solution. Bioresource Technol 2011; 102: 8877-8884.

[20] Mohan, D, Pittman Jr, CU, Bricka, M, Smith, F, Yancey, B, Mohammed, J, *et al*. Sorption of Arsenic, Cadmium, and Lead by Chars produced from Fast Pyrolysis of Wood and Bark During Bio-oil Production. J Colloid Interf Sci 2007; 310: 57-73.

[21] Cao, X, Ma, L, Bin, G, Harris, W. Dairy Manure Derived Biochar Effectively Sorbs Lead and Atrazine. Environ Sci Technol 2009; 43: 3285-3295.

[22] Liu, Z, Zhang, FS. Removal of Lead from Water using Biochar Prepared from Hydrothermal Liquefaction of Biomass. J Hazard Mater 2009; 167: 933-939.

[23] Lagergren, S. About the Theory of So-Called Adsorption of Soluble Substances. Kungliga Svenska Vetenskapsakademiens, Handlinger 1898; 24: 1-39.

[24] Olgun, A, Atar, N. Equilibrium, Thermodynamics and Kinetic Studies for the Adsorption of Lead (II) and Nickel (II) onto Clay Mixture Containing Boron Impurity. J Ind Eng Chem 2012; 18: 1751-1757.

[25] Ho, YS, McKay, G. Sorption of Dye from Aqueous Solution by Peat. Chem Eng J 1998; 70: 115-124.

[26] Weber, WJ, Morris, JC. Kinetics of Adsorption on Carbon from Solution. J Sanitary Eng Div Proceed Am Soc Civil Eng 1963; 89: 31-59.

[27] Gomez-Serrano, V, Macias-Garcia, A, Espinosa-Mansilla, A, Valenzuella-Calahorro, C. Adsorption of Mercury, Cadmium and Lead from Aqueous Solution on Heat-Treated and Sulphurized Activated Carbon. Water Res 1998; 32: 1-4.

[28] Kolodyńska, D, Wnętrzak, R, Leahy, JJ, Hayes, MHB, Kwapiński, W, Hubicki, Z. Kinetics and Adsorptive Characterization of Biochar in Metal Ions Removal. Chem Eng J 2012; 197: 295-305.

[29] Lao, C, Zelendon, Z, Gamisans, X, Sole, M. Sorption of Cd(II) and Pb(II) from Aqueous Solutions by Low-Rank Coal (Leonardite). Sep Purif Technol 2005; 45: 79-85.

[30] Liu, Z, Zhang, FS. Removal of Copper (II) and Phenol from Aqueous Solution using Porous Carbons Derived from Hydrothermal Chars. Desalination 2011; 267: 101-106.

[31] Ramana, DKV, Reddy, DHK, Yu, JS, Seshaiah, K. Pigeon Peas Hulls Waste as Potential Adsorbent for Removal of Pb(II) and Ni(II) from Water. Chem Eng J 2012; 197: 24-33.

[32] Anwar, J, Shafique, U, uz-Zaman, W, Salman, M, Dar, A, Anwar, S. Removal of Pb(II) and Cd(II) from Water by Adsorption on Peels of Banana. Bioresource Technol 2010; 101: 1752-1755.

[33] Malairajan, S, Peters, E. Removal of Toxic Heavy Metals from Synthetic Wastewater using a Novel Biocarbon Technology. J Environ Chem Eng 2013. dx.doi.org/10.1016/j.jece.2013.07.030

[34] Atar, N, Olgun, A, Wang, S. Adsorption of Cadmium (II) and Zinc (II) on Boron Enrichment Process Waste in Aqueous Solutions: Batch and Fixed-Bed System Studies. Chem Eng J 2012; 192: 1-7.

[35] Naiya, TK, Bhattacharya, AK, Das, SK. Adsorption of Cd(II) and Pb(II) from Aqueous Solutions on Activated Alumina. J Colloid Interf Sci 2009; 333: 14-26.

[36] Olgun, A, Atar, N. Removal of Copper and Cobalt from Aqueous Solution onto Waste Containing Boron Impurity. Chem Eng J 2011; 167:140-147.

[37] Yu, B, Zhang, Y, Shukla, A, Shukla, SS, Dorris, KL. The Removal of Heavy Metal from Aqueous Solutions by Sawdust Adsorption-Removal of Copper. J Hazard Mater 2000; 80: 33-42.

[38] Li, PHY, Bruce, RL, Hobday, MD. A Pseudo First Order Rate Model for the Adsorption of an Organic Adsorbate in Aqueous Solution. J Chem Technol Biotechnol 1999; 74: 55-59.

[39] Foo, KY, Hameed, BH. Microwave-Assisted Preparation and Adsorption Performance of Activated Carbon from Biodiesel Industry Solid Residue: Influence of Operational Parameters. Bioresource Technol 2012; 103: 398-404.

[40] Qiu, H, Lv, L, Pan, B, Zhang, Q, Zhang, W, Zhang, Q. Critical Review in Adsorption Kinetic Models. J Zhejiang Univ Sci A 2009; 10: 716-724.

[41] Ozcan, A, Ozcan, AS. Adsorption of Acid Red 57 from Aqueous Solutions onto Surfactant-Modified Sepiolite. J Hazard Mater 2005; 125: 252-259.

[42] Wang, CP, Wu, JZ, Sun, HW, Wang, T, Liu, HB, Chang, Y. Adsorption of Pb(II) Ion from Aqueous Solutions by Tourmaline as a Novel Adsorbent. Ind Eng Chem Res 2011; 50: 8515-8523.

[43] Ozkaya, B. Adsorption and Desorption of Phenol on Activated Carbon and a Comparison of Isotherm Models. J Hazard Mater 2006; 129: 158-163.

[44] Mukherjee, S, Kumar, S, Misra, AK, Fan, M. Removal of Phenols from Water Environment by Activated Carbon, Bagasse Ash and Wood Charcoal. Chem Eng J 2007; 129: 133-142.

[45] Acharya, J, Sahu, JN, Mohanty, CR, Meikap, BC. Removal of Lead (II) from Wastewater by Activated Carbon Developed from Tamarind Wood by Zinc Chloride Activation. Chem Eng J 2009; 129: 249-262.

[46] Rao, MM, Ramesh, A, Rao, GPC, Seshaiah, K. Removal of Copper and Cadmium from Aqueous Solution by Activated Carbon Derived from *Ceiba pentandra* Hulls. J Hazard Mater 2006; 129: 123-129.

[47] Wang, Y, Tang, WX, Cheng, YM, Zhan, LT, Li, ZZ, Tang, Q. Adsorption Behaviour and Mechanism of Cd(II) on Loess Soil China. J Hazard Mater 2009; 172: 30-37.

[48] Boudrahem, F, Sonalah, A, Aissani-Benissad, F. Pb(II) and Cd(II) Removal from Aqueous Solution using Activated Carbon Developed from Coffee Residue Activated with Phosphoric Acid and Zinc Chloride. J Chem Eng Data 2011; 56: 1946-1955.

[49] El-Sofany, EA, Zaher, WF, Aly, HF. Sorption Potential of Impregnated Charcoal for Removal of Heavy metals from Phosphoric Acid. J Hazard Mater 2009; 165: 623-629.

[50] Elouear, Z, Bouzid, J, Boujelben, N, Feki, M, Montiel, A. The Use of Exhausted Olive Cake Ash (EOCA) as a Low Cost Adsorbent for the Removal of Toxic Metal Ions from Aqueous Solutions. Fuel 2008; 87: 2582-2589.

Chapter 6

Preparation of Mesoporous Carbon Monolith from Waste Plant Material

6.1 Introduction

The carbon materials prepared in Chapter 4 of this thesis are non-porous and in powder-like form which makes it difficult for the direct use of these materials in certain applications. Production of porous carbon materials from cheap naturally occurring precursors through environmentally friendly processes is a hot topic in modern materials science. Porous materials are generally classified based on the size of their pores (micro- < 2 nm), meso- 2–50 nm, and macroporous > 50 nm) and are widely considered as promising adsorbents due to their unique properties, such as, high surface areas, large pore volumes, regular and tunable pore sizes, and the well-arranged porous structure which can easily be modified or functionalized to fit into different kinds of purpose [1,2]. This study presents a novel concept using readily available and sustainable organic waste material as a precursor for the synthesis of porous carbon monolith. It aimed at providing a cost effective strategy for the production of advanced material through a green process which does not involve the use of too many chemicals, and also provides a platform for converting waste material into a useful form for different applications, therefore reducing environmental pollution.

Carbon monoliths with mesostructure have received widespread interest due to their structural features, such as, high surface area, high thermal stability and chemical inertness, and their promising applications as adsorbents, catalyst support, and electrode materials for electrochemical double-layer capacitors (EDLCs) [3-6]. Nanocasting methods utilising mesoporous silica materials as “hard template” have been the traditional way of preparing these materials. This method however, is costly and involves several steps to prepare the scaffolds which are normally sacrificed along with the surfactant templates [3]. The pore system of the mesoporous carbon is inversely replicated from the silica template and the morphology of the silica is usually preserved in the carbon, making it difficult for the direct control of the mesostructural property and morphology [7]. The use of mesoporous silica material is unsuitable as a template from the standpoint of morphology control because it is difficult to impregnate the pores of silica membrane with carbon precursor, and thus to maintain the continuous membrane and membrane adhesion to the substrate [7]. Silica monoliths

have been used in the past to fabricate corresponding carbon monolith using different approaches [8-14], the long processing time and high-cost of the synthesis makes it difficult for the method to be employed for large scale manufacturing of the materials [15]. This drawback has stimulated the search for the development of alternative time-saving and scalable synthesis of mesoporous carbon monoliths [15]. The "soft-template" method is expected to be more flexible in the synthesis of monolithic carbon materials in terms of scaling up and lowering the cost [3,16]. It is a method of organic-organic self-assembly involving the use of polymerizable precursor and block copolymer templates based on the principle of liquid-crystal templating [3]. This soft-template approach in general, uses cross-linked polymeric materials, such as, resorcinol-formaldehyde [3], resorcinol-phloroglucinol-formaldehyde [7], phenol-formaldehyde [4], as the carbon-yielding component and amphiphilic block copolymer usually F127 [3,5-7], CTAB [17], P123 [18], and mixed F127and P123 [4], as pore-forming component. The acidic route in particular affords carbons with better-developed mesostructure than that prepared under basic conditions [16]. Using the soft-template approach a family of mesoporous carbons have been synthesised using the hydrothermal approach [3-6,15], aqueous reaction routes under atmospheric pressure at relatively low temperatures [19,20], or via the evaporation-induced self-assembly (EISA) [21-23].

Hydrothermal synthesis route has also been extensively used in the preparation of carbonaceous material, as well as in the inorganic synthesis of nanomaterials, zeolites, ion-conductors and catalysts under controlled temperature and pressure [24-28]. This powerful method is faster and more energy efficient than conventional aqueous chemical processing conditions [4]. Evaporation-induced self-assembly (EISA) method on the other hand has been used recently and has proven to be an attractive alternative to the synthesis of carbon film and monoliths, although structural disfigurement of the resultant materials always take place [29]. The direct synthesis of mesoporous carbon with well-ordered pore systems and perfect macroscopic morphologies using EISA still pose a great challenge, because of the difficulty in controlling the solvent evaporation rate [3].

The use of microwave heating and waste plant materials as carbon precursor in the synthesis of carbon monolith to the best of my knowledge is absent in literature, despite the advantages of using microwave heating over the conventional oven heating,

and the reduction in cost of production the use of readily available and sustainable waste plant materials as carbon precursors will bring into the synthesis of monolithic carbon materials. It would therefore be significant, if the carbon monoliths could be synthesised through a one-step process that is economical and convenient like using microwave heating in place of the conventional oven heating and using a waste plant material as carbon precursor.

In this chapter, the aim is to use microwave-assisted hydrothermal process and the evaporation-induced self-assembly (EISA) approach to prepare carbon monoliths from waste plant material. The effect of different conditions, namely microwave temperature and time, and the ratio of the waste plant material to the template (pluronic F127) on the synthesis will also be considered.

6.2 Synthesis Routes for the Formation of Mesoporous Carbon Monolith

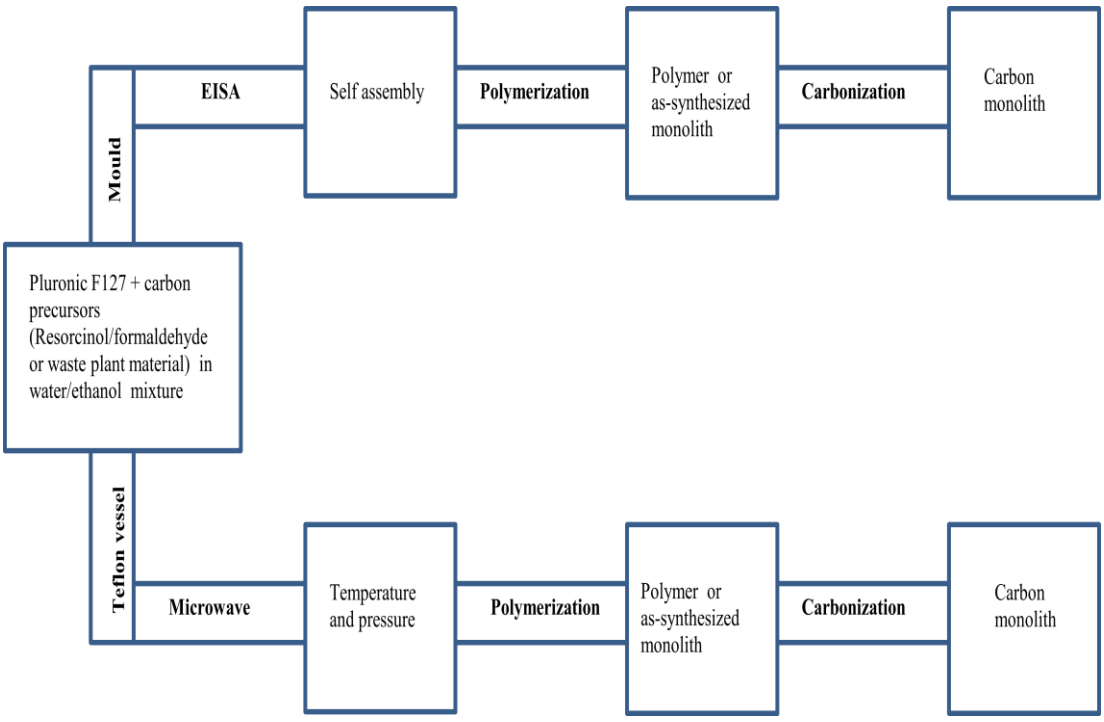

Figure 6.1: Formation of mesoporous carbons monolith through different routes. Temperature and pressure enhances the polymerization rate under the microwave-assisted route making it faster than the EISA route in which the evaporation of the solvent drives the assembly between the reacting molecules.

The synthesis route for the formation of carbon monoliths with mesostructure through organic-organic self-assembly is by strong and collective interactions involving the reacting species [21]. The formation routes for carbon monoliths with mesostructure is shown in Figure 6.1. In the first instance, polymerization slowly takes place between the carbon precursors (e.g. resorcinol and formaldehyde) forming water-soluble oligomers which have plenty of hydroxyl groups. These hydroxyl groups are capable of interacting through hydrogen bonding with the polyethylene oxide (PEO) segments of the amphiphilic triblock copolymer [30]. A strong interaction between the oligomers and the template would result and drive the assembly process between the (resorcinol-formaldehyde) polymer and the pluronic F127 [31]. The processing condition of the phase-segregated polymer phase determines the periodicity and the pore size distribution of the resulting carbon materials [3]. It is expected that under the microwave-assisted hydrothermal synthesis, the temperature and pressure play an important role in enhancing the interactions between the molecules, thereby inducing a faster rate of polymerization, and this can accelerate the phase separation. The reaction mixture, which is homogenous, separates slowly into two distinct layers, the upper layer made up of ethanol and water, and the lower layer made up of polymer/F127. A polymer monolith with rigid mesostructure is obtained from the lower phase on further polymerization. This results in increased tolerance to internal pressure during the drying and carbonization process, leading to the absence of macrocracks accompanying the uniform structural shrinkage. The template decomposes on carbonization changing the polymer monolith to a carbon monolith leading to the formation of mesopores [3].

In the case of the evaporation-induced self-assembly, the evaporation of the solvent drives the assembly between the oligomers and F127. The challenge in using evaporation-induced self-assembly is the difficulty in controlling the rate of evaporation due to the shape of the mould which makes the reaction mixture only have a small area in contact with the atmosphere and also due to the presence of water and in such situation it is difficult for phase separation to reach equilibrium, except if an external force is applied such separation could be facilitated resulting in a higher ordered structure [3].

6.3 Materials and Methods

6.3.1 Materials

Poly(ethylene oxide)-b-poly(propylene oxide)-b-poly(ethylene oxide) triblock copolymer Pluronic F127 ($EO_{106}PO_{70}EO_{106}$) and resorcinol were purchased from Sigma Aldrich, UK, formaldehyde and ethanol were purchased from Fischer Scientific, UK, while 37 % hydrochloric acid was purchased from Romil, UK. The *Prosopis africana* shell is a waste plant material of Nigerian origin. It was collected in Benue State, Nigeria and was dried, crushed and sieved to 212 µm size. The *Prosopis africana* shell has been described in Chapter 4.

6.3.2 Methods

6.3.2.1 Microwave-Assisted Hydrothermal Synthesis of Carbon Monolith

The synthesis was carried out in microwave oven (MARS, CEM, Milton Keynes, UK equipped with XP1500 digestion vessels). The pressure was monitored in the reference vessel during the reaction using a pressure sensor, while the temperature was monitored using an infrared fibre optic sensor installed in a ceramic sleeve in the same vessel. The microwave power used was 400W.

In order to study the effectiveness of microwave heating in the hydrothermal synthesis of carbon monolith, before using waste plant material as carbon precursor in such synthesis, a repeat of previously reported method by Liu *et al.* [3] using conventional oven heating was carried out in the microwave oven. In a typical synthesis, 2.5 g of pluronic F127 and 1.65 g of resorcinol were dissolved in a mixture of deionised water and ethanol (20 mL each). A colourless solution was obtained after the mixture was stirred for about 15 minutes. 0.2 g of 37 % hydrochloric acid was then added to the resulting solution. It was then stirred for 1 hour, after which 2.5 g of formaldehyde was added in dropwise. The reaction mixture was vigorously stirred for another 1 hour and it was poured into a microwave reaction vessel made of Teflon. It was then placed in a microwave. The mixture was heated between 50-100 ºC in the microwave which was set to ramp to a given temperature in 5 minutes and was held at the given temperature for 5-20 minutes. The maximum pressure attained during the process was 0.32 MPa. The reaction system was allowed to cool down to room temperature and the resulting polymer monolith was collected by filtration using

Whatman filter paper number 3, ashless 11 cm, washed several times with de-ionised water, poured into a mould and dried in a conventional oven at 50 ºC for 12 hours, and then 80 °C for 12 hours. This made the colour of the polymer monolith to change from cream to orange. After this, the resulting polymer monolith was carbonized in a tubular furnace under an inert environment of nitrogen flow with a heating rate of 5 ºC/min, and then keeping the temperature at 600 ºC for 6 hours to obtain the carbon monolith. The synthesized carbon monolith were denoted as CM_{x-y}, where x and y represent temperature and time in the microwave respectively.

For the microwave-assisted hydrothermal synthesis of carbon monolith using waste plant material as carbon precursor, the method of Liu *et al.* [3] was also adopted with modification. In a typical synthesis, 2.5 g of the pluronic F127 was dissolved in a mixture of deionized water and ethanol (20 mL each). 2.5-7.5 g of *Prosopis africana* shell was added. This was followed by the addition of 0.2 g of 37 % hydrochloric acid. The reaction mixture was then stirred for 1 hour and was poured into the microwave reaction vessel made of Teflon and treated the same way as stated above.

6.3.2.2 Evaporation-Induced Self-Assembly Synthesis of Carbon Monoliths

The method of Liu *et al.* [3] was adopted, but the carbon precursor in this study is a waste plant material. In a typical synthesis, 2.5 g of the pluronic F127 was dissolved in a mixture of deionized water (20 mL) and ethanol (20 mL) in a conical flask. 2.5 g of *Prosopis africana* shell was added. This was followed by the addition of 0.2 g of 37 % hydrochloric acid. The reaction mixture was then stirred for 1 hour and it was left open for 72 hours at room temperature to enable the ethanol to evaporate. The reaction mixture was then transferred into moulds of different sizes and dried in a conventional oven at 50 ºC for 12 hours and 80 ºC for 12 hours. The obtained monolith was carbonized in a tubular furnace under an inert atmosphere of nitrogen flow with the heating rate of 5 ºC/min, and keeping the temperature at 600 ºC for 6 hours to obtain the corresponding carbon monolith.

6.4 Characterization

The characterization of the materials was carried out using a wide range of instruments. N_2 adsorption and desorption isotherms were measured on a Micromeritics Tristar BET-N_2 surface area analyser, before carrying out the analysis

the samples were degassed at 120 ºC for 3 hours. The Brunauer-Emmett-Teller (BET) model was used for calculating the specific surface area (S_{BET}), while the pore size distributions were calculated using the Barett-Joyner-Halenda (BJH) model. Fourier transform infrared (FT-IR) spectra were collected on a Thermoscientific Nicolet 380 FT-IR using KBr pellets of the solid samples. Each sample was investigated in the wavenumber range of 4000–525 cm^{-1} using 16 scans at a spectral resolution wavenumber of 4 cm^{-1}. The morphology and particle size was visualised using a ZEISS EVO 60 scanning electron microscopy (SEM), the samples were coated with gold and platinum alloy and impregnated on a sticky disc before analysis.

6.5 Results and Discussion

6.5.1 Microwave-Assisted Hydrothermal Synthesis of Carbon Monolith using Resorcinol and Formaldehyde as Carbon Precursor

6.5.1.1 Effect of Temperature on the Synthesis

At a reaction temperature of 50 ºC for 5-20 minutes, no phase separation was observed in the microwave vessel, this could probably be because the temperature and pressure generated were not sufficient or too low to enhance the polymerization reaction between the hydroxyl group of the oligomer and the polyethylene oxide (PEO) segment of the template [3]. At 75 ºC for 20, 15, 10 and 5 minutes, a small amount of cream gel-like product was obtained, but on drying in the oven at 50 ºC for 12 hours and 80 ºC for 12 hours, it turned to an orange gel which attached to the walls of the mould and could not be removed for further study, which could be attributed to the formation of lowly cross-linked resorcinol-formaldehyde polymer [5], indicating that the polymer monolith was not rigid enough and required further polymerization. At 100 ºC, a large amount of cream gel-like product was obtained, which on drying in the oven at 50 ºC for 12 hours and 80 ºC for 12 hours turned to a solid orange polymer monolith which took the shape of the mould in which it was dried. Irrespective of the time, microwave-assisted hydrothermal synthesis at 100 ºC produced a rigid polymer monolith; the difference was only in the yield. At 120 ºC for 20, 15, 10 and 5 minutes, the product obtained was an orange foam-like solid, which could probably be because the temperature and pressure were too high for the polymerization process.

6.5.1.2 Effect of Time on the Synthesis

The effect of time on the microwave-assisted hydrothermal synthesis was investigated at a constant temperature of 100 ºC, since this temperature was found to be optimal for the synthesis, while the time for the synthesis was varied from 5-20 minutes. The yield increased with time until 20 minutes, and after that the yield was almost the same as that of 20 minutes and because of this, syntheses above 20 minutes were not investigated further. All carbon monoliths synthesized at 100 ºC showed a Type IV isotherm based on the IUPAC system of classification [32] with capillary condensation at P/P_0 = 0.5–0.8 and pore size distribution in the range of 6.4-7.7 nm (Appendix 1-4), while the SEM images (Appendix 5) of all the synthesized monoliths were made up of microspheres of different sizes in the range of 10-20 µm. Table 6.1 shows a summary of the structural properties for the carbon monoliths prepared by varying the time at 100 ºC. Due to the similarities in the properties of the synthesized carbon monolith further discussion was limited to the synthesis at 100 ºC for 20 minutes ($CM_{100\text{-}20}$) which was found to have the highest yield for the synthesis in this study.

Carbon Monolith (100 °C)	**Yield (%)**	**BET surface area (m^2/g)**	**Pore size (nm)**	**Total pore volume (cm^3/g)**	**[a]Micropore volume (cm^3/g)**	**[b]Mesopore volume (cm^3/g)**
$CM_{100\text{-}20}$	55±0.50	697±36	6.4±0.0	0.85±0.12	0.14±0.08	0.71±0.04
$CM_{100\text{-}15}$	54±1.05	665±28	6.5±0.1	0.75±0.05	0.14±0.10	0.61±0.15
$CM_{100\text{-}10}$	51±0.75	646±42	7.7±0.5	0.67±0.05	0.15±0.02	0.52±0.07
$CM_{100\text{-}5}$	47±2.33	630±35	7.7±0.3	0.58±0.03	0.13±0.03	0.45±0.06

[a] The micropore volume was calculated from the t-plot method.

[b]The mesopore volume is the difference between the total pore volume and the micropore volume.

Table 6.1: Structural properties for microwave-assisted carbon monoliths using resorcinol and formaldehyde as carbon precursor

Figure 6.2 (a and b) shows the photographs of the polymer monolith and the corresponding carbon monoliths respectively. The polymer monoliths (Figure 6.2 a) showed good bulk macroscopic appearance and are very stable and crack-free. The shape of the polymer monoliths can be changed by changing the shape of the moulds. The carbon monoliths (Figure 6.2 b) obtained after carbonization at 600 ºC for 6 hours remained crack-free, although the volume shrinks to about 50%, while the colour changes from orange to black, the monolithic morphology was still preserved. The high yield for the carbon monolith and the relatively high speed of the microwave-assisted hydrothermal route suggest that this synthetic route could be of importance for the large-scale production of mesoporous monolithic carbon materials [4].

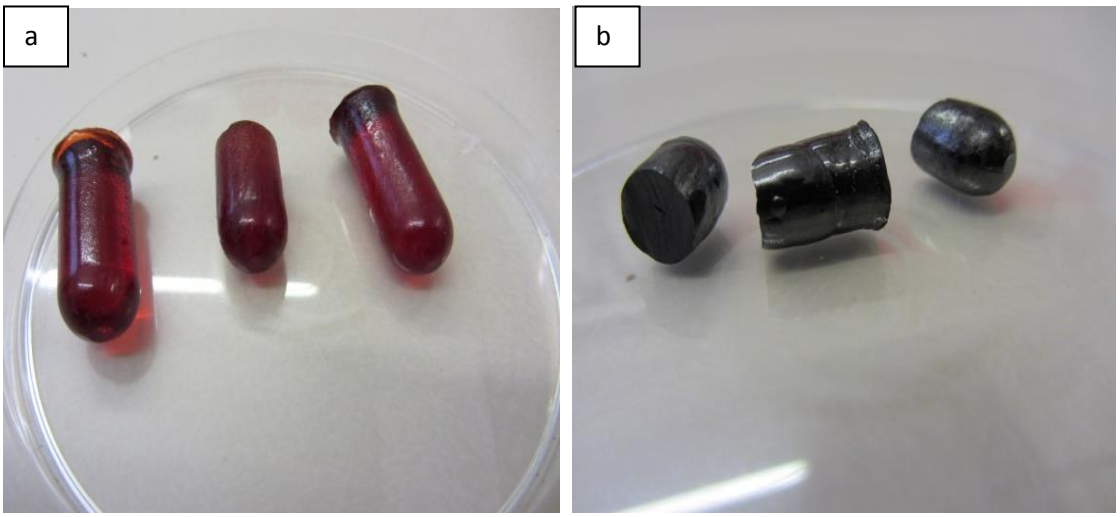

Figure 6.2: Photographs of (a) polymer monolith (b) carbon monolith from microwave-assisted hydrothermal synthesis using resorcinol and formaldehyde as carbon precursor. The carbon monolith remained stable, crack-free, and maintained the monolithic shape despite the shrinkage during the high temperature carbonization.

The scanning electron microscope (SEM) provided more information about the structural morphologies of the carbon monolith. The SEM of the polymer monolith Figure 6.3 (a), shows a material that is non-porous. After carbonization, Figure 6.3 (b), porous carbon monoliths with fused sphere-like microparticles of different sizes (10-20 µm) were obtained, which result from the decomposition of the template (Pluronic F127) during the carbonization process opening up the pores, and leaving behind the carbon precursors which grew into the sphere-like microparticles and also remained as carbonaceous pore wall [7].

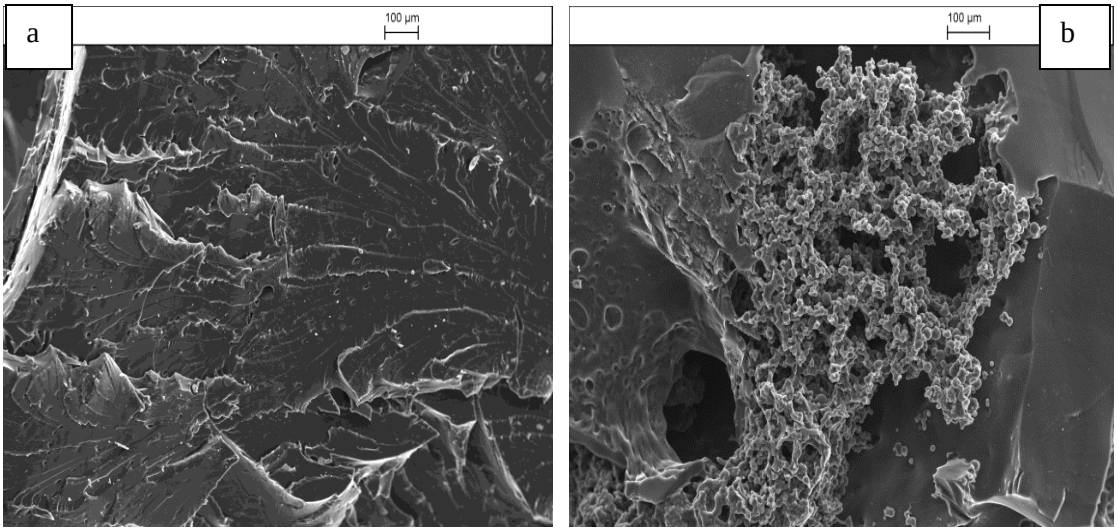

Figure 6.3: SEM images of (a) polymer monolith (b) carbon monolith from microwave-assisted hydrothermal synthesis using resorcinol and formaldehyde as carbon precursor. The template decomposed on carbonization forming the pores as seen in the carbon monolith leaving the carbon precursor that formed the pore walls.

A further insight into the changes in the material and pore generation on carbonization was provided by the nitrogen sorption measurements performed on the polymer and carbon monoliths. Figures 6.4 (a-c) show the N_2 adsorption-desorption isotherms of the polymer monolith, carbon monoliths, and the pore size distribution of the carbon monolith. The polymer monolith showed a Type II isotherm, which is a typical isotherm for a non-porous material [32], while a typical Type-IV isotherm with a hysteresis loop, which is a characteristic exhibited by mesoporous materials was obtained for the carbon monolith [5], with a clear step which is associated with the filling of mesopores due to capillary condensation at approximately P/P_0 = 0.5–0.8, suggesting the synthesized carbon monolith has a uniform mesopore [4]. It has a narrow pore size distribution of 6.4 nm and BET surface area of 697 m^2/g. It has been reported that mesoporous carbonaceous material obtained using triblock copolymers as template also possess micropores [33,34]. The increase in the amount of gas adsorbed at low relative pressure ($P/P_0 < 0.1$) for the carbon monolith (Figure 6.4 b) confirms the presence of the micropores in the framework [3]. The high surface area and pore volume (Table 6.1) is an indication that the synthesized carbon monolith would exhibit excellent performance in applications, such as, adsorption of pollutants, energy storage and catalysis [4,35].

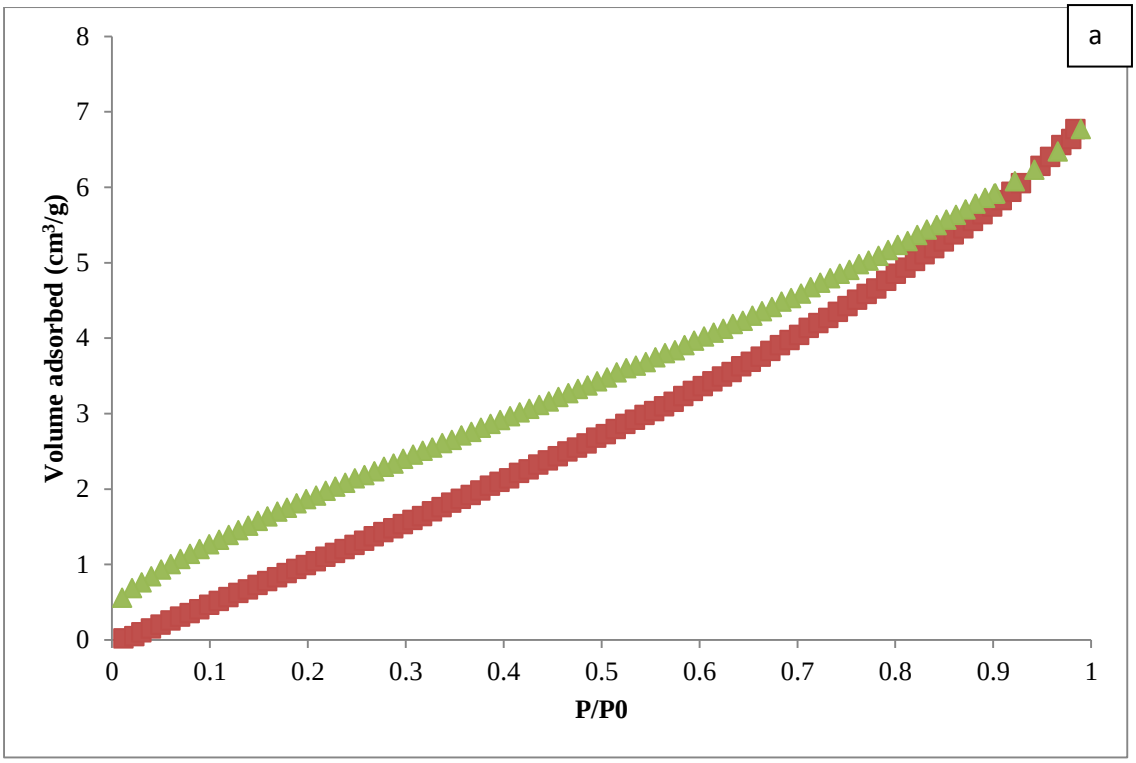

Figure 6.4 (a): N_2 adsorption-desorption isotherm of polymer monolith, showing a Type II isotherm which is a characteristic exhibited by a non-porous material.

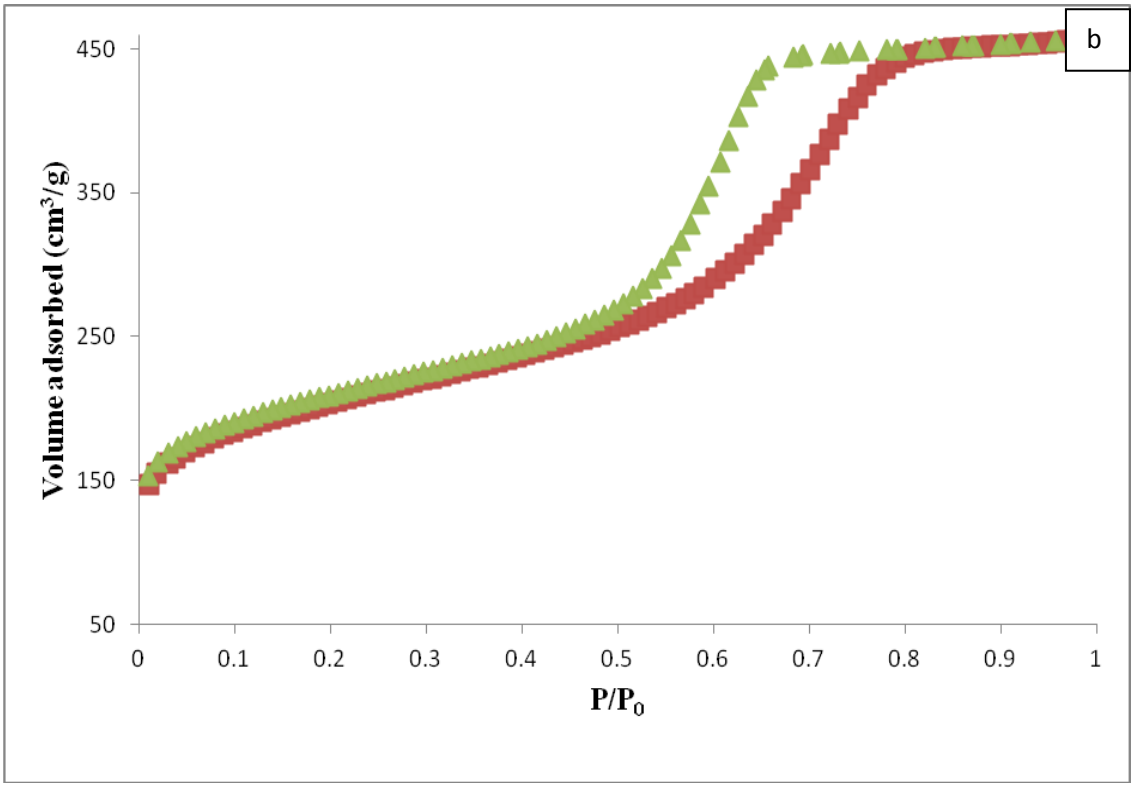

Figure 6.4 (b): N_2 adsorption-desorption isotherm for carbon monolith, showing a Type IV isotherm with a hysteresis loop, which is a characteristic exhibited by mesoporous materials. The increase in gas adsorption at $P/P_0 < 0.1$ indicates the presence of micropores.

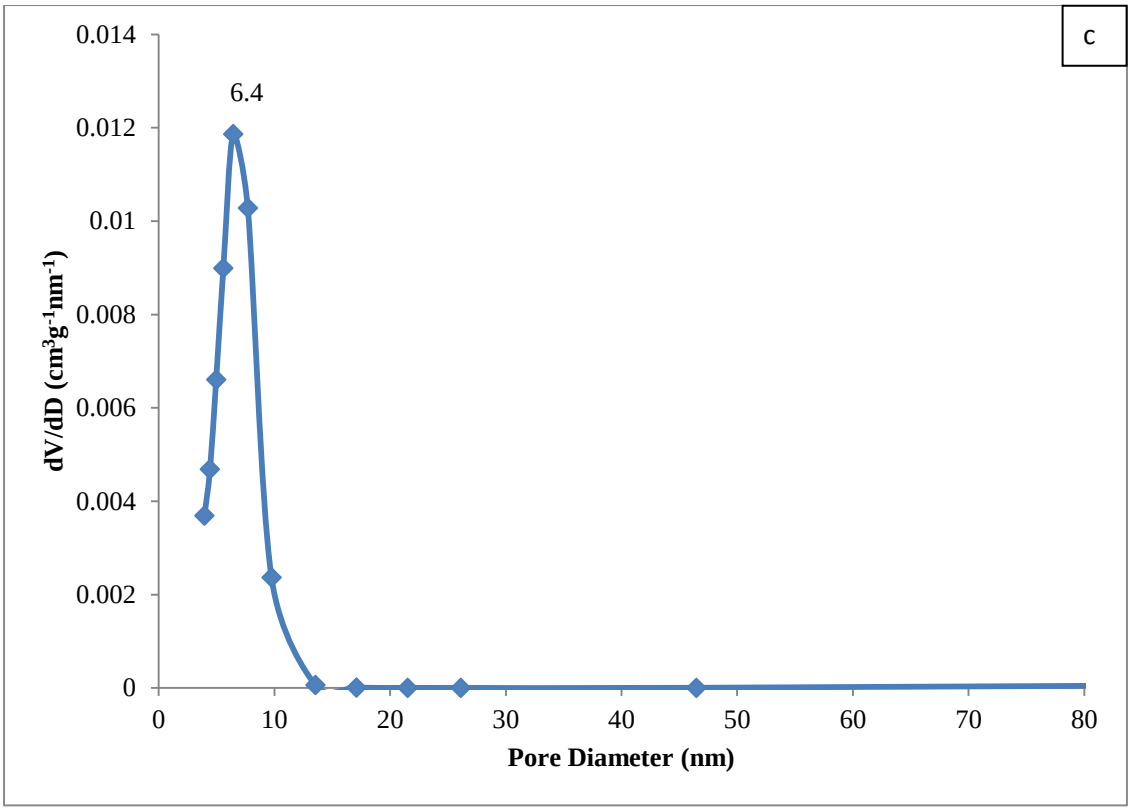

Figure 6.4 (c): Pore size distribution for carbon monolith from microwave-assisted hydrothermal synthesis using resorcinol and formaldehyde as carbon precursor, showing a narrow pore size of 6.4 nm which is in the mesopore range.

The FTIR-KBr analysis gave further insight into the chemical composition of the carbon monolith. Figure 6.5 shows the FT-IR spectra of the polymer monoliths (red) and the corresponding carbon monolith (green). The spectra have different shapes, indicating a clear change in the framework. The determination of the main functional groups for a given wavelength is based on previous report [3,5] and summarized in Table 6.2. A broad band present at about 3600-3000 cm^{-1} is due to –OH stretching, showing the presence of a large number of phenolic groups in the polymer monolith. The peaks at about 1600-1400 cm^{-1} are due to the C-C stretching vibration of tri-substituted aromatic ring structure of phenolic resin framework of the resorcinol-formaldehyde, were retained after carbonization indicating the aromatic nature of the carbon monolith. The peaks at about 1200-950 and 3000-2800 cm^{-1} which could be assigned to the C-O and C-H stretching vibrations arising from the triblock copolymer F127 also disappeared in the carbon monolith confirming the removal of F127 by decomposition after the carbonization. The peaks below 950 cm^{-1} are due to aromatic C-H bending vibrations.

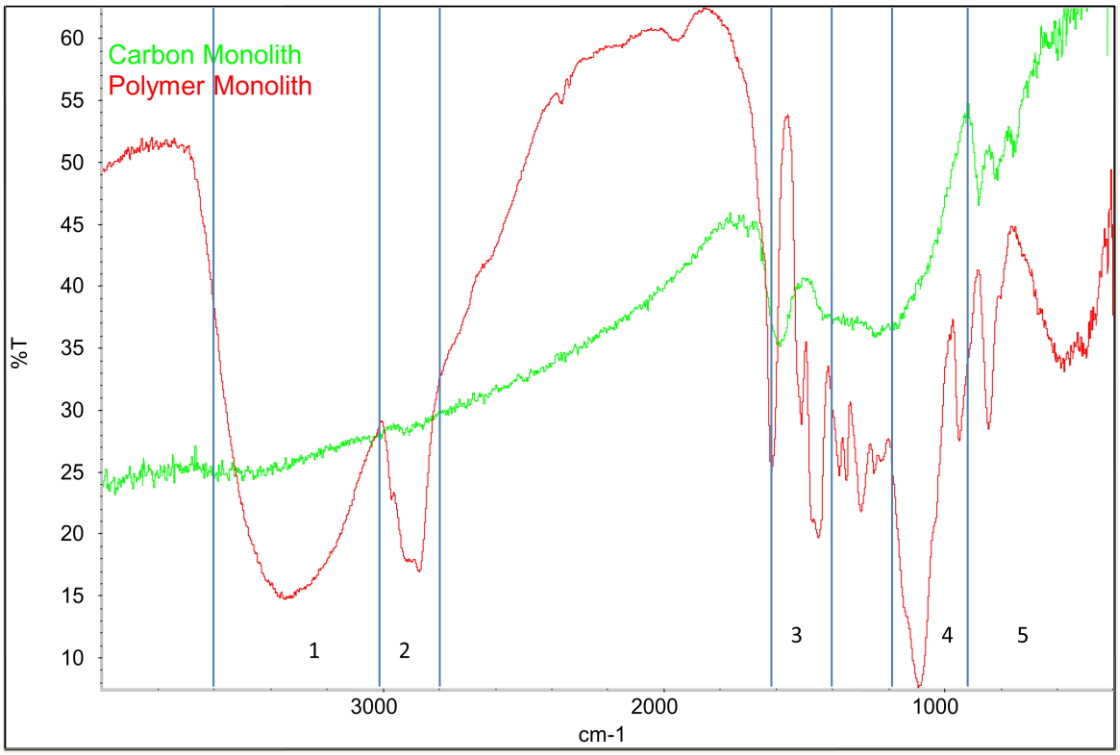

Figure 6.5: FTIR-KBr spectra of polymer monolith (red) and carbon monolith (green) from microwave-assisted hydrothermal synthesis, showing the different sections and the changes in the spectra due to the decomposition of the template during the carbonization process (assignment of functional group is in Table 6.2).

Section	Wavelength range (cm^{-1})	Functional group	Description
1	3600-3000	O-H stretching	Due to the presence of a large number of phenolic groups in the polymer monolith
2	3000-2800	C-H stretching	Due to the stretching vibrations of C-H bond in the triblock copolymer F127
3	1600-1400	C-C stretching	Due to the stretching vibration of tri-substituted aromatic ring structure of phenolic resin framework of the resorcinol-formaldehyde
4	1200-950	C-O stretching	Due to the stretching vibrations of C-O bond in the triblock copolymer F127
5	< 950	C-H bending	Due to aromatic C–H bending vibrations

Table 6.2: Assignment of the main functional groups to FTIR-KBR peaks of microwave-assisted hydrothermal synthesis using resorcinol and formaldehyde as carbon precursor.

The results obtained in this study in minutes using the microwave-assisted hydrothermal carbonization is consistent with previous reports in literature which took days and hours using the conventional method of oven heating [3,4]. Therefore, the use of microwave heating could be a time saving strategy in the synthesis of monolithic carbon materials. However, the microwave-assisted hydrothermal synthesis using waste plant material as carbon precursor was unsuccessful because the as-synthesized monolith cracked, which could be attributed to the low solubility of the waste plant material in water, coupled with a steric hindrance, due to the large amount of the groups present within the waste plant material (*Prosopis africana* shell), making the fabrication of a crack-free monolith difficult at the applied temperature and pressure [36]. This feature could limit the use of biomasses in the hydrothermal synthesis of monolithic carbon material. However, when the evaporation-induced self-assembly (EISA) approach was used in the synthesis of carbon monolith using waste plant material (*Prosopis africana* shell) as a source of cheap and readily available carbon precursor in replace of widely studied resorcinol and formaldehyde, a crack-free carbon monolith was obtained and the result for the synthesis is discussed below.

6.5.2 Evaporation-Induced Self-Assembly Synthesis of Carbon Monoliths using Waste Plant Material as Carbon Precursor

As mentioned earlier, the aim of this chapter is to use a waste plant material as carbon precursor in the synthesis of carbon monolith. The reason for this is because, it is thought that the high numbers of hydroxyl groups of the oligomers present in the plant material will provide the great driving force needed for the self-assembly interaction with the polyethylene oxide (PEO) segments of the amphiphilic triblock copolymer through hydrogen bonding [30]. This factor is very important for the preferential organisation of the carbon precursors according the spatial arrangement of the hydrophilic block of the F127 [3]. It is also believed that the oligomers in the plant material in addition, can further polymerize to thermosetting polymers with cross-linked nanostructure, resulting in high carbon content and mesoporous structure after carbonization in an inert atmosphere.

Figure 6.6: Photographs of (a) as-synthesized monolith (b) carbon monolith from evaporation-induced self-assembly using waste plant material as carbon precursor. The carbon monolith remained crack-free despite structural shrinkage during the high temperature carbonization.

Photographs of the as-synthesized and the corresponding carbon monoliths are shown in Figure 6.6. Very stable carbon samples that retained the shape of the monolith were obtained after carbonization. However, the volume shrinks to about 75% of the original volume. Despite the reduction in volume during the carbonization process, the carbon monolith remained crack-free indicating high thermal stability.

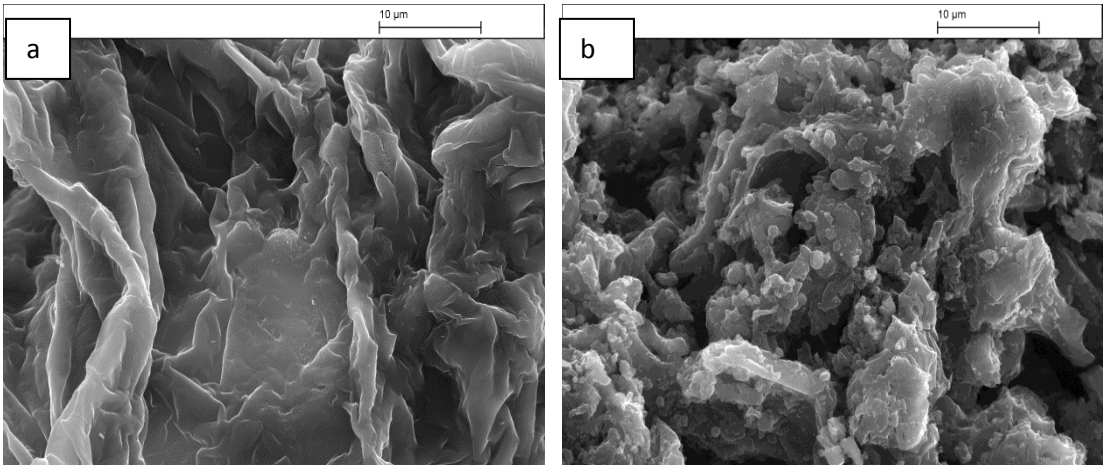

Figure 6.7: SEM images of (a) as-synthesized monolith (b) carbon monolith from evaporation-induced self-assembly using waste plant material as carbon precursor, showing the change in morphology of the monolith after the decomposition of the template during carbonization.

The scanning electron microscope (SEM) provided information about the structural morphologies of the synthesized material. Figure 6.7 shows the SEM images of the as-synthesized (a) and the carbon monolith (b). The as-synthesized monolith shows a network of fibrous structures typical of lignocellulosic material, while small

sphere-like microparticles ~1 μm in diameter were seen on the surface of the carbon monolith resulting from the evolutional development of plant tissue [35].

The N_2 adsorption-desorption isotherm of the as-synthesized and carbon monolith shown in Figures 6.8 (a-c) gave a further insight into the porosity of the material. A Type II isotherm was obtained for the as-synthesized monolith, implying that it is non porous, while a Type-IV isotherm was obtained with hysteresis loop and a clear capillary condensation step at P/P_0 ~0.4-0.8, which is a characteristic exhibited by mesoporous materials [5], was obtained for the carbon monolith. It has a narrow pore size distribution centred at 6.5 nm calculated using the BJH method indicating uniform mesopore, with a surface area of 219 m^2/g and a total pore volume of 0.21 cm^3/g. The pore system of the carbon monolith is almost completely mesopores, as it contains very few numbers of micropores from the t-plot analysis (Table 6.3).

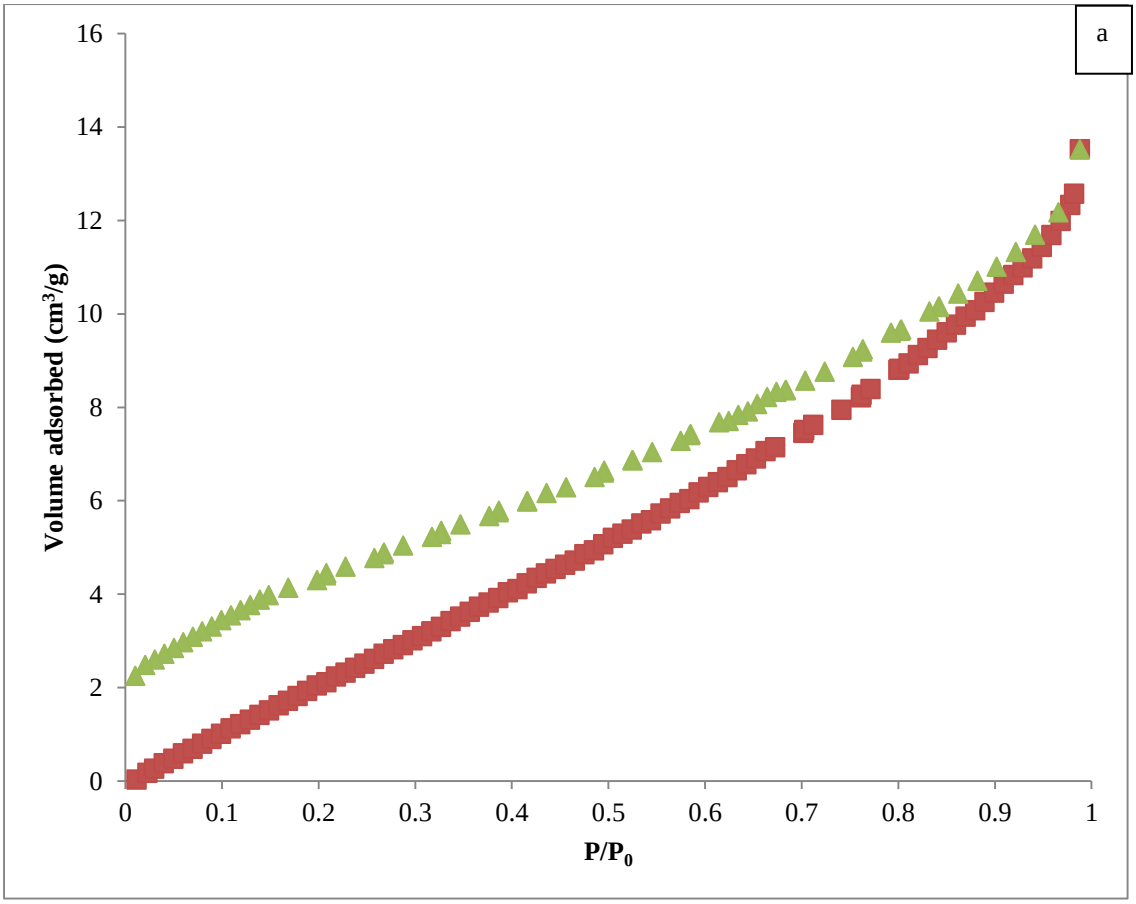

Figure 6.8(a): N_2 adsorption-desorption isotherm of the as-synthesized monolith, showing a Type II isotherm which is a typical isotherm exhibited by a non-porous material.

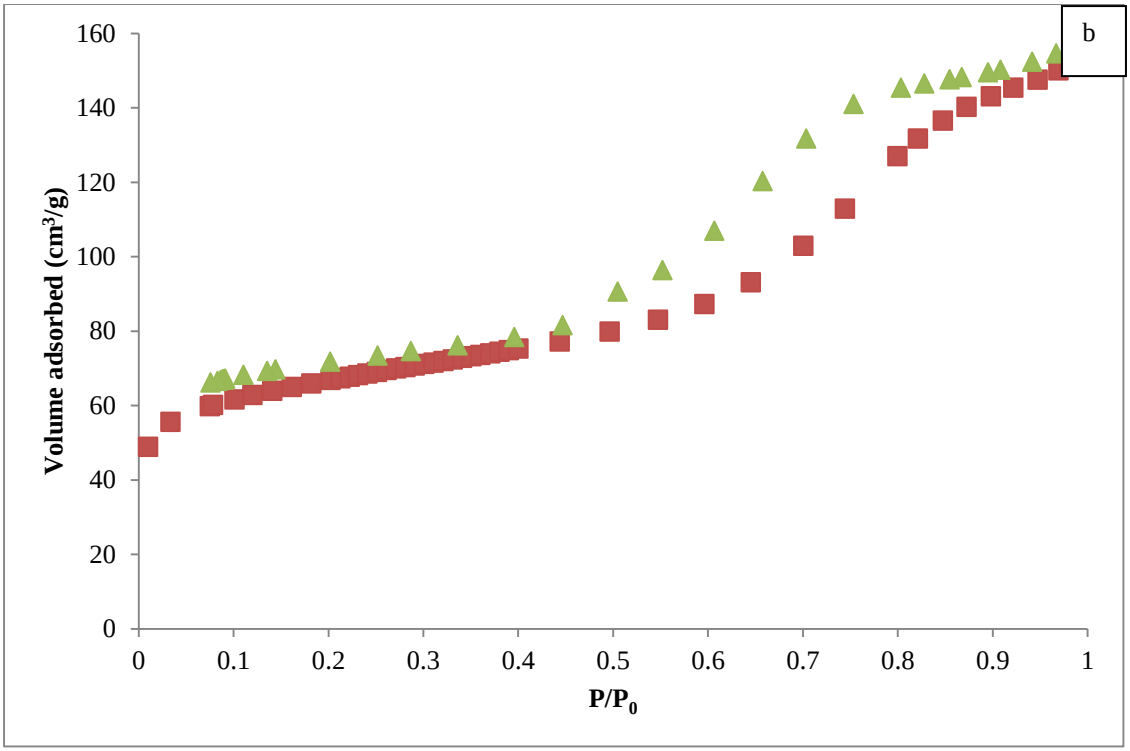

Figure 6.8(b): N_2 adsorption-desorption isotherm of the carbon monolith, showing a Type IV isotherm with a hysteresis loop which is typical of a mesoporous materials. The increase in gas adsorption at $P/P_0 < 0.1$ indicates the presence of micropores.

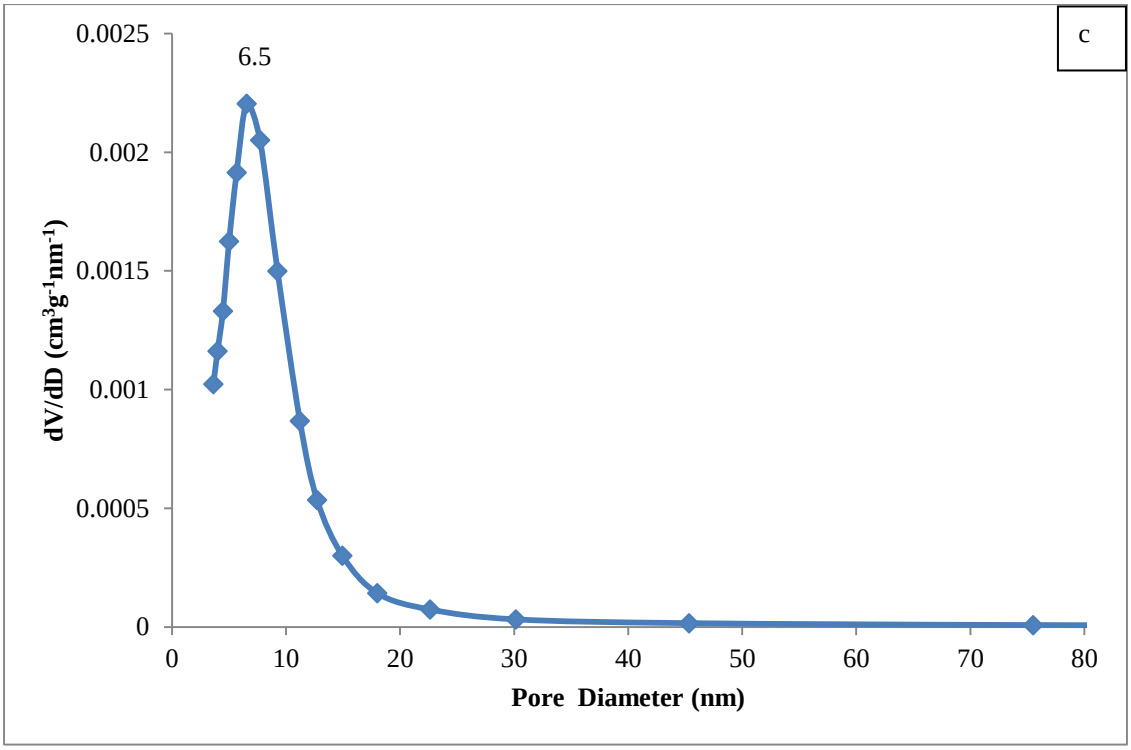

Figure 6.8(c): Pore size distribution of the carbon monolith from evaporation-induced self-assembly using waste plant material as carbon precursor, showing a narrow pore size in the mesopore range.

F127:*Prosopis africana* shell	Surface Area (m^2/g)	Pore Size (nm)	Total Pore Volume(cm^3/g)	[a]Micropore volume (cm^3/g)	[b]Mesopore volume (cm^3/g)
1:1	219±12	6.5±0.0	0.21±0.01	0.05±0.00	0.16±0.01
1:2	146±8	6.5±0.1	0.18±0.02	0.03±0.01	0.15±0.01
1:3	0.14±0.04	-	-	-	-

[a] The micropore volume was calculated from the t-plot method.

[b]The mesopore volume is the difference between the total pore volume and the micropore volume.

Table 6.3: Structural properties for carbon monoliths by evaporation-induced self-assembly using waste plant material as carbon precursor

The effect of different conditions on the synthesis was investigated by varying the ratio of the plant material to the pluronic F127. This is because to obtain a mesostructure based on the principles of organic-organic self-assembly the carbon precursor is very important [3]. The time for the reaction was also varied from 24-72 hours. As the amount of the waste plant material used was increased to 5 g, while the amount of the pluronic F127 was kept constant (ratio 1:2 of template:waste plant material), the synthesised carbon monolith was still mesoporous and also has a narrow pore size distribution of 6.5 nm as shown in Figures 6.9 (a and b), however the surface area reduced to 146 m^2/g, which was due to the increase in the amount of plant material used to the template which is the pore forming component. An important criterion to use the template successfully is to adequately load the precursors into the porous network, which is normally carried out by an efficient impregnation of the solution within the pores of the template avoiding as much as possible only surface coating [36]. When 7.5 g of the plant material was used (ratio 1:3); a non-porous material was obtained (Table 6.3). Figures 6.10 (a-c) shows that as the ratio of the *Prosopis africana* shell to the pluronic F127 increased the morphology of the obtained carbon monolith becomes non-porous and more plant-like, obviously due to the increase in the amount of the *Prosopis africana* shell added and also indicating that the amount of template used is insufficient for the waste plant material. These results show the possibility of easily changing the surface area, pore size distribution and pore volume of carbon monoliths, without necessarily changing the monolithic aspect and the macro-morphology, which could help in tailoring the porous structure to fit into specific applications [36]. The summary of the structural properties for the different ratios is

given in Table 6.3. For the effect of time, when 24 and 48 hours were used, the synthesized carbon monolith cracked and when the time was more than 72 hours no significant difference was observed in the carbon monolith. In this study, the optimal reaction condition was found to be ratio 1:1 (template:plant material) and a reaction time of 72 hours.

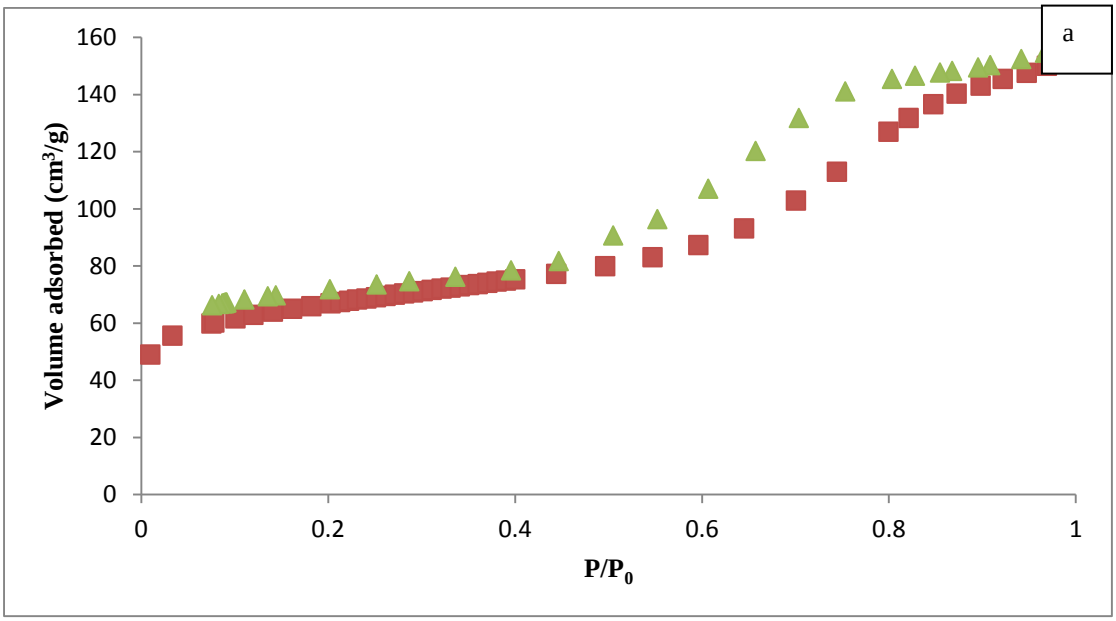

Figure 6.9 (a): N_2 adsorption-desorption isotherm of carbon monolith obtained using ratio 1:2 of template:waste plant material. The carbon monolith exhibits a Type IV isotherm with a hysteresis loop which is typical of a mesoporous material.

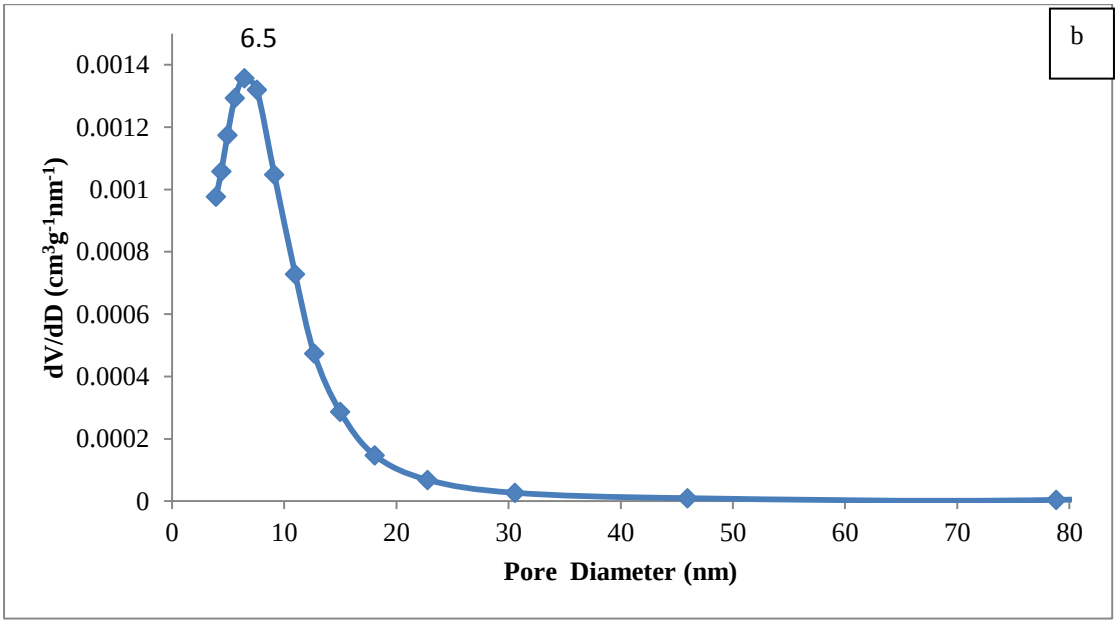

Figure 6.9 (b): Pore size distribution for carbon monolith obtained using ratio 1:2 of template:waste plant material, showing pore size in the mesopore range.

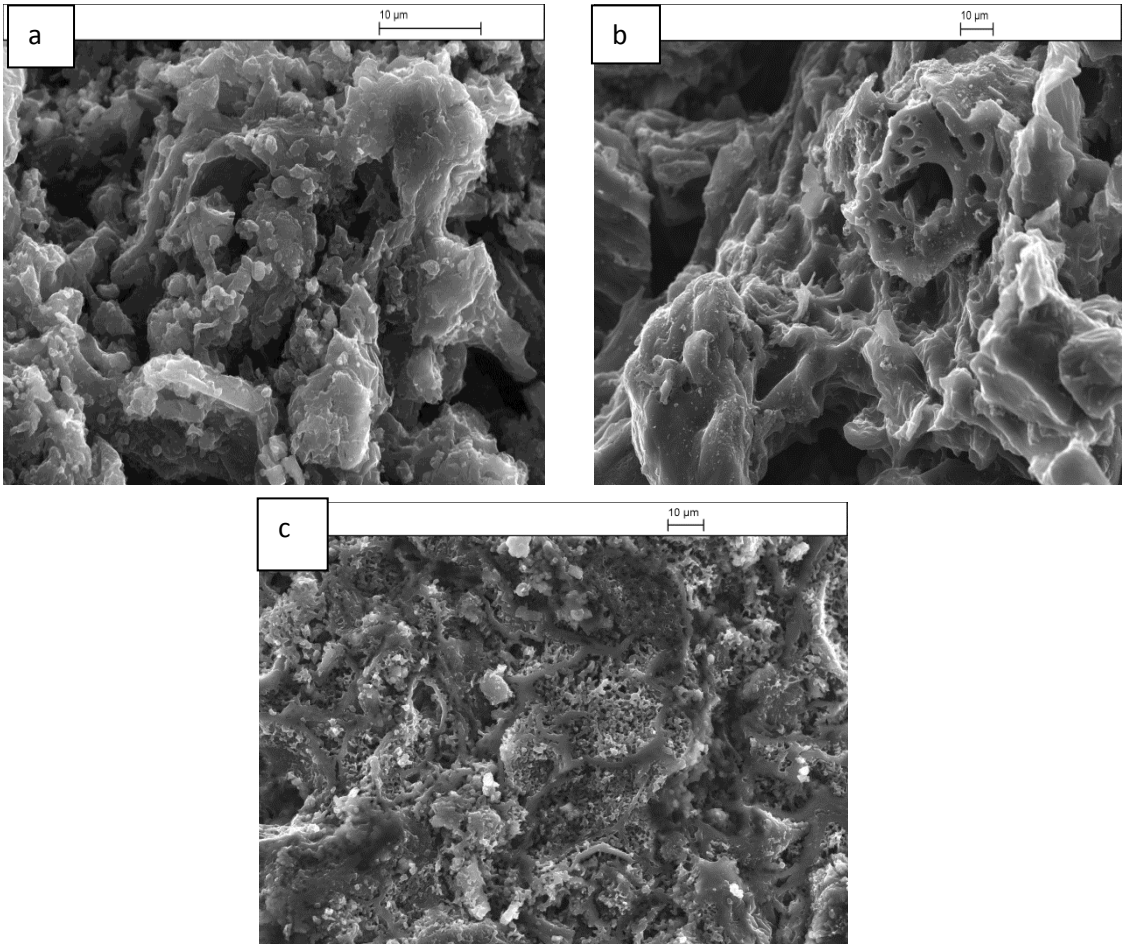

Figure 6.10: SEM images of carbon monoliths using different ratios of template:waste plant material (a) 1:1 (b) 1:2 (c) 1:3, showing the absence of pores in (c).

The FTIR-KBr analysis gave further insight into the chemical composition of the carbon monolith. Figure 6.11 shows the FT-IR spectra of the as-synthesized (red) and the carbon monoliths (blue). The spectra have different shapes due to change in framework and high carbon content after carbonization. The determination of the main functional groups for a given wavelength is based on a previous report by Liu *et al*. [3] and as reported in Chapter 4. A broad band at about 3400 cm^{-1} is due to the –OH stretching of the phenolic groups in the as-synthesized monolith. The peaks at about 1600-1500 and 1450-1200 cm^{-1} are due to the C=C stretching vibration of the aromatic structure in the plant material, and C-H bending vibration of aliphatic structures in the pluronic F127 and the plant material respectively. The peaks at 2900 and 1000 cm^{-1} which are respectively due to the C-H and C-O stretching vibrations in the plant materials and F127 almost disappeared after carbonization confirming template decomposition. The peaks below 1000 cm^{-1} are due to aromatic C-H bending vibrations.

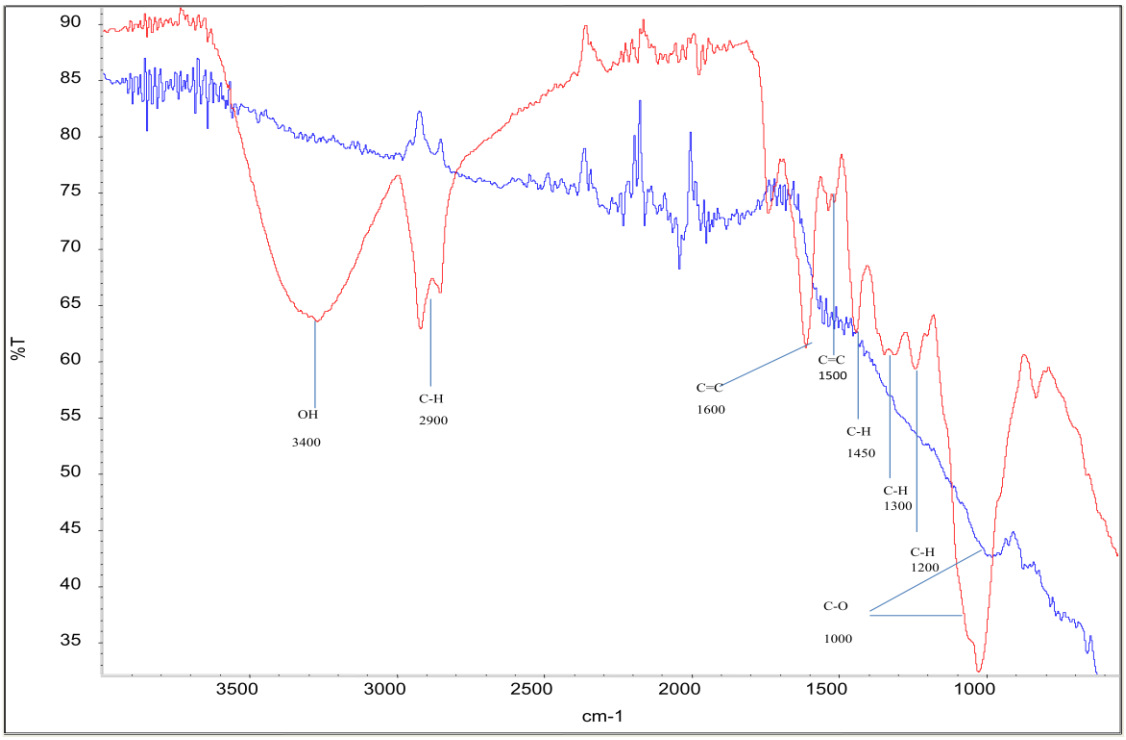

Figure 6.11: FTIR-KBr spectra showing the main functional groups in the as-synthesized (red) and carbon monolith (blue) using waste plant material as carbon precursor

6.6 Conclusion

Microwave-assisted hydrothermal method employing triblock co-polymer F127 as template and rescorcinol and formaldehyde as carbon precursors, and evaporation-induced self-assembly using a waste plant material as a carbon precursor have been used to synthesise carbon monoliths. The preliminary results showed that the microwave-assisted hydrothermal process has an excellent advantage in the synthesis of carbon monolith, as it requires shorter time to obtain similar results as those obtained via the conventional hydrothermal route using oven heating, while the evaporation-induced self-assembly approach offers a new route to the synthesis of carbon monolith with high surface area and good mechanical stability when compared to the hydrochar and biochar from the same material and this can improve the performance of such carbon materials.

6.7 References

[1] Wu, Z, Zhao, D. Ordered Mesoporous Materials as Adsorbents. Chem Comm 2011; 47: 3332–3338.

[2] Xu, LY, Shi, ZG, Feng, YQ. Preparation of a Carbon Monolith with Bimodal Perfusion Pores. Micropor Mesopor Mater 2008; 115: 618-623.

[3] Liu, L, Wang, FY, Shao, G, Yuan, Z. A Low-Temperature Autoclaving Route to Synthesize Carbon Materials with an Ordered Mesostructure. Carbon 2010; 48: 2089-2099.

[4] Huang, Y, Cai, H, Feng, D, Gu, D, Deng, Y, Tu, B, *et al*. One-Step Hydrothermal Synthesis of Ordered Mesostructured Carbonaceous Monoliths with Hierarchical Porosities. Chem Comm 2008; 2641-2643.

[5] Liu, D, Lei, J, Guo, L, Deng, K. Simple Hydrothermal Synthesis of Ordered Mesoporous Carbons from Resorcinol and Hexamine. Carbon 2011; 49: 2113-2119.

[6] Li, M, Xue, J. Ordered Mesoporous Carbon Nanoparticles with Well-Controlled Morphologies from Sphere to Rod via a Soft-Template Route. J Colloid Interf Sci 2012; 377: 169-175.

[7] Tanaka, S, Nakatani, N, Doi, A, Miyake, Y. Preparation of Ordered Mesoporous Carbon Membranes by a Soft-Templating Method. Carbon 2011; 49: 3184-3189.

[8] Nakanishi, K, Soga, N. Phase Separation in Silica Sol-Gel System Containing Polyacrylic Acid: Gel Formation Behaviour and Effect of Solvent Composition. J Non-Cryst Solids 1992; 139: 1-13.

[9] Hu, YS, Adelhelm, P, Smarsly, BM, Hore, S, Antonietti, M, Maier, J. Synthesis of Hierarchically Porous Carbon with Ordered Microstructure and their Application in Rechargeable Lithium Batteries with High Rate Capacity. Adv Funct Mater 2007; 17: 1873-1878.

[10] Shi, ZG, Feng, YQ, Xu, L, Da, SL, Zhang, M. Adding a Micropore Framework to a Parent Activated Carbon by Carbon Deposition from Methane and Ethylene. Carbon 2003; 41: 2653-2655.

[11] Wang, L, Lin, S, Lin, K, Yin, C, Liang, D, Di, Y, *et al*. A Facile Synthesis of Highly Ordered Mesoporous Carbon Monolith with Mechanically Stable Mesostructure and Superior Conductivity from SBA-15 Powder. Micropor Mesopor Mater 2005; 85: 136-142.

[12] Wang, L, Zhao, Y, Lin, K, Zhao, X, Shan, Z, Di, Y, *et al*. Carbon with High Thermal Conductivity, Prepared from Ribbon-Shaped Mesophase Pitch-Based Fibers. Carbon 2006; 44: 1298-1301.

[13] Lu, AH, Smatt, JH, Lindén, M. Combined Surface and Volume Templating of Highly Porous Nanocast Carbon Monolith. Adv Funct Mater 2005; 15: 865-871.

[14] Wang, ZY, Li, F, Ergang, NS, Stein, A. Effects of Hierarchial Architecture on Electronic and Mechanical Properties of Nanocast Monolith Porous Carbons and Carbon-Carbon Nanocomposite. Chem Mater 2006; 18: 5543-5553.

[15] Hao, G, Li, W, Li, W, Wang, S, Wang, G, Qi, L, *et al*. Lysine-Assisted Rapid Synthesis of Crack-Free Hierarchical Carbon Monoliths with a Hexagonal Array of Mesopores. Carbon 2011; 49: 3762-3772.

[16] Górka, J, Jaroniec, M. Hierarchically Porous Phenolic Resin-Based Carbons Obtained by Block Copolymer-Colloidal Silica Templating and Post-Synthesis Activation with Carbon dioxide and Water Vapor. Carbon 2011; 49: 154-160.

[17] Li, ZJ, Yan, WF, Dai, S. A Novel Vesicular Carbon Synthesized Using Amphiphilic Carbonaceous Material and Micelle Templating Approach. Carbon 2004; 42: 767-770.

[18] Kim, TW, Kleitz, F, Paul, B, Ryoo, RJ. MCM-48-Like Large Mesoporous Silicas with Tailored Pore Structure: Facile Synthesis Domain in a Ternary Triblock Copolymer-Butanol-Water System. Am Chem Soc 2005; 127: 7601-7610.

[19] Zhang, FQ, Meng, Y, Gu, D, Yan, Y, Chen, Z, Tu, B, *et al*. An Aqueous Cooperative Assembly Route to Synthesize Ordered Mesoporous Carbons with Controlled Structures and Morphology. Chem Mater 2006; 18: 5279-5288.

[20] Zhang, FQ, Meng, Y, Gu, D, Yan, Y, Yu, CZ, Tu, B, *et al*. A Facile Aqueous Route to Synthesize Highly Ordered Mesoporous Polymer and Carbon Framework with *Ia3d* Bicontinous Cubic Structure. J Am Chem Soc 2005; 127: 13508-13509.

[21] Liang, CD, Hong, K, Guiochon, GA, Mays, JW, Dai, S. Synthesis of a Large-Scale Highly Ordered Porous Carbon Film by Self-Assembly of Block Copolymers. Angew Chem Int Ed 2004; 43: 5785-5789.

[22] Tanaka, S, Nishiyama, N, Egashira, Y, Ueyama, K. Synthesis of Ordered Mesoporous Carbons with Channel Structure from an Organic-Organic Composites. Chem Comm 2005; 2125-2127.

[23] Meng, Y, Gu, D, Zhang, FQ, Shi, YF, Cheng, L, Feng, D, *et al*. A Family of Highly Ordered Mesoporous Polymer Resin and Carbon Structures from Organic-Organic Self-aAsembly. Chem Mater 2006; 18: 4447-4464.

[24] Antonietti, M, Titirici, MM, Thomas, A, Yu, SH, Muller, JO. A Direct Synthesis of Mesoporous Carbons with Bicontinuous Pore Morphology from Crude Plant Material by Hydrothermal Carbonization. Chem Mater 2007; 19: 4205-4212.

[25] Sevilla, M, Fuertes, AB. Chemical and Structural Properties of Carbonaceous Products Obtained by Hydrothermal Carbonization of Saccharides. Chem-Eur J 2009; 15: 4195-4203.

[26] Vercaemst, C, Ide, M, Allaert, B, Ledoux, N, Verpoort, F, van der Voort, P. Ultra-Fast Hydrothermal Synthesis of Diastereoselective Pure Ethenylene-Bridged Periodic Mesoporous Organosilicas. Chem Comm 2007; 2261-2263.

[27] Cushing, BL, Kolesnichenko, VL, O'Connor, CJ. Recent Advances in the Liquid-Phase Syntheses of Inorganic Nanoparticles. Chem Rev 2004; 104: 3893-3946.

[28] Cundy, CS, Cox, PA. The Hydrothermal Synthesis of Zeolite: History and Development from the Earliest Days to the Present Time. Chem Rev 2003; 103: 663-701.

[29] Tian, BZ, Liu, X, Solovyoy, LA, Liu, Z, Yang, HF, Zhang, ZD, *et al*. Facile Synthesis and Characterization of Novel Mesoporous and Mesorelief Oxides with Gyroidal Structures. J Am Chem Soc 2004; 126: 865-875.

[30] Meng, Y, Gu, D, Zhang, FQ, Shi, Y, Yang, H, Li, Z, *et al*. Ordered Mesoporous Polymers and Homologous Carbon Frameworks, Amphiphilic Surfactant Templating and Direct Transformation. Angew Chem Int Ed 2005; 44: 7053-7059.

[31] Gao, P, Wang, A, Wang, X, Zhang, T. Synthesis of Highly Ordered Ir-Containing Mesoporous Carbon Materials by Organic-Organic Self Assembly. Chem Mater 2008; 20: 1881-1888.

[32] Sing, KSW, Everett, DH, Haul, RAW, Moscou, L, Pierotti, RA, Rouquerol, *et al*. Reporting Physisorption Data for Gas/Solid Systems. Pure Appl Chem 1985; 57: 603-619.

[33] Wan, Y, Shi, YF, Zhao, D. Designed Synthesis of Mesoporous Solids via Nonionic-Surfactant-Templating Approach. Chem Commun 2007; 897-926.

[34] Wan, Y, Zhao, D. On the Controllable Soft-Templating Approach to Mesoporous Silicates. Chem Rev 2007; 107: 2821-2860.

[35] Huang, CH, Doong, RA. Sugarcane Bagasse as the Scaffold for Mass Production of Hierarchically Porous Carbon Monoliths by Surface Self-Assembly. Micropor Mesopor Mater 2012; 147: 47-52.

[36] Yu, L, Bruna, N, Sakaushi, K, Eckert, J, Titirici, MM. Hydrothermal Nanocasting: Synthesis of Hierarchically Porous Carbon Monoliths and their Application in Lithium–Sulfur Batteries. Carbon 2013; 61: 245-253.

Chapter 7

Composting of *Prosopis africana* Shell and Effect of Organic Pollutant on Composting Process

7.1 Introduction

In the previous chapters the waste material (*Prosopis africana* shell) was processed by pyrolysis, but this method requires specific technology and energy input. Composting is a well proven process for transforming waste into a useful material and its application for treating metal contaminated soils has been studied in detail as reported in the literature and also at Hull [1]. Unlike pyrolysis treatments, composting represents a simple technology and low cost approach in waste management. It provides a platform for the sustainable reuse of the biodegradable fraction of the organic waste materials which is both microbial and nutrient rich. Details of the process have already been carried out in Chapter 1 (1.3.4). Composting has been shown to improve soil properties, contribute to the partial dissipation of organic pollutants through concentration decrease, suppress most pathogenic organisms, decrease the bioavailability of heavy metals, and stabilizes the organic material in the final compost before being applied in soils [2-4]. However, even with a developed technological infrastructure, the resultant material (compost) can be difficult to utilise if there are no sufficient markets or outlets for its use. Therefore, one of the potential challenges with composted materials is to develop suitable end uses for the material generated. The addition of selected organic substrate (amendment) to enhance the bioremediation process can improve the products and overcome any drawback in the process efficiency [5].

For the composting process to be successful and applied in the bioremediation of contaminated sites and soils, a number of physical, chemical, and biological factors that determine the microbial accessibility to the target molecules are very important [6,7]. The bioavailability of the pollutants, the nature and content of the waste or soil organic matter, which is largely composed of humic acids (HAs) have important roles to play [8-10]. The presence of organic matter would appear to greatly enhance the removal of organic pollutant [11], however, the exact mechanisms regarding the removal are still not very clear. The mechanisms for the removal of organics include complete or partial mineralisation or fixation to organic matter as non-extractable

residues (NER) [2,12]. However, the results of such bioremediation approaches are contradictory. For example, Joyce *et al.* [13] showed that generally PAHs were removed during the active composting phases with scant removal during the latter curing phases while, Sayara *et al.* [5] recommended the use of mature compost as opposed to immature compost for the removal of PAHs. Therefore, conclusions between studies may vary due to the different experimental/analytical approaches used.

Environmental pollution resulting from organic pollutants is a major problem in Nigeria due to her huge natural resources. Petrochemical pollution from oil spillage which is one of the anthropogenic sources of organic pollutants, mostly polycyclic aromatic hydrocarbons (PAHs) in the environment as mentioned previously in Chapter 2 (2.2.2), occurs on a regular basis. Bioremediation through composting has shown to be a major environmental process for the remediation of PAHs pollution in terrestrial and aquatic ecosystems [14]. This is usually achieved through biostimulation (addition of substrates, such as, starch to enhance the degradation process) or bioaugmentation (addition of microorganisms capable of degrading the pollutants) of the contaminated environment [7,15]. Interest in this area of research has been on the increase with the bioremediation of two and three ring PAHs being well documented, and the degradation and detoxification of anthracene and other PAHs by micro-organisms, such as, bacteria and fungus have been well studied [16-23]. Whilst degradation of organic compounds has been studied numerous times in composting environments, the effect of the organic pollutant on the composting process itself to the best of my knowledge has not been investigated. It will therefore be necessary for such study to be carried out.

As part of the investigation, starch and anthracene amendments, alongside unamended controls were used, and the total dry matter and extracellular enzyme activities were monitored in order to understand what is going on in the composting environment. Complex carbohydrate polymers, such as starch, are degraded, in part, by a consortium of enzymes excreted by the indigenous microflora. For the purposes of this study, two extracellular enzymes (α-and β- glucosidase) were selected. α-glucosidases are enzymes involved in hydrolysing α-1,4-glucosidic bonds in complex carbohydrates, such as starch, to release the glucose monomers. This is in contrast to the β-glucosidase which act on β-1,4-glucosidic bonds found in substrates, such as, cellulose. Therefore, it is expected that the activity of the α-glucosidases will increase

as a result of starch amendment to a composting process, while the activity of the β-glucosidase is expected to be unaffected. The use of extracellular enzyme analysis to investigate starch degradation with its focal enzyme (α-glucosidase) alongside a non-specific substrate (β-glucosidase) during the composting process has been shown to be promising [24,25].

The initial composting experiments were carried using *Prosopis africana* shell a waste product from Nigeria, however work then continued with UK sourced waste material (green compost). This material could be used for the study without having to import large quantities of waste material. In order to investigate the effect of organic pollutants on the composting process, a simple PAH (anthracene), Figure 7.1, was used as a model compound that has been widely studied in the composting environment. It is not acutely toxic, carcinogenic, or mutagenic like other PAHs [16]. However, its solubility in water is high because of its low molecular weight; therefore, it can be found at a more significant level in the aquatic environment compared to most of the other PAHs and as such can be a threat to the environment, its presence has been detected in industrial effluents, in water run-offs, in surface water and groundwater, in sediments, as well as in drinking water [16]. The effluents from industries, such as, synfuel industry, shale oil plants, petroleum refineries, and industries using coal-derived products are most likely to contain anthracene and other PAHs. It has also been reported that anthracene, pyrene and phenanthrene are the ideal chemicals for bioremediation through composting process [13].

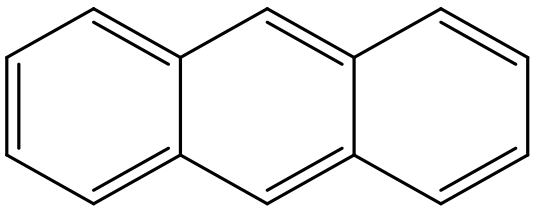

Figure 7.1: Structure of Anthracene

The aims of this chapter are

- To investigate whether the waste material (*Prosopis africana* shell) can be composted.
- To study the effect of an organic pollutant (anthracene) during a starch amended co-composting process

7.2 Materials and Methods

7.2.1 Materials

All chemicals used in this study were of analytical grade and were used subsequently without further purification. Anthracene (97% purity) was purchased from Sigma-Aldrich, UK. Acetone was purchased from Fisher Scientific, UK. The corn starch was purchased from Tesco supermarket in Hull, UK. Stock solution of anthracene (4 g/L) was prepared in acetone and diluted to the required concentration. *Prosopis africana* shell, a Nigerian waste material was used in the preparation of the compost, while green wastes compost obtained from a commercial operator in the UK was used to study the effect of organic pollutant (anthracene) on the composting process.

7.2.2 Methods

7.2.2.1 Composting of the *Prosopis africana* shell

50 g each of the pulverized *Prosopis africana* shell were weighed into Twelve (12) different flasks of known weight. 50 mL of water was added to each of the flasks and the whole content in each flask was weighed and placed in an incubator at 30 °C. After four days three (3) flasks and their contents were taken out of the incubator and weighed, after which they were dried in an oven at 105 °C for 72 hours. The dried composts were removed from the oven, allowed to cool down to room temperature and weighed to obtain the weight lost (loss in dry matter). The same procedure was carried out for the remaining flasks on the 11^{th}, 17^{th} and 29^{th} day.

7.2.2.2 Effects of Organic Pollutant during a Starch Amended Co-Composting Process

In order to investigate the effects of polycyclic aromatic hydrocarbon (anthracene) during a starch amended co-composting process the following three experiments were set up. It should be noted that these experimental set-ups are exploratory due to absence of an established method in literature.

Small scale mesocosms were prepared in 250 mL conical flasks of known weight. As a cost-effective starch amendment, food grade corn flour (aka cornstarch; as in the wet milled product from maize) was used. Anthracene amendments were

prepared by dissolving anthracene in acetone (4 g/L) and adding it to the compost. All mesocosms were incubated at 30 °C. Previous studies have shown starch degradation to be independent of temperature when compared to higher thermophilic temperatures [24,25]. Furthermore, the use of a lower temperature eliminated the requirement for moisture regulation during the experiment so evaporation was minimal over the time period used. Each mesocosm was sampled to destruction.

Experiment one

This experiment was set-up to see if a given concentration of anthracene will have effect on the total dry matter and the extracellular enzyme activity. 50 g of compost was amended with 10 g of starch, 400 mg/kg of anthracene, and 60 mL of distilled water. Control was prepared without anthracene and starch, the other set-ups were with starch no anthracene, and anthracene no starch. For each of the four treatments, five samples were prepared, which were sampled on a weekly basis for five weeks.

Experiment two

The effects of increasing anthracene concentration were studied in this experiment. 40 g of compost was amended with 125-750 mg/kg of anthracene, 60 mL of distilled water and 10 g starch. Sampling was carried out after one week of composting. Control was prepared without anthracene and starch.

Experiment three

This experiment was a repeat of experiment one using a higher concentration of anthracene with replication. 100 g of compost was amended with 10 g of starch, 60 mL of water and 1 g/kg of anthracene. Control was prepared without anthracene and starch, the other set-ups were with starch no anthracene, and anthracene no starch. For each of the four treatments, six samples were prepared. The first sampling period was after a week. Sampling continued on a weekly basis for further two weeks. This experiment was replicated.

Loss in Dry Matter

At sampling, the total weight (including flask) of the mesocosm was recorded. One gram of waste material was removed for slurry preparation. The remainder of the

material was used for the determination of moisture content. Moisture content was calculated by measuring the weight loss, after oven drying, at 105 °C, for 72 hours. The total wet weight, absolute value of moisture content and dry weight (the total wet weight minus the total moisture content) of each mesocosm was then calculated based on the moisture content and the total wet weight of the mesocosm at sampling (loss on ignition method).

Extracellular Enzyme Analysis (EEA)

Slurries were prepared from the samples by adding 1 g (wet weight) of sample to 99 mL of sterile water. It was subsequently diluted to 1 g/L final concentration. The extracellular enzyme analysis for the activities of (alpha) α- and (beta) β- glucosidase were assayed using the model fluorogenic substrate with methylumbelliferone (MUF) as the fluorescing agent based on the principles of Hoppe [26]. 240 µL of waste slurries (1 g/L) were placed into 1.5 mL microcentrifuge tubes. 10 µl of respective 5 mM α- and β-glucosidase substrates (4-methylumbelliferyl α-D-glucopyranoside and 4-methylumbelliferyl β-D-glucopyranoside respectively; Sigma) were added to each tube. Negative controls, consisting of slurries, that have been boiled for 10 minutes and then cooled before the addition of the assay enzyme substrates, were used in correcting for the background fluorescence and activity for each sample. After incubation, the samples were centrifuged for 2 minutes at 10 000 rpm. In order to measure the fluorescence of each of the samples, 200 µl was added to a microtitre plate containing 16 µL of pH 10 borate buffer solution (Sigma). It was quantified using a fluorometer (FLU-Ostar OPTIMA, BMG LABTECH Ltd., UK) which has a fitted excitation filter at 350 nm and an emission filter at 460 nm. The blank sample fluorescence reading was subtracted from the positive sample to correct for background florescence. Concentrations of samples were determined using a straight line calibration curve with standard solutions of 4-methylumbellifone (Sigma).

7.2.2.3 Statistical Analysis

Linear regression analysis and a two way ANOVA model (Stata v7.0, Stata Corporation, College Station, Texas, USA) were used to assess the effects of time, starch and anthracene on the total dry matter and enzyme activity for each enzyme substrate.

7.3 Results and Discussion

7.3.1 Composting of the *Prosopis africana* shell

The results for the loss in total dry matter for *Prosopis africana* shell is shown in Figure 7.2. The rapid loss in dry matter corresponds to the active phase of the composting process [27]; and it occurred within the first 14 days of the composting process. The greatest loss in dry matter of about 30% occurred during this period. The active phase was followed by maturation phase (14-29 day) which was characterized by decline in the loss in dry matter accounting for about 5.8 % of the total loss in dry matter, which showed the stability of the compost after the active phase [27]. The trend for the loss in dry matter is consistent with previous reports [27-29]. The total loss in dry matter was close to the 40% found for the composting of olive mill wastewater with olive leaves [29]. Further experiments would be required on larger scale (preferably in Nigeria) to demonstrate the effectiveness of the composting process.

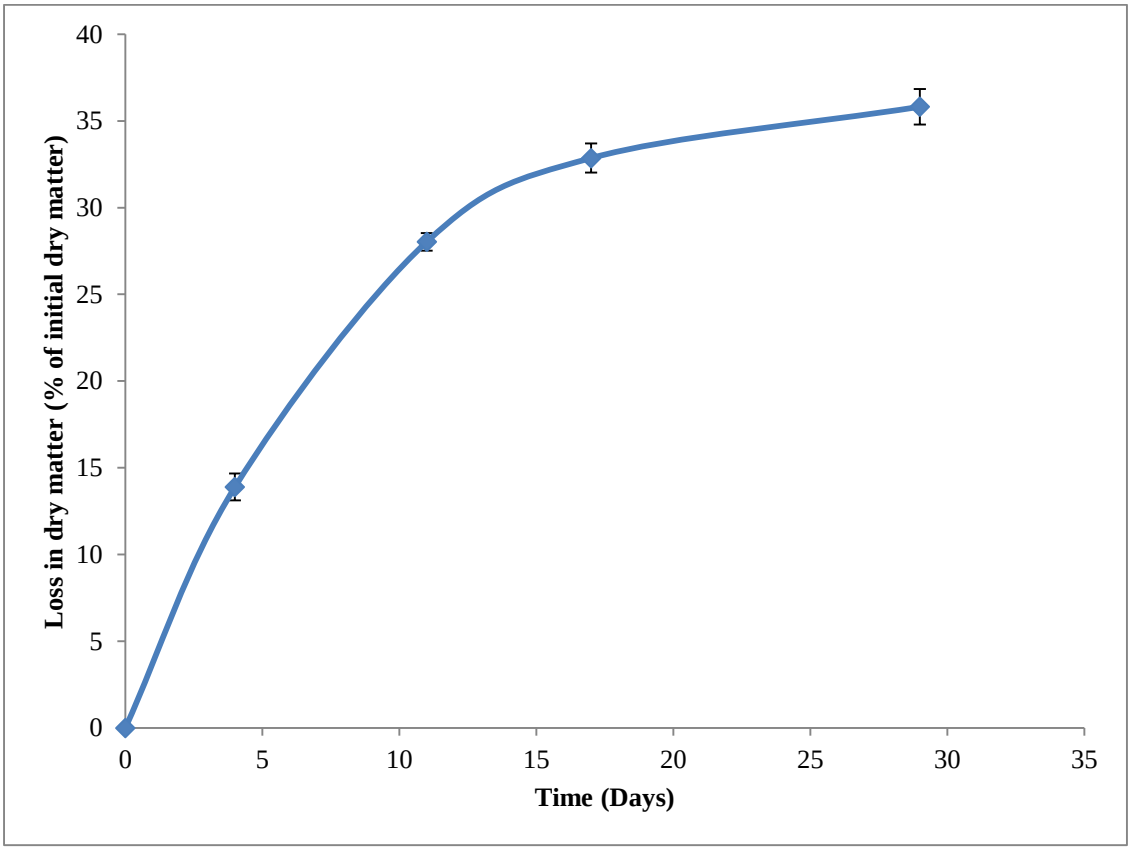

Figure 7.2: Loss in dry matter during the composting of *Prosopis africana* shell. The loss in dry matter was rapid during the active phase of composting (0-14 day) and decline afterwards during the maturation phase (14-29), (n=3).

7.3.2 Effects of Organic Pollutant during a Starch Amended Co-Composting Process

The use of compost in the bioremediation of organic compounds is regarded as effective method for remediation. Degradation of PAHs in particular have been studied numerous times in composting environments however, the underlying fundamental mechanism is unclear [1]. There is a potential for failure if the correct conditions are not put in place. The question is what are the correct conditions if we do not know the exact mechanism? It is therefore necessary to have a thorough understanding of process conditions which will allow for a proper optimisation of the bioremediation technique and could subsequently lead to a better result. Therefore, this aspect of the study presents a different and novel perspective from previous studies, as it aimed at investigating the effect of an organic pollutant (anthracene) on the composting process, and to understand such effect and possible interaction during a starch amended co-composting process.

The results for the loss in dry matter for the three experiments are presented in Figures 7.3-7.5. In experiment one, there were declines in organic matter for all treatments (Figure 7.3). From each of these treatments, regression analysis (Appendix 6) revealed that each of these declines were statistically significant ($p < 0.05$). The decline in dry matter for the control compost, the anthracene amended compost, and the starch amended compost are generally consistent with certain assumptions, i.e., that starch amended compost degrades more rapidly than the control. The control compost in this instance was not affected by anthracene. However, there appears to be an effect of anthracene on the decline in dry matter in the starch amended compost. These composts show increased dry matter content that cannot be explained by the additional amounts of dry matter introduced by the anthracene amendment. Using two way ANOVA (Appendix 7 a), the data shows that time, starch addition and anthracene amendment were all statistically significant ($p<0.05$) in determining the total dry matter.

In experiment two (Figure 7.4), the effect of increasing anthracence concentration was investigated. This, however, did not produce a significant effect with regard to increasing anthracene concentration and the total dry matter contents of the seven starch amended compost ranged from 44.5 to 45 grams.

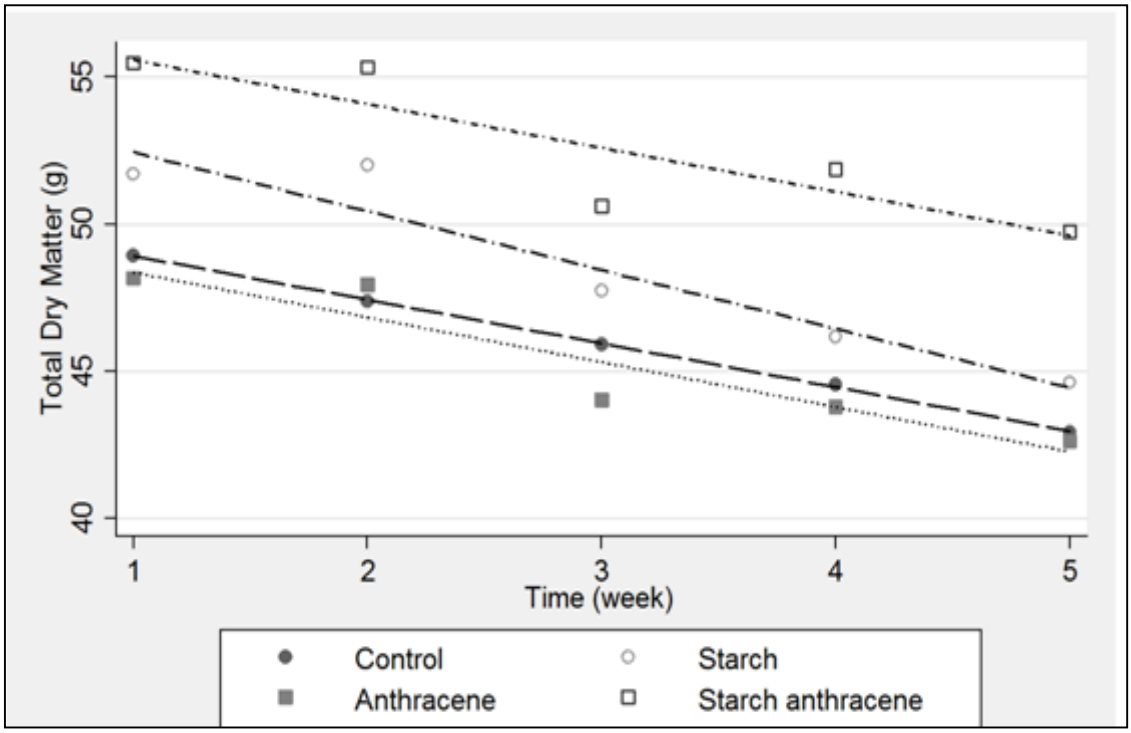

Figure 7.3: Loss in dry matter for experiment one, showing the decline in organic matter for all the treatments.

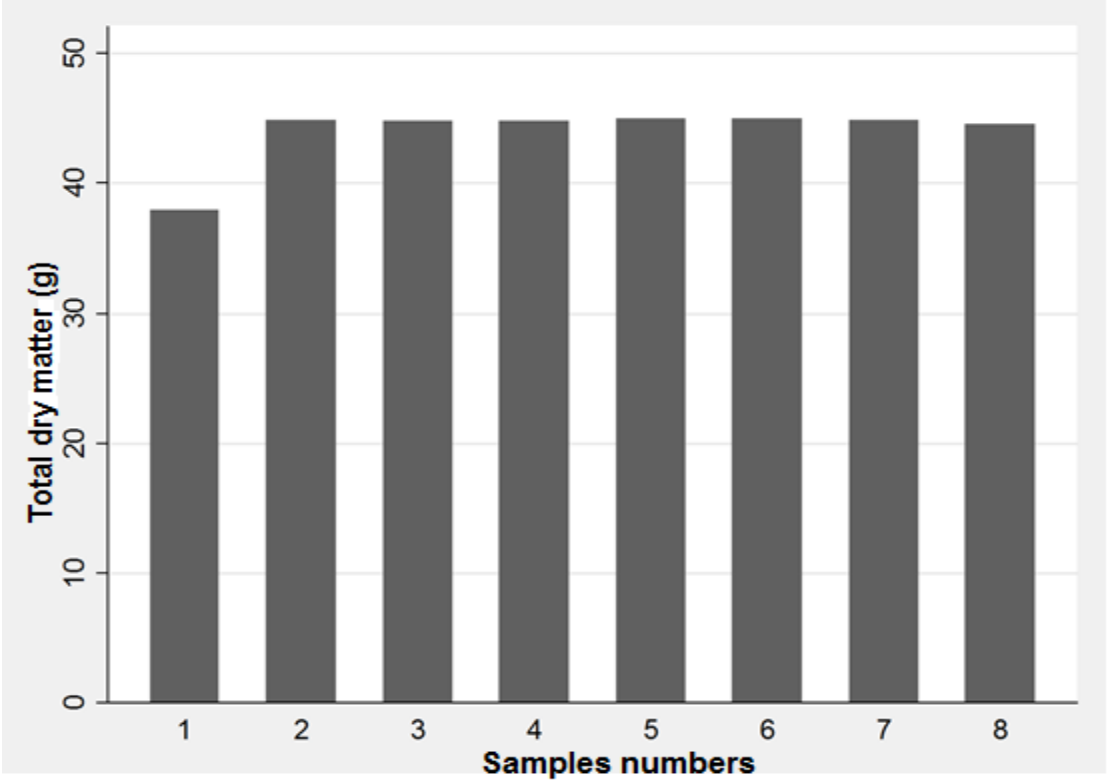

Figure 7.4: Loss in dry matter for experiment two, showing no significant effect of the increasing anthracene concentration. Sample 1 = Control, sample 2 = compost + starch no anthracene, samples 3-8 contains increasing concentrations of anthracene (125-750 mg/kg)

In experiment three (Figure 7.5), the observed trend was similar to that of experiment one. Again two way ANOVA (Appendix 7 b) revealed that time, starch addition and anthracene were all statistically significant ($p<0.05$) in determining the total dry matter in experiment three. However, regression analysis (Appendix 8) of the individual treatments reveals that only the starch amendment with anthracene shows a significant ($p=0.027$) decrease. Although samples were replicated in the experiment, compared to experiment one only three time periods were investigated, thus experiment one had an extended time period.

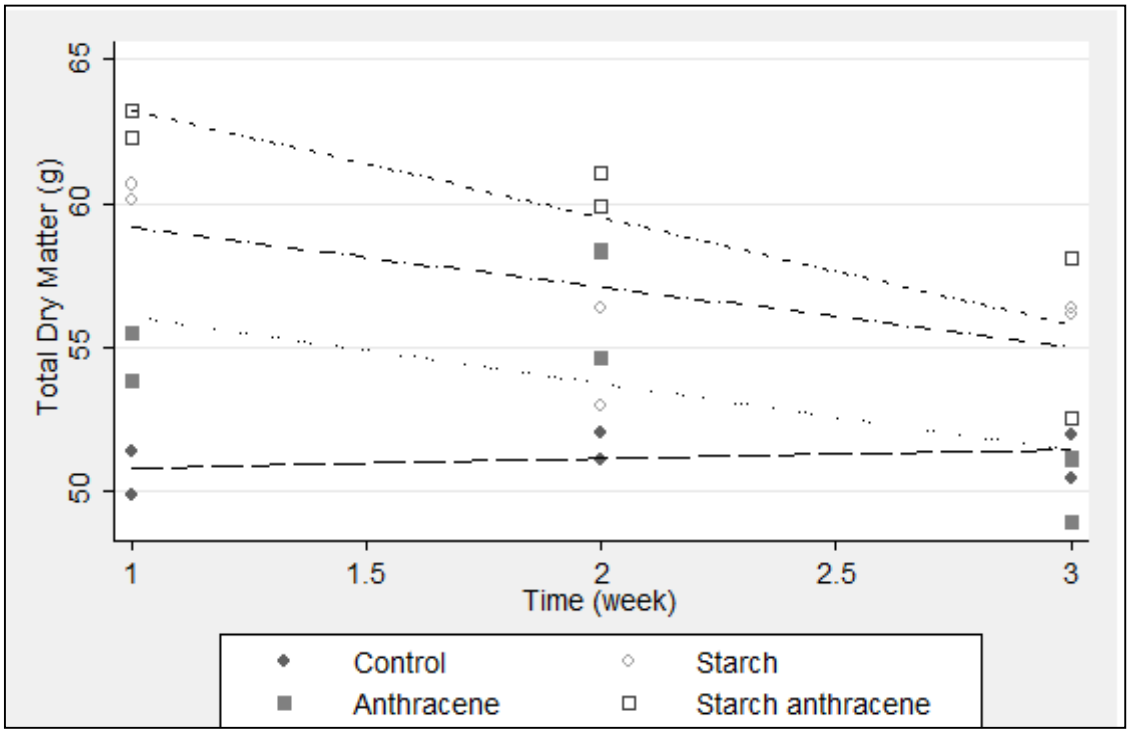

Figure 7.5: Loss in dry matter for experiment three, showing the decline in organic matter for all the treatments.

The results for the extracellular enzyme analysis (EEA) for the three experiments are presented in Figures 7.6-7.8. In experiment one, results of two way ANOVA (Appendix 9 a) revealed that anthracene addition was a significant variable for α-glucosidase activity. Surprisingly starch addition was not significant and although elevated activities of α-glucosidase activity could be seen in the starch and anthracene compost, starch addition alone did not promote α- glucosidase activity whereas anthracene addition alone did (Figure 7.6). β-glucosidase activity, relative to α- glucosidase activity, remained low in all samples and was not significantly affected by time, starch or anthracene addition (Appendix 9 b).

In experiment two (Figure 7.7), there was no apparent trend in α-glucosidase activity with increasing anthracene concentration and unlike experiment one, starch addition alone enhanced α- glucosidase activity. These data were more consistent with no effect of anthracene.

Figure 7.6: Enzyme analysis for experiment one, showing elevated activities of α-glucosidase activity in the starch and anthracene amended compost.

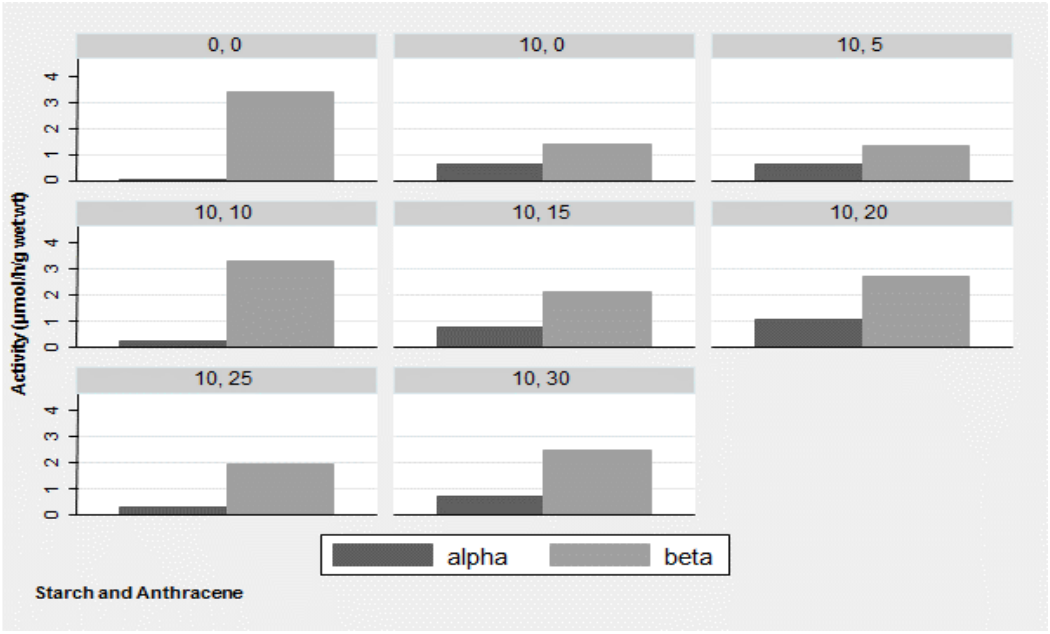

Figure 7.7: Enzyme analysis for experiment two, showing no apparent trend in α-glucosidase activity with increasing anthracene concentration and unlike experiment one, starch addition alone enhanced α- glucosidase activity.

Finally in experiment three, results of two way ANOVA (Appendix 10 a and b) revealed no statistically significant effect of either starch or anthracene addition on α-or β-glucosidase. However, enhanced α-glucosidase activity was observed in samples from both starch amended and starch and anthracene amended treatments (Figure 7.8).

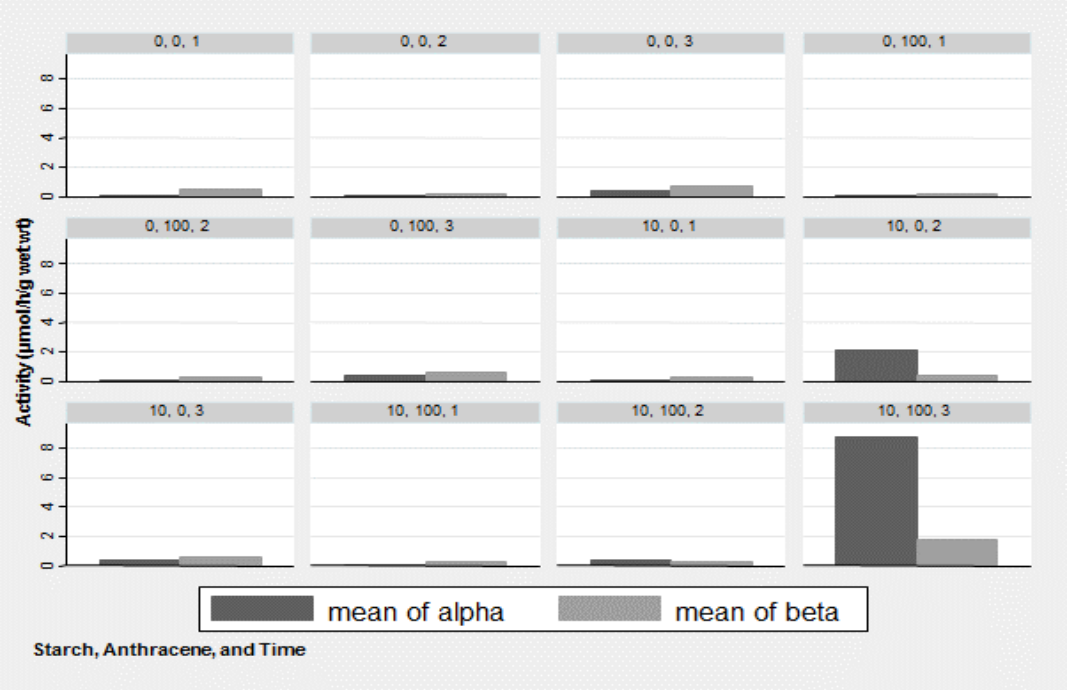

Figure 7.8: Enzyme analysis for experiment three, showing enhanced α-glucosidase activity in starch amended and starch and anthracene amended treatments

Previous experiments have demonstrated a link between starch degradation and glucosidase activity, but it is not always clear that this relationship is strictly adhered to in all composting environments [24,25]. From the results obtained in this study, it can be seen that without performing the experiments for the effects of anthracene on the composting process at the same time, it became very difficult to have the same result each time the experiment was carried out. In this respect, the attempts to link starch degradation with a glucosidase activity were ambitious. As noted by Adams and Scott [25] empirical evidence between extracellular enzyme analysis (EEA) and their focal polymer (starch in this study) appear almost completely absent from the composting literature. In experiment one, the starch amended compost failed to demonstrate a glucosidase activity and the activation by anthracene was unexpected. Qasemian *et al.* [30] demonstrated that various enzyme activities increased after anthracene addition to a soil environment; however this was over a period of months. In all three experiments, however, the interaction between the anthracene and starch consistently produced

enhanced activities of α-glucosidase suggesting that, as an enzyme partially responsible for starch degradation, that starch degradation would not be inhibited by anthracene. However, it would appear that some form of toxic effect is being produced by anthracene addition since in both experiments one and three the interaction of starch and anthracene produced a level of dry matter that was higher than expected. Although persistent, anthracene is not regarded as a particularly toxic organic pollutant. On investigating anthracene toxicity, Bonnet *et al.* [16] showed that anthracene had no biocidal effect on eukaryotic microorganisms, but did show a biostatic effect on these organisms. The effects of a biostatic as opposed to a biocidal response on α-glucosidase after starch amendment could be interesting, since there is already a microbial presence in the compost, a biostatic response may inhibit succession of starch hydrolysing organisms, but not necessarily inhibit expression of hydrolytic enzyme by the resident biomass and since the microbial community is not growing as a result of this biostatic effect of the anthracene, the higher level of the dry matter obtained in experiment one and three for the anthracene and starch amended compost could be as a result of fewer microorganisms present in the compost when compared with the starch amended compost making the decomposition process slower. Therefore, whilst apparent enzyme activity is increased, this may not necessarily be related to the true enzyme dynamics in the system.

7.4 Conclusion

The preliminary composting experiment with the *Prosopis africana* shell demonstrated that it could be composted. However, due to insufficient material, a UK based green waste compost was selected for further studies in order to understand the effect of organic pollutant (anthracene) during a starch amended co-composting process. The effect monitored through the total dry matter and extracellular enzyme activities of both starch specific (α-glucosidase) and non-specific (β-glucosidase) substrate showed that the effect of anthracene addition alone was not highly significant on the composting process; however the interaction between the anthracene and starch consistently produced effects on the total dry matter and α-glucosidase which is novel. The result from this study could further be used to design experiment to describe the magnitude of such interaction.

7.5 References

[1] Greenway, GM, Song, QJ. Heavy Metal Speciation in Composting Process. J Environ Monit 2002; 4: 300-305.

[2] Lashermes, G, Barriuso, E, Houot, S. Dissipation Pathways of Organic Pollutants during the Composting of Organic Wastes. Chemosphere 2012; 87: 137-143.

[3] Amir, S, Hafidi, M, Merlina, G, Hamdi, H, Revel, JC. Fate of Polycyclic Aromatic Hydrocarbons during Composting of Lagooning Sewage Sludge. Chemosphere 2005; 58: 449-458.

[4] Pakou, C, Kornaros, M, Stamatelatou, K, Lyberatos, G. On the Fate of LAS, NPEOs and DEHP in Municipal Sewage Sludge during Composting. Bioresource Technol 2009; 100: 1634-1642.

[5] Sayara, T, Sarrà, M, Sánchez, A. Effects of Compost Stability and Contaminant Concentration on the Bioremediation of PAHs-Contaminated Soil through Composting. J Hazard Mater 2010; 179: 999-1006.

[6] Semple, KT, Reid, BJ, Fermor, TR. Impact of Composting Strategies on the Treatment of Soils Contaminated with Organic Pollutants. Environ Pollut 2001; 112: 269-283.

[7] Wick, LY, Remer, R, Wurz, B, Reichenbach, J, Braun, S, Schafer, F, *et al*. Effect of Fungal Hyphae on the Access of Bacteria to Phenanthrene in Soil. Environ Sci Technol 2007; 41: 500-505.

[8] Cornelissen, G, Gustafsson, O, Bucheli, TD, Jonker, MTO, Koelmans, AA, van Noort, PCM. Extensive Sorption of Organic Compounds to Black Carbon, Coal, and Kerogen in Sediments and Soils: Mechanisms and Consequences for Distribution, Bioaccumulation, and Biodegradation. Environ Sci Technol 2005; 39: 6881-6895.

[9] Thorn, KA, Pennington, JC, Kennedy, KR, Cox, LG, Hayes, CA, Porter, BE. N-15 NMR Study of the Immobilization of 2,4- and 2,6-Dinitrotoluene in Aerobic Compost. Environ Sci Technol 2008; 42: 2542-2550.

[10] Grosser, RJ, Friedrich, M, Ward, DM, Inskeep, WP. Effect of Model Sorptive Phases on Phenanthrene Biodegradation: Different Enrichment Conditions Influence Bioavailability and Selection of Phenanthrene-Degrading Isolates. Appl Environ Microbiol 2000; 66: 2695-2702.

[11] Juhasz, AL, Naidu, R. Bioremediation of High Molecular Weight Polycyclic Aromatic Hydrocarbons: A Review of the Microbial Degradation of Benzo[a]pyrene. Int Biodeter Biodegr 2000; 45: 57-88.

[12] Barriuso, E, Benoit, P, Dubus, IG. Formation of Pesticide Nonextractable (Bound) Residues in Soil: Magnitude, Controlling Factors and Reversibility. Environ Sci Technol 2008; 42: 1845-1854.

[13] Joyce, JF, Sato, C, Cardenas, R, Surampalli, RY. Composting of Polycyclic Aromatic Hydrocarbons in Simulated Municipal Solid Waste. Water Environ Res 1998; 70: 356-361.

[14] Kästner, M, Mahro, B. Microbial Degradation of Polycyclic Aromatic Hydrocarbons in Soils Affected by the Organic Matrix of Compost. Appl Microbiol Biotechnol 1996; 44: 668-675.

[15] Bamforth, SM, Singleton, I. Bioremediation of Polycyclic Aromatic Hydrocarbons: Current Knowledge and Future Directions. J Chem Technol Biotechnol 2005; 80: 723-736.

[16] Bonnet, JL, Guiraud, P, Dusser, M, Kadri, M, Laffosse, J, Steiman, R, *et al*. Assessment of Anthracene Toxicity toward Environmental Eukaryotic Microorganisms: *Tetrahymena pyriformis* and selected Micromycetes. Ecotox Environ Safe 2005; 60: 87-100

[17] Boonchan, S, Britz, ML, Stanley, GA. Surfactant-Enhanced Biodegradation of High Molecular Weight Polycyclic Aromatic Hydrocarbons by *Stenotrophomonas maltophilia*. Biotechnol Bioeng 1998; 59: 482-494.

[18] Hamdi, H, Benzarti, S, Manusadzianas, L. Aoyama, I, Jedidi, N. Bioaugmentation and Biostimulation Effects on PAH Dissipation and Soil Ecotoxicity under Controlled Conditions. Soil Biol Biochem 2007; 39: 1926-1935.

[19] Borràs, E, Caminal, G, Sarrà, M, Novotný, C. Effect of Soil Bacteria on the Ability of Polycyclic Aromatic Hydrocarbons (PAHs) Removal by *Trametes versicolor* and *Irpex lacteus* from Contaminated Soil. Soil Biol Biochem 2010; 42: 2087-2093.

[20] Cerniglia, CE. Biodegradation of Polycyclic Aromatic Hydrocarbons. Curr Opin Biotech 1993; 4: 331-338.

[21] Harayama, S. Polycyclic Aromatic Hydrocarbon Bioremediation Design. Curr Opin Biotech 1997; 8: 268-273.

[22] Kelley, L, Freeman, JP, Evans, FE, Cerniglia, CE. Identification of Metabolites from the Degradation of Fluoranthene by *Mycobacterium* sp. Strain PYR-1. Appl Environ Microbiol 1993; 59: 800-806.

[23] Müncnerová, D, Augustin, J. Fungal Metabolism and Detoxification of Polycyclic Aromatic Hydrocarbons: A Review. Bioresource Technol 1994; 48: 97-106.

[24] Adams, JDW, Umapathy, D. Composting of Green Waste: Observations from Windrow Trials and Bench-Scale Experiments. Environ Technol 2008; 29: 1149-1155.

[25] Adams, JDW, Scott, KM. Enzymatic Analyses Demonstrate Thermal Adaptation of α-Glucosidase Activity in Starch Amended Gully Waste. Bioresource Technol 2013; 127: 231-235.

[26] Hoppe, H. Use of Fluorogenic Model Substrates for Extracellular Enzyme Activity (EEA) Measurement of Bacteria. In Handbook of Methods in Aquatic Microbial Ecology, ed by Kemp PF, Sherr, BF, Sherr, EB, Cole, JJ. Lewis Publishers, Boca Raton, FL, USA, 1993.

[27] Bernal, MP, Navarro, AF, Roig, A, Cegarra, J, Garcia, D. Carbon and Nitrogen Transformation during Composting of Sweet Sorghum Bagasse. Biol Fertil Soils 1996; 22: 141-148.

[28] Paredes, C, Roig, A, Bernal, MP, Sánchez-Monedero, MA, Cegarra, J. Evolution of Organic Matter and Nitrogen during Co-Composting of Olive Mill Wastewater with Solid Organic Wastes. Biol Fertil Soils 2000; 32: 222-227.

[29] García-Gómez, A, Roig, A, Bernal, MP. Composting of the Solid Fraction of Olive Mill Wastewater with Olive Leaves: Organic Matter Degradation and Biological Activity. Bioresource Technol 2003; 86: 59-64.

[30] Qasemian, L, Guiral, D, Ziarelli, F, Dang, TKV, Farnet, A. Effects of Anthracene on Microbial Activities and Organic Matter Decomposition in a *Pinus halepensis* Litter from a Mediterranean Coastal Area. Soil Biol Biochem 2012; 46: 148-154.

Chapter 8

General Conclusions and Suggestions for Future Work

8.1 General Conclusions

Pollution arising from waste materials is a global problem and there is an urgent need for the proper management of the environment as this is an important requirement for overall and sustainable development. There are different approaches to the management of waste materials, such as, incineration, landfilling, pyrolysis, anaerobic digestion and composting. However, environmental impacts, such as, generation of greenhouse gases (carbon dioxide and methane), and contamination of water bodies by the leachate are the major concerns when incineration and landfilling are used. Application of other waste management strategies of pyrolysis (wet and dry) and composting will help in the proper management of the environment without the above mentioned impacts.

Over the last two to three decades, various environmental and developmental action plans have been put in place by world leaders and this had led to leaders of individual governments taking different approaches to manage their environment, but obtaining the right approach to tackle it is still a challenge to some governments, especially in developing countries. Despite the measures put up by the Nigerian Government, such as establishment of regulatory institutions, proper documentation on the volume of waste generated is still lacking, and landfill and incineration methods of waste management are still in practice in different part of the country.

Pyrolysis and composting have been shown to be a more environmentally friendly way of waste management and the products from these processes if properly managed can be further utilized as sources of low cost materials in other fields, especially in the environment. However, care should be taken in using these approaches, because if it not properly carried out may also lead to environmental pollution. Therefore, the use of standardized methods should be advocated. In dry pyrolysis, there are some drawbacks which the wet pyrolysis approach of hydrothermal carbonization sets out to address. However, the time consuming nature of the conventional method of hydrothermal carbonization needs to be sped up to meet the frequent requirements of environmental monitoring. Thus, the microwave-assisted

hydrothermal carbonization approach was used to prepare carbonaceous material from waste plant materials in this thesis. Three different waste materials *Prosopis africana* shell, rapeseed husk and coconut shell were subjected to hydrothermal carbonization using the conventional and microwave-assisted approach. The prepared materials showed similarities in their physical and chemical properties. The degree of carbonization of the material depends on the nature of the material, and the process condition (time and temperature of carbonization). Soft and hard biomass have different structural disintegration pathways, which was obvious from the level of carbonization observed in the waste materials. In comparison *Prosopis africana* shell and rapeseed husk show more carbonization and decomposition due to their soft nature, while the coconut shell showed a lower degree of carbonization and decomposition when subjected to the same preparation conditions. The time and temperature of carbonization were also found to have a significant effect on the percentage yield of the process. A decrease in percentage yield was observed with increase in time and temperature for the soft biomass (*Prosopis africana* shell, rapeseed husk), while the hard biomass (coconut shell) showed an opposite behaviour. In all cases the microwave-assisted hydrothermal carbonization took a shorter time and showed a higher degree of carbonization than the conventional approach. The microwave-assisted hydrothermal carbonization process therefore offers a new route to the synthesis of carbon materials and requires a shorter time to prepare the materials when compared to the conventional method.

The carbon materials from dry pyrolysis (biochar) and wet pyrolysis using the microwave-assisted hydrothermal process (hydrochar) were also applied in the removal of some heavy metals from aqueous solution and showed excellent performance in removing the heavy metals studied, and in comparison with other adsorbents previously reported proved to be better, as the materials have higher adsorption capacities. Interestingly, the hydrochar from microwave-assisted hydrothermal carbonization, which is a green chemistry approach, was capable of adsorbing the metal ions more effectively from aqueous solution than the biochar because of the more oxygen-containing functional groups on the surface. The maximum adsorption capacities were 45.3 and 31.3 mg/g for Pb^{2+} and 38.3 and 29.9 mg/g for Cd^{2+} on the hydrochar and biochar respectively. The adsorption data were modelled using pseudo first-order and pseudo second-order kinetics. The results fitted pseudo second-order

kinetics more than pseudo-first-order kinetics and the adsorption data could be better described using the Langmuir isotherm model than the Freundlich isotherm model. The intraparticle diffusion model was also used to study the diffusion mechanism of the adsorption process and the result indicated that metal ions diffusion into pores is not the dominating factor that controlled the mechanism of the adsorption process. The thermodynamic results indicated that the adsorption process for the metal ions was a spontaneous and endothermic process.

The carbon materials prepared from the pyrolysis and the hydrothermal carbonization of the waste materials were useful, but are in powdered form, non-porous and have small surface areas. In order to enhance the performance of the processed waste material as an adsorbent, porous carbon monoliths were synthesized. The microwave-assisted process was applied in the synthesis of the carbon monolith. Mesoporous carbon monolith that compared well with those synthesized through the conventional route of oven heating was obtained using resorcinol and formaldehyde as the carbon precursor and pluronic F127 as the template. This method of synthesis offers a new route to synthesis of carbon monolith with mesostructure as a shorter time is required in the microwave-assisted synthesis. However, the use of the microwave-assisted hydrothermal carbonization in the synthesis of carbon monolith using waste plant material (*Prosopis africana* shell) as a cheap and readily available carbon precursor and pluronic F127 as template was not successful as the synthesized monolith cracked, but by using evaporation-induced self-assembly (EISA), crack-free mesoporous carbon monolith was obtained. This type of process has not been previously reported in literature. The preliminary results showed a very good prospect and this could offer a newer and cheaper route to the synthesis of porous carbon monolith. It could also be a better way of processing waste materials into a useful product, as the synthesized carbon monolith has a higher surface area and porosity than the biochar and the hydrochar prepared from the same material.

Composting has been used as a low cost alternative to other methods of waste management. The initial composting experiment proved that the *Prosopis africana* shell can be composted. The effects of an organic pollutant (anthracene) during a starch amended co-composting process with green waste compost monitored through the total dry matter and extracellular enzyme (α- and β-glucosidase) activities showed that the effect of anthracene was not highly significant in this study. However, the interaction

between the anthracene and starch had effects on the total dry matter and α-glucosidase activity which is novel.

8.2 Suggestion for Future Work

Long processing time and high-cost are the challenges facing the available methods for the synthesis of carbon monoliths making it difficult for the methods to be employed for large scale manufacturing of the materials. These challenges have stimulated the search for the development of an alternative cheap, time-saving and scalable approach to the synthesis of carbon monoliths. The results obtained using the microwave heating has shown that the synthesis time could be reduced if this approach is used. Also, using waste plant material as a cheap and readily available carbon precursor can reduce the high-cost of production. It is rational therefore to suggest that these approaches are applied in the synthesis of materials, especially carbon monoliths. The carbon monoliths prepared using these approaches deserve further investigation. They can be applied in different fields, such as, adsorption, catalysis, and as electrode materials for electrochemical double-layer capacitors (EDLCs). This will be useful in assessing the prepared materials as compared to those that are presently available. Also, the synthesis of carbon monolith in the microwave using plant material as the carbon precursor should be explored further, as this if successful will reduce the time and cost of the synthesis simultaneously.

Functionalising and magnetising the hydrochar during the microwave-assisted hydrothermal carbonization could lead to synthesis of carbon materials that could be fit for specific applications, such as, adsorption and catalysis. Although functionalising hydrochar is not something new, carrying it out in the microwave could be faster when compared to the methods that are being presently used. The microwave-assisted hydrothermal conversion process should be applied to other types of waste materials outside the waste biomass, such as, animal and industrial waste and in the process remove these materials which could constitute nuisance to the environment and convert them to useful products for different applications. Research should also be carried out to separate and characterize the bio-oil from the aqueous products of the microwave-assisted hydrothermal carbonization process. The biochar, hydrochar and compost from these waste materials should also be applied to agricultural soil alone or together to see

their effects on crop growth and in the remediation of agricultural soil contaminated with organics and heavy metals. The synergistic effect of these products could enhance a better and faster remediation of such soil and also improve the soil properties for agricultural purposes.

The interaction between the anthracene and starch during a starch amended co-composting should be further investigated by designing experiment to describe the magnitude of such interactions. In view of this, I suggest that such interaction should be studied under the same composting environment. If possible, these effects should be confirmed outside the laboratory using soils contaminated with PAHs, for example petrochemical polluted soils.

Appendix

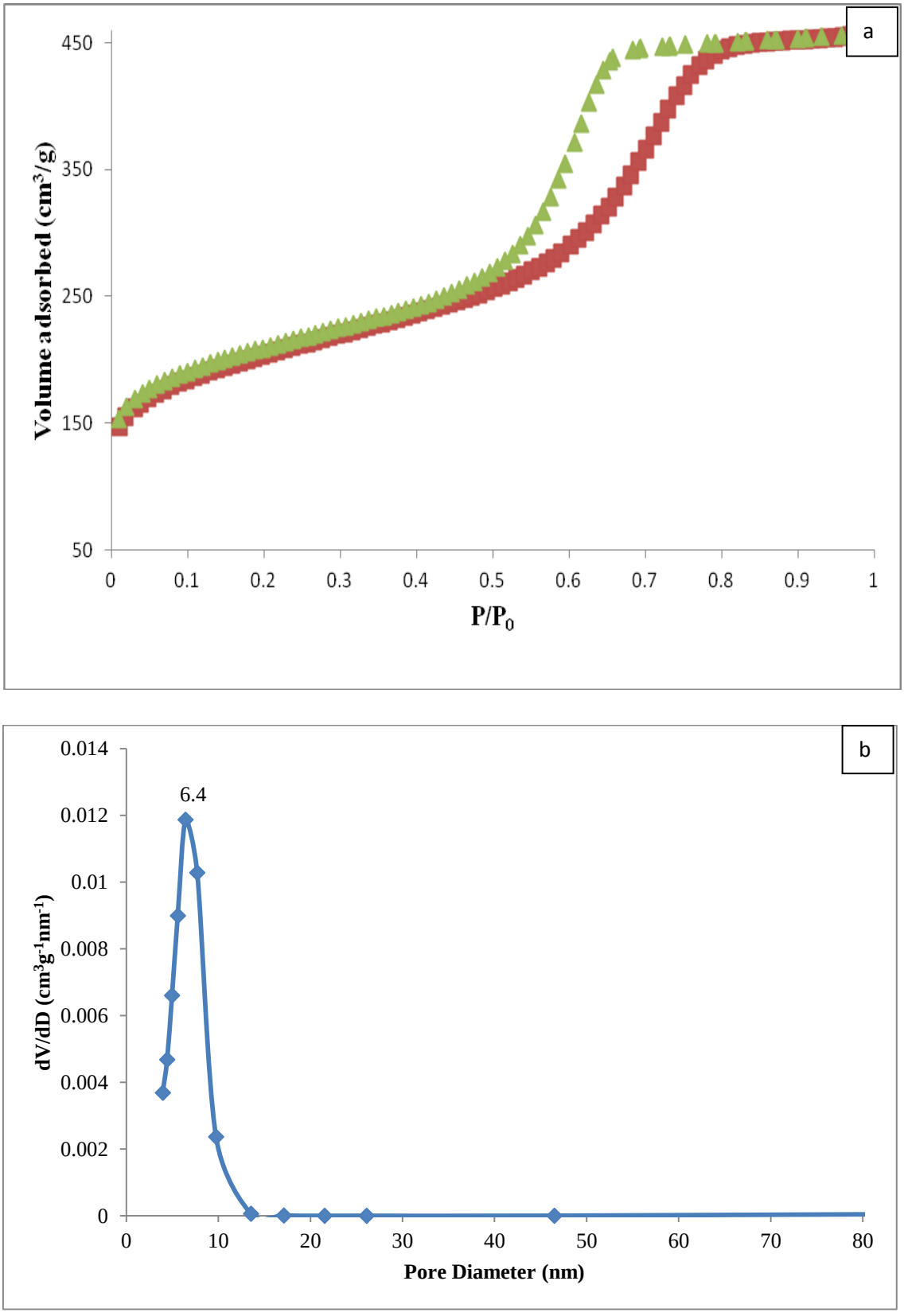

Appendix 1: (a) N_2 sorption isotherm and (b) pore size distribution of $CM_{100\text{-}20}$

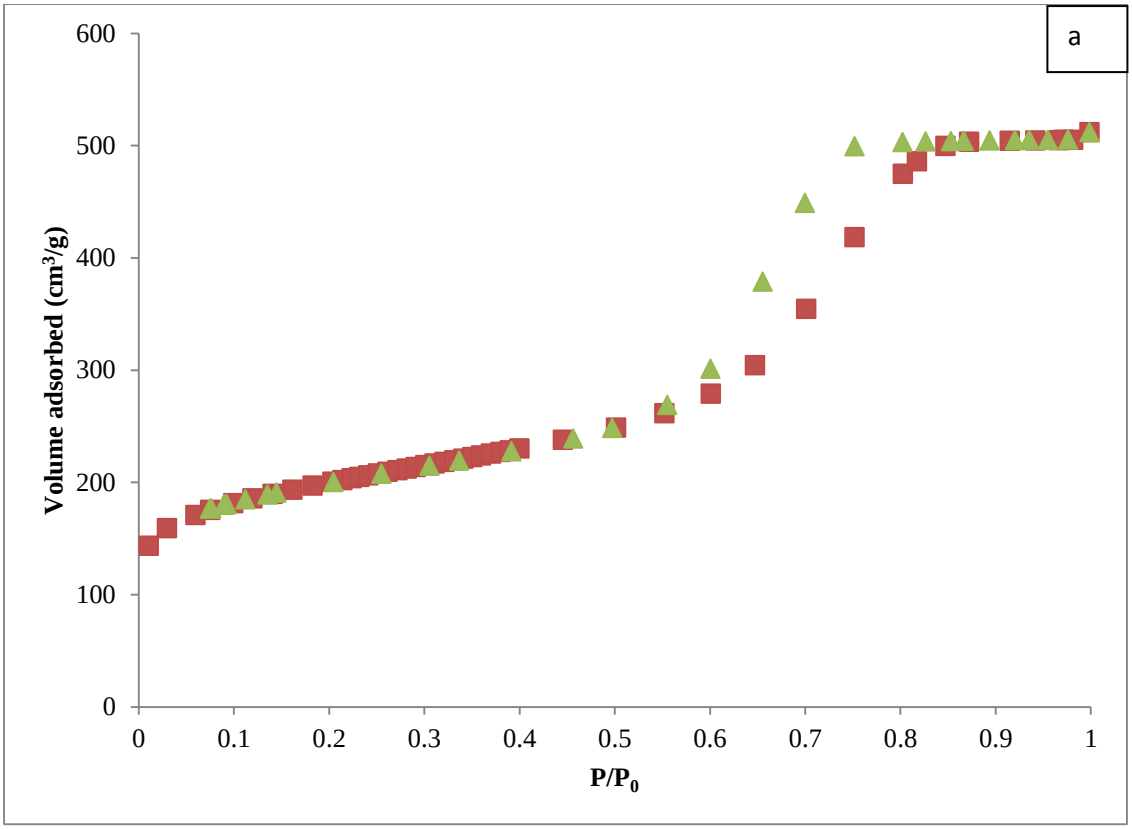

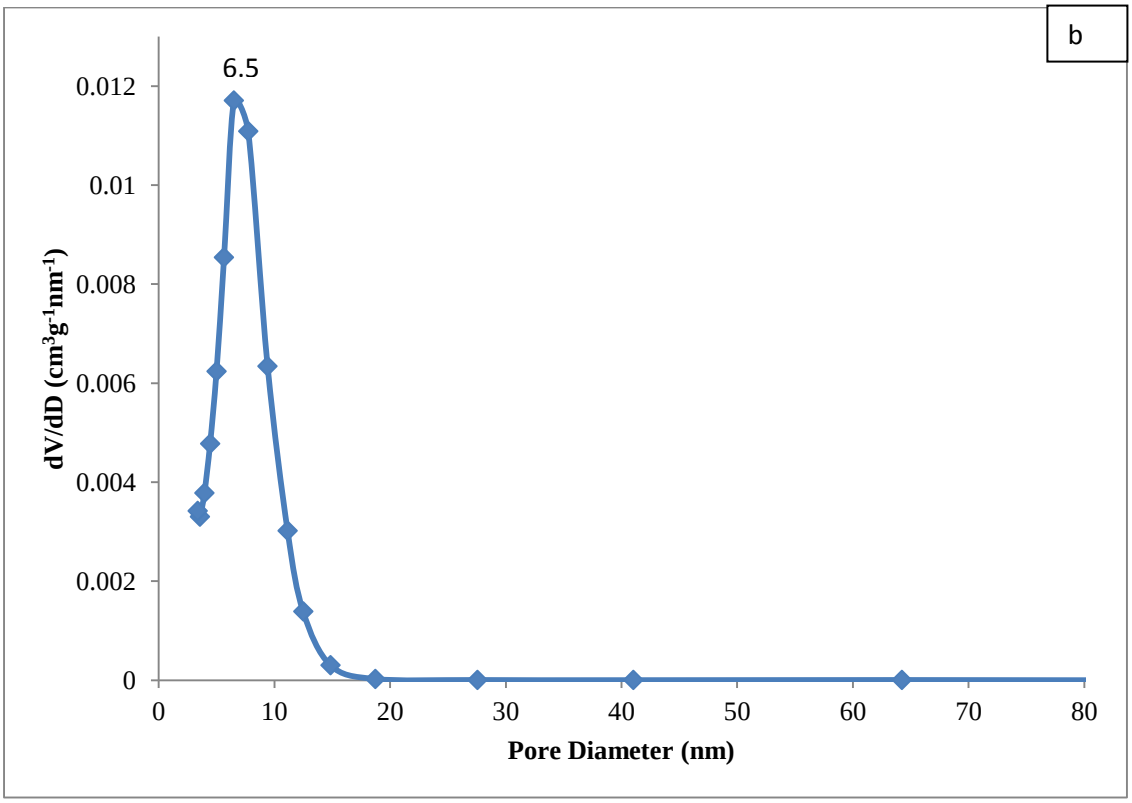

Appendix 2: (a) N_2 sorption isotherm and (b) pore size distribution of $CM_{100\text{-}15}$

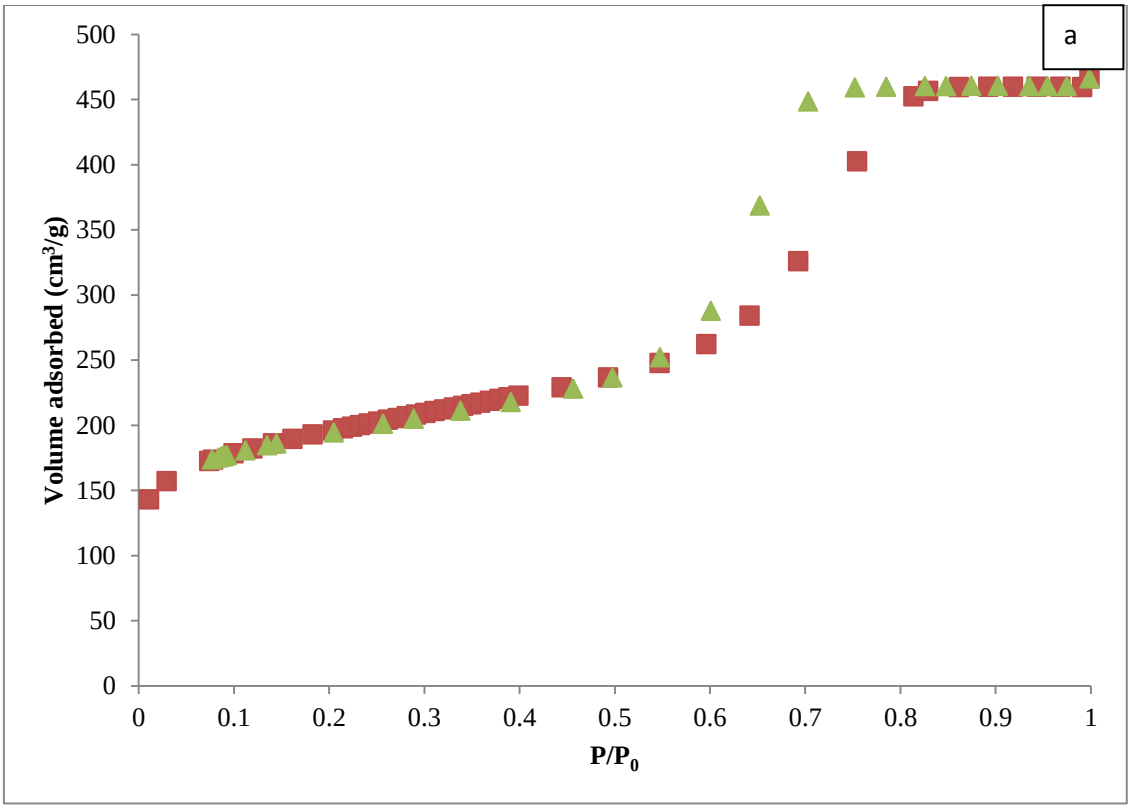

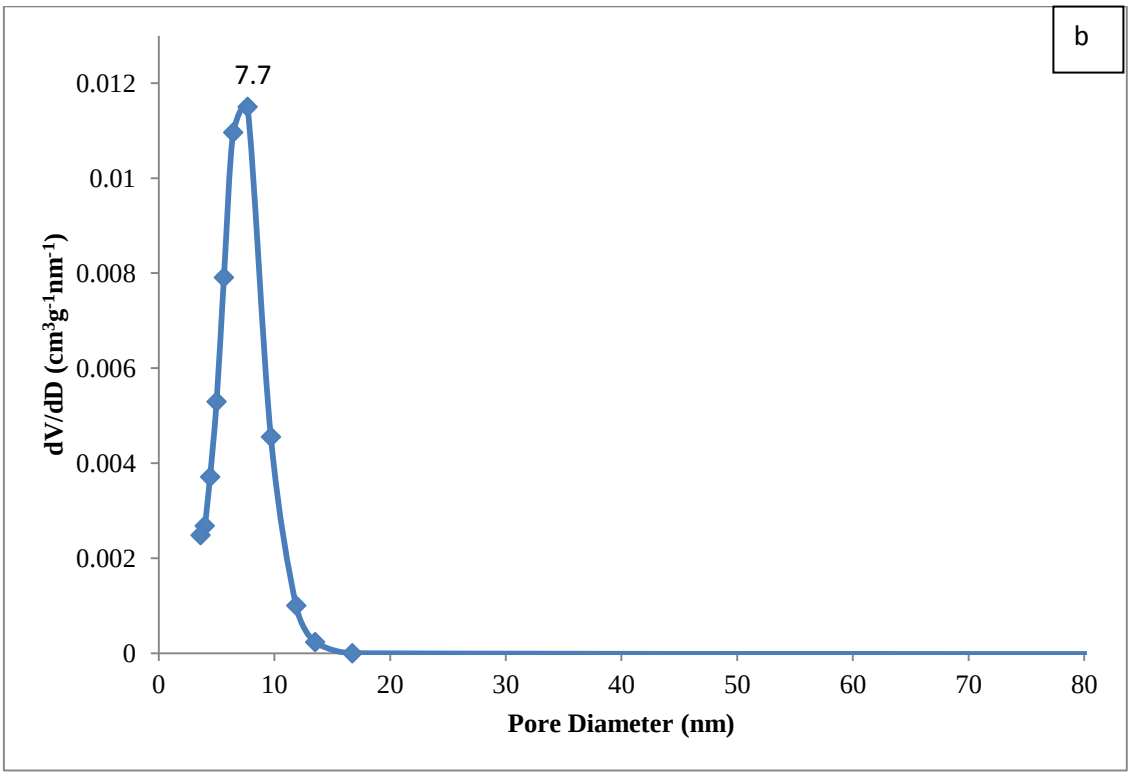

Appendix 3: (a) N_2 sorption isotherm and (b) pore size distribution of $CM_{100\text{-}10}$

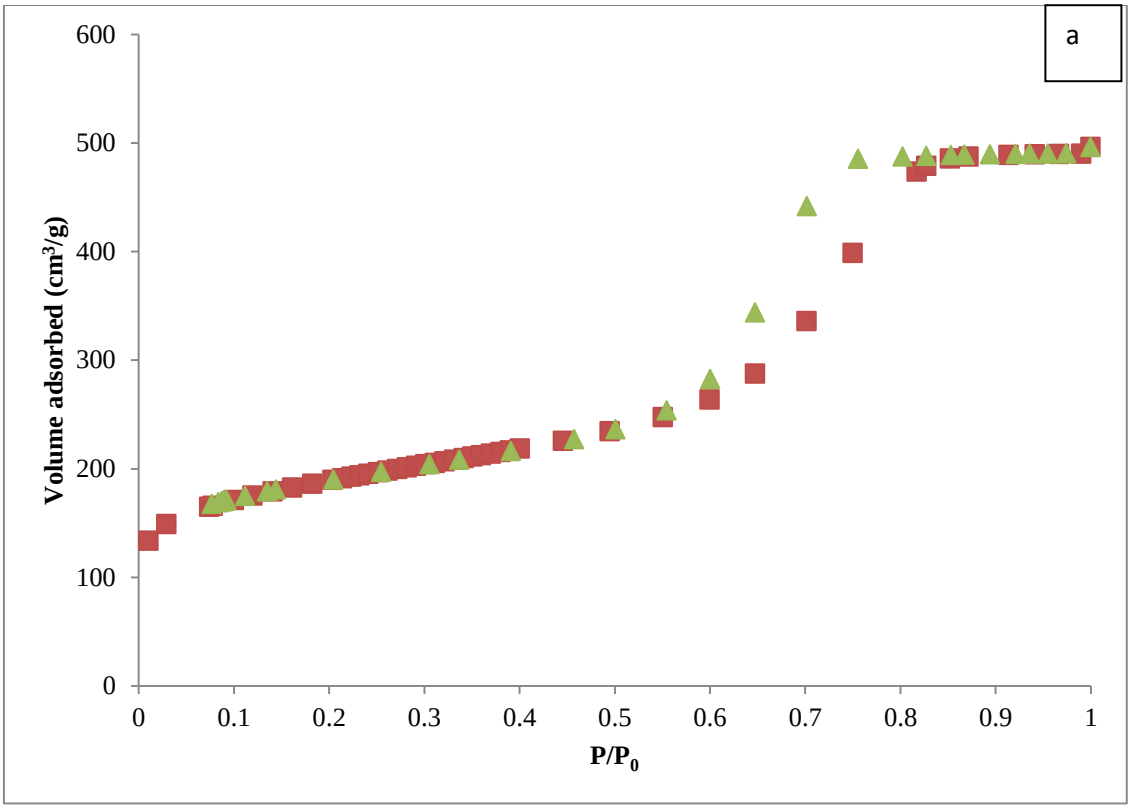

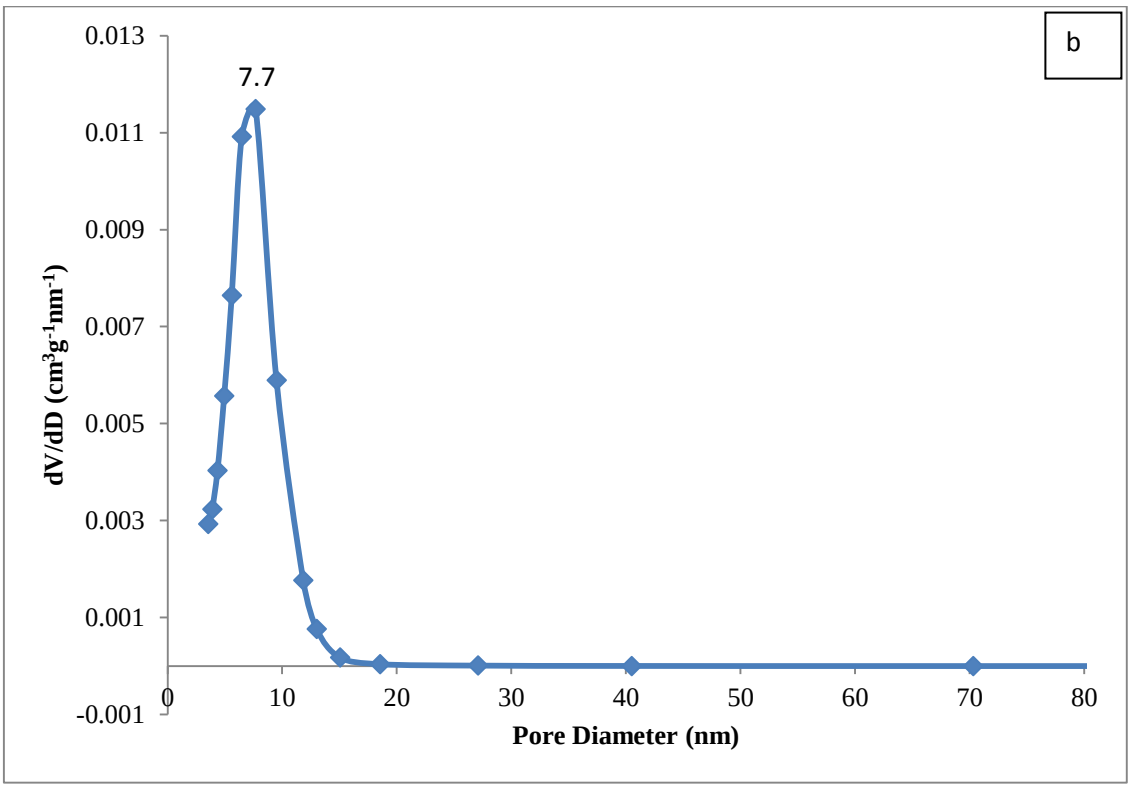

Appendix 4: (a) N_2 sorption isotherm and (b) pore size distribution of $CM_{100\text{-}5}$

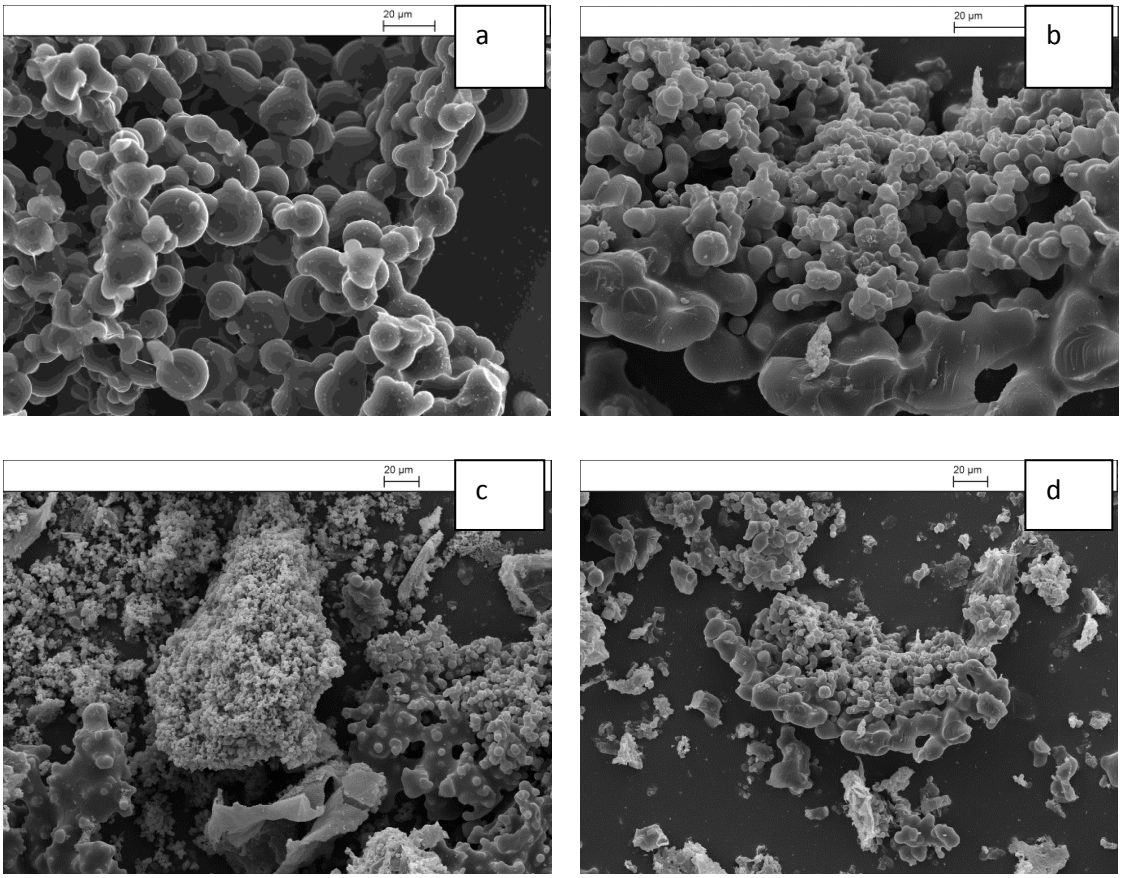

Appendix 5: SEM images of (a) $CM_{100\text{-}20}$ (b) $CM_{100\text{-}15}$ (c) $CM_{100\text{-}10}$ (d) $CM_{100\text{-}5}$

Source	SS	df	MS	Number of obs = 5
Model	22.13	1	22.13	F(1, 3) = 5075.00
Residual	0.013	3	0.0043	Prob > F = 0.0000
Total	22.15	4	5.53	R-squared = 0.9994
				Adj R-squared = 0.9992
				Root MSE = 0.0661

Total dry	Coef.	Std. Err.	t	P>t	[95% Conf.	Interval]
Time	-1.48	0.020	-71.24	0.000	-1.55	-1.42
_cons	50.40	0.069	727.69	0.000	50.18	50.62

Appendix 6 (a): Regression analysis, total dry matter with time, if starch=0 & anthracene=0

Source	SS	df	MS	Number of obs = 5
Model	39.96	1	39.96	F (1, 3) = 33.38
Residual	3.59	3	1.19	Prob > F = 0.0103
Total	43.55	4	10.88	R-squared = 0.9175
				Adj R-squared = 0.8900
				Root MSE = 1.0943

-Total dry	Coef.	Std. Err.	t	P>t	[95% Conf.	Interval]
Time	-1.99	0.34	-5.78	0.010	-3.10	-0.89
_cons	54.44	1.14	47.44	0.000	50.79	58.09

Appendix 6 (b): Regression analysis, total dry matter with time, if starch=10 & anthracene=0

Source	SS	df	MS	Number of obs = 5
Model	23.24	1	23.24	F (1, 3) = 22.85
Residual	3.05	3	1.01	Prob > F = 0.0174
Total	26.29	4	6.57	R-squared = 0.8840
				Adj R-squared = 0.8453
				Root MSE = 1.0086

Total dry	Coef.	Std. Err.	t	P>t	[95% Conf.	Interval]
Time	-1.52	0.31	-4.78	0.017	-2.53	-0.50
_cons	49.88	1.05	47.16	0.000	46.52	53.25

Appendix 6 (c): Regression analysis, total dry matter with time, if starch=0 & anthracene=20

--Source	SS	df	MS	Number of obs = 5
Model	22.24	1	22.24	F (1, 3) = 10.98
Residual	6.07	3	2.02	Prob > F = 0.0453
Total	28.32	4	7.08	R-squared = 0.7854
				Adj R-squared = 0.7139
				Root MSE = 1.4233

Total dry	Coef.	Std. Err.	t	P>t	[95% Conf.	Interval]
Time	-1.49	0.45	-3.31	0.045	-2.92	-0.05
_cons	57.07	1.49	38.24	0.000	52.32	61.82

Appendix 6 (d): Regression analysis, total dry matter with time, if starch=10 & anthracene=20

Source	Partial SS	df	MS	F	Prob > F
Model	249.35	6	41.56	15.42	0.0000
Starch	119.88	1	119.88	44.47	0.0000
Anthracene	15.53	1	15.52	5.76	0.0321
Time	113.95	4	28.49	10.57	0.0005
Residual	35.04	13	2.70		

Appendix 7 (a): ANOVA results for loss in dry matter under different treatments for experiment one. R^2 for the overall model is 0.8768

Source	Partial SS	df	MS	F	Prob > F
Model	309.26	4	77.32	13.21	0.0000
Starch	207.88	1	207.88	35.51	0.0000
Anthracene	37.94	1	37.94	6.48	0.0197
Time	63.44	2	31.72	5.42	0.0137
Residual	111.24	19	5.86		
Total	420.50	23	18.28		

Appendix 7 (b): ANOVA results for loss in dry matter under different treatments for experiment three. R^2 for the overall model is 0.7355

Source	SS	df	MS	Number of obs = 6
Model	0.39	1	0.39	F (1, 4) = 0.49
Residual	3.18	4	0.79	Prob > F = 0.5216
Total	3.57	5	0.71	R-squared = 0.1096
				Adj R-squared = -0.1130
				Root MSE = .89265

-- Total dry	Coef.	Std. Err.	t	P>t	[95% Conf. Interval]	
--Time	0.31	0.44	0.70	0.522	-0.92	1.55
_cons	50.47	0.96	52.35	0.000	47.79	53.14

Appendix 8 (a): Regression analysis, total dry matter with time, if starch=0 & anthracene=0

Source	SS	df	MS	Number of obs = 6
Model	17.20	1	17.20	F (1, 4) = 2.94
Residual	23.44	4	5.86	Prob > F = 0.1618
Total	40.64	5	8.12	R-squared = 0.4233
				Adj R-squared = 0.2791
				Root MSE = 2.4208

Total dry	Coef.	Std. Err.	t	P>t	[95% Conf. Interval]	
Time	-2.07	1.21	-1.71	0.162	-5.43	1.28
_cons	61.23	2.61	23.42	0.000	53.97	68.49

Appendix 8 (b): Regression analysis, total dry matter with time, if starch=10 & anthrancene=0

Source	SS	df	MS		Number of obs = 6	
Model	55.94	1	55.94		F (1, 4) = 11.55	
Residual	19.37	4	4.84		Prob > F = 0.0273	
Total	75.31	5	15.06		R-squared = 0.7428	
					Adj R-squared = 0.6785	
					Root MSE = 2.2007	

Total dry	Coef.	Std. Err.	t	P>t	[95% Conf. Interval]	
Time	-3.73	1.10	-3.40	0.027	-6.79	-0.68
_cons	66.97	2.37	28.18	0.000	60.37	73.57

Appendix 8 (c): Regression analysis, total dry matter with time, if starch=10 & anthracene=100

Source	SS	df	MS		Number of obs = 6	
Model	21.61	1	21.61		F (1, 4) = 2.59	
Residual	33.45	4	8.36		Prob > F = 0.1831	
Total	55.07	5	11.01		R-squared = 0.3926	
					Adj R-squared = 0.2407	
					Root MSE = 2.8919	

Total dry	Coef.	Std. Err.	t	P>t	[95% Conf. Interval]	
Time	-2.32	1.44	-1.61	0.183	-6.33	1.68
Cons	58.36	3.12	18.68	0.000	49.68	67.03

Appendix 8 (d): Regression analysis, total dry matter with time, if starch=0 & anthracene=100

Source	Partial SS	df	MS	F	Prob > F
Model	17.89	6	2.98	4.35	0.0126
Time	1.89	4	0.47	0.69	0.6110
Anthracene	13.72	1	13.72	20.01	0.0006
Starch	2.276	1	2.27	3.32	0.0916
Residual	8.91	13	0.68		
Total	26.81	19	1.41		

Appendix 9 (a): ANOVA results for α-glucosidase activity for experiment one. R^2 for the overall model is 0.6674

Source	Partial SS	df	MS	F	Prob > F
Model	.029	6	0.0049	1.31	0.3180
Week	.012	4	0.0030	0.82	0.5374
Anthracene	.013	1	0.013	3.62	0.0795
Starch	.0037	1	0.0037	1.00	0.3348
Residual	.048	13	0.0037		
Total	.078	19	0.0041		

Appendix 9 (b): ANOVA results for β--glucosidase activity for experiment one. R^2 for the overall model is 0.3775

Source	Partial SS	df	MS	F	Prob>F
Model	52.00	4	13.00	1.59	0.2189
Starch	18.77	1	18.77	2.29	0.1467
Anthracene	7.55	1	7.55	0.92	0.3492
Time	25.67	2	12.83	1.57	0.2348
Residual	155.80	19	8.20		
Total	207.81	23	9.03		

Appendix 10 (a): ANOVA results for α-glucosidase activity for experiment three. R^2 for the overall model is 0.2503

Source	Partial SS	df	MS	F	Prob > F
Model	2852837.92	4	713209.47	2.71	0.0610
Starch	244016.66	1	244016.66	0.93	0.3476
Anthracene	82134.00	1	82134.00	0.31	0.5828
Time	2526687.25	2	1263343.62	4.80	0.0205
Residual	4997846.08	19	263044.53		
Total	7850684.00	23	341334.08		

Appendix 10 (b): ANOVA results for β--glucosidase activity for experiment three. R^2 for the overall model is 0.3634